

Protein-Mediated Membrane Fusion: New Insights from the Reptilian
Reovirus p14 Fusion Protein

by

Jennifer A. Corcoran

Submitted in partial fulfillment for the requirements of the degree of Doctor of
Philosophy

at

Dalhousie University
Halifax, Nova Scotia
November, 2003

© by Jennifer A. Corcoran, 2003



National Library
of Canada

Bibliothèque nationale
du Canada

Acquisitions and
Bibliographic Services

Acquisitions et
services bibliographiques

395 Wellington Street
Ottawa ON K1A 0N4
Canada

395, rue Wellington
Ottawa ON K1A 0N4
Canada

Your file Votre référence

ISBN: 0-612-89820-2

Our file Notre référence

ISBN: 0-612-89820-2

The author has granted a non-exclusive licence allowing the National Library of Canada to reproduce, loan, distribute or sell copies of this thesis in microform, paper or electronic formats.

L'auteur a accordé une licence non exclusive permettant à la Bibliothèque nationale du Canada de reproduire, prêter, distribuer ou vendre des copies de cette thèse sous la forme de microfiche/film, de reproduction sur papier ou sur format électronique.

The author retains ownership of the copyright in this thesis. Neither the thesis nor substantial extracts from it may be printed or otherwise reproduced without the author's permission.

L'auteur conserve la propriété du droit d'auteur qui protège cette thèse. Ni la thèse ni des extraits substantiels de celle-ci ne doivent être imprimés ou autrement reproduits sans son autorisation.

In compliance with the Canadian Privacy Act some supporting forms may have been removed from this dissertation.

Conformément à la loi canadienne sur la protection de la vie privée, quelques formulaires secondaires ont été enlevés de ce manuscrit.

While these forms may be included in the document page count, their removal does not represent any loss of content from the dissertation.

Bien que ces formulaires aient inclus dans la pagination, il n'y aura aucun contenu manquant.

Canada

DALHOUSIE UNIVERSITY
DEPARTMENT OF MICROBIOLOGY AND IMMUNOLOGY

The undersigned hereby certify that they have read and recommend to the Faculty of Graduate Studies for acceptance a thesis entitled “Protein-Mediated Membrane Fusion: New Insights from the Reptilian Reovirus p14 Fusion Protein” by Jennifer A. Corcoran in partial fulfillment of the requirements for the degree of Doctor of Philosophy.

Dated: December 8, 2003

External Examiner: _____

Research Supervisor: _____

Examining Committee: _____

Departmental Representative: _____

DALHOUSIE UNIVERSITY

DATE: November 7, 2003

AUTHOR: Jennifer A. Corcoran

TITLE: Protein-Mediated Membrane Fusion: New Insights from the
Reptilian Reovirus p14 Fusion Protein.

DEPARTMENT OR SCHOOL: Microbiology and Immunology

DEGREE: Ph.D. CONVOCATION: May YEAR: 2004

Permission is herewith granted to Dalhousie University to circulate and to have copied for non-commercial purposes, at its discretion, the above title upon the request of individuals or institutions.

The author reserves other publication rights, and neither the thesis nor extensive extracts from it may be printed or otherwise reproduced without the author's written permission.

The author attests that permission has been obtained for the use of any copyrighted material appearing in the thesis (other than the brief excerpts requiring only proper acknowledgement in scholarly writing), and that all such use is clearly acknowledged.

Table of Contents	Page
List of Tables	viii
List of Figures	ix
Abstract	xi
List of Abbreviations and Symbols	xii
Acknowledgements	xv
 Chapter 1	
Introduction	1
Overview	1
1.1 Membrane fusion in pure lipid bilayers	3
1.1.A Membrane lipids	3
1.1.B Factors that promote/prevent membrane fusion	4
1.1.C Techniques used to study membrane fusion	7
1.1.D Membrane fusion of pure lipid bilayers	12
1.2 Biological membrane fusion	19
1.2.A Biological membranes	19
1.2.B Biological membrane fusion	20
1.2.C The fusion pore is a fluctuating lipid junction between two lipid bilayers held in place by a protein scaffold	21
1.2.D A transient proteinaceous fusion pore is followed by a lipidic pore	29
1.2.E The fusion pore is proteinaceous until lipid is recruited to break the protein ring	30
1.2.F Summary of models	31
1.3 Fusion proteins encoded by enveloped viruses	33
1.3.A An introduction to viral fusion proteins	33
1.3.B Viral fusion proteins are metastable	38
1.3.C Membrane interacting region I – the transmembrane anchor	45
1.3.D Membrane interacting region II – the fusion peptide	48
1.3.E Other membrane interacting regions	53
1.4 Cellular fusion proteins	59
1.4.A Intracellular fusion	59
1.4.B Intercellular fusion	64
1.5 Reoviruses encode membrane fusion proteins	70
1.6 Figures	74

Chapter 2		80
Materials and Methods		
2.1	Cells and virus	80
2.2	Materials	81
2.3	Cloning and sequencing	81
2.4	p14 protein and antiserum production	84
2.5	p14-proteoliposome production	85
2.6	Transfection and cell staining	86
2.7	Syncytial indexing	87
2.8	Antibody inhibition	87
2.9	<i>In vitro</i> transcription and translation	88
2.10	Radiolabeling	88
2.11	Pulse-labeling	89
2.12	Membrane fractionation	89
2.13	Immune precipitation	90
2.14	Co-immune precipitation	91
2.15	Cell staining with fluorescent dyes	91
2.16	Co-fluorescence using p14-GFP	92
2.17	Chemical cross-linking	94
2.18	Cholesterol depletion	95
2.19	Detergent-resistant membrane fractionation	95
2.20	Sucrose density gradient centrifugation	96
2.21	Western blotting	96
Chapter 3		98
Membrane Fusion Mediated by a Type III Protein with an External Myristylated Amino Terminus		
3.1	Overview	98
3.2	Introduction	99
3.3	Results	102
3.4	Discussion	110
3.5	Figures	119
Chapter 4		130
An atypical fusion protein from a nonenveloped virus contains a looped internal fusion peptide within its essential 40-residue N-terminal ectodomain.		
4.1	Overview	130
4.2	Introduction	131
4.3	Results	137
4.4	Discussion	147
4.5	Figures and Tables	155

Chapter 5	161
The 14 kDa membrane fusion protein of reptilian reovirus is a homomultimer.	
5.1 Overview	161
5.2 Introduction	162
5.3 Results	166
5.4 Discussion	177
5.5 Figures and Tables	187
Chapter 6	199
A nonenveloped virus membrane fusion protein localizes to lubrol-resistant membrane microdomains: possible role of cell protrusions in the mechanism of p14 cell-cell fusion.	
6.1 Overview	199
6.2 Introduction	201
6.3 Results	205
6.4 Discussion	215
6.5 Figures	224
Chapter 7	231
Conclusions	
7.1 Summary	231
7.2 Model	233
7.3 Figures	241
References	244
Appendix A	283
Supplementary material for experiments performed by collaborators	
Supplementary Materials and Methods	
1.1 Circular dichroism	283
1.2 Preparation of large unilamellar vesicles	283
1.3 Lipid mixing assay	284
1.4 Solution NMR spectroscopy	285
1.5 Quantification of cholesterol effects on fusion	286
1.6 Supplementary Figures and Tables	288

Appendix B	294
Primers	
Appendix C	297
Letters of copyright permission	

List of Tables	Page
1.1 Class I viral fusion proteins	35
1.2 Class II viral fusion proteins	37
1.3 Unclassified viral fusion proteins	38
1.4 Transmembrane anchor sequences	48
1.5 Fusion peptide sequences	52
1.6 Sequences of other membrane-interacting regions	57
1.7 Candidate cellular fusion peptide sequences	66
1.8 Fusogenic reovirus species	70
5.1 Cross-linking reagents	191

List of Figures	Page
1.1 The molecular shape of a membrane lipid influences the structure it forms in an aqueous environment.	74
1.2 The stalk-pore model of membrane fusion.	75
1.3 Influenza hemagglutinin (HA) undergoes conformational rearrangement in response to acid pH.	76
1.4 The structure(s) of representative Class I and Class II viral fusion proteins.	77
1.5 The boomerang model.	78
1.6 Members of the genus orthoreovirus.	79
3.1 The first open reading frame on the RRV bicistronic S1 genome segment encodes a p14 fusion protein.	119
3.2 Sequence-predicted structural motifs in p14.	120
3.3 p14 is a surface-localized integral membrane protein.	122
3.4 p14 assumes an N _{exo} /C _{cyt} surface membrane topology.	123
3.5 p14 is not N-glycosylated.	124
3.6 The C-terminal 37 amino acids of p14 are dispensable for fusion.	125
3.7 N-terminal myristylation of p14 is essential for cell fusion.	126
3.8 p14 translocates its myristylated N-terminus across the membrane.	127
3.9 The V9T substitution eliminates p14-induced membrane fusion.	128
3.10 Structural motifs in the reovirus FAST proteins.	129
4.1 p14 contains a hydrophobic patch in its ectodomain.	155
4.2 The p14 hydrophobic patch and may form a loop.	156
4.3 Site-specific substitution of amino acids within the p14 hydrophobic patch motif that alter the formation of the loop or its hydrophobic face but not overall hydrophobicity impair fusion.	158
4.4 Reversal of the position of the loop-stabilizing charged residues within the p14 hydrophobic patch motif restores fusion.	159
4.5 The amino acid sequence of the p14 hydrophobic patch is compared with a moderately hydrophobic stretch in BRV p15.	160
5.1 Structural motifs in p14.	187
5.2 Substituted or tagged p14 constructs exert a <i>trans</i> -dominant negative effect on the ability of authentic p14 to mediate fusion.	188
5.3 Co-immune precipitation indicates that p14 is a homomultimer.	190
5.4 <i>In vitro</i> chemical cross-linking indicates that p14 is a homomultimer.	192
5.5 p14 traffics through the ER-Golgi pathway to the cell surface.	194
5.6 p14 multimerization may occur within the first 15 minutes of protein synthesis.	196
5.7 The degradation profile of the ARV p10 protein.	197
5.8 A structural model of p14 indicates possible regions of interaction between p14 monomers.	198

6.1	p14-fusion requires plasma membrane cholesterol.	224
6.2	p14 localizes to the Lubrol-resistant membrane fraction by ultracentrifugation.	225
6.3	p14 localizes to Lubrol- and Triton X-100-resistant membrane microdomains by sucrose density gradient analysis.	227
6.4	Placental alkaline phosphatase (PLAP) localizes to Triton X-100-resistant membrane microdomains.	228
6.5	p14 localizes preferentially to Lubrol-rafts.	229
6.6	p14 localizes to regions of cell protrusions.	230
7.1	A hypothetical free energy diagram of the membrane fusion reaction.	241
7.2	A model of p14-mediated fusion.	242
7.3	The p14 fusion protein in action, as illustrated by a short video. (to view with enclosed CD)	243

Abstract

Reptilian reovirus (RRV) is one of a limited number of non-enveloped viruses capable of inducing cell-cell fusion. A small, hydrophobic, basic, 125 amino acid fusion protein termed p14, is encoded by the first open reading frame (orf) of a bicistronic viral mRNA. Sequence comparisons to previously characterized reovirus fusion proteins identified p14 as a new member of the reovirus fusion-associated small transmembrane (FAST) protein family.

p14 contains several key structural and functional motifs. A C-proximal proline-rich motif and N-glycosylation consensus sequence are not required for fusion activity, whereas N-terminal myristylation of p14 is an essential component of the fusion mechanism. p14 is a Type III (N_{exo}/C_{cyt}) integral membrane protein. This topology results in the co-translational translocation of the essential myristylated N-terminal domain of p14 across the membrane. Site-directed mutagenesis, circular dichroism and an *in vitro* liposome fusion assay identified an N-proximal hydrophobic patch (HP) as a fusion motif integral to the p14-fusion mechanism. Solution NMR spectroscopy identified a β -structured loop near the N terminus, with the C-terminal residues remaining unstructured. Certain substitutions in the HP that resulted in a fusion-minus phenotype also exerted a dominant negative effect on authentic p14-induced syncytium formation, suggesting p14 may multimerize. A co-immune precipitation assay indicated that p14 forms homomultimers. *In vitro* chemical cross-linking confirmed the close association of p14 monomers, and suggested p14 may form dimers. The mechanism of p14-mediated fusion depends on the presence of cholesterol in the plasma membrane. p14 localizes to two types of detergent-resistant membrane microdomains; however, fluorescence microscopy suggested that a greater population of the protein resided in cholesterol-dependent Lubrol-resistant membranes. It is possible that p14 may utilize Lubrol-rafts to target cell membrane protrusions as its preferred site of fusion initiation.

Based on these studies, the following model for p14-mediated membrane fusion is proposed. RRV p14 adopts a membrane topology that externalizes its myristylated N-terminal domain, allowing the fatty acid to associate with the exoplasmic leaflet of the membrane. A critical number of p14 multimers localize to cholesterol-rich Lubrol-resistant membrane microdomains in non-planar regions of the plasma membrane. The hydrophobic patch dehydrates the intercellular space and/or interacts with one or both membranes, mediating membrane perturbation. The membrane-embedded myristic acid reversibly dissociates from the donor membrane and/or interacts with the target membrane, to increase membrane perturbation. The membrane-interacting regions of a critical number of p14 multimers mediate sufficient alteration of lipid bilayer structure that membrane merger is the result. This study accentuates the diversity and unusual properties of p14 and the FAST protein family as a third distinct class of viral membrane fusion proteins.

List of Abbreviations and Symbols

σ C	sigma C, ARV cell attachment protein
Δ G	Gibbs free energy
β -Me	β -mercaptoethanol
ADAM	<i>a</i> disintegrin and metalloprotease domain protein
AE	free energy of activation
APG	p-azidophenyl glyoxal monohydrate
ARV	avian reovirus (<i>Reoviridae</i>)
ASLV	avian sarcoma leukosis virus (<i>Retroviridae</i>)
B56	Brij 56
B58	Brij 58
BFA	brefeldin A
BRV	baboon reovirus (<i>Reoviridae</i>)
C	carboxy terminus
CD	circular dichroism
Ci	Curie
CMC	critical micellar concentration
CMM	canine microsomal membranes
CSFV	classical swine fever virus (<i>Flaviviridae</i>)
CT	cytoplasmic tail
DHBV	duck hepatitis B virus (<i>Hepadnaviridae</i>)
DMSO	dimethyl sulfoxide
DOPC	dioleoylphosphatidylcholine
DOPE	dioleoylphosphatidylethanolamine
DRM	detergent-resistant membrane
DSC	differential scanning calorimetry
DST	disuccinimidyl tartrate
DTSSP	dithiobis(sulfosuccinimidylpropionate)
E	envelope protein of alpha- and flaviviruses (E1/E is the fusion subunit)
EFF-1	epithelial fusion failure protein
EGS	ethylene glycobis(succinimidylsuccinate)
env	envelope protein of retroviruses (the fusion subunit)
ER	endoplasmic reticulum
F	fusion protein of paramyxoviruses (F1 is fusion subunit)
FAST	fusion-associated small transmembrane protein
FBS	fetal bovine serum
FITC	fluorescein
G	glycoprotein of rhabdoviruses (fusion subunit)
GFP	green fluorescent protein
gp	glycoprotein (often used to describe retrovirus fusion subunit)
GPI	glycosylphosphatidylinositol
G-stem	truncated construct of the VSV G-protein
HA	hemagglutinin protein of influenza virus (HA2 is fusion subunit)

HBSS	Hank's buffered saline solution
HBV	hepatitis B virus (<i>Hepadnaviridae</i>)
HCV	hepatitis C virus (<i>Flaviviridae</i>)
HERV	human endogenous retrovirus (<i>Retroviridae</i>)
HII	hexagonal II phase
HIV	human immunodeficiency virus (<i>Retroviridae</i>)
HP	hydrophobic patch
hpt	hours post-transfection
HRSV	human respiratory syncytial virus (<i>Paramyxoviridae</i>)
HSV	herpes simplex virus (<i>Herpesviridae</i>)
HTLV	human T-cell leukemia virus (<i>Retroviridae</i>)
LB	Lubrol WX
LPC	lysophosphatidylcholine
LsAg	large surface antigen of hepadnaviruses
LUV	large unilamellar vesicle
M β CD	methyl- β -cyclodextrin
MHV	mouse hepatitis virus (<i>Coronaviridae</i>)
MMLV	murine Moloney leukemia virus (<i>Retroviridae</i>)
MOI	multiplicity of infection
MRV	mammalian reovirus (<i>Reoviridae</i>)
MSD	membrane-spanning domain
myr	myristic acid
N	amino terminus
NBV	Nelson Bay virus (<i>Reoviridae</i>)
NDV	Newcastle disease virus (<i>Paramyxoviridae</i>)
NMR	nuclear magnetic resonance
N-NBD-PE	N-(7-nitro-2,1,3-benzoxadiazol-4-yl) phosphatidylethanolamine
NpTNE	NP-40-containing Tris-NaCl-EDTA buffer
N-Rh-PE	N-(lissamine Rhodamine B sulfonyl) phosphatidylethanolamine
OG	octylglucoside
ORF	open reading frame
p14-2HAC	p14 construct with two HA epitopes on the C-terminus
p14-2HAN	p14 construct with two HA epitopes between residues 7 and 8
PA	phosphatidic acid
PBS	phosphate-buffered saline
PC	phosphatidylcholine
PE	phosphatidylethanolamine
PEG	poly(ethylene glycol)
PLAP	placental alkaline phosphatase
PS	phosphatidylserine
RIPA	radio immune precipitation buffer
RRV	reptilian reovirus (<i>Reoviridae</i>)
RSV	respiratory syncytial virus (<i>Paramyxoviridae</i>)
RV	rabies virus (<i>Rhabdoviridae</i>)
S	surface protein of coronaviruses (fusion subunit is S2)
SDS	sodium dodecyl sulfate

SDS-PAGE	sodium dodecyl sulfate polyacrylamide electrophoresis
SE	standard error
SFV	Semliki Forest virus (<i>Togaviridae</i>)
SGL	sphingolipid
SIV	simian immunodeficiency virus (<i>Retroviridae</i>)
SNARE	soluble N-ethylmaleimide-sensitive factor attachment receptor
SsAg	small surface antigen of hepadnaviruses (the fusion subunit)
SUV	small unilamellar vesicle
SV5	simian virus 5 (<i>Paramyxoviridae</i>)
TBEV	tick-borne encephalitis virus (<i>Flaviviridae</i>)
TCA	trichloroacetic acid
TFE	trifluoroethane
TGN	trans-Golgi network
TM	transmembrane protein of retroviruses (fusion subunit)
TMC	transmonolayer or transmembrane contact
TMD	transmembrane domain
TNE	Tris-NaCl-EDTA buffer
TX	Triton X-100
TxTNE	Triton X-100 Tris-NaCl-EDTA buffer
V0	hydrophobic subunit of the vacuolar ATPase pump
VSV	vesicular stomatitis virus (<i>Rhabdoviridae</i>)

Acknowledgements

The efforts of many people contributed to this work; I would like to thank them now.

I would like to thank the following scientific collaborators. Drs. R. F. Epand and R. M. Epand (MacMaster University) collaborated on the study of the p14 fusion peptide and contributed Fig 1.1, 1.2.A-C, and Table 1.1 in Appendix A. Drs. R. Syvitski and D. Jakeman (Faculty of Pharmacy, Dalhousie University) collaborated on the structural determination of the p14 hydrophobic patch motif, and contributed Fig 1.3, Appendix A. Mr. J. Salsman (Duncan lab) collaborated on the study of the cholesterol dependence of the p14 fusion mechanism and contributed Fig 1.4.A-B, Appendix A. Mr. J. Salsman also generously donated the electron micrograph displayed in Fig 7.2.

I would like to acknowledge the generous donation of scientific materials. Dr. W. Ahne (University of Munich) donated the python isolate of reptilian reovirus. Dr. D. Brown (SUNY) donated the PLAP mammalian expression vector. Dr. N. Ridgway (Dalhousie University) donated the N-BP-2 cell line. Dr. M. Shmulevitz (formerly of the Duncan lab) donated the ARV p10-2HAN clone.

I would like express my gratitude to my examining committee. Thanks to Dr. M. Whitt, for agreeing to travel Dalhousie University for my Ph.D. defense, especially as it will entail travel to Canada in December. Much thanks to the committee members, who have provided suggestions, advice, and encouraging words over the years: Dr. D. Byers, Dr. N. Ridgway, Dr. R. Singer, and Dr. D. Stoltz. To Dr. Don Stoltz and former committee member, Dr. Mike Carpenter, thank you both for your encouragement and mentoring of my interest in virology. I hold you both entirely responsible for this foolish graduate school undertaking.

I would also like to acknowledge all the support from members of the department: lab neighbors, the administrative staff (especially Jess!), and Dr. G. Johnston, for his leadership.

It feels like the many years that I have been a Ph.D. student in the Duncan lab have flown by; there are many individuals who have come and gone during that time, and made my graduate school experience a better one. To former members of the lab: Maya, Denisa, Steve, The Boy, Kenny, Paul, Christian – thanks for lots of laughs in the early years. Kenny, a special thanks for your help with the making of the p14-fusion movie. DM, thanks for all the ten minute talks, your quick-witted nature, and mostly, my friends. To the former honours students with whom I was lucky enough to work with: Ryan, Erin, Joanna, Claire, and Julie – thanks for your patience, your enthusiasm for the lab, and really, for teaching me more than I taught you. I remember the year of ‘the girls’ fondly. A special thanks to Ryan for excellent preliminary work on p14-myristylation. Thank you, Jing, for expert technical assistance, exquisite cell culture care, and your ability to work happily with and even organize such a crazy group. It was joyful to work with you, and remember, if you ever tire of working with Roy, just give me a call. Thank you Sam, for endless talks, for sharing in the misery and the joy, and for your friendship. Yo to the

girls, Deniz and Jayme, thanks for your comedic prowess, however unintentional, and for your geeky nature – it is always good to have someone equally geeky to talk to about science. To Roberto, thanks for your intentional comedic prowess and wisdom as a scientist. To Tara1 and Tara2, thanks for joining the crusade of radiation safety, keeping the girls in line, and laughing at my jokes.

To the esteemed leader of the lab, Roy, I run out of words when it comes time to express such a debt of gratitude. As a graduate student supervisor, you are a rare find; your approachability, generosity, sense of humor, enthusiasm for science, and true concern for your students has not gone unnoticed, or unappreciated. Thank you for everything.

The Ph.D. process is a long one. I think graduate students go through stages of Ph.D. ‘growth’ along the way. The first stage involves an all-encompassing enthusiasm for science, non-stop talking about the importance of basic research at parties (when you still go to parties), happily working on weekends, feeling challenged. The second stage involves a dangerous cycle of frustration and anger, love of your research (when you get a good result), then more frustration and anger, then more joy, and so on. The last stage involves months of sitting at home alone in your pajamas at your computer. Thank you to all my friends and family who are not in research, yet put up with these stages.

My family has provided so much encouragement, not only for this latest endeavor, but throughout my life. It is a rare and wonderful thing to know that you have five people that you can depend on, and look up to. My uncle, Father Rocci, is one of the most gentle and caring people I know. My dad can always be counted on for drives, videotaping, rules to live by, and a dry sense of humor. He was the first scientist I ever knew, and the biggest scientific influence in my life. My brother Joe and I share a love of music (though he has all the talent in that regard), but also a love of science and books; his intellect is astounding. My sister, Beth, has a joie de vivre like no one else I have ever met; she has been my best friend, my partner in crime, my enthusiastic supporter, my fun with abandon. My mom is my role model. She is responsible for bringing a shy child out of her shell, with steadfast support and encouraging words. She taught me to write. By example, she taught me not to be afraid of hard work or difficult challenges. I could not have asked for better.

To my second family, Alexis, Peter, Mike, and Kate, thank you for giving me a home away from home, for your kindness, generosity, love, and for Rob. To my husband Rob, you more than anyone know the challenges that come hand in hand with the successes of research. Your unique sense of humor and sense of being drives me nuts and keeps me sane. You are my biggest support; you denounce my enemies with vigor and love my friends. You make everything about my world better.

Chapter 1

Introduction

Overview

Membrane fusion involves the merging of two lipid bilayers and a redistribution of aqueous contents and bilayer components (reviewed in Section 1.1). The fusion reaction proceeds through intermediates in which phospholipids are not arranged in bilayers and monolayers are highly curved. These lipid intermediates are energetically unfavorable, as biological membranes are submitted to strong repulsive hydration and electrostatic barriers. In biological membrane fusion, fusion proteins overcome these thermodynamic barriers.

Biological membrane fusion is both an essential and a tightly regulated process, involved in enveloped virus entry, intracellular vesicle trafficking, fertilization, muscle cell differentiation, and placenta formation (Blumenthal *et al.*, 2003; Jahn *et al.*, 2003). Viral and cellular fusion proteins not only overcome the thermodynamic barrier to membrane merger, but also regulate where it occurs in space and time. Numerous models of protein-mediated fusion suggest that the fusion protein(s) acts as a catalyst to lower the activation energy barrier of unfavorable lipidic intermediates. Other models propose that the fusion protein(s) directly mediates fusion by creating intermediate structures that are comprised of the fusion protein itself. These models (Section 1.2), and membrane fusion proteins from both enveloped viruses (Section 1.3) and cellular systems (Section 1.4) will be discussed.

Select members of the *Reoviridae* family induce cell-cell fusion and multinucleated syncytium formation in infected cells – a very unusual feature for a

nonenveloped virus. These fusion-associated small transmembrane proteins (FAST) are not required for reovirus entry into the cell, and are not essential for the life cycle of the virus. Investigation of these small, unusual, non-essential FAST proteins promises to further our understanding of the minimal structural features of a fusion protein necessary to catalyze the thermodynamically unfavorable process of membrane fusion. In this study, the newest member of the FAST protein family, p14, has been identified and characterized, and a working model of p14-mediated membrane fusion is proposed.

1.1 Membrane fusion in pure lipid bilayers

1.1.A Membrane lipids

Membrane lipids are amphipathic molecules (described in Mathews and van Holde, 1996). Each lipid is comprised of a hydrophilic polar head group and two hydrophobic fatty acid tails. The lipid bilayer is stabilized predominantly by entropy-driven hydrophobic forces that promote the association of the non-polar fatty acid tails (Smith and Haymet, 1993). Van der Waals interactions between the hydrocarbon regions of the molecule act to further promote bilayer formation. The polar head groups associate with water, giving membrane lipids the propensity to form micellar and bilayer structures in an aqueous environment. The acyl chains of lipids can be saturated or unsaturated hydrocarbons; often membrane lipids will have one of each. There are three classes of lipids interspersed with cholesterol in biological membranes: glycerophospholipids, sphingolipids, and glycosphingolipids (Mathews and van Holde, 1996). The structural properties of the different membrane lipids influence their ability to function in biological processes such as membrane fusion.

Glycerophospholipids

The polar head group (R) of each glycerophospholipid contains a phosphorylated glycerol molecule (glycerol-3-phosphate). Two acyl chains are attached to the glycerol. The R group varies, and confers different biochemical and functional properties to different members of this lipid class. Phosphatidic acid is the simplest member of this group; all others are derivatives of this basic phospholipid structure.

Sphingolipids and glycosphingolipids

Sphingolipids are built on the long-chain amino acid sphingosine rather than glycerol-3-phosphate. Fatty acid linkage to the amino group creates ceramide; further modification to the hydroxyl group of sphingosine creates other structurally different lipids: e.g., addition of a phosphocholine group gives sphingomyelin. Sphingosine lipids that contain sugar moieties attached to the sphingosine hydroxyl are called glycosphingolipids.

Cholesterol:

Cholesterol is structurally different from most membrane lipids. It is weakly amphipathic due to its one hydroxyl group on a planar structure of fused cyclohexane (three) and cyclopropane (one) rings. This gives cholesterol a bulky rigid structure, and the addition of cholesterol to membranes tends to add rigidity and disrupt the regularity of the membrane structure.

1.1.B Factors that promote/prevent membrane fusion

The study of membrane fusion in artificial lipid bilayers has led to the identification of some chemical and physical properties of lipids that influence their inherent propensity to fuse. These properties will be introduced below, and expanded on further during the discussion of models of membrane fusion. As well, lipid bilayers in close apposition are subject to a number of opposing forces (Zimmerberg *et al.*, 1993) which will be discussed.

Electrostatic repulsion

Electrostatic repulsion exists between like charges on the polar head groups of membrane lipids. In the case of natural membranes this force is only weakly repulsive (Stegmann *et al.*, 1989).

Van der Waals attraction

When hydrophobic regions of a membrane bilayer are exposed as a result of stress on that membrane, this creates a Van der Waals attractive force between the hydrophobic moieties. This force will promote membrane fusion, but only occurs at interbilayer distances of approximately 1 nm (Helm *et al.*, 1989).

Hydration repulsion

At the interbilayer distances that precede membrane merger (1-3 nm), the major force preventing molecular contact of lipids is hydration repulsion (Rand and Parsegian, 1984). This force arises from the work it takes to remove the shell of water molecules bound to polar head groups. This force is significant at interbilayer distances of 2 nm or less and it increases exponentially as the distance between two opposing membranes decreases (Stegmann *et al.*, 1989). Chemical agents that reduce the hydration repulsion force promote membrane fusion. For example, the divalent cation Ca^{2+} dehydrates the space between phosphatidylserine (PS) bilayers by forming a *trans* complex with the negatively charged phospholipid head group (Zimmerberg *et al.*, 1993). Because of the strong binding affinity of Ca^{2+} for PS, structural water is removed from the membrane surface (Ohki, 1982). Similarly, the polymer polyethylene glycol (discussed below) dehydrates the interbilayer space and promotes close aggregation of lipid membranes (summarized in Lentz and Lee, 1999).

Membrane tension

Strong adhesion between membranes of fixed volume, or cross-linking of vesicles with divalent cations, can increase the surface tension of lipid monolayers and promote fusion (Ohki, 1982; Chanturiya *et al.*, 2000). Bridging the polar groups of adjacent PS together

with Ca^{2+} not only reduces hydration repulsion, but creates stress on the membrane, and causes more hydrocarbons to be revealed to water. The surface tension of the bilayer increases proportionally with the increase in overall hydrophobicity of the membrane surface. Monovalent cations do not cause fusion of PS bilayers as they do not bridge two polar groups to create the requisite membrane surface tension. *In vitro* application of osmotic stress to a liposome membrane to achieve high membrane tension also promotes fusion (Zimmerberg *et al.*, 1993).

Spontaneous/intrinsic curvature

The lipid rearrangements that are believed to occur during the intermediate stage(s) of membrane fusion involve non-bilayer structures. The ability of membrane lipids to form such non-bilayer structures can be predicted by their molecular shape (Cullis *et al.*, 1986; Zimmerberg *et al.*, 1993). Each membrane lipid possesses a different inherent shape, and this shape predicts the propensity of a lipid monolayer to bend. Spontaneous or intrinsic curvature is defined from the perspective of the hydrophobic interior of a membrane bilayer looking out toward the polar headgroups. From this perspective, intrinsic curvature is considered positive when concave, and negative when convex (Blumenthal *et al.*, 2003). The inherent shape of each membrane lipid is based on the volume occupied by its polar head group relative to that of its fatty acid tails (cartooned in Fig 1.1). Cylindrical shaped lipids (phosphatidylcholine or PC) tend to form planar bilayers of negligible curvature. Inverted cone-shaped lipids (lysophosphatidylcholine or LPC) possess a large polar group relative to their hydrophobic base, and prefer to form micellar structures with intrinsic positive curvature. Cone-shaped lipids (phosphatidylethanolamine or PE) have small polar head groups and prefer to form non-

bilayer phases such as inverted micelles and the hexagonal II (H_{II}) phase with spontaneous negative curvature. The process of membrane fusion, in both artificial lipid bilayers and in a biological setting (discussed more below), is sensitive to modulations of lipid composition in a manner that correlates with the spontaneous curvature of the membrane lipids (Roos and Choppin, 1985; Zimmerberg *et al.*, 1993; Epand, 1997). For example, an increased proportion of unsaturated fatty acids, PE, or phosphatidic acid (PA) promotes spontaneous negative curvature and increases fusion, while the addition of LPC promotes positive curvature and inhibits fusion (Zimmerberg *et al.*, 1993; Epand, 1997; Hague *et al.*, 2001).

1.1.C Techniques used to study membrane fusion

The overwhelming problem with the study of the molecular details of the membrane fusion reaction is that it proceeds extremely rapidly (micro-milliseconds; Mayer, 1999; Jahn *et al.*, 2003). To overcome this hurdle, many techniques have been developed for the study of membrane merger *in vitro* using pure phospholipid bilayers as the simplest possible model system. Such model membranes have allowed the identification of individual components and events in the membrane fusion process. Often investigators attempt to slow or stall the membrane fusion reaction to observe the intermediate stages of fusion. As well, biophysicists have inferred the structures of the intermediates predicted to be involved in membrane fusion by theoretical calculation of the energy cost of their formation. Some techniques used to study membrane fusion are discussed below.

Liposomes

The use of artificial membrane vesicles termed liposomes has provided much information regarding how the chemical and physical properties of lipids influence the fusion reaction (Hague *et al.*, 2001). Bilayers in water tend to form spherical vesicular structures in which each monolayer is curved; the amount of curvature depends on both the intrinsic curvature of the constituent lipids and the method used to make the vesicle (sonication, extrusion, vortexing; Epand, 1997, 2003; Lentz and Lee, 1999). Liposomes are created to have different diameters: small unilamellar vesicles (SUVs) are 20 - 100 nm in diameter and are created by sonication that introduces energy into the liposome. SUVs possess a high degree of positive curvature in the outer monolayer and negative curvature in the inner monolayer. The high stress and high energy of these vesicles makes them very fusogenic in response to small perturbations (peptides, cations, PEG; Blumenthal *et al.*, 2003). Large unilamellar vesicles (LUVs; 100-500 nm in diameter) are more stable and more accurately estimate parameters that affect cell-cell fusion. One of the great advantages of such artificial systems is that the composition of the liposome can be varied, and the effect of lipid composition on membrane fusion assessed. Lipid vesicles are often treated with potential fusogens (chemical, proteinaceous) to study the effect of various conditions on the fusion process (Epand, 1997, 2003; Lentz and Lee, 1999).

Planar phospholipid bilayers

The deposition of a lipid bilayer onto a flat surface creates a way to study membrane fusion in a more stable bilayer system and gives a close approximation of a cell membrane. Fusion of phospholipid vesicles to planar phospholipid membranes (Chanturiya *et al.*, 1997, and references therein) mimics the fusion of an exocytic vesicle

with the plasma membrane or an enveloped virus with the host cell membrane. This technique has also been used to study the early steps in fusion pore formation using electrophysiological measurements of ion conductance across the bilayer (Epad, 1997; Chanturiya *et al.*, 1997).

Cation (Ca^{2+})-induced fusion of anionic (PS) lipid vesicles and acid-induced fusion of PE lipid vesicles

Three steps have been identified in the membrane fusion process: aggregation, membrane destabilization, and fusion. When the above approaches are used to study the steps of membrane fusion, the aggregation and destabilization steps cannot be distinguished. For example, calcium induces interbilayer dehydration required for liposome aggregation and the membrane tension that is needed for outer leaflet destabilization. Thus, though these assays have in the past been very useful (Okhi, 1982; Ellens *et al.*, 1985), they will not be discussed further.

Polyethylene glycol (PEG)-induced liposome aggregation

PEG is a hydrophilic polymer that dehydrates membrane surfaces, forcing close contact between membranes and causing aggregation of liposomes and cells (Arnold *et al.*, 1983). PEG induces near molecular contact between opposing membranes, but does not modify the bilayer sufficiently to induce fusion (Lentz and Lee, 1999). Aggregated liposomes do not fuse unless the bilayer is disrupted (Lentz *et al.*, 1992), similar to what has been observed for cellular fusion (cells 2-3 nm apart do not fuse). However, PEG-aggregated phospholipid vesicles do fuse if the lipid packing density of the outer leaflet is altered (Lee and Lentz, 1997b). This can be achieved by high intrinsic negative curvature, acyl chain unsaturation in fusion-prone SUVs, small amphipathic peptides, or other

factors that promote imperfect outer leaflet packing (Lentz and Lee, 1999). Thus PEG has been used extensively to help understand the factors that allow two opposing lipid membranes to progress from close apposition to fusion.

Assays to detect membrane fusion

Membrane fusion is measured by assays that detect both the merging of lipid bilayers and luminal continuity that accompanies merger of opposing membranes (Blumenthal *et al.*, 2003). The assays have the advantage of being quantitative as well as qualitative.

Lipid mixing

Lipid-mixing assays assess when two lipid bilayers have merged and the lipids within those bilayers begin to intermix. These assays can be used in artificial lipid systems (Struck *et al.*, 1981) or to monitor fusion of biological membranes (Hoekstra *et al.*, 1984). Lipid-mixing assays are based on the following principle. One population of cells/liposomes is labeled with either a self-quenching concentration of a fluorescent dye conjugated to a saturated hydrocarbon chain (e.g., octadecyl Rhodamine B chloride [R18]) or with two fluorophores, an energy donor and energy acceptor (e.g., N-[7-nitro-2,1,3-benzoxadiazol-4-yl] and N-[lissamine Rhodamine B sulfonyl], respectively) coupled to the free amino group of phosphatidylethanolamine for incorporation into the lipid bilayer. In the latter scenario, the emission band of the energy donor overlaps with the excitation band of the energy acceptor. At high concentrations, the energy from a photon absorbed by the energy donor is transferred to the energy acceptor, which fluoresces as a result. These labeled membranes are then mixed with a population of unlabelled cells/liposomes. Upon dilution of the R18 probe during fusion between labeled

and unlabeled membranes, there is a time-dependent enhancement of fluorescence intensity. For the resonance energy transfer system, the increase in fluorescence emission for the energy donor is linearly proportional to the amount of membrane mixing.

Lipid-mixing assays are widely used to study fusion in many systems. Disadvantages of this approach include high background fluorescence and the fact that redistribution of lipid probes can signify either complete fusion or hemifusion, where only two contacting monolayers have merged. Advantages of this system include sensitivity and the fact that R18 will spontaneously insert into membranes, allowing labeling of biological membranes (Blumenthal *et al.*, 2003).

Content mixing

Content-mixing assays monitor the mixing of aqueous contents of liposomes/cells. Liposome:liposome fusion assays often use the fluorophore 1-aminonaphthalene-3,6,8-trisulfonic acid (ANTS) and its quencher N,N'-p-xylylenebis(pyridinium bromide) (DPX). In the ANTS/DPX assay, ANTS is encapsulated in one population of liposomes and DPX in the other; when fusion occurs and luminal contents of the liposomes intermix, this results in the quenching of ANTS fluorescence (Ellens *et al.*, 1985). The linkage of fluorophores such as fluorescein isothiocyanate or tetramethylrhodamine to a high-molecular-weight dextran followed by entrapping dextrans at self-quenching concentrations provides another popular marker (Stutzin, 1986; Epand *et al.*, 1999). Loaded liposomes can then be assessed for fusion with empty liposomes or cells by measuring the dequenching of the fluorescence that occurs as the labeled-dextran is diluted.

Electrophysiological approaches

Electrophysiological measurements are able to detect the opening of fusion pores less than 2 nm in diameter with millisecond resolution. Whole-cell capacitance measures the change in the capacitance of a cell (normally constant) when it increases as a result of an increase in surface area. These measurements depend upon ion gradients across the membrane being measured, and thus slow fluctuating alterations in capacitance suggest small pore opening and closing (Zimmerberg *et al.*, 1993). The conductance of a fusion pore can be calculated from such electrical measurements of cells or planar lipid bilayers. The early stages of fusion pore formation can also be assayed by measuring the passage of hydrogen ions through a fusion pore from an unlabelled population of liposomes prepared at low pH into a population of liposomes that has entrapped the fluorophore 8-hydroxy-pyrene-1,3,6-trisulfonic acid (HPTS). The fluorescent intensity of HPTS decreases at low pH, and the decrease is proportional to the amount of hydrogen ion movement between two vesicles and is thus an indicator of fusion-pore formation (Lee and Lentz, 1998).

Electron microscopy

Electron microscopy as a tool to study membrane fusion is limited due to the rapidity of the reaction, but does remain an important tool to distinguish real fusion (indicated by lipid mixing) from vesicle disintegration (Blumenthal *et al.*, 2003).

1.1.D Membrane fusion of pure lipid bilayers

Despite extensive study of membrane fusion *in vitro* and *in vivo*, the lipid rearrangements that need to occur in order to merge two bilayers, and the nature of the intermediate

structures in the fusion reaction, remain a matter of debate. Several theories about the nature of membrane fusion in pure lipid bilayers are discussed below.

The original stalk model of membrane fusion

Biological membrane fusion is believed to proceed through lipidic intermediate structures; thus pure lipid bilayers have been used to estimate and investigate such structures (Lentz and Lee, 1999). The most widely accepted model of the lipid rearrangements that occur during the fusion reaction derives from the original theory proposed by Kozlov and Markin (1983 [in Russian]; summarized in Kozlov *et al.*, 1989; Zimmerberg *et al.*, 1993; Blumenthal *et al.*, 2003; illustrated in Fig 1.2.A). This theory suggests that if the hydration repulsion force is overcome, two bilayers in close apposition fluctuate, and rather than remaining bilayer structures, the contacting outer monolayers merge to form a stalk. The 'stalk' joins the lipid components of the outer leaflets of the two bilayers; the merger of these outer leaflets is termed hemifusion. Hemifusion is defined as the merger of contacting monolayers without merger of inner monolayers or fusion pore formation (Blumenthal *et al.*, 2003). The net curvature of the stalk structure (Fig 1.2.A) is negative, so the formation of this intermediate should be favored by lipids with negative intrinsic monolayer curvature in the contacting leaflets (Zimmerberg *et al.*, 1993). In the stalk structure the inner monolayers are not merged, and thus continuity between the two aqueous compartments is prevented. Subsequent to its formation, the stalk is proposed to widen, forming a second intermediate called the hemifusion diaphragm/septum or trans-monolayer (or trans-membrane) contact (TMC; Siegel, 1999). Rather than form an extended septum, this intermediate ruptures into a

fusion pore. In this environment, the formation of a fusion pore is promoted by lipids of positive spontaneous curvature in the inner leaflet (Kozlov *et al.*, 1989) and by factors that increase membrane tension. Thus, membranes with outer leaflets comprised of negative spontaneous curvature and inner leaflets with positive curvature are optimal for fusion according to the stalk model (Zimmerberg *et al.*, 1993).

Evidence from in vitro fusion systems that supports the stalk model

Lentz and co-workers have made significant contributions to the study of membrane fusion in pure bilayer systems using PEG-aggregated small unilamellar phospholipid vesicles (SUVs) (summarized in Lentz and Lee, 1999). In their experiments, PEG is used to dehydrate the interbilayer space and bring SUVs into near molecular contact. However, close contact between bilayers is not sufficient to induce fusion (Massenburg and Lentz, 1993); fusion requires packing disruption of the outer leaflets of contacting bilayers (Lee and Lentz, 1997b; Talbot *et al.*, 1997). Perturbation of a vesicle with phospholipase A2 (which hydrolyzes a small amount of lipid from outer leaflet of SUV) or cardiolipin (a diphosphatidylglycerol molecule which induces negative spontaneous curvature due to its molecular shape) produces an imbalance in membrane lipid packing and induces fusion of PEG-aggregated vesicles (Lee and Lentz, 1997b). LPC addition to the outer leaflets of these vesicles reverses fusion, whereas the presence of LPC in the inner leaflet has no effect (did not encourage or discourage fusion; Lee and Lentz, 1997b). Unsaturated fatty acid tails also promote fusion. These studies are consistent with the stalk as a lipidic intermediate in the fusion reaction and hint that the stalk structure

may be the high-energy intermediate, the formation of which requires large activation energy.

A three-step mechanism for PEG-mediated phospholipid vesicle fusion was proposed by Lee and Lentz (1997a): (1) the formation of a reversible intermediate that consists of a dynamic mixture of two unstable forms, a hemi-fused stalk and a transient small fusion pore (which at this stage both can still revert to the prefusion state); (2) the stalk matures to a semi-stable hemifusion septum; and (3) irreversible formation of the fusion pore occurs when the septum widens and becomes unstable. By measuring lipid probe and proton redistribution between phospholipid vesicles, these authors determined the time course, rate, and activation energy of each step (Lee and Lentz, 1997a; Lee and Lentz, 1998). The activation energies for the first and last steps of the process are similar to those observed in protein-mediated fusion systems (discussed below in Section 1.2), suggesting that merger of the outer leaflets precedes merger of the inner leaflets, consistent with the stalk model. The formation of a hemifusion intermediate prior to complete fusion has also been observed experimentally in other protein-free systems (Chernomordik *et al.*, 1995a; Chanturiya *et al.*, 1997). As well, other investigators used proton transfer to show that fusion-pore flickering occurs in pure lipid bilayer systems, suggesting that pore flicker does not result from the formation of a proteinaceous channel (discussed in Section 1.2). This observation further supports the assertion that membrane fusion proceeds through a stalk-like hemi-fused lipidic structure.

The energy cost of stalk formation

Both theoretical calculations and experimental evidence suggest that the stalk structure is a high-energy intermediate of the membrane fusion reaction, likely to have a free energy substantially larger than that of the pre-fusion state (stable lipid bilayers; Kozlovsky and Kozlov, 2002; Epand, 2003). Theoretical estimates of this energy consider two major contributions to the energy of the stalk: (1) the bending of planar monolayers into non-planar structures; and (2), the formation of a void space in the stalk structure created by the unequal bending of outer *versus* inner leaflets (Fig 1.2.A.; Siegel, 1993). The energy cost of bending depends on the spontaneous curvature of the bilayer, while the energy cost of the void space produced by this structure is based on the predicted surface area of the void. Based on these theoretical calculations, the free energy of the stalk was estimated to be so large (150-200 kT) that it was questioned whether this structure could form during the fusion process (Siegel, 1993, 1999).

Resolution of the energy crisis of the stalk

Kozlovsky and Kozlov (2002) propose an alteration of the stalk structure that deals with this energy crisis (Fig 1.2.B). Their new theoretical model is based on lipid tilt and oblique packing of hydrocarbon chains with respect to the membrane. The free energy of the stalk structure is estimated by theoretically calculating the energy needed to bend planar monolayers so sharply that they accommodate the formation of a stalk structure without creating any void space. This requires that individual lipid molecules that comprise the stalk have to tilt relative to the plane of the bilayer, expose hydrophobic regions to water, and elongate acyl chains. This tilting of lipids occurs at an energy cost,

which is theoretically calculated from experimental data on the phase transition of lipids from bilayer to non-bilayer structures. In this calculation, the energy of the stalk is estimated without any assumption of void space, creating the new stalk structure shown in Fig 1.2.B (Kozlovsky and Kozlov, 2002). This more realistically shaped stalk has considerably lower energy relative to that of planar bilayers (45-50 kT for monolayers with low spontaneous curvature) that can even become negative for bilayers of substantial negative intrinsic curvature. In this new theoretical model, the overall area of the stalk structure is reduced. As depicted, the modified stalk fulfills the definition of both a stalk and a hemifusion diaphragm at the same time (Fig 1.2.B). With the very first merger of the outer leaflets of two fusing bilayers, the inner monolayers are already deformed so that they touch one another (as previously described for the hemifusion diaphragm/TMC; Kozlovsky and Kozlov, 2002).

Experimental observation of a stalk-like structure

The unstable and highly transient nature of lipidic intermediates of membrane fusion has made their direct observation difficult; thus, the lipid rearrangements have been inferred from theoretical calculations. Yang and Huang (2002, 2003) present the first direct observation of a stalk structure to validate these theoretical models. Diphytanoyl phosphatidylcholine (DPhPC; a lipid with negative spontaneous curvature) bilayers were spread on a flat substrate and exposed to high humidity; under these conditions the lipid formed a stack of parallel bilayers (3.5 nm thick) intercalated with water layers (1 nm thick). Direct dehydration was used to induce contact between two apposing bilayers. When the relative humidity was reduced to 70-80%, point contacts occurred between

bilayers, and the two contacting monolayers merged into a stalk-like structure in a regular three-dimensional pattern. This regular array allowed the authors to use crystallographic techniques to determine the three-dimensional structure of the stalk-like structure at low resolution. Further reduction in humidity gave a diffraction pattern consistent with the inverted hexagonal (H_{II}) phase of lipids, confirming speculation that the stalk was an intermediate state between the lamellar and H_{II} phases. These studies provide the first experimental confirmation of the stalk hypothesis of membrane fusion and suggest that the stalk structure is the natural consequence of molecular contact of two bilayers with sufficient spontaneous negative curvature. Further study by Yang *et al.* (2003a) determined that the stalk-like structure also exists in lipid mixtures of dioleoylphosphatidylcholine (DOPC) and dioleoylphosphatidylethanolamine (DOPE), but that this intermediate phase between lamellar and H_{II} exists only for a certain range of spontaneous negative curvature (ratio of DOPC:DOPE must not exceed 1:2). The observation of a distorted hexagonal phase in the multi-component lipid bilayers also implies that lipid components may adjust their local concentrations to alter local spontaneous curvature in a manner that allows the minimal energy structure to form. This suggests that perhaps the energy of membrane fusion intermediates may be lower than calculated theoretically, as spontaneous curvature may not be a constant in a mixed monolayer. In a biological situation, this implies that the local adjustment of membrane lipid composition (by lipid diffusion or flip-flop) may have a significant fusion-promoting effect.

1.2 Biological membrane fusion

1.2.A Biological membranes

Biological membranes are inherently stable, composed of a complex mixture of lipids that provide plasticity and adaptability to the environment (Stegmann *et al.*, 1989; Blumenthal *et al.*, 2003). Different cell types contain different proportions of each lipid molecule, giving function-specific roles to membranes for many cell types. This has important implications for processes such as cell signaling, membrane permeability, and membrane fusion. Biological membranes are also asymmetric. Generally, the extracellular leaflet of a plasma membrane or the luminal leaflet of an organelle membrane is rich in lipids with zero intrinsic curvature (phosphatidylcholine, sphingomyelin), while the cytosolic leaflet is comprised of lipids with intrinsic negative curvature (phosphatidylethanolamine, phosphatidylserine). Glycolipids such as glycosphingolipids are found in the outer leaflet of the plasma membrane (Mathews and van Holde, 1986). This distribution results in a cell membrane that is highly stable, and a cytoplasmic vesicle that is fusion-prone. In addition, the cell surface is decorated not only with glycolipids, but also with glycoproteins that together form a hydrated glycocalyx estimated to be 30-40 nm thick, preventing the aggregation of two opposing cell membranes (Springer, 1990). However, on the basis of electron microscopy we know that cell membranes must come into close contact for fusion to occur (Knutton and Pasternak, 1979). Even upon dehydration, the large size of cell surface structures such as adhesion molecules that project perpendicularly from the cell surface (ranging in size from 5-30

nm; Springer, 1990) also prevents the close molecular contact that must precede fusion. Despite this, intermembrane distances vary depending on the site of the cell surface, and can decrease to approximately 3-7 nm for point contacts of microvilli and gap junctions (Springer, 1990, and references therein).

1.2.B Biological membrane fusion

It is a generally accepted belief that biological membrane fusion is protein-mediated. What, then, is the role of the fusion protein? Fusion proteins provide specificity to the membrane fusion reaction, and limit its occurrence in time and space (Blumenthal *et al.*, 2003). Fusion proteins are often involved in mediating close apposition of two membranes. Fusion proteins reduce the energy barrier that prevents membrane fusion, a barrier that appears to be higher in a biological system than in a pure lipid bilayer. How fusion proteins do this remains a mystery. Do these proteins lower the activation barrier to fusion because they raise the energy of the reactants by destabilization of the prefusion bilayers, or do they lower the energy cost of the intermediate state(s) in the fusion reaction? For viral membrane fusion, it has been suggested that triggered conformational alterations in fusion protein structure provide energy to drive the membrane fusion reaction (Carr and Kim, 1993; Weissenhorn *et al.*, 1999). If so, how is this conformational energy captured, or if fusion proteins can lower the activation energy barrier that prevents the membrane fusion reaction, is a direct input of energy even required (Epanand, 2003)? Finally, do fusion proteins act like catalysts, by promoting the formation of lipid-based structures that precede membrane merger, or do they play a direct role in forming the fusion pore structure? The discussion that follows attempts to

answer some of these questions by illustrating current models of protein-mediated fusion. Though the focus of this discussion is the catalytic role of fusion proteins and how they mediate the lipid rearrangements that precede membrane merger, evidence that suggests fusion proteins are directly required for the formation of a proteinaceous fusion pore will also be discussed. In sections 1.3 and 1.4, the fusion proteins that mediate this reaction will be examined in more detail. This discussion is intended to provide sufficient background information regarding protein-mediated membrane fusion to allow the reader to appreciate the unique nature of the reoviral FAST protein family member named p14.

1.2.C The fusion pore is a fluctuating lipid junction between two lipid bilayers held in place by a protein scaffold

Fusion of pure lipid bilayers is similar to biological fusion

Lee and Lentz (1998) used PEG-mediated fusion of pure lipid bilayers to study the kinetic steps of the membrane fusion process and determine the activation energy associated with each step. They determined the activation energy for the creation of the stalk intermediate to be 37 kcal/mol; this value is very similar to that calculated for the process of fusion between vesicular stomatitis virus (VSV) and erythrocyte ghosts (42 kcal/mol; Clague *et al.*, 1990). The series of kinetic steps of fusion in a pure bilayer system are the same as those for biological fusion: the formation of an initial, transient fusion pore, redistribution of lipid indicating hemifusion, and redistribution of small, then large, aqueous compartment markers (Zimmerberg *et al.*, 1994; Blumenthal *et al.*, 1996; Lee and Lentz, 1997a, 1998; Chanturiya *et al.*, 1997; Leikina and Chernomordik, 2000;

Frolov *et al.*, 2000). In PEG-aggregated model membranes, fusion will not proceed until the activation energy barrier that prevents merger is lowered, often by raising the energy of the prefusion state through altered bilayer curvature (Lee and Lentz, 1997b). As with fusion of pure lipid bilayers, membrane curvature also affects protein-mediated fusion; it is inhibited by the addition of lysophosphatidylcholine to the outer leaflet and promoted by oleic acid (a *cis*-unsaturated fatty acid with negative intrinsic curvature; Chernomordik *et al.*, 1999). The activation energy of the third step in membrane fusion of model membranes, fusion pore formation, was calculated by Lee and Lentz (1998) to be 22 kcal/mol, whereas Oberhauser *et al.* (1992) calculated the energy of this process for secretory granule release as 23 kcal/mol. This correspondence again argues that fusion pore formation proceeds by the same lipidic rearrangement in both systems.

Influenza hemagglutinin is a prototype fusion protein

Since the determination of the influenza virus membrane fusion protein, hemagglutinin (HA) structure to a resolution of 3 Å in 1981 (Wilson *et al.*, 1981), many of the detailed models of protein-mediated membrane fusion are based on the study of HA. Though this protein and its components that contribute to membrane fusion activity are discussed in greater detail in Section 1.3, along with other examples of viral fusion proteins, it is introduced here to discuss HA-mediated membrane fusion models.

The HA protein is a trimeric Type I integral membrane glycoprotein embedded in the influenza virus lipid envelope. Each trimer consists of three copies of two disulfide-linked subunits: HA1, the receptor-binding domain, and HA2, the fusion domain. HA at neutral pH (Wilson *et al.*, 1981; shown in Fig 1.3.A, C) was crystallized without its

transmembrane and cytoplasmic domains. The HA trimer extends 130 Å perpendicularly from the virus envelope. The stalk of the structure is comprised of a triple-stranded α -helical coiled coil that stabilizes the trimer (HA2), while the HA1 domain forms a globular β -structured head (pictured in Fig 1.3.C). In its neutral pH form, the three N-terminal fusion peptides of HA2 are buried in the trimer interface 35 Å from the viral membrane. In the acid-exposed HA (lacking the transmembrane and cytoplasmic domains and the N-terminal HA2 hydrophobic fusion peptide), the coiled-coil stalk has extended and the fusion peptide is extruded from its buried location; it is believed to interact with either the target cell membrane or the viral envelope (Bullough *et al.*, 1994; shown in Fig 1.3.B, C). The refolding reaction of HA, as inferred from crystallographic structures, occurs as follows (Bullough *et al.*, 1994; Chen *et al.*, 1999; Tamm, 2003). The anti-parallel helices that lie on the outside of the native structure are connected by long loops to the N-terminal end of the central coiled coil dissociate and extend the central coiled coil. The N-terminal half of the central coiled coil remains intact while the C-terminal region (proximal to the viral envelope) is reorganized and turns 180° to pack in anti-parallel fashion against the central coiled coil. These two conformational changes result in a redirection of the N- and C-termini of HA2 from the bottom to the top of the coiled coil, where they interact to form a cap structure (Chen *et al.*, 1999; compare Figs 1.3.A and B).

Cast-and-retrieve model

This model suggests that the HA protein uses membrane anchors in both the viral envelope (the transmembrane domain) and the target cell membrane (the fusion peptide)

to bend the two opposing membranes (Zimmerberg *et al.*, 1993). Membrane tension becomes so large that it is more energetically favorable for these two opposing membranes to merge into a stalk structure than to remain as closely opposed highly curved bilayers. In the prefusion state, the two membranes are at a minimum of 130 Å apart (the height of the HA molecule). Upon exposure to low pH, the fusion peptides are released from their buried position. The fusion peptide region (to be discussed further in Section 1.3.D) is 20 amino acids in length; however, the 15 amino acids C-terminal to the hydrophobic peptide are believed to form a β -structured tethering sequence. Taken together, these 35 amino acids can extend, at maximum, a distance of 119 Å (axial length of 3.4 Å per residue) from its original location in the native structure (35 Å above the surface of the viral membrane; Wilson *et al.*, 1981) (summarized in Zimmerberg *et al.*, 1993). The fusion peptide (100 Å away) is within reach of the target membrane, where it is proposed to insert. The interaction of the fusion peptide with the membrane is thermodynamically favorable, releases energy, and causes secondary structural alteration of the N-terminal 21 amino acids into an α -helix. The discrete structural alteration of these 21 amino acids from an extended form to an α -helix causes a contraction of 40 Å, and exerts a bending force on the target membrane. If the fusion peptides of several HA trimers act in concert, the force generated could pull the target membrane 30-40 Å closer to the viral envelope. The tension of the fusion peptide as a result of this contraction could force the HA molecules to tilt outward, in turn bending the viral envelope outward toward the target membrane. According to this model, the curvature of both membranes (in the area encircled by the HA proteins) becomes so great that it is more favorable for

the two membranes to interact, thereby relieving the membrane tension that results from such extreme bending of bilayers (Zimmerberg *et al.*, 1993).

Spring-loaded model

Since the determination of the acid-exposed HA structure, extensive study on the role of the conformational rearrangement of HA has attempted to couple protein structural remodeling with the lipid rearrangements that occur during membrane fusion. The spring-loaded model has become widely accepted; it suggests that the native form of HA is a kinetically trapped metastable structure (Carr and Kim, 1993; Weissenhorn *et al.*, 1999; discussed further in Section 1.3.B). This model is based on a spring-loaded mechanism because the prefusion structure of HA is primed for a conformational rearrangement that leads to membrane fusion (Eckert and Kim, 1997). When exposed to acidic pH, metastable HA undergoes triggered structural alteration to the low energy form crystallized by Bullough *et al.* (1994) and Chen *et al.* (1999) (sometimes referred to as the six-helix bundle). In this model, structural rearrangement of HA achieves the following: (1) the previously buried fusion peptide is repositioned 100 Å by extension of the central coiled coil at the N terminus and is believed to interact with the target membrane; (2) the C-terminal α -helical region refolds and makes a 180° turn that reorients the remaining C-terminal helices antiparallel to the central coiled coil (Fig 1.3.A-C). These two changes generate the low energy form of HA and place the fusion peptide and transmembrane anchor at the same end of the molecule. The energy provided by the 2nd conformational alteration of the HA trimer (reorientation of the C-terminal helix-hinge) is believed to mechanically pull the two membranes close enough together

that the stressed bilayers will first form a stalk, followed by a fusion pore. Due to the high-energy barrier that prevents membrane fusion, this model suggests that the cooperation of several HA trimers recruited to the fusion site will be required. If these conformational rearrangements pull the two membranes together, the interbilayer distance would be reduced from 130 Å to 15 Å (the diameter of a triple-stranded coiled coil), overcoming much of the hydration repulsion force and creating surface membrane tension to promote lipid rearrangement (Weissenhorn *et al.*, 1999). The central dogma of this model, that the acid-induced conformational change of HA, through the formation of extensive coiled coils, can release adequate free energy to overcome the barriers to membrane fusion (Blumenthal *et al.*, 2003), is discussed further in Section 1.3.B.

Dimple model

Kozlov and Chernomordik (1998) suggest a mechanism by which the acid-induced conformational change of the HA trimer mediates the release of the fusion peptide, which then inserts into the viral envelope, not the target cell membrane. Thus, the conformation of HA that is usually considered to be inactive is of primary importance in this model. Extension of the HA coiled coil pulls on the inserted fusion peptide (similar to that proposed in the ‘cast-and-retrieve’ model, except that the fusion peptide is embedded in a different membrane) and causes the membrane surrounding each HA trimer to bend in a saddle-like shape. To minimize membrane tension, the HA-containing membrane elements cluster into a ring. The cooperative effect of a ring of HA molecules provides sufficient pull to the HA-containing membrane that the protein-free membrane central to the protein ring responds to the membrane bending stresses by inducing outward

dimpling of the viral envelope or the HA-expressing membrane. The growth of this membrane dimple toward the target membrane provides close contact between opposing membranes. The top of the dimple is a region of highly stressed membrane with considerable curvature; bending stresses at the top of the dimple facilitate stalk formation as the dimple reaches the opposing membrane. This model provides the link missing in other models of protein-mediated fusion by directly coupling protein structural remodeling with the rearrangement of lipid bilayers. Because the HA molecules are excluded from the top of the dimple, the fusion reaction proceeds by the same lipid rearrangements observed in protein-free bilayers (Chernomordik *et al.*, 1999).

Hydrophobic defect

In a variation on the theme of the dimple model, Bentz (2000a) suggests that the conformational change of HA is coupled with the formation of a hydrophobic defect in the viral or HA-expressing membrane. Thus, fusion peptides that insert in the viral envelope are considered in this model. After insertion, extension of the central coiled coil extracts the fusion peptide from the outer monolayer of the viral envelope and redirects it 100 Å towards the target membrane, where it embeds. For an isolated HA molecule, the hydrophobic defect created in the outer leaflet of the viral envelope will be quickly filled by lipid diffusion. For those fusion peptides in a group of HA molecules, the aggregated transmembrane domains will restrict lipid flow (restricted hemifusion; Chernomordik *et al.*, 1998; Leikina and Chernomordik, 2000), creating a hydrophobic defect that exposes both lipid acyl chains and non-polar residues of HA transmembrane anchors to water (Bentz, 2000a). As the defect cannot be relieved by recruitment of lipid from the viral

membrane, lipid from the outer monolayer of the opposing target membrane is recruited, creating the first fusion intermediate, a stalk. The fusion peptides embedded in the target membrane may facilitate this process. This model proposes that fusion will not progress without a sufficiently large aggregate of HA molecules at the site of initiation because the transmembrane domains of HA are required to restrict lipid flow into the hydrophobic defect.

The hydrophobic defect model shares some similarities with the dimple model proposed by Kozlov and Chernomordik (1998; also described in Chernomordik *et al.*, 1999). However, the dimple model does not describe a role for the state of restricted hemifusion, deemed as the necessary precursor to fusion pore formation, while unrestricted hemifusion represents a dead-end pathway (Chernomordik *et al.*, 1998; Leikina and Chernomordik, 2000). Nonetheless, the two models are not mutually exclusive and can be combined as follows. Insertion of the HA fusion peptide into the viral membrane, and subsequent coiled-coil rearrangements of HA cause the central membrane to dimple outward (Kozlov and Chernomordik, 1998), after which the ring of HA molecules at the site of dimpling will tighten and restrict lipid flow to the central membrane. At this point, the dimple can no longer grow outward, and the tension of the coiled coils pulling on the fusion peptides will extract a proportion of the hydrophobic peptides from the viral membrane, resulting in their insertion into the target membrane (Bentz, 2000a). A stalk could then form from the combination of the incomplete membrane dimple and the hydrophobic void that recruits lipids from the target membrane to heal the defect (Bentz, 2000a).

1.2.D A transient protein fusion pore is followed by a lipidic pore

HA- or influenza virus-mediated fusion is preceded by the formation of small transient pores in the target membrane (less than 26 Å in diameter, not large enough to allow passage of 3-kDa dextran; Bonnafeous and Stegmann, 2000). These small pores persist after pH neutralization (designed to stop the acid-induced conformational rearrangement of HA) and stay open for minutes to hours, suggesting that they are proteinaceous (Stegmann, 2000). In the model, Bonnafeous and Stegmann (2000) propose that these initial fusion pores form anywhere in the target membrane and are comprised of a cluster of HA fusion peptides. Upon further aggregation of HA molecules and complex formation, a larger pore forms that allows leakage of dextran molecules out of the target liposome. When 'leakage pores' come into contact with the viral/HA-containing membrane, fusion is initiated. It is suggested that the edge of the expanding pore in the target membrane contains exposed hydrophobic regions that are thermodynamically unfavorable, and thus the leakage pore recruits lipid from the outer leaflet of the viral membrane. From here, membrane fusion proceeds according to the stalk model, beginning with the formation of a hemifusion diaphragm (Bonnafeous and Stegmann, 2000).

The evidence in support of the formation of a transient proteinaceous pore also supports the suggestion that fusion proceeds through lipidic rearrangements that are restricted by a ring of HA molecules. This state has been termed restricted hemifusion, and is defined as an absence of lipid mixing or fusion-pore formation that can be revealed

by transformation into complete fusion when treated with certain amphipathic molecules or hypotonic shock (Chernomordik *et al.*, 1998; Chernomordik *et al.*, 1999; Leikina and Chernomordik, 2000). Restricted hemifusion, and hemifusion in general, is not expected to result in the leakage of target liposomal contents that was observed (Stegmann, 2000; Bonnafous and Stegmann, 2000), supporting the assertion that early pores may be proteinaceous. Conversely, the kinetic steps of membrane fusion described for pure lipid bilayers also include the occurrence of small transient pores before lipid mixing or content mixing are observed (Lee and Lentz, 1997a), indicating that early pores may be lipidic in nature.

1.2.E The fusion pore is proteinaceous until lipid is recruited to break the protein ring

Most theories relating to the intermediates in membrane fusion propose that such intermediates are mediated, either exclusively or predominantly, by lipidic structures. However, a recent study using a candidate cellular fusion protein implicated in yeast vacuolar fusion has revitalized debate over whether the central intermediates in the fusion reaction are lipidic or proteinaceous. This candidate fusion protein is V0, the hydrophobic subunit of the vacuolar ATPase (Peters *et al.*, 2001). V0 is a proteolipid, a protein that can be extracted along with membrane lipids into chloroform-methanol (Zimmerberg, 2001). The model proposes that dimerization of two *trans* V0 complexes in opposing vacuolar membranes forms a gap-junction-like structure, which then opens radially to allow the inclusion of lipid molecules into the pore. Models of fusion based on HA and other viral proteins do not support this new model. It is difficult to imagine how the

transmembrane domains of HA and other fusion proteins would form a pore/channel; not only do these sequences lack any channel-forming motif, but the amino acid sequences of the transmembrane domains of viral fusion proteins (both within and between viral families) are variable. GPI-linked HA that lacks a transmembrane anchor is unable to mediate complete fusion (see Section 1.3.C), yet still causes the formation of small transient pores that are experimentally similar to those formed by authentic HA. Furthermore, the conductance of the initial fusion pores in both protein-mediated fusion and pure lipid bilayers varies greatly. In contrast, proteinaceous pores would be expected to have more fixed conductance levels due to uniform pore size.

1.2.F Summary of models

From the preceding discussion of various models of protein-mediated fusion in biological systems, the predominant role of a fusion protein emerges as a membrane-merger catalyst, unlikely to be a direct component of the membrane fusion intermediate state (e.g. fusion pore). Membrane fusion proteins are clearly believed to alter the activation energy barrier that prevents spontaneous membrane merger, but how this is accomplished (by altering the energy of the lipidic intermediates of fusion or by direct input of energy) is still a matter of debate. As the majority of the models discussed here were based on the viral fusion protein, HA, (with the exception of the protein pore model, based on V0), a comparative evaluation of other fusion proteins is warranted. The following two sections therefore discuss important components of both viral (Section 1.3) and candidate cellular (Section 1.4) membrane fusion proteins to broaden a perspective of how membrane

fusion proceeds in all biological systems. This study will then contrast the features of these membrane fusion proteins with those of the FAST protein p14.

1.3 Fusion proteins encoded by enveloped viruses

1.3.A An introduction to viral fusion proteins

All enveloped viruses encode a membrane fusion protein(s) that is embedded in the viral envelope. These proteins are essential for the virus life cycle, as they are responsible for mediating effective entry of the virus particle into the host cell. Penetration of the host cell membrane occurs by membrane fusion of the viral envelope with the plasma or endosomal membrane. The membrane fusion activity of these proteins must be tightly controlled to ensure that the fusion process occurs at the right time and in the right place (White, 1990). Thus, fusion proteins are activated by triggers such as receptor binding, co-receptor binding, and/or endosomal acidification. For the remainder of this review, the precise regulation of these proteins and their importance in the virus life cycle will be ignored. Instead, the discussion will focus on the properties of these proteins that play important roles in the ability to facilitate membrane merger.

Viral fusion proteins have been classified into different groups predominantly on the basis of their structure. Those fusion proteins for which detailed structural information is lacking are classified on the basis of similar structural motifs or biochemical characterization.

Class I fusion proteins:

Class I viral fusion proteins form rod-like structures that extend perpendicularly outward from the viral membrane as visualized by electron microscopy (Dutch *et al.*, 1999;

Weissenhorn *et al.*, 1999). In the case of HA, immunoelectron microscopy with domain-specific monoclonal antibodies showed that the transmembrane anchor and N-terminal fusion peptide are at the same end of the molecule (Skehel *et al.*, 1982; Weissenhorn *et al.*, 1999, and references therein). These rods are α -helical and very stable. Using x-ray crystallography and NMR techniques, partial structures of many Class I viral fusion proteins have been solved (references in Table 1.1; Fig 1.4.A). These structures are based on synthetic peptides of the heptad-repeat regions of the protein or the bacterially expressed fusion-protein ectodomain (membrane-interacting regions, and in some cases with hinge regions removed). In all the Class I proteins, a central coiled coil comprised of the N-terminal heptad repeat is observed, and the three C-terminal α -helices often pack antiparallel to the central coiled coil (Skehel and Wiley, 1998; Fig 1.4.A). This structure is termed the six-helix bundle and results in the localization of the N-terminal fusion peptide and the C-terminal transmembrane anchor at the same end of the molecule. For mouse hepatitis virus (MHV), the crystal structure has not been solved; however, synthetic peptides of the heptad repeats form an α -helical rod-like structure 14.5 nm in length as determined by electron microscopy (Bosch *et al.*, 2003).

Influenza HA is the only viral fusion protein for which there is structural information available for both pre- (neutral pH) and post- (acidic pH) fusion states (Fig 1.3.A-C). This has led to the structure-based proposed conformational changes described in Section 1.2 (Wilson *et al.*, 1981; Bullough *et al.*, 1994; Chen *et al.*, 1999). For other Class I proteins, the structural details of the triggered conformational change are not known. However, human immunodeficiency virus Type 1 (HIV-1) gp41, simian immunodeficiency virus (SIV) gp41, Moloney murine leukemia virus (MMLV) TM, and

Ebola virus GP2 all adopt a low-energy structure similar to the low-pH form of HA, leading to speculation that similar conformational remodeling occurs for all Class I fusion proteins (Skehel and Wiley, 1998; Weissenhorn *et al.*, 1999; Fig 1.4.A). This structural information is supported by biochemical studies that use synthetic peptides of the heptad repeat regions to inhibit the conformational change (to be discussed in Section 1.3.B). By analogy with HA, all Class I fusion proteins are thought to exist in two conformations: a metastable form complexed with the receptor-binding domain and a low-energy six-helix bundle.

Table 1.1 Class I viral fusion proteins

Virus	Virus Family	Protein	Reference(s) for structural characterization
Influenza	orthomyxo	HA2	Wilson <i>et al.</i> , 1981; Bullough <i>et al.</i> 1994; Chen <i>et al.</i> , 1999
HTLV	retro	gp21	Kobe <i>et al.</i> , 1999
MMLV	retro	gp21	Fass <i>et al.</i> , 1996
Visna	retro	TM	Malashkevich <i>et al.</i> , 2001
HIV-1	retro	gp41	Chan <i>et al.</i> , 1997; Tan <i>et al.</i> , 1997; Weissenhorn <i>et al.</i> , 1997
SIV	retro	gp41	Caffrey <i>et al.</i> , 1998; Malashkevich <i>et al.</i> , 1998; Yang <i>et al.</i> , 1999
Ebola	filo	gp2	Weissenhorn <i>et al.</i> , 1998a,b; Malashkevich <i>et al.</i> , 1999
MHV	corona	S2	Bosch <i>et al.</i> , 2003 **proteomic and biochemical approach
SV5	paramyxo	F1	Baker <i>et al.</i> , 1999
HRSV	paramyxo	F1	Zhao <i>et al.</i> , 2000
NDV	paramyxo	F	Chen <i>et al.</i> , 2001

Class II viral fusion proteins

Class II fusion proteins do not extend perpendicularly to the viral membrane in rod-like stem structures, are not rich in α -helix, and do not form coiled coils. These proteins are completely different in structure from the Class I proteins. From electron microscopy and X-ray crystallographic studies on both isolated fusion protein (soluble ectodomain

portion) and the whole virus, the structure of many of these proteins has been solved (references in Table 1.2; example in Fig 1.4.B). Class II proteins lie flat against the viral envelope to create an icosahedral scaffold (often in combination with another glycoprotein) that covers most of the viral surface. Each monomer is composed of three predominantly β -structured domains. These proteins do not possess N-terminal fusion peptides; instead, the sequences that are predicted to be fusion peptides are contained within a loop structure at the distal end of domain II. In the native structure of the tick-borne encephalitis virus (TBEV) E homodimer, the fusion-peptide loop of one monomer is constrained by a disulfide bridge and buried by the carbohydrate chain of the other monomer (summarized in Heinz and Allison, 2001; Fig 1.4.B).

The Semliki Forest virus (SFV) particle icosahedral shell comprised of viral glycoproteins rearranges upon exposure to low pH (Haag *et al.*, 2002). The rearrangement facilitates the alteration of the E1:E2 heterodimer into the E1 homotrimeric form involved in mediating membrane fusion (Gibbons *et al.*, 2003), and tilts the E1 protein outward from the viral envelope. Recently, the structure of the soluble E1 homotrimer was described using both electron microscopy and crystallographic techniques (Gibbons *et al.*, 2003). The implications of the triggered structural remodeling of the Class II fusion proteins for the fusion mechanism, analogous to the coiled-coil rearrangements of Class I fusion proteins, will be discussed in Section 1.3.B.

Table 1.2 Class II viral fusion proteins

Virus	Virus Family	Protein	Reference(s) for structural characterization
SFV	toga	E1	Lescar <i>et al.</i> , 2001; Haag <i>et al.</i> , 2002; Gibbons <i>et al.</i> , 2003
Dengue	flavi	E	Kuhn <i>et al.</i> , 2002
CSFV	flavi	E2	Garry and Dash, 2003 **proteomics approach
TBEV	flavi	E	Rey <i>et al.</i> , 1995
Hepatitis C	flavi	E2	Garry and Dash, 2003 **proteomics approach

Unclassified fusion proteins from enveloped viruses

The fusion mechanism of many enveloped viruses remains undetermined. For members of the herpesvirus family, four glycoproteins (gB, gD, gH, gL) are required for virus-cell and cell-cell fusion; thus, dissecting the role of each protein in the fusion pathway is complex (Muggeridge, 2000). The mechanism of fusion requires that gD bind one of a number of possible receptors (Pertel *et al.*, 2001), and is regulated by the anti-fusion activity of another glycoprotein, gK (Avitabile *et al.*, 2003). The fusion mechanism of vaccinia virus involves a 14-kDa protein that is present on the surface of intracellular mature virions (Gong *et al.*, 1990). This protein is a trimer and contains a central coiled coil, but lacks a membrane-spanning domain and an obvious fusion peptide (Vázquez *et al.*, 1998; Vázquez and Esteban, 1999). The vaccinia virus p14 protein is anchored to the membrane by protein-protein interactions with a 21-kDa membrane-spanning protein (Rodriguez *et al.*, 1993). Hepadnaviruses (hepatitis B virus, duck hepatitis B virus) encode three or two versions of the surface glycoprotein, respectively. The smallest glycoprotein, small surface antigen (SsAg), is believed to mediate the membrane fusion event required for entry. A fusion peptide has been defined at the N terminus of this protein. Though there is no structural information available for this protein, it is a

polytopic membrane-spanning protein and thus is unlikely to adopt a structure that is similar to that of either Class I or Class II proteins (summarized in Cooper *et al.*, 2003).

There is no x-ray crystallographic or NMR spectroscopic information for the G protein of the rhabdoviruses, vesicular stomatitis virus (VSV) and rabies virus (RV) (Gaudin *et al.*, 1995). Like Class I fusion proteins, G is a trimer, but the oligomeric structure of G is not stable and at neutral pH the protein exists in equilibrium between monomeric and trimeric states (Zagouras and Rose, 1993). Like Class II fusion proteins, the fusion peptide of G is internal to the amino acid sequence of the protein (Whitt *et al.*, 1990, Zhang and Ghosh, 1994). Upon exposure to low pH, the G protein undergoes a conformational rearrangement that stabilizes the trimer; however, unlike Class I and Class II protein remodeling, these structural changes are reversible (Gaudin *et al.*, 1991; Gaudin, 2000). This feature alone sets this protein apart from other viral fusion proteins, and has prompted investigators to suggest that the rhabdoviruses encode a third distinct class of fusion proteins.

Table 1.3 Unclassified viral fusion proteins (no structural information)

Virus	Virus Family	Protein	Reference(s) – descriptive no structure
Vaccinia	pox	14 kDa	Gong <i>et al.</i> , 1990; Vázquez and Esteban, 1999
HSV-2	herpes	gD, gB, gH, gL	Muggeridge, 2000
Rabies	rhabdo	G	reviewed in Gaudin <i>et al.</i> , 1995
VSV	rhabdo	G	reviewed in Gaudin <i>et al.</i> , 1995
HBV	hepadna	SsAg	Cooper <i>et al.</i> , 2003

1.3.B Viral fusion proteins are metastable

Many investigators believe that viral membrane fusion proteins are metastable structures that are poised to undergo fusion-mediating structural rearrangement in response to an

appropriate trigger (Carr and Kim, 1993; Weissenhorn *et al.*, 1999). As described in section 1.2, the spring-loaded mechanism of HA-mediated fusion suggests that conformational alteration from the kinetically trapped high-energy structure to the low energy form drives the thermodynamically unfavorable process of membrane fusion. The evidence that supports and contradicts this model will be discussed.

Support for the role of metastability

Many viral fusion proteins are synthesized as precursor proteins (e.g. HA0) that fold and oligomerize in the endoplasmic reticulum, and are subsequently proteolytically cleaved (e.g. to HA1 and HA2) during trafficking to the cell surface. For members of Class I (influenza HA, Ebola gp, paramyxovirus F, and HIV-1 env), proteolytic cleavage produces two domains, a globular receptor-binding domain and a membrane-anchored rod-like fusion domain, that remain covalently or non-covalently associated (Hallenberger *et al.*, 1992; Volchkov *et al.*, 1998; Weissenhorn *et al.*, 1999, and references therein). This cleavage event is essential for the infectivity of these viruses. It places the fusion peptide at or near the N terminus of the fusion domain, and is believed to generate a fusion protein that is trapped in a metastable folding state by virtue of interactions with the receptor-binding domain (summarized in Weissenhorn *et al.*, 1999). Class II fusion proteins are not proteolytically cleaved from a precursor form, but are synthesized in association with a second glycoprotein, the cleavage of which is required for fusion. During synthesis in the endoplasmic reticulum, the E1 spike protein of Semliki Forest virus (SFV) associates with the transmembrane precursor protein p62 to form a heterodimer; the two proteins traffic together to the plasma membrane. P62 is

processed by proteolytic cleavage into the E2 and E3 subunits (the mature spike protein is a trimer of E1/E2 heterodimers), and this cleavage is required to activate the E1 subunit for fusion (Zhang *et al.*, 2003). For the alphavirus termed Sindbis virus, proteolytic cleavage of the precursor PE2 is required for fusion-protein E1 activation and infectivity (Smit *et al.*, 2001). Proper folding of the flavivirus Tick-borne encephalitis virus (TBEV) E protein can only be achieved when it is coexpressed with the envelope glycoprotein prM (precursor of M) as a heterodimer. Co-synthesis with prM promotes the correct folding of E (Lorenz *et al.*, 2002). The subsequent proteolytic cleavage of prM is required to activate membrane fusion (Stadler *et al.*, 1997).

Not only is proteolytic cleavage required to generate the active form of both the Class I and Class II fusion proteins, but many investigators believe the cleavage event is essential to generate a native form of the protein that is metastable, and that then remodels in response to a fusion trigger. Does the conformational rearrangement that occurs when these proteins are triggered drive the fusion reaction, or does the trigger simply generate a 'fusion-active' conformation of the protein that can mediate membrane merger independently of the refolding reaction itself? Synthetic peptides that interact with different regions of the coiled coil, differential binding of monoclonal antibodies, and altered sensitivity to proteinase K, were used to map the structural remodeling of Class I proteins that occurs with fusion (Doms *et al.*, 1985; White and Wilson, 1987; Puri *et al.*, 1990). Studies on the energetics of refolding suggest that the six-helix bundle is at a lower energy than the native structure and that the refolding reaction is thus irreversible (Carr and Kim, 1993). Intrinsic fluorescence demonstrates a remarkable alteration in trp-fluorescence melting profile of influenza HA at neutral and acid pH (Rugroik *et al.*, 1986;

Remeta *et al.*, 2002). Raising the temperature or adding denaturants has been shown to induce an HA structure that is indistinguishable from the low pH form (Ruigrok *et al.*, 1986; Carr *et al.*, 1997). Elevated temperature was also associated with activation of fusion for paramyxoviruses (Wharton *et al.*, 2000). Mutations that disrupt formation of the coiled coil, or weaken interactions that are involved in six-helix bundle formation, abolish fusion (Wild *et al.*, 1994; Weng and Weiss, 1998; Qiao *et al.*, 1999; Gruenke *et al.*, 2002). Synthetic peptides that bind to the heptad-repeat regions of Class I fusion proteins also prevent the formation of the six-helix bundle and abolish fusion (Joshi *et al.*, 1998). All this evidence points to the importance of the structural transition that occurs in response to the fusion trigger, but does not answer whether it is the transition itself or the final conformation of the protein that is required for fusion.

Peptide-inhibition studies indicated that six-helix bundle formation is directly coupled to the merging of membranes. These results support a structural transition of HIV-1 gp41 and SV5 F1, and not the end product of this transition, that is required to facilitate fusion (Melikyan *et al.*, 2000; Russell *et al.*, 2001). In an investigation of the temporal order of HIV-1 gp41 six-helix bundle formation relative to the formation of the fusion pore, Melikyan *et al.* (2000) discovered that formation of the six-helix bundle is coincident with fusion and cannot be detected before fusion-pore formation. Russell *et al.* (2001) used N- and C-terminal heptad-repeat synthetic peptides and LPC-mediated fusion arrest to show that, for the SV5 F1 protein, the formation of the six-helix bundle structure and fusion are concurrent events. These studies support the role of structural remodeling of a metastable protein to a low-energy form as an integral component of the fusion mechanism.

The presence of heat or urea did not induce fusion at neutral pH for the Class II fusion proteins of SFV (E1) and TBEV (E), though both proteins demonstrated a remarkable change in intrinsic fluorescence melting profile at different pHs (Gibbons *et al.*, 2000; Stiasny *et al.*, 2001). The E1 protein structure was altered after this treatment and subsequent virus infectivity was abolished (Gibbons *et al.*, 2000). The post-fusion structure, the E1/E homotrimer, was highly resistant to the same treatment, suggesting its increased stability relative to native dimer. These authors suggest that, like Class I fusion proteins, the Class II proteins E1 and E adopt a native folding state that is metastable; however, the conformational alterations required to mediate fusion by Class II viruses are more complex than for Class I (Gibbons *et al.*, 2000; Stiasny *et al.*, 2001). The unclassified fusion protein, duck hepatitis B virus SsAg, contains a sequence that connects the first two transmembrane domains of the polytopic protein. This domain can also traverse the membrane, suggesting an alternative mechanism of fusion peptide exposure (the fusion peptide is at the N terminus, and extends into the first membrane-spanning domain). This structural alteration may create a spring-loaded structure in the native state, similar to that described for Class I and II fusion proteins (Grgacic *et al.*, 2000).

Evidence against the role of metastability

A construct of the murine coronavirus JHMV with a mutated protease-cleavage site (prevents proteolytic processing of the S protein into functional S1 and S2 subunits) was expressed using vaccinia virus and transient transfection. The cleavage-minus S protein caused a delayed onset of fusion, yet fusion still occurred despite the fact that no S1/S2

cleavage products were detected (Taguchi, 1993). That proteolytic cleavage of a precursor fusion protein is not required to prime the fusion domain suggests that the native state of the S protein may not be metastable, or that metastability is not essential for fusion ability. Similarly, a recombinant Ebola virus was engineered to lack the proteolytic cleavage site that generates gp1 and 2. This recombinant virus was viable, suggesting that the cleavage event is not essential (Neumann *et al.*, 2002). The glycoprotein G, encoded by the rhabdoviruses VSV and rabies virus, is not synthesized as a precursor; thus, no activating proteolytic cleavage event occurs to prime these proteins, again contradicting the essential role of a metastable protein in the fusion process.

The rhabdovirus G protein also lacks distinguishing structural features (e.g. coiled coils) to place it in one of the defined classes of fusion proteins. The VSV G glycoprotein clearly undergoes conformational rearrangements when exposed to acidic pH, as demonstrated by intrinsic fluorescence and binding of a fluorescent probe (Crimmins *et al.*, 1983; Carneiro *et al.*, 2001). The conformational change increases exposure of a hydrophobic region. However, the fusion process of G protein has been shown to be reversible; that is, the low-pH-triggered conformational changes that do occur concomitant with fusion are not irreversible end products. This suggests that the rhabdoviral G protein is not metastable in its native state (Crimmins *et al.*, 1983; Clague *et al.*, 1990; Gaudin, 2000). The thermal stability of the native and low-pH form of VSV G as determined by Trp-fluorescence melting profiles at neutral and acidic pH do not differ (Yao *et al.*, 2003). Furthermore, the membrane fusion activity of G is not induced by heat or denaturant, further suggesting that the native G protein is not in a metastable state (Yao *et al.*, 2003).

Recent investigations have used differential scanning calorimetry (DSC) to re-evaluate the proposed metastability of native HA, as an isolated protein or in intact virus particles (Epand and Epand, 2002, 2003; Remeta *et al.*, 2002). The unfolding of a protein that is in a kinetically trapped high-energy state is an exothermic process and should result in the release of energy that can be measured by DSC. However, neither isolated HA nor whole influenza virus particles exhibited an exothermic unfolding process. This result contradicts a central dogma of the spring-loaded model of membrane fusion, that the native fusion-protein structure alters in a manner that provides energy to the fusion reaction. Epand and Epand (2002, 2003) suggest an alternative role for the conformational rearrangements of HA that do occur and are required for the fusion mechanism. Exposure of HA to acidic pH correlates with a change in tertiary structure, a greater susceptibility to proteinase K digestion, and a loss of trimer stability in SDS (Epand and Epand, 2002). Thus, perhaps the 'fusion-active' HA is a dissociated trimer. Though the HA molecule rearranges in response to low pH, the native form of this protein is not in a metastable state as a consequence of the HA1 subunit constraining the HA2 from adopting an extended coiled-coil and six-helix bundle structure (Epand and Epand, 2003).

In summary, numerous lines of evidence are beginning to contradict the belief that the native state of fusion proteins such as HA exists in a metastable conformation, and that the structural remodeling of this protein provides energy to drive the fusion reaction. As will be discussed further, the reovirus FAST proteins also do not appear to have the size or structural capability to undergo energy-producing alterations in structure.

1.3.C Membrane-interacting region I: the transmembrane anchor

Though many of the studies on viral membrane fusion proteins focus on the role of structural remodeling of the ectodomain, the role of the membrane-interacting regions of these proteins is equally important to the fusion process. Current research on the importance of the transmembrane anchor supports two different theories: (1) this region serves an anchoring role, and/or (2) this domain is involved in the fusion process, specifically fusion-pore formation.

Pioneering studies that substituted the transmembrane domain (TMD) of influenza HA and HIV-1 gp41 with a glycosylphosphatidylinositol (GPI) anchor (to create constructs GPI-HA and GPI-gp41, respectively) pointed to the essential nature of this domain (Salzwedel *et al.*, 1993; Kemble *et al.*, 1994). GPI-HA and GPI-gp41 mediate hemifusion, not complete fusion, as fusion pores do not form. Armstrong *et al.* (2000) show that the TMD must completely span the lipid bilayer for complete fusion to occur (minimum length 17 residues); if not, only hemifusion takes place. It is possible that the TMD must be tightly anchored into the viral membrane to provide the requisite membrane tension for the hemifusion diaphragm to proceed to a fusion pore. Leikina and Chernomordik (2000) speculate that HA-GPI may not be able to cause the restricted hemifusion required for the fusion process. As a result, the lipid-anchored HA protein progresses down the alternative, dead-end pathway of unrestricted hemifusion.

As viral fusion proteins possess distinct TMD with different motifs, it is difficult to pinpoint the properties within this domain that may be essential for fusion-pore formation (Schroth-Diez *et al.*, 2000). To test whether a precise amino acid sequence was

required, Melikyan *et al.* (1999) constructed chimeric proteins comprised of the intact HA ectodomain and different combinations of TMD and cytoplasmic tail (CT). These combinations included the TMD and/or CT of HA itself, or that of an unrelated integral membrane protein (polyimmunoglobulin receptor; PIRG). The chimeric HA protein with a foreign TMD supported fusion, suggesting that one role of this region is to provide a stable anchor. However, the ability of the chimeric HA to mediate fusion was dependent on the combination of TMD and CT in the molecule, suggesting a more complex role. Though fusion-competent chimeric molecules indicate there is wide latitude in the nature of the TMD that can support fusion, certain constructs of HA that contained amino acid substitutions within the TMD abolished fusion (Melikyan *et al.*, 1999). The VSV G protein TMD requires two glycine residues for fusion-pore formation (Cleverley and Lenard, 1998). Individual alteration of each glycine residue reduced fusion activity, while constructs containing two altered glycine residues demonstrated a hemifusion phenotype. This suggests that at least one TMD gly residue is necessary for late events in the fusion process. Interestingly, gly residues are more than twice as abundant in the TM domains of viral fusion proteins than in those of non-fusion proteins (Table 1.4). Cleverley and Lenard (1998) propose that a glycine hinge increases compression and negative curvature of the viral envelope and expansion of the hemifusion diaphragm until the perturbed lipids form a fusion pore. Substitution of a proline (with gly, ala, or val) in the TMD of the Moloney murine leukemia virus (MMLV) env protein dramatically impaired fusion (Taylor and Sanders, 1999), also supporting this model. On the other hand, when the TMD of a fusion protein (VSV G) was replaced with a TMD from any of four different unrelated proteins, fusion activity was retained (Odell *et al.*, 1997). However, each of the

substituted transmembrane-domain sequences was glycine-rich, making it difficult to interpret these results. Mutagenesis of the transmembrane domain of gH, one of the four glycoproteins that is required for herpesvirus-mediated cell-cell fusion, abolished syncytium formation when expressed along with gB, gD, and gL. Specific substitution of conserved glycines within this TMD also impaired cell-cell fusion (Harman *et al.*, 2002). Thus, the debate regarding the role of the transmembrane anchor in the fusion process remains. Although it is clear that a variety of membrane-anchoring sequences can substitute for the TMD of fusion proteins and mediate function, it is possible that this domain requires a particular amino acid character (rich in glycines and other small amino acids; Odell *et al.*, 1997).

The effect of a synthetic peptide of the VSV G TMD on PEG-mediated fusion of SUVs was assessed (Dennison *et al.*, 2002). The TMD peptide enhanced the rate but not the extent of lipid mixing, while a mutant peptide (essential di-glycine motif altered to di-alanine) significantly inhibited the extent of fusion-pore formation. These authors suggest that the authentic TMD peptide stabilizes non-lamellar structures to promote fusion-pore formation (Dennison *et al.*, 2002), which underscores the important role of the TMD in the fusion process.

Table 1.4 Transmembrane anchor sequences

Fusion Protein	Transmembrane anchor sequence (glycine residues in bold)	Reference
Influenza A HA2	QILAIYSTVASSLVLLVSL G AISFWMCS	Veit <i>et al.</i> , 1991
HIV-1 gp41	IFIMIV GGLVGL RIVFAVLSIVN	Willey <i>et al.</i> , 1986
Sendai F1	TVITIIIVVMVILVVIIIVIVIVLY	McGinnes and Morrison, 1986
RSV F1	IMITIIIVIIIVILLSLIAVGLLLYC	McGinnes and Morrison, 1986
NDV F1	ALITYIVLTIISLVF G ILSLVLACYLMI	Chambers <i>et al.</i> , 1986
Measles F1	IVYILIAVCL GGLIG IPALICCC	Buckland <i>et al.</i> , 1987
SV5	VLSIIAICL GSLGL LILILLLLSVVVW	McGinnes and Morrison, 1986
MMLV TM	SPWFTTLISTIM G PLIVLLMILL F GPCI LN	Ragheb and Anderson, 1994
Dengue E	STSLSVSLVLV G VVTLYL G AMVQA	Deubel <i>et al.</i> , 1986
SFV E1	IS GGLG AFA G AILVLVVVTCIGL	Garoff <i>et al.</i> , 1980
Sindbis E1	LF GG ASSLLI IG LMIFACSMMLTST	Dalgarno <i>et al.</i> , 1983
Rabies G	YVLMTAGAM IG LVLI F SLMTWC	Seif <i>et al.</i> , 1985
VSV G	SSIASFFFI IGLIIG LFLVL	Brun <i>et al.</i> , 1995

1.3.D Membrane-interacting region II: the fusion peptide

There are a number of criteria that define a fusion peptide. These segments are often rich in glycine residues and, for the Class I fusion proteins, are found at or near the N terminus of the fusion protein domain (Durell *et al.*, 1997; Skehel *et al.*, 2001). In contrast, Class II fusion proteins and the rhabdoviral fusion proteins locate fusion peptides internally, within the amino acid sequence of the fusion protein (Whitt *et al.*, 1990; Shome and Kielian, 2001). These internal fusion peptides are often less hydrophobic than those located at the N terminus (Whitt *et al.*, 1990; Zhang and Ghosh, 1994). Mutation of the fusion-peptide region often leads to loss of fusion activity of the protein (Zhang and Ghosh, 1994; Frederickson and Whitt, 1995; Delos and White, 2000; Delos *et al.*, 2000; Allison *et al.*, 2001; Cross *et al.*, 2001; Epand *et al.*, 2001a). Synthetic

peptide analogues of the fusion peptide motif possess membrane destabilizing activity and the ability to mediate lipid mixing *in vitro* (Epand, 2003). Finally, these regions are usually highly conserved within fusion proteins encoded by different virus strains within the same family, though they have little homology with fusion peptide motifs from disparate families (Nieva and Agirre, 2003).

The hydrophobic nature of N-terminal fusion peptides precludes the use of x-ray crystallography and solution NMR spectroscopy for the resolution of the structure of this region (Yang *et al.*, 2001). To prevent fusion-protein aggregation in aqueous solution, the Class I fusion proteins used for crystallization lacks this N-terminal hydrophobic region (Table 1.1). In contrast, internal fusion peptides were not removed from the native structures of Class II fusion proteins, and localize to looped regions in their high-resolution structures (Rey *et al.*, 1995; Lescar *et al.*, 2001; Kuhn *et al.*, 2002). Spectroscopic techniques such as circular dichroism (CD) have been used to assess the secondary structure of fusion-peptide analogues, and for the influenza HA this region appears to be uniformly α -helical when inserted into the membrane at an oblique angle (summarized in Wharton *et al.*, 1988; Lüneberg *et al.*, 1995; Epand, 2003). CD techniques have been less informative for the HIV-1 gp41 fusion peptide, as different experiments have shown different secondary-structure propensity (Martin *et al.*, 1993; Martin *et al.*, 1996; Yang *et al.*, 2001). However, the recent use of solution NMR spectroscopic techniques on a soluble version of the HA fusion peptide indicates that the membrane-inserted fusion peptide undergoes conformational rearrangement when acid-exposed. The first 10 amino acids form an α -helix at both neutral and acidic pH and residues 11-13 form a turn, and redirect the peptide so that it forms a wide V. The C-

terminal region is disordered at neutral pH and adopts a short (residues 14-18) 3_{10} -helix at low pH (Han *et al.*, 2001). This inverted-V structure places the bulky hydrophobic residues into a pocket within the V, and a ridge of glycine residues on the surface-exposed edge of the N-terminal α -helix (Tamm, 2003). This helix-hinge-helix motif has also been predicted for the HIV-1 gp41 fusion peptide (derived from FTR spectroscopy of a ^{13}C -labeled fusion peptide; Gordon *et al.*, 2002).

A major role of the conformational alteration in structure of both Class I and Class II fusion proteins in response to the fusion-activating trigger is to release the previously buried fusion peptide to allow it to interact with either the target or viral membrane. With acid-exposure, the fusion peptide of HA moves approximately 100 Å relative to the rest of the molecule (Carr and Kim, 1993). The fusion-mediating structural rearrangement of the Class II fusion proteins involves a redistribution from dimer to trimer of the proteins that comprise the icosahedral scaffold (Haag *et al.*, 2002). This is believed to facilitate the subsequent interaction of the internal fusion peptide (located in a small loop at one end of each monomer, buried in the dimer and exposed upon trimerization) with the membrane (Heinz and Allison, 2001; Gibbons *et al.*, 2003). That fusion peptides interact with membranes is clear, but how do these amphipathic motifs modulate lipid bilayers to drive the membrane fusion reaction forward?

Recent development of a host-guest system that renders the HA fusion peptide water-soluble (Han and Tamm, 2000a) allowed an investigation of the thermodynamics of fusion-peptide insertion into a lipid bilayer. As with other amphipathic peptides, membrane insertion is coupled with refolding of the peptide, a process that is energetically favorable (Tamm, 2003). Li *et al.* (2003) demonstrated that for the HA N-

terminal fusion peptide, membrane insertion is a thermodynamically favorable event driven by enthalpy and opposed by entropy (Li *et al.*, 2003). This result suggests that the thermodynamic event is not driven by the hydrophobic effect. As the peptide inserts more deeply into the bilayer, more energy is released. The authors also estimate that about half the enthalpy of binding is due to folding and half due to membrane insertion. The folding of the HA fusion-peptide V-structure and its ability to deeply insert into the lipid bilayer are important components of the thermodynamic impetus that drives fusion (Li *et al.*, 2003).

Amphipathic fusion peptides are also believed to mediate dehydration of the intercellular water layer (Han *et al.*, 1999), one of the predominant thermodynamic barriers that prevents biological-membrane fusion (Rand, 1981; Zimmerberg *et al.*, 1993). Synthetic fusion peptides possess the ability to modulate membrane curvature and perturb the bilayer state, as evidenced by assays that measure their ability to induce non-bilayer lipid phases in pure bilayer systems (Epand and Epand, 2000; Peisajovich *et al.*, 2000a). The curvature-modulating ability of synthetic peptides correlates with the conditions required for fusion-protein function; for example, HA fusion peptide only modulates curvature at acidic pH (Epand and Epand, 1994). Fusion-protein multimerization may promote the self-association of fusion peptides in a manner that promotes enhanced fusogenicity (Yang *et al.*, 2003b). Fusion peptide motifs also possess structural plasticity, likely as a result of their glycine/alanine-rich nature (Davies *et al.*, 1998; Pécheur *et al.*, 2000; Wong, 2003). Synthetic constructs of fusion peptides can readily interconvert between α -helical and β -structured conformations (Epand, 1998). It is possible that the interconversion between α -helix and β -strand facilitates the

membrane insertion/disruption necessary for fusion (Peisajovich *et al.*, 2000a; Tamm, 2003). This conformational flexibility in response to pH is illustrated by the structure of the HA fusion peptide (Han *et al.*, 2001).

Table 1.5 Fusion-peptide sequences

Type	Fusion Protein	Fusion Peptide Sequence	Reference
N-terminal/N-proximal	Influenza HA2	GLFGAIAGFIENGWEG	Skehel <i>et al.</i> , 2001
	HIV gp41	GVFVLGFLGFLATAGS	Skehel <i>et al.</i> , 2001
	Sendai F1	FFGAVIGTIALGVATSA	Skehel <i>et al.</i> , 2001
	RSV F1	FLGFLLGVGSAIASGV	Skehel <i>et al.</i> , 2001
	Ebola GP2	EGAAIGLAWIPYFGPAA	Suárez <i>et al.</i> , 2003
	Measles F1	FAGVVLAGAALGVATA	Samuel and Shai, 2001
	HIV gp41	AVGIGALFLGFLGAAGSTMGARS	Skehel <i>et al.</i> , 2001
	FeLV env	EPISLTVALMLGGLTVGGIAAGVGTGTK	Davies <i>et al.</i> , 1998
	HBV SHBsAg	MENITSGFLGPLLVLQAGFFLLTR	Rodriguez-Crespo <i>et al.</i> , 1996
	SIV gp41	GVFVLGFLGFLA	Cladera <i>et al.</i> , 1999
	AS/LV env	RIFASILAPGVAAAQALREIERL	Delos <i>et al.</i> , 2000
	VSV G	QGTWLNPGFPPQSCGYATV	Delos <i>et al.</i> , 2000
Internal	TBE E	DRGWGNHCGFLFGKSSIVACVKAA	Allison <i>et al.</i> , 2001
	SFV E1	DYQCKVYTGVPFMWGGAYCFCD	Shome and Kielian, 2001
	HCV E1	DLLVGSATLCSALYVGDLGGSVF	Garry and Dash, 2003

Boomerang model of HA-mediated fusion

Tamm has studied the HA fusion peptide extensively, and combined his studies on the fusion peptide region with the classical spring-loaded model of HA-mediated fusion to generate the boomerang theory (Fig 1.5.A-C; Tamm, 2003). In this model, low pH extrudes the buried fusion peptide, and extension of the central coiled-coil region of HA orients the fusion peptide toward the target membrane, where it inserts. Insertion of the

fusion peptide, its concomitant refolding, and the extension of the coiled coil are exothermic processes, releasing energy that can be utilized to pull the two opposing membranes together. Aggregation of several HA trimers at the fusion site is likely required for this event. As the C-terminal coiled-coil region refolds, the HA ectodomain tilts, and the fusion and transmembrane domains are brought within close proximity, though still embedded in two separate, closely apposed and highly curved and stressed membranes. This step is referred to as boomerang retrieval (Tamm, 2003). At this stage, outer membrane leaflets begin to mix, and likely the membrane perturbing actions of the fusion peptide and TMD facilitate hemifusion. However, in Tamm's model, a direct interaction between the fusion peptide and the TMD is required to open the fusion pore, as follows. The conserved glycine ridge in the N-terminal arm of the fusion peptide is a candidate region for mediating helix-helix interactions with the TMD α -helix. The fusion peptide can then slide along the TMD, thereby opening the V-shaped conformation of the fusion peptide into a more extended α -helix. This action is proposed to open the fusion pore (Tamm, 2003). The fusion peptide and TMD of several HA trimers are likely required for this process.

1.3.E Other membrane-interacting regions

The spring-loaded model of membrane fusion proposes that each viral fusion protein contains a single fusion peptide that is solely responsible for destabilization of the target membrane during the fusion process. More recently, the role of the transmembrane anchor in the donor membrane has been realized. However, in addition to these two membrane-interacting regions, other regions of viral membrane protein have recently

been proposed to interact with membranes, promoting their merger (Peisajovich and Shai, 2003).

Class I fusion peptides contain two regions of heptad repeats integral to coiled-coil formation. More recent studies have proposed an additional role for the N-terminal heptad repeat in the fusion mechanism of influenza HA, HIV-1 gp41, and paramyxovirus F1. Epand *et al.* (1999) used a 127-amino-acid segment of HA, comprised of the N-terminal fusion peptide, the N-terminal heptad repeat and the loop region, to demonstrate that this construct mediates lipid mixing of liposomes in a pH-dependent and more efficient manner than does the N-terminal fusion peptide alone. This suggests that the extra amino acid residues may contribute to and/or modulate the membrane interactions of the N-terminal fusion peptide. This 127-amino-acid HA construct was subsequently shown to induce cell-cell hemifusion between two cells that expressed adhesion molecules (Leikina *et al.*, 2001). In a similar study, Ghosh and Shai (1999) compared the ability of various constructs of the paramyxovirus F protein to mediate liposome fusion. These included a 33-amino-acid construct of the N-terminal fusion peptide and a 70-amino-acid construct of the fusion peptide plus the N-terminal heptad repeat. Only the 70-amino-acid construct was able to mediate lipid mixing, whereas the shorter peptide, a mutant fusion peptide and a mutant heptad repeat did not. Similarly, extension of the HIV-1 gp41 N-terminal fusion peptide by the 17 predominantly polar amino acids that follow the hydrophobic peptide significantly increased lipid mixing (Peisajovich *et al.*, 2000a). These authors speculate that the addition of the polar region facilitates the correct oligomerization of the peptide to enhance its fusion ability.

That the transmembrane anchor of fusion proteins provides more than just an anchoring role in the membrane has been discussed. However, the pre-transmembrane region (that for some fusion proteins spans the C-terminal heptad-repeat sequence) has been shown to play an important and direct role in fusion. Suárez *et al.* (2000) investigated the membrane-interacting potential of the pre-transmembrane region of the gp41 ectodomain that showed a tendency to partition into the membrane interface, using the hydrophobicity scale developed by Wimley and White (described in Nieva and Suárez, 2000). A synthetic peptide of this region partitions into membranes (demonstrated by intrinsic fluorescence) and induced lipid mixing and leakage of liposome contents (Suárez *et al.*, 2000). Furthermore, lipid mixing and leakage assays using equimolar amounts of the membrane-proximal peptide and the N-terminal fusion peptide suggested that these two regions co-operated to potentiate the membrane destabilizing effects. These authors were the first to propose the importance of the membrane-proximal domain to the fusion mechanism, and note that many fusion proteins also contain a pre-transmembrane fusion that is rich in aromatic residues (Table 1.6; Suárez *et al.*, 2000). Epand and Epand (2001) investigated the role of the pre-transmembrane region in the TM protein of a spumaretrovirus, human foamy virus. A synthetic peptide to this region induced lipid mixing *in vitro*; when added in conjunction with the N-terminal fusion peptide of foamy virus TM, a synergistic effect occurred. Site-directed mutagenesis of the aromatic residues within the pre-transmembrane region of HIV-1 gp41 and HPIV-2 F1 abolished fusion (Munoz-Barroso *et al.*, 1999; Salzwedel *et al.*, 1999; Tong *et al.*, 2001). Kliger *et al.* (2000) propose the following amended model of HIV-1 gp41-mediated membrane fusion. This model suggests that the

interaction of the N-terminal fusion peptide with the target membrane and formation of the six-helix bundle is followed by the dissociation of the six-helix bundle to allow other membrane-interacting segments (e.g., the pre-transmembrane domain) to interact with the membrane in a manner that further promotes membrane merger. While the transmembrane anchor and fusion peptide are believed to penetrate into the hydrophobic core of the membrane, the pre-transmembrane region is proposed to bind to the surface of the membrane (Kliger *et al.*, 2000).

The membrane-proximal region of the VSV G protein possesses the unique ability to potentiate the membrane fusion activity of other viral glycoproteins (VSV New Jersey G protein, SV5 F1, HIV-1 gp41; Jeetendra *et al.*, 2002). This feature requires a minimum of 14 amino acids within the pre-transmembrane region to potentiate SV5-mediated syncytium formation. When analyzed alone, a truncated VSV G protein comprised of the membrane-proximal stem, the transmembrane anchor, and the cytoplasmic domain (G-stem) was able to induce cell-cell hemifusion (Jeetendra *et al.*, 2002). Rupture of the hemifusion diaphragm with chlorpromazine indicated that G-stem-induced hemifusion was a functional precursor to complete fusion. The authors suggest that the pre-transmembrane region of the G protein has the ability to alter membrane curvature, facilitating the lipid rearrangement and membrane destabilization required to form the stalk intermediate (Jeetendra *et al.*, 2002).

The ectodomain of the fusion protein of paramyxoviruses is larger than that of influenza HA or HIV-1 gp41. At approximately 500 amino acids, there is a long stretch of protein (more than 280 amino acids) between the N-terminal and C-terminal heptad-repeat regions implicated in coiled-coil formation (Russell *et al.*, 2001). It has been

proposed that C-terminal to the heptad repeat, the F1 protein of Sendai virus contains a second fusion peptide that is similar in nature to the N-terminal fusion peptide of HIV-1 gp41 (Peisajovich *et al.*, 2000b). A synthetic peptide of this region induced lipid mixing at a concentration that was less than that required for the N-terminal fusion peptide. The authors suggest that this internal fusion peptide also interacts with the target membrane during the fusion process and may in fact mediate the initial interaction of the F1 ectodomain with the opposing membrane, as it is located in the loop region at the top of the native structure (Peisajovich *et al.*, 2000b). A synthetic peptide that corresponds to this internal fusion peptide also inhibits Sendai virus fusion (Ghosh *et al.*, 2000). Measles virus F1 has also been shown to contain an internal fusion peptide, suggesting that this is an integral feature of the fusion mechanism of all paramyxoviruses (Samuel and Shai, 2001).

Table 1.6 Sequences of other membrane-interacting regions

Type	Viral protein	Membrane-interacting sequence (aromatic residues in bold)
Pre-transmembrane region	HIV-1 gp41	ELLELDK W ASL W N W FNITN W L W YIK L F
	Foamy virus gp47	GN F LSGTAQGI F GT A F SLLG Y LKPILIG
	Ebola gp2	PHD F VDKTLPDQGDNDN W W T G W RQ W IP
	Influenza A HA	AESLQNRIQIDPVKLSSG Y KDIIL W F S F
	Sendai F	SKAELEKARKILSEVGR W YNSRET V IT
	Sindbis E1	PHKNDQEFQAAISKTS W S W L F AL F GG A
	Hepatitis C E2	VVDVQ Y L Y GIGSAVVS F AIK W E Y VLLL
	VSV G	TGLSKNPIELVEG W F S S W KSSIAS F F F
Internal fusion peptide	Sendai F1	YFGLLTAFGSNFG
	Measles F1	YTEILSLFGPSLR

Samuel and Shai (2001) and Suárez *et al.* (2000).

Epand (2003) has analyzed the membrane-interacting regions of many viral fusion proteins. He proposes a mechanism of protein-mediated fusion that differs from the common paradigm. Epand used differential scanning calorimetry to show that the HA fusion protein does not exist in a metastable native state (Epand and Epand, 2002, 2003). Indeed, a truncated 127-amino-acid HA ectodomain that has already adopted the post-fusion conformation is able to mediate cell-cell hemifusion (Leikina *et al.*, 2001). There are several possible explanations for how membrane fusion proteins can lower the activation energy barrier that prevents membrane merger (even though the reactants and products of the fusion process are energetically similar; Epand, 2003). The triggered conformational change is essential to expose the fusion peptide; subsequent insertion of the fusion peptide into the target membrane is a thermodynamically favorable process (Li *et al.*, 2003). Membrane-interacting regions of the fusion proteins, including the fusion peptide, transmembrane anchor, pre-transmembrane region, heptad repeats, and internal fusion peptides, may function in concert to dehydrate the interbilayer space and disrupt the membrane bilayer to lower this activation energy barrier. The concerted action of a critical number of fusion proteins, and their membrane-interacting segments, may cause sufficient perturbation of the pre-fusion bilayer state that membrane fusion occurs, without the requirement of a metastable fusion protein. This alternate view may provide a framework for how p14 and the other FAST proteins function as membrane fusion proteins.

1.4 Cellular fusion proteins

The complex cellular machinery that regulates and mediates essential intra- and intercellular membrane fusion events is beginning to come into focus (Brunger, 2001). Despite this, a detailed molecular view of how cellular fusion proteins modulate membrane lipid bilayers is still lacking. The extensive regulatory machinery is not described here; instead, this review focuses on candidate fusion proteins that may play a direct role in membrane merger.

1.4.A Intracellular fusion

Intracellular fusion between vesicles and their target membranes is a highly regulated, specific, and efficient process (e.g., synaptic-vesicle / plasma-membrane fusion occurs within milliseconds) that requires complex interactions of a host of regulatory factors in addition to the presence of membrane fusion proteins. The many regulatory players that tether the two opposing membranes together (long coiled-coil proteins), regulate the length of time of the tethering process (Rabs), and proofread the actual fusion event (SM proteins) is not discussed here. For recent reviews on the regulation of intracellular fusion, see Gerst (2003) and Jahn *et al.* (2003).

The SNARE hypothesis was proposed in 1993; it states that the specificity of intracellular fusion events and the core of the fusion machinery is controlled and comprised of the SNARE (soluble *N*-ethylmaleimide-sensitive factor attachment receptor) proteins (Söllner *et al.*, 1993). It proposes that SNARE proteins localize to each individual subcellular compartment, tagging that membrane with a molecular

identification. At its simplest level, a SNARE localized to a vesicular membrane (v-SNARE) must pair with its cognate partner(s), two target-membrane-localized (t-) SNAREs. Only cognate partners can form the SNARE complex that drives fusion (Söllner *et al.*, 1993). The human genome contains 35 SNARE proteins and yeast contain 21; this degree of variety does not provide enough molecular tags, and thus the theory is clearly an oversimplification (Bock *et al.*, 2001). In addition, SNARE pairing is not based on the simple v-SNARE:t-SNARE ratio of 1:2, but rather on the conservation of residues that mediate interaction between the partners (3 glutamines, 1 arginine). This has led to a revised nomenclature that describes the individual components of the SNARE complex as a Q- or R-SNARE (each complex requires two Q-SNAREs and one R-SNARE; Bock *et al.*, 2001). That said, the SNARE proteins do play an integral role in the fusion mechanism itself.

The structure of a well-characterized recombinant synaptic fusion complex (v-SNARE is synaptobrevin; t-SNAREs are syntaxin and SNAP-25) was described by Sutton *et al.* (1998). In this crystal structure, the three SNARE proteins complex to form an α -helical rod-like structure similar to that found in the Class I fusion proteins (Skehel and Wiley, 1998). The transmembrane anchors of synaptobrevin and syntaxin are both oriented at the same end of the four-helix rod (with two helices supplied by SNAP-25). The four-helical bundle and the orientation of the membrane-anchoring components of the structure suggested that SNARE complex may mediate intracellular vesicle fusion in a manner similar to that of the Class I viral fusion proteins (Skehel and Wiley, 1998). A mechanism was suggested whereby cognate SNAREs in two opposing membranes would interact at first using their N-terminal regions, and subsequently assemble into the rod-

like structure by a mechanism that 'zippered' the α -helices together from N to C terminus. Based on the spring-loaded model of HA-fusion, the 'zippering' of the SNARE complex and the thermodynamic favorability of complex formation was proposed to pull the two apposing membranes together (Skehel and Wiley, 1998).

There exists much evidence to support the important role of cognate SNARE assembly into *trans* complexes that dock two opposing membranes together and provide a level of specificity to the reaction (summarized in Jahn *et al.*, 2003). However, the assertion that this protein complex is the minimal machinery required for the fusion event remains a controversial claim. Weber *et al.* (1998) used a liposome fusion assay to demonstrate that SNAREs were the minimal fusion machinery. Critics of this study question whether the liposome fusion system represents a physiological situation, and posit that the SUVs used in the experiments were fusion-prone. Indeed, PEG-mediated aggregation can fuse SUVs (20-100 nm in diameter) that are highly curved and fusion-prone (Lentz *et al.*, 1992). The mean diameter of liposomes used by Weber *et al.* (1998) was 45 nm; perhaps these membranes contained the outer-leaflet packing defects that allow fusion of closely apposed membranes (Lentz *et al.*, 1992; Lentz and Lee, 1999). Furthermore, the rate of fusion observed *in vitro* (minutes to hours) was slow relative to the rapid (micro to millisecond) fusion events that occur in synaptic-vesicle exocytosis (Mayer, 1999). Evidence to support these studies showed that when the transmembrane anchors of syntaxin and synaptobrevin were replaced with a phospholipid, close apposition of vesicles but no membrane fusion occurred (McNew *et al.*, 2000). However, an isoprenoid-anchored v-SNARE was sufficient to mediate fusion when the anchor

spanned the entire bilayer, suggesting that for the SNARE proteins, the role of transmembrane domain is that of stable membrane-anchor.

Biological membranes are more complex than the synthetic phospholipid membranes of liposomes, and their membrane composition makes them unlikely to fuse. Further, biological membranes have a protein content of 30-70%, making their propensity to fuse significantly different from that of liposomes (Mayer, 1999). To address this criticism, Rothman and co-workers recently demonstrated cell-cell fusion using flipped SNAREs. In this study, the cognate SNAREs were expressed in cells in a flipped orientation so that rather than face the cytoplasm, the bulk of the protein resided on the cell surface. Surface biotinylation demonstrated that a proportion of the flipped SNAREs were expressed on the cell surface and a cell-cell fusion assay demonstrated that flipped SNAREs did indeed mediate cell fusion (Hu *et al.*, 2003). The v-SNARE-expressing cells were fluorescently labeled with a cytoplasmically localized red fluorescent protein; the t-SNARE-expressing cells were labeled with a nuclear-localized cyan-fluorescent protein; fused cells demonstrated a red cytoplasm surrounding blue nuclei. That the SNARE complex can mediate cell-cell fusion suggests that the nature of the fusing membrane or size of the vesicle may not have artificially improved the *in vitro* results. As well, other candidate 'fusion' factors normally found in the cytoplasm are not present in the extracellular milieu, a feature of this paper that addresses critics of the SNARE hypothesis who believe that the actual fusion event is mediated by as yet undefined cytoplasmic molecules (to be discussed).

Bentz (2000a) considers that the SNAREpins may function similar to HA in a model of membrane fusion based on the hydrophobic defect. This model (described in

section 1.2) necessitates that the candidate fusion protein contain a fusion peptide. Such a putative fusion peptide is proposed to exist in the v-SNARE synaptobrevin2 (Table 1.7; Jahn and Südhof, 1994), in the center of the coiled-coil domain of the SNARE-complex structure (Sutton *et al.*, 1998). As SNAREs are believed to be unstructured before complex formation, Bentz proposes that in the pre-fusion v-SNARE, the putative fusion peptide embeds in the vesicle membrane. After docking and four-helical bundle formation, the structural remodeling pulls the fusion peptide out of the vesicle membrane. If lipid flow is restricted by the presence of other vesicular membrane proteins, a hydrophobic defect is created and membrane fusion proceeds as described in Section 1.2. The data of McNew *et al.* (2000) supports this model, as it predicts that the v-SNARE, but not the t-SNARE, would require a membrane-spanning domain that spans the entire bilayer to restrict lipid flow from the vesicle membrane to the defect (Bentz, 2000a).

Studies of homotypic vacuolar fusion in yeast suggest that other fusion protein factors are required downstream of SNAREpin docking (Ungermann *et al.*, 1998). By dissecting the steps that precede the actual fusion event (tethering, docking) the authors show that SNAREpins can be dissociated prior to the fusion event. When the fusion block is removed, membrane merger proceeds despite the fact that the SNARE complex is dissociated. Ungermann *et al.* (1998) suggest that though SNAREs are integral to the vacuole fusion event to mediate docking and close apposition of membranes, an unknown downstream molecule(s) that is activated by calcium and the calcium-dependent enzyme calmodulin is responsible for the actual merger of membranes. Peters *et al.* (2001) identify this unknown factor as the V0 subunit of the vacuolar ATPase pump. The V0 subunit is a complex of six proteolipids that form a ring in the vacuolar membrane. When

signaled by the V1 subunit, V0 subunits form the proton pump used to acidify the vacuole. However, Peters *et al.* (2001) suggest that V0 has a second, V1-independent, role. In response to the dual trigger of calcium and calmodulin, *trans*-V0 complexes in opposing membranes dimerize to form a proteinaceous fusion pore. This event is presumed to happen downstream of SNARE-mediated docking of two vacuolar membranes together. After pore formation, calmodulin is proposed to promote pore widening and, as the proteolipid subunits disperse, lipids of the bilayer invade the proteolipid complex and eventually replace the V0 subunits. This discovery has led to a re-evaluation of current models that suggest fusion proceeds through lipidic subunits and has generated the protein-pore theory discussed in Section 1.2. However, there is as yet no evidence whether the V0 proteolipid fusion pore exists in any other fusion system (Almers, 2001). In addition, V0 mutants are not lethal, and yeast cells lacking this protein can survive on acidic rich media. This observation has prompted investigators to question the universality of the V0 fusion mechanism (Jahn *et al.*, 2003).

1.4.B Intercellular fusion

Intercellular membrane fusion events are essential for such cellular processes as gamete fertilization, muscle fiber formation, and the formation of the maternal-fetal interface layer in the placenta (Blumenthal *et al.*, 2003). In each case, the membrane fusion machinery is not defined; the candidate fusion proteins are discussed below.

Fertilization

The final steps of sperm-egg interaction (following the acrosome reaction and dissolution of the egg's protective coating) involve the adhesion of the sperm plasma membrane to

the egg plasma membrane, and their subsequent membrane merger (Talbot *et al.*, 2003). The sperm glycoprotein, fertilin, was the first protein identified as important in these final fertilization events. Fertilin is a heterodimer of α - and β -subunits, and is a member of the ADAM (*a disintegrin and metalloprotease*) transmembrane protein family (Schlöndorff and Blobel, 1999). Monoclonal antibodies directed against β -fertilin implicate this subunit as important for membrane adhesion, while the α subunit has been suggested to be the fusion effector (Talbot *et al.*, 2003). A region in α -fertilin has been modeled as an amphipathic α -helix and is proposed to act in a manner similar to that of a viral fusion peptide in the fusion reaction (Table 1.7; Blobel *et al.*, 1992). A model for the activity of α -fertilin suggests that after adhesion of the sperm and egg membrane (mediated by β -fertilin), α -fertilin undergoes structural alteration that permits its fusion peptide to interact with the egg plasma membrane (Bigler *et al.*, 1997). However, sperm from α -fertilin knockout mice are still capable of gamete fusion (Cho *et al.*, 2000), and some mammalian species have been shown to lack the gene for α -fertilin (Waters and White, 1997), making it unlikely that fertilin is the sole protein responsible for sperm-egg membrane fusion.

If fertilin is important in sperm-egg fusion, this sperm ADAM must be redundant with other proteins (Talbot *et al.*, 2003). New candidate fusion proteins have arisen from studies of the egg plasma membrane. Removal of egg GPI-linked proteins using phosphatidylinositol-specific phospholipase C results in a marked decrease in egg-sperm fusion but little effect on binding of sperm to egg (Coonrod *et al.*, 1999). Mice lacking the tetraspanin protein CD9 display complete loss of membrane fusion activity; the addition of antibodies against CD9 has the same inhibitory effect (Kaji *et al.*, 2000;

Miyado *et al.*, 2000). Identification of the potential role(s) of these new candidate fusion proteins in membrane merger remains.

Interestingly, CD9 and other tetraspanin proteins have been identified as players in other cell-cell fusion systems. Antibodies directed against CD9 have no effect on canine distemper virus-cell fusion, but prevent cell-cell fusion of infected cells (Schmid *et al.*, 2000). Similarly, infection of cells with feline immunodeficiency virus (FIV) at a step after virus entry is inhibited by antibodies to CD9 (Willett *et al.*, 1997), while the CD82 tetraspanin protein modulates the characteristics of infection with human T-cell leukemia virus type 1 (Pique *et al.*, 2000). Finally, a genetic screen has identified a candidate fusion protein involved in cell membrane merger of yeast gametes, encoded by the *PRM1* gene (Heiman and Walter, 2000). This gene encodes a multi-spanning transmembrane protein that localizes to sites of cell-cell contact when it is deleted, yeast mating is severely impaired. In these mating-impaired cells, electron microscopy indicates that cells are closely apposed but their membranes remain unmerged (Heiman and Walter, 2000).

Table 1.7 Candidate cellular fusion peptide sequences

Candidate fusion protein	Fusion Peptide Sequence	Reference
synaptobrevin (v-SNARE)	QVDEVVDIMRVNVDKYLE	Jahn and Südhof, 1994
mouse fertilin- α	KLVCCTDVRYLPKVKPLHSLQVPY	Huovila <i>et al.</i> , 1996
guinea pig fertilin- α	KLICGIISSIPPIRALFAAIQIP	Huovila <i>et al.</i> , 1996
meltrin- α	GGASRPVIGTNAVSIETNIPQQEGGRI L	Huovila <i>et al.</i> , 1996
<i>C. elegans</i> EFF-1	SMIIPPLPAIVGQGARAICL	Moher <i>et al.</i> , 2002

Myoblast and developmental fusion

Skeletal muscles are multinucleated cells that form during development by the aggregation and fusion of precursor myoblasts. Much investigation of myoblast and developmental cell-cell fusion has utilized genetically manipulated organisms such as *Drosophila* or *Caenorhabditis elegans* (these topics are reviewed in Shemer and Podbilewicz, 2003; Taylor, 2000). Though many of these studies have identified important genes in the regulatory process of developmental fusion, Mohler *et al.* (2002) recently identified a candidate fusion gene from *C. elegans*, named *eff-1* (epithelial fusion failure-1). Several lines of evidence suggest that the EFF-1 protein may be directly involved in membrane fusion. (1) EFF-1 is a Type 1 integral membrane glycoprotein with a large N-terminal ectodomain and lacks coiled coils, but does contain a putative internal fusion peptide (Table 1.7). (2) *eff-1* mutants fail to promote epithelial cell fusion *in vivo*. (3) Sites of cell-fusion initiation in epithelial cells (adherens junctions; Mohler *et al.*, 1998) remain intact in *eff-1* mutants, suggesting that it is the fusion process itself and not the close apposition of cells that is blocked. (4) The ectodomain of EFF-1 contains the predicted consensus sequence for a phospholipase A2 active site, raising the interesting possibility that EFF-1 could alter the lipid packing density of its own or the target membrane during fusion (Shemer and Podbilewicz, 2003).

In mammalian cells, the study of myotube formation in cell culture has indicated some interesting parallels with gamete fertilization. A homolog of fertilin, meltrin- α , has been linked with myotube formation (Yagami-Hiromasa *et al.*, 1995; Huovila *et al.*, 1996). In addition, antibodies against the tetraspanin protein CD9, as well as antibodies against other multi-spanning proteins, delay myotube formation, while overexpression of

CD9 is associated with an increase in fusion activity (Tachibana and Helmer, 1999). The formation of multinucleated myotubes from precursor myoblasts has shown that the early stages of fusion of these differentiating cells requires the transient cell-surface externalization of phosphatidylserine (PS) at sites of cell-cell contact (van den Eijnde *et al.*, 2001). Addition of annexin V (which binds PS) to cells in culture blocks myotube formation, whereas a mutant form of annexin V that is unable to bind PS does not. These authors show that differentiating myoblasts require PS externalization for myotube formation. Though PS externalization is often associated with an early stage of apoptosis, in this case, this observation is not related to apoptosis and is not inhibited by compounds that block the apoptotic cascade (van den Eijnde *et al.*, 2001). These results suggest that PS externalization may modulate the cell-membrane character to create a plasma membrane that is receptive to the cell-cell fusion events that occur early in differentiation. Consistent with this hypothesis is the observation that proliferating myoblast cells were resistant to Sendai virus-mediated cell-cell fusion; however, after differentiation these cells became susceptible to fusion (Hirayama *et al.*, 1999). The timing of myoblast susceptibility to Sendai virus suggests that it may be related to the PS externalization that occurs with myoblast differentiation.

Syncytiotrophoblast fusion

Successful formation of the syncytiotrophoblast layer is essential for embryo implantation and for the formation and function of the maternal-fetal barrier in the placenta (Pötgens *et al.*, 2003). Attempts to discern the factors that promote the initial cell-cell and cell-syncytium fusion events critical for maintenance determined that early

steps of the apoptotic cascade precede syncytial fusion in trophoblasts (Huppertz *et al.*, 1999). Specifically, PS is translocated from the inner to the outer leaflet of the plasma membrane and this event is essential for fusion. Addition of mouse monoclonal antibodies against PS blocks syncytium formation in more than one *in vitro* model system (Lynden *et al.*, 1993; Adler *et al.*, 1995). This feature is similar to what is seen for myoblast fusion, and indeed some investigators have suggested that the candidate myoblast fusion protein meltrin is also involved in syncytial trophoblast fusion, as meltrin- α mRNA was detected in mononuclear blood cells of the placenta (Gilpin *et al.*, 1998).

A more recent discovery suggests that the protein that mediates the essential cell-cell fusion between trophoblasts is the env protein of human endogenous retrovirus (HERV-W), re-named syncytin (Mi *et al.*, 2000). Syncytin is expressed at high levels in the placenta and at low levels in the testis, but is not expressed in other tissues. The provirus that expresses syncytin also contains inactivating mutations in the other viral genes, suggesting selective preservation of the *env* gene (Stoye and Coffin, 2000). Transient transfection of syncytin into cells in culture induced syncytium formation that could be inhibited by the addition of antibodies against syncytin (Mi *et al.*, 2000). However, the promiscuous nature of the fusion ability of syncytin makes it unclear how it can mediate and regulate the precisely timed fusion events that it has been deemed responsible for. Additional regulatory mechanisms are assumed to exist (Pötgens *et al.*, 2003).

1.5 Reoviruses encode membrane fusion proteins

The family *Reoviridae* is a large group of nonenveloped viruses with a genome of 10-12 segments of double-stranded RNA (Nibert and Schiff, 2001). The ten genera within this family display disparate biochemical, structural, and biological properties and illustrate diversity within the family. Highly unusual for a nonenveloped virus, members of four genera of the *Reoviridae* family induce multinucleated syncytium formation *in vivo* and *in vitro* (Table 1.8, and references therein).

Table 1.8 Fusogenic reovirus species

Genus	Fusion	Fusogenic members	Reference(s)
Cypovirus	N	-	
Fijivirus	N	-	
Oryzavirus	N	-	
Coltivirus	N	-	
Phytoreovirus	N	-	
Seadornavirus	N	-	
Rotavirus	Y	Porcine rotavirus (A)	Gelberg <i>et al.</i> , 1990
		Porcine-like (non-A) rotavirus	Theil and Saif, 1985
		Rat rotavirus (non-A)	Vonderfecht <i>et al.</i> , 1984
Orbivirus	Y	Rabbit syncytium virus	Theil and McCloskey, 1991
Aquareovirus	Y	Species groups A-F, including Salmon virus	Winton <i>et al.</i> , 1987; Attoui <i>et al.</i> , 2002
Orthoreovirus	Y	Avian reovirus	Kawamura <i>et al.</i> , 1965
		Muscovy duck reovirus	Kuntz-Simon <i>et al.</i> , 2002
		Nelson Bay virus	Gard and Compans, 1970
		Baboon reovirus	Duncan <i>et al.</i> , 1995
		Reptilian reovirus	Ahne <i>et al.</i> , 1987; Vieler <i>et al.</i> , 1994; Lamirande <i>et al.</i> , 1999; Duncan <i>et al.</i> , 2003

For enveloped viruses, syncytium formation is a direct result of the mechanisms used by these viruses to enter and exit cells (White, 1990). These viruses use a membrane

fusion protein embedded in their lipid envelope to effect virus entry; progeny virus must re-acquire the fusion glycoprotein(s) during budding and egress from an infected cell. Thus, the presence of membrane-embedded virally-encoded fusion proteins on the cell surface often results in the formation of multinucleated cells during the course of infection, and may facilitate cell-cell spread of the virus, promoting pathogenicity. Of the syncytium-inducing members of the family *Reoviridae*, the avian reoviruses (ARV; genus orthoreovirus) have been studied most extensively. For ARV, cell-cell fusion is not an essential component of the virus life cycle, but syncytium formation does promote rapid egress from infected cells (Duncan *et al.*, 1996). The characterization of two avian reovirus strains with different syncytium-inducing abilities indicates that the cell-fusion property is likely associated with increased pathogenicity in the host. However, it is not a requirement for virus replication, as a weakly fusogenic strain of ARV replicated equally well or better than a highly fusogenic strain in cell culture (Duncan and Sullivan, 1998).

Inclusion of potential species into the orthoreovirus genus requires four characteristics: ten segments of dsRNA (grouped into three large, three medium, and four small size classes based on electrophoretic mobility), one polycistronic S-class genome segment, a double-shelled nucleocapsid approximately 85 nm in diameter, and isolation from a vertebrate host (Nibert and Schiff, 2001). The prototype species of the genus orthoreovirus, mammalian reovirus (MRV; 4 serotypes; Nibert and Schiff, 2001; Attoui *et al.*, 2001), like most nonenveloped viruses, is non-fusogenic. However, a subgroup of orthoreoviruses is fusogenic (Duncan, 1999; Fig 1.6). These include the avian reoviruses (77 isolates, all fusogenic), two atypical mammalian reoviruses (Nelson Bay virus [NBV]; Baboon reovirus [BRV]), and a recently described species, a reptilian reovirus




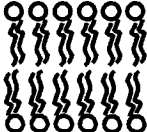

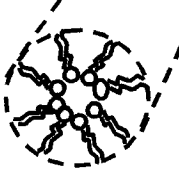
(RRV) isolated from a python (Fig 1.6; Table 1.8, and references therein). Syncytium-inducing reptilian reoviruses have also been isolated from other snakes (rattlesnake, tree boa, ratsnake, viper), iguanas, and lizards (Blahak *et al.*, 1995; Lamirande *et al.*, 1999; Vieler *et al.*, 1994, and references therein) and preliminary descriptive analyses suggest that these as-yet-unclassified agents may also be the same species (Blahak *et al.*, 1995; Duncan *et al.*, 2003).

The polycistronic S-class segment common to all orthoreoviruses has been shown to influence the pathogenic properties of the virus. For the non-fusogenic MRV, $\sigma 1s$ (a non-structural protein encoded by the MRV bicistronic S1 genome segment) is implicated in G2/M cell-cycle arrest (Poggioli *et al.*, 2001); for the fusogenic orthoreoviruses, the first open reading frame of the polycistron encodes the fusion protein of ARV, NBV, and BRV (p10, p10, and p15, respectively; Shmulevitz and Duncan, 2000; Dawe and Duncan, 2002). For RRV, this first open-reading frame is also predicted to encode a cell-fusion protein (p14), though no direct sequence similarity exists between this putative fusion protein and those previously characterized (Duncan *et al.*, 2003). The study described in this thesis was undertaken to confirm and characterize the cell-cell fusion ability of the reptilian reovirus putative fusion protein, p14.

A novel member of the reovirus fusion-associated small transmembrane (FAST) protein family, p14, was identified and characterized. Structural features/motifs that are essential for the mechanism of p14-mediated membrane fusion include the following: Type III ($N_{\text{exo}}/C_{\text{cyt}}$) integral membrane association, N-terminal modification by myristate, and an internal fusion peptide motif. The role of these structural features, of p14-

homomultimerization, and of cell surface localization to distinct microdomains provide a framework for an hypothesis of how p14 facilitates membrane merger.

1.6 Figures

Membrane Lipid	Molecular Shape	Structure in Water
A Lysophosphatidylcholine		
B Phosphatidylcholine		
C Phosphatidylethanolamine		



 represents a an inverted cone-shaped lipid with one fatty acid tail
 represents a membrane lipid with two fatty acid tails

Fig 1.1 The molecular shape of a membrane lipid influences the structure it forms in an aqueous environment. **(A)** Lysophosphatidylcholine and other inverted cone lipids prefer micellar structures. **(B)** Phosphatidylcholine and other cylindrical lipids prefer the planar bilayer phase. **(C)** Phosphatidylethanolamine and other cone lipids prefer the non-bilayer hexagonal II phase.

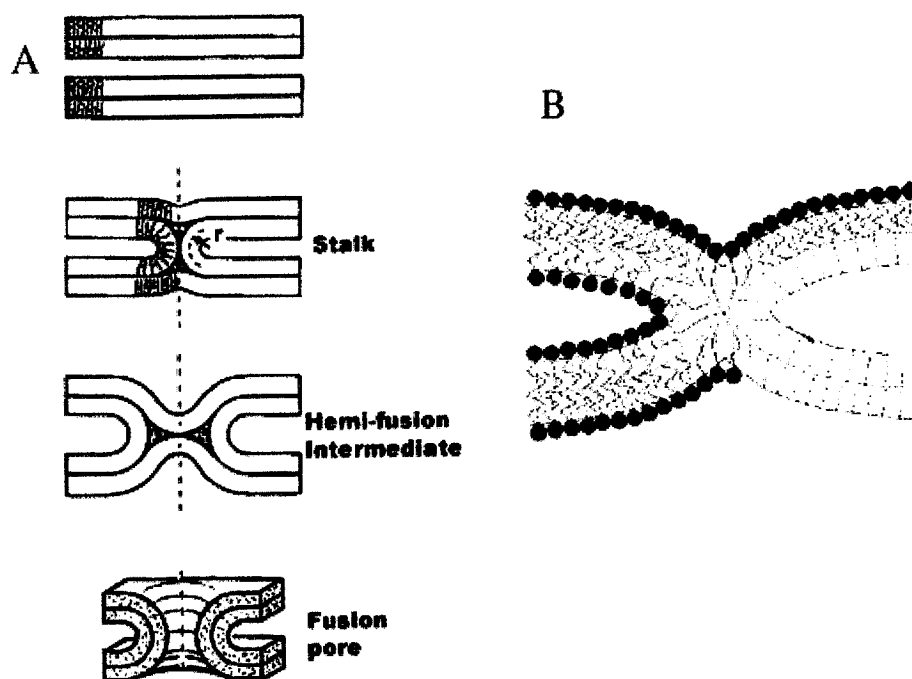


Fig 1.2 The stalk-pore model of membrane fusion. **(A)** This model, originally proposed by Kozlov and Markin (1983), suggests that close apposition of two bilayers leads to the formation of a stalk intermediate where the two outer leaflets of the membrane have merged. Contact, but not merger, of the inner leaflets, results in a second intermediate that is referred to as the hemi-fusion diaphragm or trans-monolayer contact. As this diaphragm widens, a fusion pore is formed that allows intermixing of lipid and aqueous compartments. **(B)** The new stalk structure proposed by Kozlovsky and Kozlov (2002) does not have any void space in the structure and is more energetically favorable. Reprinted with permission from Chemical Reviews, Vol 103, Blumenthal *et al.* (2003). ©2003 American Chemical Society.

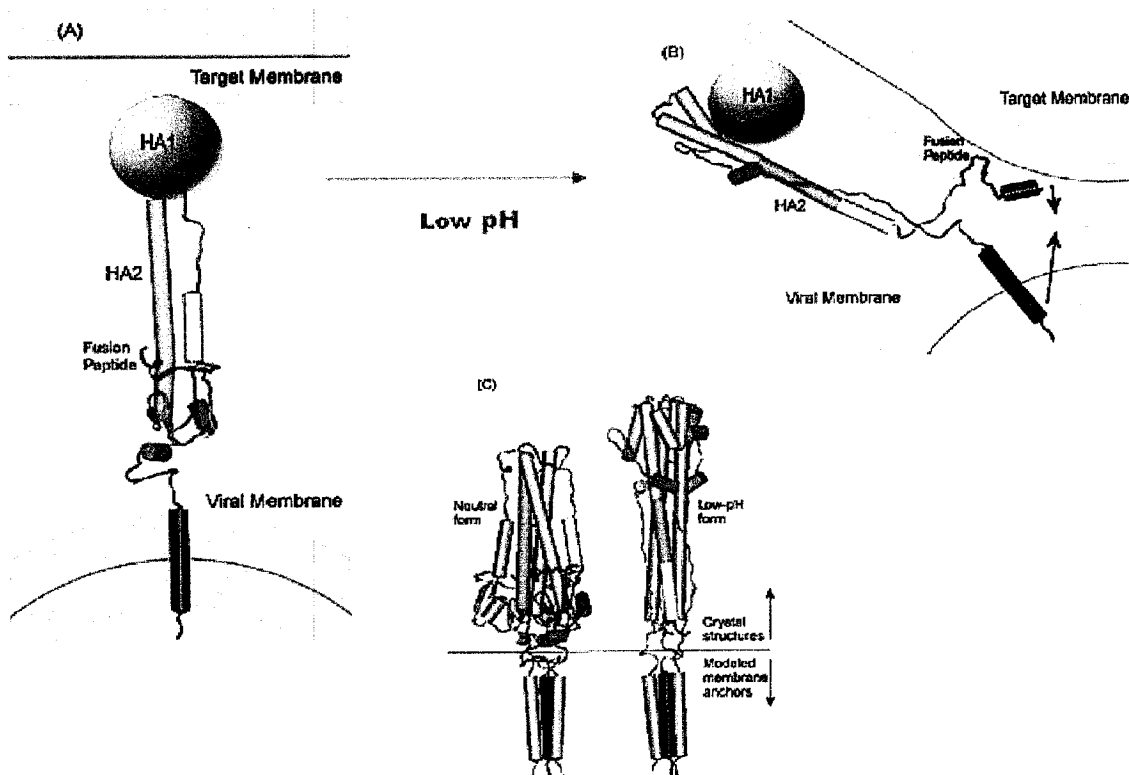


Fig 1.3 Influenza hemagglutinin (HA) undergoes conformational rearrangement in response to acid pH. For clarity, only one monomer is shown in A and B, and the HA1 domain is depicted as a sphere (A and B) or not at all (C). **(A)** The native form of HA (Wilson *et al.*, 1981). **(B)** The low-pH structure of HA (Chen *et al.*, 1999). The structural remodeling reaction was inferred from these static structures. HA1 dissociates from the HA2 subunit. HA2 rearranges as follows. (1) The green loop adopts a helical conformation, while the N-terminal region of the cyan α -helix converts to a loop, shifting the coiled coil. (2) The C-terminal region of the cyan α -helix reorients anti-parallel to the new coiled coil. (3) The connecting region between the cyan α -helix and the transmembrane domain is extended. (4) Residues from both the N-terminal and C-terminal regions combine to form a stabilizing cap-structure. **(C)** The trimeric form of HA at neutral and acid pH. Reprinted with permission from Chemical Reviews, Vol 103, Blumenthal *et al.* (2003). ©2003 American Chemical Society.

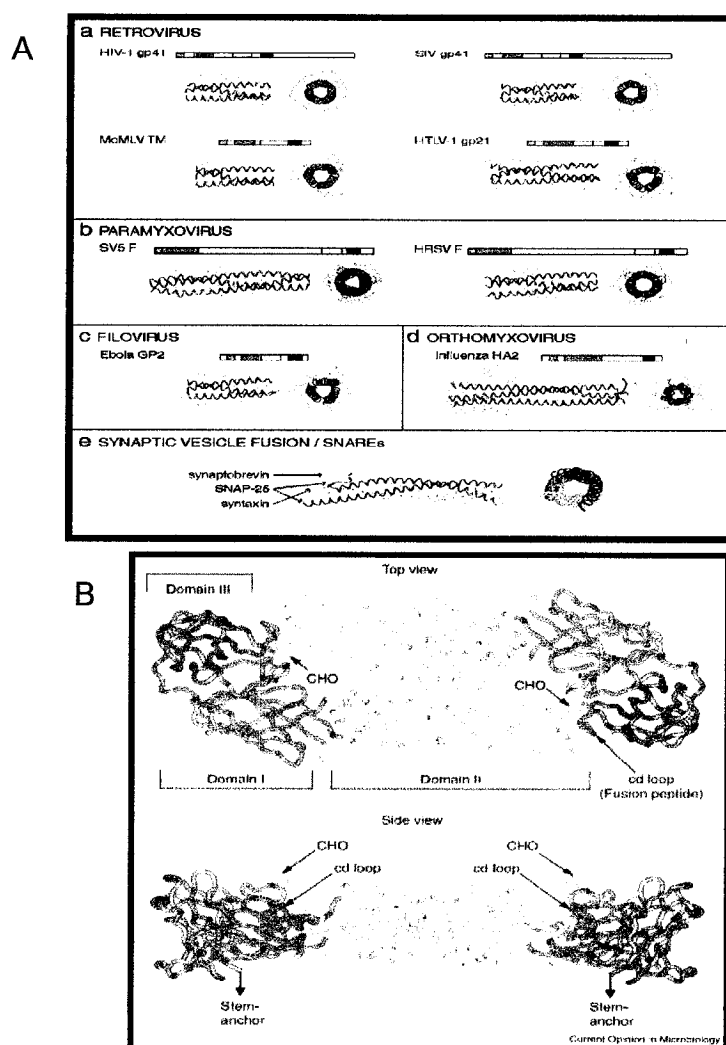


Fig 1.4 The structure(s) of representative Class I and Class II viral fusion proteins. **(A)** The protein cores of Class I viral and intracellular membrane fusion proteins are shown. The N-terminal heptad repeat (blue), the C-terminal heptad repeat (yellow), the fusion peptide (red), and the transmembrane domain (black) are indicated in the primary structure. The tertiary structures (side view and end view both pictured) are comprised of the heptad-repeat regions that form the central coiled coil; however, both the fusion peptide and transmembrane domains would be expected to reside at the same end of the structure (right side as pictured in side view of coiled coil). Reprinted, with permission, from the Annual Review of Biochemistry, Vol 70, Eckert and Kim, ©2001, by Annual Reviews www.annualreviews.org. **(B)** The native structure of a Class II fusion protein (tick-borne encephalitis virus E protein). The three domains, location of the fusion peptide (within the cd loop, buried by the carbohydrate chain on Asn 154 of the opposite monomer), and point of stem anchor (transmembrane domain) attachment are indicated. Reprinted from Current Opinion in Microbiology, Vol 4, Heinz and Allison, "The machinery for flavivirus fusion with host cell membranes", pp450-455, ©2001, with permission from Elsevier.

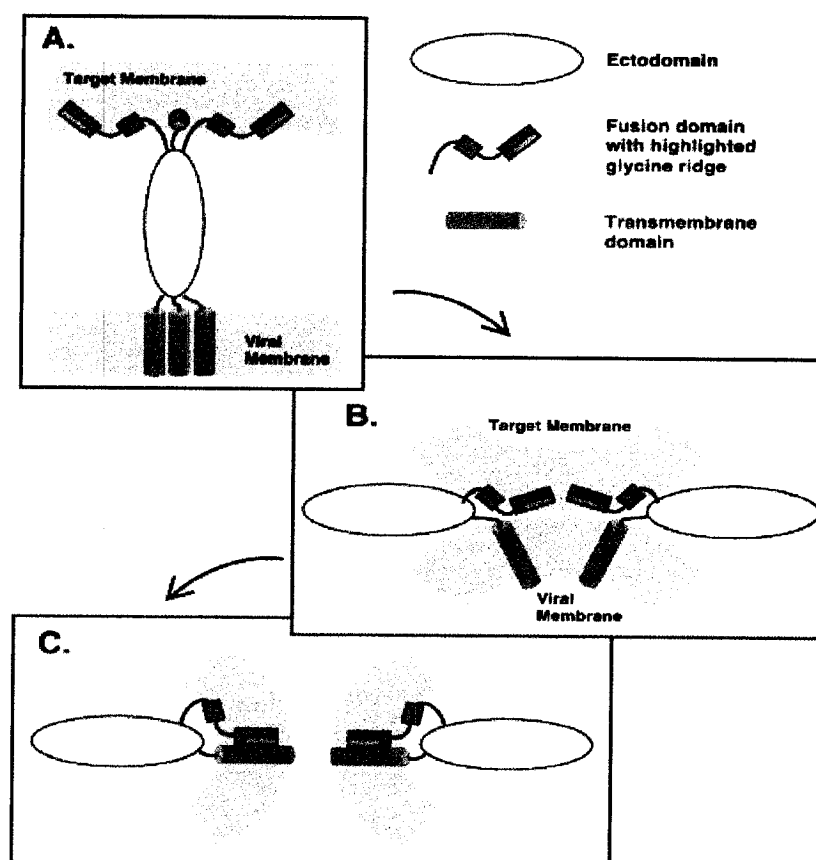


Fig 1.5 The boomerang model. **(A)** Exposure to low pH induces a conformational rearrangement in HA that reorients the V-shaped fusion peptide towards the target membrane, where it inserts. Membrane insertion triggers discrete secondary-structural alteration of the fusion peptide and is thermodynamically favorable. **(B)** Refolding at the C-terminal hinge of the HA ectodomain tilts the molecule and pulls the two membranes into close apposition. Hemifusion is predicted to occur at this stage. **(C)** The V-shaped fusion peptide is proposed to interact with the transmembrane domain using the glycine ridge. This interaction facilitates opening of the fusion pore. Reprinted from *Biochimica et Biophysica Acta – Biomembranes*, Vol 1614, Issue 1, Tamm, “Hypothesis: spring-loaded boomerang mechanism of influenza hemagglutinin-mediated membrane fusion”, pp14-23, ©2003, with permission from Elsevier.

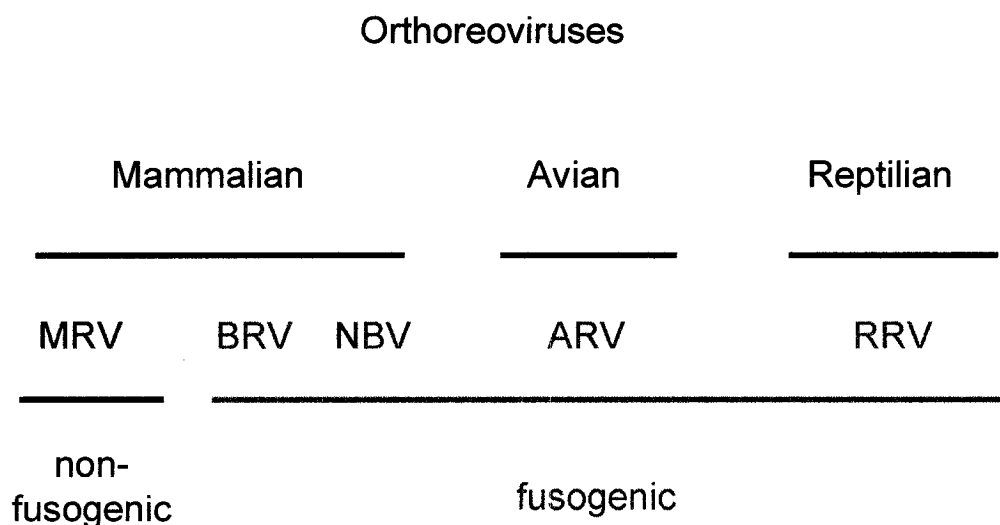


Fig 1.6 Members of the genus orthoreovirus. The genus is subdivided into the fusogenic and non-fusogenic subgroups. Of the fusogenic orthoreoviruses, there are four species: avian reovirus (ARV), Nelson Bay virus (NBV), Baboon reovirus (BRV), and Reptilian reovirus (RRV). The non-fusogenic orthoreoviruses include the prototype species, mammalian reovirus (MRV). Reprinted from *Virology*, Vol 260, Duncan, "Extensive sequence divergence and phylogenetic relationships between the fusogenic and nonfusogenic orthoreoviruses: a species proposal", pp316-328, ©1999, with permission from Elsevier.

Chapter 2

Materials and Methods

2.1 Cells and Virus

Vero and QM5 cells (Antin and Ordahl, 1991) were maintained at 37°C in a 5% CO₂ atmosphere in medium 199 with Earle's salts containing 100 U of penicillin and streptomycin per ml and 5% or 10% heat-inactivated fetal bovine serum (FBS). Sf21 (*Spodoptera frugiperda*) cells used for expression of p14 protein from recombinant baculoviruses were obtained from Lois Murray (Dalhousie University) and maintained in suspension at 27°C in a shaker incubator in SF900II medium (Life Technologies) supplemented with 3% heat-inactivated fetal bovine serum. N-BP-2 cells (CHO cells with a defect in the site-2 protease needed to activate the SREBP-responsive genes, and which cannot synthesize cholesterol *de novo* unless the transfected site-2 gene is induced [Pai *et al.*, 1998]) were maintained in DMEM supplemented with 5% FBS, oleate, mevalonate, and cholesterol. N-BP-2 cells were obtained from Neale Ridgway (Dalhousie University). 12CA5 anti-HA mouse hybridoma cells (obtained from Mark Naghtigal, Dalhousie University) were grown in RPMI 1640 medium containing 10% heat-inactivated fetal bovine serum and 100 U of penicillin and streptomycin per ml.

Reptilian reovirus isolated from the kidney of a python (*Python regius*) (Ahne *et al.*, 1987), was obtained from W. Ahne (University of Munich, Munich, Germany). The virus was passaged at low multiplicity of infection (MOI) in Vero cells at 27°C.

2.2 Materials

The p14 peptide was synthesized by Dalton Chemical Laboratories (Toronto, Ontario) in two forms: myristyl-GSGPSNFBHAPGEAIVTGLEKGADKVAGT-amide and acetyl-GSGPSNFBHAPGEAIVTGLEKGADKVAGT-amide. Both were purified to >95% purity by high-performance liquid chromatography. All lipids were purchased from Avanti Polar Lipids. Lubrol was purchased from Serva; all other detergents and cholesterol-depleting reagents (methyl- β -cyclodextrin, lovastatin and U18666A) were from Sigma-Aldrich.

2.3 Cloning and Sequencing

The procedure for cDNA synthesis and cloning of reoviral genome segments is described in detail elsewhere (Duncan, 1999). Briefly, reptilian reoviral genomic dsRNA was isolated from concentrated virus (Duncan *et al.*, 1995). After polyA-tail addition to the RNA, cDNA was created using an oligo(dT)-*NotI* primer and Superscript RT (Life Technologies Inc.). Amplified cDNA was isolated, *NotI*-digested, gel-purified, cloned into the *NotI* site of pBlueScriptIISK (pBSK) (Stratagene), and transformed into *E. coli* DH5 α cells made competent by CaCl₂ treatment. Clones containing cDNA inserts the approximate size of the full-length S-class genomic dsRNA were sequenced completely in both directions (Robarts Research Institute DNA Sequencing Facility, London, Ontario). In this manner, full-length cDNA corresponding to the S1 genome segment of RRV was cloned into pBSK. The S1 genome segment clone was then subcloned into the mammalian expression vector pcDNA3 (Invitrogen) for further analysis.

The full-length S1 genome segment, and each of the two open reading frames on this genome segment (p14 and σ C), were subcloned into pcDNA3 (Invitrogen) using the restriction sites *HindIII* and *EcoRI* (primers in Table I). The pcDNA3-p14 clone was then used as a template to generate the following tagged and site-specific substituted p14 constructs. Two HA-epitope tags were added in tandem (separated by a single glycine linker) to either the C terminus of p14 (p14-2HAC) or to the N-terminal domain (p14-2HAN) following amino acid 7 (to avoid alteration of the myristylation consensus sequence). Each 2HA-tagged construct was generated in two steps, by first generating a singly-tagged clone (p14HAN or p14HAC), and then using the singly-tagged clone as the template for addition of the second tag. P14-HAN, p14-HAC and p14-2HAC were created using 50 ng of template, 2 U of *Vent* DNA polymerase (NEB), and 100 ng of each primer; p14-2HAN was created using 50 ng of template, 2.5 U of Cloned *Pfu* DNA polymerase (Stratagene), and 125 ng of each primer, both according to the instructions of the respective manufacturers (primers in Table II). To create p14-GFP, the p14 ORF was amplified by PCR using primers in Table I and inserted into the *HindIII/BamHI* restriction sites of the restriction enzyme-digested pEGFP-N1 vector (Clontech).

p14 constructs containing site-specific amino acid substitutions were created using the Quick Change Site-Directed Mutagenesis Kit (Stratagene). Each reaction used 50 ng of template DNA, 2.5 U of *Pfu Turbo* DNA polymerase, and 125 ng of each primer (see Table III). After amplification, PCR products were digested with 10 U *DpnI* to remove the methylated template DNA. The unmethylated product was transformed into *E. coli* DH5 α cells made competent by CaCl₂ treatment.

A recombinant baculovirus expressing the p14 fusion protein under the control of the polyhedrin promoter was created using the Bac-To-Bac Baculovirus Cloning and Expression System (Life Technologies). The p14 ORF was subcloned into the pFastBac1 transfer vector by PCR amplification using primers that incorporated an in-frame enterokinase-cleavable C-terminal 6xhistidine tag and restriction sites for *Sall* and *NotI* into the PCR product (primers in Table I). pFastBac1-p14-6His was transformed into *E. coli* DH10BAC competent cells (Life Technologies). DH10BAC cells contain a baculovirus shuttle vector (bacmid). Site-specific transposition of the pFastBac1-p14-6His expression cassette into the bacmid creates a recombinant baculovirus. The bacmid DNA was isolated from *E. coli* using alkaline lysis, and subjected to agarose (0.5%) gel electrophoresis for 12 hours at 23 volts. PCR analysis of the transposition region of the recombinant bacmid using M13/pUC forward and reverse primers (Life Technologies) was used to confirm insertion of the p14-6His ORF. Five μ l of p14-6His bacmid DNA and 6 μ l CellFECTIN (Life Technologies) in SF900II medium (Life Technologies) were used to transfect subconfluent Sf21 cells for 5 hours at 27 °C. The transfection medium was removed and replaced with SF900II medium supplemented with 3% fetal bovine serum. After 3 days at 27°C, the recombinant baculovirus-containing supernatant was harvested and passaged 3 times in Sf21 cells using an MOI of 0.01 – 0.1. p14-6xHis recombinant baculovirus titer was determined by plaque assay.

All pcDNA3 and pFastBac1 clones were confirmed by dideoxy sequencing (Thermo Sequenase Radiolabeled Terminator Cycle Sequencing Kit (USB)) according to the manufacturer's instructions. pEGFP clones were confirmed by sequencing at Robarts Research Institute, DNA Sequencing Facility (London, Ontario). A mammalian

expression vector containing the cDNA for placental alkaline phosphatase (PLAP) (Berger *et al.*, 1987) was generously donated by D. Brown (State University of New York). The ARV p10-2HAN clone (Shmulevitz and Duncan, 2000) was generously donated by M. Shmulevitz (this lab).

2.4 p14 protein and antiserum production

Sf21 cells were grown to a cell density of approximately 3.25×10^6 /ml and then infected with p14 recombinant baculovirus at a MOI of 0.05 to 0.08. At 48 hours post-infection, infected cells were harvested and centrifuged at $1000 \times g$ for 10 minutes.

The resulting cell pellet was lysed with extraction buffer (50 mM sodium phosphate, 300mM NaCl, 1.6% Igepal [NP-40], pH 7.0). Insoluble debris was pelleted and the supernatant, containing p14, was then added to TALON® Metal Affinity Resin (Clontech) and shaken gently for 3 hours at 4° C to begin initial purification. The resin was then washed with extraction buffer twice to remove unbound protein and p14 eluted from the resin with elution buffer (50 mM sodium phosphate, 300 mM NaCl, 150 mM imidazole, 1.6% Igepal [NP-40], pH 7.0). The eluate was dialyzed against 50 mM HEPES, 150 mM NaCl, 1.6% Igepal [NP-40], pH 7.0 at 4°C for 12 hours and further purified using HiTrap SP HP ion-exchange columns (Amersham Pharmacia Biotech). p14 was eluted from the column using 50 mM HEPES, 300 mM NaCl, 1.6% octylglucoside (OG). The p14 concentration was determined by the Bio-Rad DC protein assay and routinely adjusted to approximately 1 mg/ml. The purity of the protein, which ranged from 90 to 95%, was estimated by sodium-dodecyl-sulfate polyacrylamide-gel electrophoresis (SDS-PAGE, 15% acrylamide) and silver-staining (Blum *et al.*, 1987).

For p14 antiserum production, 500 μ g of the p14 protein was used for injection into New Zealand White rabbits. For the initial injection, 500 μ l of p14 protein (1 mg/ml) in elution buffer was mixed with 500 μ l of Freund Complete Adjuvant (Sigma) 30 minutes before being administered at three sites (two intramuscular and one subcutaneous). For the remaining 5 injections, protein was mixed with Freund Incomplete Adjuvant (Sigma). Injections were administered every 6 weeks to boost the antibody response against p14. Rabbit polyclonal antiserum raised against avian reovirus-176 was previously described (Duncan *et al.*, 1996).

For the production of 12CA5 anti-HA (IgG2b κ), the cell supernatant from 12CA5 mouse hybridoma cells was concentrated by precipitation with 35% ammonium sulfate (approximate concentration of anti-HA, 1.6 μ g/ μ l). IgG2b isotype control was purchased from Cedarlane Laboratories. A mouse monoclonal anti-placental alkaline phosphatase (PLAP; Clone A89) was purchased from Dako.

2.5 p14 proteoliposome production (for chemical cross-linking)

The molar ratio of lipids in the liposome formulations used here was 60:30:10 of dioleoylphosphatidylcholine (DOPC) : dioleoylphosphatidylethanolamine (DOPE) : cholesterol. All lipids were dissolved in chloroform, mixed in a 100-ml pear flask containing glass beads and dried under vacuum for 2 hours. The resulting lipid film was hydrated by vigorous vortexing in 10 mM HEPES (pH 7.4) and 150 mM NaCl at room temperature to generate 20 mM multilamellar vesicles. The liposomes were passed 20 times through a 400-nm polycarbonate filter (Nucleopore) using a small-volume extrusion apparatus (Avestin). p14 was incorporated into liposomes based on the

detergent depletion method (Rigaud *et al.*, 1988). Briefly, solubilization of liposomes (4.86 mg/ml) by octylglucoside (OG) was monitored by turbidimetry (optical density at 600 nm) and 1.2 % OG was used for the procedure. It has been demonstrated that optimal proteoliposome formation rapidly occurs at the onset of liposome solubilization by OG (Rigaud *et al.*, 1995). p14 protein and liposome suspensions (in 10 mM HEPES [pH 7.4], 150 mM NaCl, 1.2 % OG) were vigorously mixed (at a final lipid concentration of 6.66 mM, a final p14 protein concentration of 0.1 mg/ml, and a final lipid:protein ratio of 48.6:1) and incubated at room temperature for 30 minutes. The detergent was removed by a multi-step dialysis at 4 °C against 500 mL buffer containing 2 g of Bio-Beads-SM-2 adsorbent (Bio-Rad). P14-proteoliposomes were isolated using sucrose density gradient ultracentrifugation.

2.6 Transfection and Cell Staining

Vero cells or QM5 cells (60 - 70% confluency) were transfected with 1 µg of DNA and 2 µl of Lipofectamine (Invitrogen) per well of a 12-well cluster plate, according to manufacturer's instructions. Co-transfections used the same total amount of DNA and lipofectamine, and a 1:1 ratio of the two clones unless otherwise indicated. Cell monolayers were fixed with methanol and stained at various times post transfection with Wright-Giemsa. Alternatively, fixed cell monolayers were immunostained as follows: cells were blocked with whole goat IgG (1:1000) in Hank's buffered saline solution (HBSS) for 30 minutes at room temperature, then primary antibody (1:800 rabbit polyclonal anti-p14) was adsorbed to cells for 45-60 minutes at room temperature. After primary antibody binding, cell monolayers were washed six times in HBSS and

secondary antibody (1:800 alkaline phosphatase-conjugated goat anti-rabbit [Jackson Immunochemicals] in blocking buffer) was adsorbed to cells, washed as described above, and substrate BCIP/NBT was added to allow colour development. Stained cells were visualized on a Nikon Diaphot inverted microscope at a magnification of 200x. Image-Pro Plus software (v.4.0) was used to capture images of stained cells.

2.7 Syncytial Indexing

The relative ability of various p14 mutants to mediate syncytium formation was quantified by a syncytial index assay. Giemsa-stained cell monolayers were visualized on a Nikon Diaphot inverted microscope at a magnification of 100x. The numbers of syncytial foci and syncytial nuclei present in 5 random fields of view were determined by microscopic examination of Giemsa-stained transfected or co-transfected cell monolayers at 100x magnification. Results were reported as the mean \pm the standard error (SE) from three separate experiments. The relative fusion ability of each compared to authentic p14 was then graphed using Slide Writer 4.0.

2.8 Antibody Inhibition

For antibody inhibition, two-fold serial dilutions of complement-fixed polyclonal anti-p14 antiserum or normal rabbit serum were added to the medium of p14-transfected cells at 4 hours post transfection. At 14-18 hours post transfection, the cell monolayers were fixed with methanol, stained with Wright-Giemsa, and examined for the presence of multinucleated syncytia.

2.9 *In vitro* transcription and translation

The full-length S1 genome segment, p14 ORF, σ C ORF, and p14 constructs containing site-specific substitutions were transcribed from 1 μ g of each *EcoRI*-linearized pcDNA3 clone using bacteriophage T7 RNA polymerase (Life Technologies). Each uncapped transcription reaction was incubated for 2 hours at 37°C. 250 ng of each RNA transcript was then translated in the presence of [3 H]-leucine (1 μ Ci per reaction) using nuclease-treated rabbit reticulocyte lysates (Promega) according to the manufacturer's instructions. *In vitro* translation reactions were then subjected to SDS-PAGE (15%), and proteins visualized by DMSO-PPO fluorography (Bonner, 1984).

2.10 Radiolabeling

p14-transfected Vero or QM5 cells in 60 mm tissue-culture dishes were labeled for 1 hour with 50 μ Ci [3 H]-leucine (Amersham Pharmacia Biotech) per ml of leucine-free medium (Sigma) at 18-24 or 12-16 hours post transfection. Alternatively, Vero cells were labeled at 18 hours post transfection for 3 hours with 20 μ Ci [3 H]-myristic acid (Amersham Pharmacia Biotech) per ml of Earle's MEM (Life Technologies). Radiolabeled cell monolayers were washed with HBSS and lysed in cold radioimmunoprecipitation assay (RIPA) buffer (50 mM Tris-HCl pH 8, 150 mM NaCl, 1 mM EDTA, 1% [v/v] Igepal [Sigma] 0.5% [w/v] sodium deoxycholate, 0.1% [w/v] SDS) containing protease inhibitors (200nM aprotinin, 1 μ M leupeptin, and 1 μ M pepstatin [Sigma]). The nuclei from radiolabeled cell lysates were pelleted for 2 minutes at 13,000 x g in a benchtop microcentrifuge, and the supernatant reserved for immunoprecipitation or direct gel analysis.

2.11 Pulse-labeling

For pulse-chase analysis of p14, transfected cells were radiolabeled for 15 minutes at 18-24 (Vero cells) or 12-16 (QM5 cells) hours post transfection, and chased for the indicated times with Earles' medium containing unlabeled leucine at 3000 times the concentration of [^3H]-leucine. Pulse-labeling of p10-2HAN-transfected QM5 cells was performed at 24 hours post transfection. Cell monolayers were washed with HBSS and lysed at 4°C in radioimmunoprecipitation assay (RIPA) buffer. For co-immunoprecipitation experiments, radiolabeled cells were removed from the tissue-culture dish by treatment with 50 mM EDTA (in phosphate-buffered saline [PBS]) for 15 minutes at room temperature, pelleted at 500 x g for 5 minutes, and lysed in 500 μl of either RIPA buffer, TxTNE buffer (50 mM Tris-HCl pH 8, 150 mM NaCl, 1mM EDTA, 1% [v/v] Triton X-100), or NpTNE buffer (50 mM Tris-HCl pH 8, 150 mM NaCl, 1mM EDTA, 1% [v/v] Igepal [NP-40]) containing protease inhibitors. In a preliminary experiment, the total cell protein in each 10-cm dish (0.5 ml lysate) was calculated using a modified Lowry assay according to the instructions of the manufacturer (BioRad DC), and the detergent:protein ratio calculated to be at minimum 25:1 (Ostermeyer *et al.*, 1999).

2.12 Membrane fractionation

QM5 cells transfected at 60-70 % confluence were labeled at 14 hours post transfection for 1 hour with 50 μCi [^3H]-leucine as above. After labeling, cells were washed with PBS and lifted off the tissue culture dish by treatment with 50 mM EDTA for 10 minutes. Cells were pelleted at 500 x g, and resuspended in 1 ml PBS. Cells were disrupted by 20

passes through a 30-gauge needle, and unbroken cells and debris were removed by centrifugation at 700 x g for 2 minutes. The supernatant was used to recover the membrane fraction of transfected cells by ultracentrifugation at 100,000 x g for 1 hour. The soluble fraction was removed and mixed 1:1 with 2x RIPA buffer, the membrane pellet was resuspended by vortexing in 1 ml 1x RIPA buffer, and both were immunoprecipitated as described below. For removal of peripherally associated membrane proteins, the membrane pellet was treated with either a salt concentration of salt (500 mM NaCl) or high pH (100 mM Na₂CO₃, pH 11.4) (Fujiki *et al.*, 1982) on ice for 30 minutes, followed by a second centrifugation at 100,000 x g for 1 hour to recover integrally associated membrane protein. All soluble and membrane fractions were then immunoprecipitated.

2.13 Immune precipitation

[³H]-leucine- or [³H]-myristate-labeled samples were diluted to a 1-ml volume in RIPA buffer. After clearing the lysate using a 1:100 dilution of normal rabbit serum and IgGSORB (The Enzyme Center), p14 was immune precipitated for 1 hour on ice using a 1:100 dilution of rabbit polyclonal anti-p14, normal rabbit serum, mouse monoclonal (IgG2b) anti-HA, or a mouse IgG2b isotype control. σC was immune precipitated using a 1:200 dilution of rabbit polyclonal anti-avian reovirus-176. Antibody-antigen complexes were recovered using fixed *Staphylococcus aureus* cells (Harlow and Lane, 1988) (used in the experiments shown in Chapters 2 and 3) or using IgGSORB (The Enzyme Center) (used in the experiments shown in Chapters 4 and 5). Pellets were washed three times with RIPA buffer, and immune complexes released by boiling in SDS

protein-sample buffer for 5 minutes. Immune precipitated protein and labeled lysates were subjected to SDS-PAGE (15% acrylamide) and visualized by DMSO-PPO fluorography.

2.14 Co-immune precipitation

[³H]-leucine-labeled transfected-cell lysates were diluted to a 0.5-ml volume in RIPA, TxTNE, or NpTNE buffer. After clearing the lysate using a 1:100 dilution of normal rabbit serum or an IgG2b isotype control, immune precipitations were performed for 1 hour on ice using a 1:100 dilution of rabbit polyclonal anti-p14, normal rabbit sera, monoclonal anti-HA, or an IgG2b control. Antibody-antigen complexes were recovered using IgGSORB (The Enzyme Center), pellets were washed three times with RIPA, TxTNE, or NpTNE buffer, and immune complexes released by boiling in SDS protein-sample buffer for 5 minutes. Immune precipitated proteins were subjected to SDS-PAGE (15% acrylamide) and visualized by DMSO-PPO fluorography.

2.15 Cell Staining with fluorescent dyes

QM5 cells were seeded in 6-well tissue-culture plates containing 18-mm square coverslips (No. 1 thickness), and transfected 20-24 hours after seeding as described above. Six hours post transfection, cell monolayers were washed twice with HBSS and either fixed with ice-cold methanol for staining of intracellular p14, or surface-stained. Permeabilized cells were blocked with either whole goat or rat IgG (1:1000) in HBSS for 30 minutes at room temperature, then primary antibody (1:800 rabbit polyclonal anti-p14

or 1:200 mouse monoclonal [IgG2b] anti-HA in blocking buffer) was adsorbed to cells for 45-60 minutes at room temperature. After primary antibody binding, cell monolayers were washed six times in HBSS and secondary antibody (1:400 FITC-conjugated goat anti-rabbit or 1:200 FITC-conjugated rat anti-mouse [Jackson Immunochemicals] in blocking buffer) was adsorbed to cells and washed as described above. Non-permeabilized cells were stained as above with the following exceptions: dilutions of 1:200 rabbit anti-p14, 1:100 mouse anti-HA, 1:100 FITC goat anti-rabbit, or 1:50 FITC rat anti-mouse (all in blocking buffer) were used and all staining was performed at 4°C; after primary antibody addition and washing, cells were fixed with ice-cold methanol and washed before secondary antibody addition. After the final HBSS wash, stained cells on coverslips were mounted on glass slides using fluorescence mounting medium (Dako). Stained cells were visualized and photographed using the 100x objective of a Zeiss LSM510 scanning argon-laser confocal microscope.

2.16 Co-fluorescence using p14-GFP

QM5 cells were seeded in 6-well tissue-culture plates containing 18-mm square coverslips (No. 1 thickness), and transfected with p14-GFP 20-24 hours after seeding as described above. At 15 hours post transfection, Brefeldin A (1 µg/ml in DMSO; Epicentre Technologies) or DMSO alone was added to cells. At 16-20 hours post transfection, cell monolayers were washed twice with HBSS and fixed with ice-cold methanol. Permeabilized cells were blocked with whole rat IgG (1:1000, Jackson Immunochemicals) in HBSS for 30 minutes at room temperature, following which an organelle-specific mouse monoclonal IgG1 antibody (1:1000 of either anti-calnexin [BD

Transduction Laboratories], anti- β -COP [Sigma], or anti-TGN38 [BD Transduction Laboratories] in blocking buffer) was adsorbed to cells for 45-60 minutes at room temperature. After primary antibody binding, cell monolayers were washed six times in HBSS and secondary antibody (1:1000 rat anti-mouse IgG1:biotin [Serotec] in blocking buffer) was adsorbed to cells and washed as described above. Streptavidin:phycoerythrin-Texas Red (1:2000) (Serotec) was adsorbed to cells and washed as described above. After the final HBSS wash, stained cells on coverslips were mounted on glass slides using fluorescence mounting medium (Dako), and visualized and photographed using the 100x objective of a Zeiss LSM510 scanning argon/neon-laser confocal microscope.

Alternatively, p14-GFP-transfected cells (some pretreated with 20 mM methyl- β -cyclodextrin [M β CD] in serum-free medium at 37°C for 20 minutes) were analyzed for detergent resistance before fixation. Individual coverslips were washed at 14 hours post transfection, and treated with either 0.5% (w/v) Lubrol or 0.5% (v/v) Triton X-100 (in HBSS buffer) by rapid immersion of the coverslip into the detergent-containing buffer 3 times for 5 seconds each. Coverslips were washed twice with HBSS and fixed with methanol at -20°C for 5 minutes. Cells on coverslips were mounted on glass slides using fluorescence mounting medium (Dako), and visualized and photographed using the 40x or 100x objective of a Zeiss LSM510 scanning argon-laser confocal microscope. Each image was recorded using the same capture parameters to best represent the amount of p14-GFP fluorescence remaining after the treatment.

2.17 Chemical Cross-linking

All cross-linking reagents were purchased from Pierce. 10-cm dishes of p14-transfected QM5 cells were radiolabeled at 13 hours post transfection. Cells were washed in PBS, removed from the tissue-culture dish by treatment with 50 mM EDTA (in PBS) for 15 minutes at room temperature, pelleted at 500 g for 5 minutes, and resuspended in 200 μ l PBS. When membrane-impermeable reagents were used, 1% NP40 was added. When an amine-reactive reagent was used (DTSSP, EGS, DST, described in Table 4.1), each cell suspension was treated with the indicated cross-linker for 2 hours at 4°C. Following incubation, each reaction was quenched with 50 mM Tris (pH 7.4) for 15 minutes at 4°C. For APG (described in Table 4.1), the first step of the cross-linking reaction (slow, arginine-reactive) was performed for 2 hours at room temperature; after UV photoactivation the fast non-specific second step was performed on ice for 15 minutes. All samples were lysed in RIPA buffer and immune precipitated with anti-p14. Each reaction was boiled in SDS protein-sample buffer (+/- β -mercaptoethanol for DTSSP reactions) for 5 minutes, and subjected to gel analysis as described above.

Duplicate samples of purified p14 (1.2 mg/ml in 50 mM HEPES, 300 mM NaCl, and 1.6% OG) were treated with the indicated amount of DTSSP for either 30 minutes at room temperature or 2 hours at 4°C. To avoid hydrolysis, powdered DTSSP was added to the reaction directly. Following incubation, the reaction was quenched with 50 mM glycine for 20 minutes at room temperature. Alternatively, p14-proteoliposomes (approximately 0.25 mg/ml p14), purified by sucrose density gradient analysis, were treated with the indicated amount of DTSSP, and the reaction incubated and quenched as described above. Each reaction was boiled in SDS protein-sample buffer (without β -

mercaptoethanol unless indicated) for 5 minutes, subjected to SDS-PAGE (15% acrylamide) and visualized by silver staining.

2.18 Cholesterol Depletion

Vero cells were treated with 2 mM methyl- β -cyclodextrin (M β CD extracts cholesterol from membranes and entraps it within its hydrophobic ring structure) approximately one hour before p14-mediated syncytium formation is first observed after transfection with p14. Cell monolayers were fixed with methanol and stained at 12 hours post transfection with Wright-Giemsa.

2.19 Detergent-Resistant Membrane Fractionation

Ten-cm dishes of QM5 cells at 60-70% confluence were transfected with p14 and labeled for 1 hour with [3 H]-leucine (50 μ Ci/ml) at 13-15 hours post transfection. After labeling, cells were washed with PBS and lifted off the tissue culture dish by treatment with 50 mM EDTA for 15 minutes. Cells were pelleted at 500 x g, and resuspended in 0.5 ml PBS, RIPA buffer, 0.5% (v/v) Triton X-100, 0.5% (w/v) Lubrol, 60 mM octylglucoside, 0.5% (v/v) Brij 56, or 0.5 % (v/v) Brij 58 (all detergents in TNE [50 mM Tris-HCl pH 8, 150 mM NaCl, 1 mM EDTA] buffer), or 0.5% (w/v) Lubrol in TNE with 1 M NaCl. All lysis buffers contained protease inhibitors (200 nM aprotinin, 1 μ M leupeptin, and 1 μ M pepstatin). When no detergent was used, cells were disrupted by 20 passes through a 30 gauge needle, and unbroken cells and debris removed by centrifugation at 700 x g for 2 minutes; when detergent-containing buffer was used, cells were lysed at 4 $^{\circ}$ C for 30-45 minutes. The cell lysate was used to recover the detergent-resistant membrane fraction

by ultracentrifugation at 100 000 x g for 1 hour. The detergent-soluble fraction was removed and mixed 1:1 with 2x RIPA buffer, the membrane pellet was resuspended by vortexing in 1 ml RIPA buffer, and both fractions were immune precipitated.

2.20 Sucrose Density Gradient Centrifugation

10-cm dishes of p14-transfected QM5 cells were labeled and removed from the tissue-culture dish using EDTA as described above. After low-speed centrifugation, the resulting cell pellets were lysed in 250 μ l of either 0.5% (w/v) Lubrol or 0.5% (v/v) TritonX-100 (in TNE buffer plus protease inhibitors) at 4 °C for 30-45 minutes. The cell lysate was then mixed with 250 μ l of 2.4 M (82.4%) sucrose, and overlaid with 1 ml of 0.9 M (30.8%), 0.5 ml of 0.8M (27.2%), 1 ml of 0.7 M (24%), and 1 ml of 0.1 M (3.4%) sucrose. When indicated, 0.1% (w/v) Lubrol was included in all sucrose fractions. Sucrose density gradients were subjected to ultracentrifugation at 332 000 x g for 16-18 hours. Fractions (0.5 ml) were carefully harvested from the top of the gradient so as not to disturb lower fractions. Each fraction was mixed 1:1 with 2x RIPA buffer and immune precipitated. PLAP-transfected QM5 cells were harvested at 24-28 hours post transfection, lysed in 0.5% (v/v) Triton X-100, and prepared for sucrose gradient analysis as described above.

2.21 Western Blotting

After sucrose density gradient ultracentrifugation, total protein in each 0.5-ml fraction was precipitated using an equal volume of 100% trichloroacetic acid (TCA) at 4 °C for 10 minutes, washed twice with 2.5% TCA, once with cold methanol, and air-dried before

being resuspended in SDS protein-sample buffer. Proteins were boiled for 5 minutes and subjected to SDS-PAGE (10% acrylamide) followed by immunoblotting using 1:2000 mouse monoclonal anti-PLAP (Dako) and 1:2000 horseradish-peroxidase-conjugated secondary antibody (Kirkegaard Perry Laboratories). Proteins were visualized by a chemiluminescence reaction according to manufacturer's instructions (Kirkegaard Perry Laboratories).

Chapter 3

Membrane fusion mediated by a Type III protein with an external myristylated amino terminus

3.1 Overview

Reptilian reovirus (RRV) is one of a limited number of non-enveloped viruses capable of inducing cell-cell fusion. A small, hydrophobic, basic, 125-amino-acid fusion protein encoded by the first open reading frame (ORF) of a bicistronic viral mRNA is responsible for this activity. Sequence comparison to previously characterized reovirus fusion proteins indicated that p14 represents a new member of the fusion-associated small transmembrane (FAST) protein family. Topological analysis revealed that p14 is a member of a subset of integral membrane proteins, the Type III ($N_{\text{exo}}/C_{\text{cyt}}$) proteins, that lack a cleavable signal sequence and use a reverse signal-anchor to direct membrane insertion. This topology results in the co-translational translocation of the essential myristylated N-terminal domain of p14 across the membrane. p14 is a novel reovirus membrane fusion protein, and further accentuates the diversity and unusual properties of the FAST protein family as a third distinct class of viral membrane fusion proteins.

3.2 Introduction

Biological membrane fusion is an essential cellular process mediated by specific fusion proteins (Stegmann *et al.*, 1989; White, 1990; Blumenthal *et al.*, 2003; Jahn *et al.*, 2003). Enveloped-virus fusion proteins have contributed extensively to the model of protein-mediated membrane fusion. They are complex, multimeric, Type I integral membrane proteins that facilitate virus entry into cells by mediating fusion between the viral envelope and the target cell membrane (White, 1990). Two distinct classes of enveloped virus fusion proteins have been identified. Class I fusion proteins are exemplified by influenza virus HA and human immunodeficiency virus gp41, and Class II proteins by alpha and flavivirus E1 and E, respectively (White, 1990; Skehel and Wiley, 1998; Weissenhorn *et al.*, 1999; Heinz and Allison, 2001; Kielian, 2002). For both classes, triggered conformational changes and/or multimer reorganization of the complex ectodomain is essential for the fusion reaction (Weissenhorn *et al.*, 1999; Heinz and Allison, 2001). This transition from a metastable to a low-energy form of the fusion protein is believed to provide energy to overcome the thermodynamic barriers that inhibit membrane merger (Carr and Kim, 1993; Gibbons *et al.*, 2000; Eckert and Kim, 2001; Stiasny *et al.*, 2001). However, the complete role of protein structure remodeling as a thermodynamic mediator of the fusion reaction remains unresolved (Epand and Epand, 2002, 2003; Remeta *et al.*, 2002).

Nonenveloped viruses lack a lipid bilayer, their entry is not dependent on membrane fusion and they do not encode membrane fusion proteins. The exception to this rule are the fusogenic species of the *Reoviridae* family (Nibert and Schiff, 2001;

summarized in Table 1.8). The reovirus fusion proteins are not part of the virus particle, and are not utilized in the virus entry process (Duncan *et al.*, 1996; Shmulevitz and Duncan, 2000; Dawe and Duncan, 2002). This class of fusion-associated small transmembrane (FAST) proteins comprises the only known examples of viral nonstructural proteins that induce cell-cell fusion, in a manner that is not required for entry or exit of the virus (Duncan *et al.*, 1996). Instead, FAST protein-mediated syncytium formation leads to more rapid virus particle egress and/or cell-cell spread during the course of an infection (Duncan *et al.*, 1996; Duncan and Sullivan, 1998).

Two reovirus FAST proteins have been identified. Avian reovirus (ARV) and Nelson Bay reovirus (NBV) encode homologous 95 to 98-amino-acid fusion proteins, termed p10 (Shmulevitz and Duncan, 2000). An atypical mammalian reovirus, baboon reovirus (BRV), encodes a non-homologous 140-amino-acid 15-kDa fusion protein (p15) that is comprised of a different arrangement of structural motifs (Dawe and Duncan, 2002). Both p10 and p15 are integral membrane proteins that lack an N-terminal signal sequence. Both are modified by fatty acids: p10 is palmitylated at an internal membrane-proximal di-cysteine motif, while p15 is N-terminally myristylated (Dawe and Duncan, 2002; Shmulevitz *et al.*, 2003b). Both proteins contain a positively charged region C-terminal to the transmembrane domain (Shmulevitz and Duncan, 2000; Dawe and Duncan, 2002). ARV p10 localizes to the plasma membrane in an ($N_{\text{exo}}/C_{\text{cyt}}$) topology that places a small N-terminal domain (approximately 40 residues) outside the cell (Shmulevitz and Duncan, 2000). The membrane topology of p15 has not been determined; however, the presence of two potential transmembrane domains and the N-

terminal myristate suggests that p15 may assume an N_{cyt} -bitopic or -polytopic membrane association (Dawe and Duncan, 2002).

The reovirus fusion proteins lack key features found in most enveloped-virus fusion proteins, including multiple heptad repeats implicated in formation of a coiled-coil stalk (found in all Class I fusion proteins; Weissenhorn *et al.*, 1999). The small size of the FAST proteins makes it difficult to envision how these proteins extend the distance between two opposing biological membranes or utilize a structural rearrangement that leads to fusion-peptide exposure and energy release that can be harnessed to drive membrane merger (White, 1990; Carr and Kim, 1993; Zimmerberg *et al.*, 1993; Skehel and Wiley, 1998). The reovirus fusion proteins are therefore unlikely to conform to this paradigm. A comparative analysis of the FAST proteins promises an enhanced understanding of these minimalist fusion proteins, and the structural features required for membrane fusion.

A reptilian reovirus (RRV) isolated from a python was recently characterized as a new species of fusogenic orthoreovirus (Ahne *et al.*, 1987; Duncan *et al.*, 2003). I now show that the p14 protein encoded by the first open reading frame on the bicistronic S1 genome segment is a third distinct member of the reovirus FAST protein family. p14 is a surface-localized Type III ($N_{\text{exo}}/C_{\text{cyt}}$) integral membrane protein that places its essential, myristylated N-terminal domain outside the cell. Although the precise role of the external myristylated N terminus of p14 in the fusion mechanism is undetermined, this discovery adds a novel structural motif to the FAST protein repertoire and a new element to be considered for models of protein-mediated membrane fusion.

3.3 Results

The 1st open reading frame of the bicistronic S1 genome segment of a reptilian reovirus encodes the fusion protein

Sequence analysis identified two sequential, partially overlapping open reading frames (ORFs) on the S1 genome segment of RRV (Fig 3.1.A; Duncan *et al.*, 2003). *In vitro* transcription and translation confirmed that this genome segment encodes two protein products: a 35-kDa homolog of the ARV cell attachment protein σ C, and a 14-kDa product (Fig 3.1.B). Transfection analysis using the S1 genome segment indicated that one of these proteins was responsible for the syncytial phenotype of RRV. Subcloning and expression revealed that the 125-amino-acid p14 protein encoded by the first ORF, when expressed by itself in transfected cells, induced extensive multinucleated syncytium formation in both transfected Vero epithelial cells and in QM5 quail cell fibroblasts (Fig 3.1.C). Immune precipitation confirmed expression of p14 in both transfected and virus-infected cells (Fig. 3.1.B).

Structural motifs in p14

The RRV p14 protein contains several predicted structural motifs (Fig 3.2). A hydropathy plot of p14 and sequence analysis identified a predicted transmembrane domain (TMD), suggesting that p14 resides as an integral membrane protein. Sequence analysis also suggested that p14 lacks a cleavable N-terminal signal sequence, suggesting that the

membrane-spanning domain may function as an internal signal anchor (Spiess, 1995). The only other region of moderate hydrophobicity occurs in the N-terminal domain (Fig 3.2.A), a region I termed the hydrophobic patch. The N-terminal domain also contains a consensus sequence for N-terminal myristylation (MGXXXS/T/A) (Towler *et al.*, 1988). The C-terminal domain is comprised of two different regions: a highly basic, membrane-proximal region (10 of the 22 residues immediately following the TM domain are basic), and a C-terminal proline-rich region (8 prolines between residues 99-112) that includes a stretch of 5 consecutive prolines. The C-terminal domain also contains a consensus sequence for N-linked glycosylation (NXS/T) at asn121. The functional significance of these sequence-predicted structural motifs was further investigated.

p14 assumes a N_{exo}/C_{cyt} surface membrane topology

Analysis of the soluble and membrane fractions from transfected QM5 cells indicated that p14 localized exclusively to the membrane pellet (Fig 3.3.A, left panel), suggesting p14 is co-translationally inserted into cellular membranes. Treatment of the membrane pellet with either high salt or high pH to extract peripheral membrane proteins (Fujiki *et al.*, 1982) did not alter p14 distribution (Fig 3.3.A), indicating the predicted p14 transmembrane domain is functional, and that p14 exists exclusively as an integral membrane-spanning protein. A known soluble protein, σ C encoded by avian reovirus, was located in the soluble fraction after σ C-transfected cells were subjected to the same procedure (Fig 3.3.A, right panel). Consistent with the membrane localization of p14, immunostaining of permeabilized cells revealed a punctuate, reticular staining pattern with concentrations of p14 in the perinuclear region, while similar staining of non-

permeabilized cells detected patchy ring fluorescence at the surface of cells (Fig 3.3.B). Furthermore, the exogenous addition of polyclonal α -p14 inhibited syncytium formation in p14-transfected cells, while normal rabbit serum did not (Fig 3.3.C). These results imply that p14 localizes to the ER-Golgi pathway, and that at least a portion of p14 trafficks to the cell surface, where it is directly involved in promoting the membrane fusion reaction.

To examine p14 membrane topology, constructs were created that contained tandem HA epitope tags added either at the C-terminus of p14 (p14-2HAC), or inserted between residues seven and eight within the N-terminal domain (p14-2HAN). The double-epitope tag at the C-terminus slowed, but did not inhibit, the extent of cell-cell fusion, while the epitope tag in the N-terminal domain abrogated polykaryon formation (Fig 3.4.A). Cells transfected with p14-2HAN or p14-2HAC were immunostained using an anti-HA monoclonal antibody, either after fixation and permeabilization to reveal intracellular fluorescence, or as live cells to detect the surface-expressed ectodomain. In permeabilized cells, both constructs generated the reticular staining pattern characteristic of authentic p14 (Fig 3.4.B panels a and b). Positive surface staining was only obtained with the p14-2HAN construct, indicating that p14 assumes a N_{exo}/C_{cyt} surface topology in the plasma membrane (Fig 3.4.B. panels c versus d).

The C terminus of p14 is dispensable for fusion activity

p14 contains a potential site for N-glycan addition (NXS/T) at asn 121. However, only a single molecular weight form of p14 was expressed in transfected cells (Figs 3.3.A, 3.5.A). When p14-transfected cells were pre-treated with tunicamycin (an inhibitor of N-

linked glycosylation), there was no effect on protein mobility (Figure 3.5.A). Neither tunicamycin treatment nor the elimination of the glycosylation site (by substitution of asparagine residue 121 with glutamine [N121Q]) affected p14-mediated cell fusion or electrophoretic mobility (Figure 3.5.A., B), indicating the p14 is not modified by glycan addition at asn 121.

Proline-rich regions can form Type II polyproline helices and are often involved in protein-protein interactions (Kay *et al.*, 2000; Reiersen and Rees, 2001). To examine the influence of the unusual C-proximal polyproline motif on p14 fusion activity, five p14 C-terminal deletion mutants (named for their length in amino acids) were assessed using a quantitative fusion assay based on the average number of syncytial nuclei per field. Deletion of the C-terminal 10-20 amino acids from p14, including the five consecutive proline residues and potential polyproline helix (residues 108-112), decreased the speed of p14-induced syncytium formation, as evidenced by a decreased syncytial index, at early times post-transfection (Fig 3.6.A). However, the overall extent of fusion remained unimpaired, as two truncated constructs of p14 containing 105 (p14-C105) and 115 (p14-C115) amino acid residues mediated the formation of large multinucleated syncytia (Fig 3.6.B) that eventually encompassed the entire cell monolayer. An 88-amino-acid version of p14 (p14-C88) that lacks all of the proline residues also displayed an impaired speed, but not extent, of fusion (Fig. 3.6.A, B). Therefore, the C-terminal 37 amino acids of p14, representing the proline-rich region (a potential polyproline helix motif) and the glycosylation site, are dispensable in the mechanism of p14-mediated fusion.

The p14-C78 construct (78 amino acids in length) was devoid of fusion activity while the p14-C83 construct (83 amino acids) retained vestigial fusion activity, initiating the formation of small syncytia that failed to progress in size over time (data not shown and Fig 3.6.A, B). The loss of fusion activity of these extended truncation constructs might have reflected ineffective co-translational membrane insertion. Immune precipitation results did indicate a slight reduction in detection of the C83 and C78 constructs in the membrane fraction (Fig 3.6.C). However, the p14-C88 construct displayed a similar level of detection in the membrane fraction yet retained the ability to fully fuse the monolayer (Fig 3.6.B). Therefore, decreased detection of these three truncated constructs most likely reflected loss of a C-proximal epitope rather than decreased membrane association. Therefore, a minimum size or structure of the p14 C-terminal domain most likely influences p14 fusion activity by altering events downstream of membrane insertion.

N-terminal myristylation of p14 is essential for fusion activity

The myristate moiety of myristylated proteins is almost always associated with the cytoplasmic leaflet of lipid bilayers (Resh, 1999). In view of the predicted $N_{\text{exo}}/C_{\text{cyt}}$ topology of p14, we anticipated that the myristylation consensus sequence would be non-functional, and therefore irrelevant for p14 function. This was not the case. Radiolabeling indicated incorporation of [^3H]myristic acid into authentic p14, but not into a construct containing a G2A substitution that eliminates the myristylation consensus sequence; both constructs were detected with a [^3H]leucine label (Fig 3.7.A). The loss of labeling of the G2A construct by myristic acid confirmed that labeling of authentic p14 reflected

incorporation of [^3H]myristic acid and implied that p14 is a myristylated integral membrane protein. In addition, the myristate moiety appears to be an essential component of p14, since the p14-G2A construct did not mediate cell-cell fusion (Fig 3.7.B). The altered fusion activity of the myristylation-minus construct did not reflect altered protein expression (Fig 3.7.A) or p14 subcellular localization, as determined by immunofluorescence (Fig 3.7.C). Therefore, the N-terminal myristylation consensus sequence of p14 is both functional and essential for p14-induced syncytium formation.

p14 translocates its myristylated N terminus across the membrane

The unexpected placement of a myristylated N-terminal domain external to the plasma membrane prompted further confirmation of p14 topology. An N-linked glycosylation site was engineered into the N-terminal domain of p14 (V9T), and N-glycosylation mapping was used to examine the topology of the p14-V9T construct. *In vitro* translation of p14 in the presence or absence of canine microsomal membranes (CMM) produced proteins with identical gel mobilities (Fig 3.8.A), confirming the sequence-predicted absence of a cleavable N-terminal signal peptide. Conversely, *in vitro* translation of p14-V9T in the presence of CMM resulted in two protein species, one with a retarded gel mobility relative to authentic p14 or to p14-V9T translated in the absence of CMM (Fig 3.8.A). The mobility shift of approximately 3 kDa is the appropriate molecular-weight alteration for one core glycan (2.5 kDa; Daniels *et al.*, 2003), and was in accord with the mobility shift of a known glycosylated control protein (Fig 3.8.A). The non-myristylated p14-G2A construct demonstrated a minor population with the same gel mobility as the glycosylated species of p14-V9T when translated in the presence of CMM (Fig 3.8.A).

This slow mobility form of p14-G2A likely adopts the opposite Type II ($N_{\text{cyt}}/C_{\text{exo}}$) topology, thereby allowing the native glycosylation site at asn121 access to the glycosylation machinery in the microsomal lumen. This result suggests that myristylation may be a minor contributor to determining an exclusive $N_{\text{exo}}/C_{\text{cyt}}$ topology for p14.

Analysis of p14-V9T in transfected Vero cells also detected two different species of p14-V9T, with a loss of the slower migrating form following treatment of cells with tunicamycin (Fig 3.8.B). To exclude the possibility that there might be two populations of p14, one with the myristylated N-terminal domain inside the cell and the other non-myristylated form in the $N_{\text{exo}}/C_{\text{cyt}}$ topology, p14-V9T-transfected cells were labeled with [^3H]myristic acid. The N-terminal domain of p14-V9T was both N-glycosylated and myristylated, as evidenced by the ability of [^3H]myristic acid to label both molecular weight forms of p14-V9T (Fig 3.8.B). These results conclusively established that the myristylated N-terminal domain of p14 is translocated into the ER lumen, and after trafficking to the plasma membrane, resides outside the cell.

Transfection analysis indicated a loss of syncytium-inducing ability due to the V9T substitution (Fig 3.9.A, panel a). The loss of fusion activity was not the result of steric hindrance by the addition of a large carbohydrate moiety, since the fusion ability of p14-V9T was not restored by the inhibition of N-linked glycosylation using tunicamycin (Fig 3.9.A, panel b). Transport of the p14-V9T construct was also not affected, as a population of p14-V9T was clearly visualized accumulating at the plasma membrane by immunofluorescence (Fig 3.9.B). Therefore, minor alteration near the N-terminus of the p14 ectodomain hydrophobic patch affects the membrane fusion activity of the protein,

independent of any effects on p14 membrane insertion, protein topology, or cell-surface localization.

3.4 Discussion

p14 is the newest member of the diverse FAST protein family

My study indicates that the RRV p14 protein is a novel reovirus FAST protein, the newest member of a diverse family of atypical viral membrane fusion proteins. While p14 shares no significant sequence similarity with previously identified FAST proteins (Shmulevitz and Duncan, 2000; Dawe and Duncan, 2002), some structural commonality between the FAST proteins does exist (Fig 3.10). All of the FAST proteins are small, basic, acylated integral membrane proteins. However, the nature of the acylation, the arrangement of the hydrophobic motifs, and the presence or absence of essential cysteine residues or proline-rich regions (Fig 3.10) leads to each FAST protein containing its own signature arrangement of structural motifs. Moreover, key structural features found in enveloped-viral fusion proteins, such as coiled-coil domains, typical fusion-peptide motifs, and large, complex, multimeric ectodomains, are absent in the FAST proteins. Clearly, the reovirus FAST proteins represent a third class of viral membrane fusion proteins, distinct from the Class I and Class II enveloped-virus fusion proteins (Skehel and Wiley, 1998; Weissenhorn *et al.*, 1999; Heinz and Allison, 2001; Kielian, 2002). The structural features of the FAST proteins, including the unique myristylated ectodomain of p14 identified here, are likely to have important implications for the mechanism of FAST-mediated membrane fusion.

The carboxyl terminus, including a polyproline motif, is non-essential for fusion

The C-terminal domain of p14 is comprised of a membrane-proximal polybasic region (a structural feature of all the FAST proteins) and a polyproline motif that is also found in BRV p15, but not in ARV p10. Of this approximately 65-residue endodomain, the terminal 37 amino acids, including the proline-rich region, are not essential for the fusion activity of p14 (Figure 3.6.A, B). Previous C-terminal truncation studies indicated that p10 also possesses a minimum size requirement (Shmulevitz and Duncan, 2000). As the ribosome protects 30-40 amino acid residues of a nascent protein (Daniels *et al.*, 2003), it was speculated by Shmulevitz and Duncan (2000) that the size minimum results from the inability of smaller p10 constructs to co-translationally translocate across the ER membrane. I found that all five p14 C-terminal deletion constructs, including a non-fusogenic 78-residue p14 construct that possesses only 29 residues C-terminal to the membrane-spanning domain, remain exclusively membrane-localized (Figure 3.6.C). This suggests that the p14 size minimum (88 amino acids) may reflect a requirement for fusion rather than for membrane targeting.

Topological analysis indicates that p14 is a Type III (N_{exo}/C_{cyt}) plasma-membrane protein

Subcellular fractionation revealed p14 resides exclusively as an integral membrane protein (Fig 3.3.A), implying co-translational membrane insertion. The absence of a cleavable signal peptide (Fig 3.8.A) indicated that p14 utilizes an internal transmembrane domain as a signal-anchor. Topological analyses using epitope tagging (Fig 3.4) and glycosylation mapping (Fig 3.8) both indicated that the small, approximately 40-residue

p14 N-terminal domain resides external to the membrane. All of these properties identified p14 as a Type III ($N_{\text{exo}}/C_{\text{cyt}}$) membrane protein (Spiess, 1995; Godor and Spiess, 2001; also referred to as Type I-SA in High and Laird, 1997). Unlike both Type I ($N_{\text{exo}}/C_{\text{cyt}}$) and Type II ($C_{\text{exo}}/N_{\text{cyt}}$) proteins that translocate sequences C-terminal to the signal peptide or signal-anchor, Type III proteins utilize reverse signal-anchors that translocate N-terminal residues which are transiently exposed to the cytosol before the signal-anchor emerges from the ribosome (Godor and Spiess, 2001). P14 contains a number of topological determinants, which all have been shown to promote a Type III ($N_{\text{exo}}/C_{\text{cyt}}$) orientation. These determinants include: (1) the C-terminal location of positively charged residues flanking the signal anchor (von Heijne and Gavel, 1988); (2) the long length of the signal-anchor sequence (Wahlberg and Spiess, 1997; Rösch *et al.*, 2000; Abell *et al.*, 2002); and (3) the small size of the translocated N-terminal domain (Denzer *et al.*, 1995). These features are found in several other Type III ($N_{\text{exo}}/C_{\text{cyt}}$) membrane proteins, including cytochrome P-450 (Sato *et al.*, 1990), mouse synaptotagmin I and II (Kida *et al.*, 2000), the Golgi-localized tumor antigen RCAS1 (Engelsberg *et al.*, 2003), the γ -secretase component PEN-2 (Crystal *et al.*, 2003), the Batten disease protein CLN3 (Mao *et al.*, 2003), and the viral proteins influenza M2 (Lamb *et al.*, 1985) and influenza B NB glycoprotein (Williams and Lamb, 1986). Protein topogenesis is commonly directed by multiple determinants which in combination generate a uniform, thus unique, topology for a given protein (Goder and Spiess, 2001). For p14 all topogenic signals favor the observed Type III ($N_{\text{exo}}/C_{\text{cyt}}$) membrane topology, making p14 the first demonstrated example of a Type III membrane fusion protein.

A reexamination of the previously characterized p10 FAST protein of ARV indicates that p10 is also a member of the Type III class of integral membrane proteins (Shmulevitz and Duncan, 2000). The p10 protein assumes an $N_{\text{exo}}/C_{\text{cyt}}$ topology, and p10 topogenic signals are typical of Type III membrane proteins, including the absence of an N-terminal signal peptide, positive charges distributed on the C-terminal side of the signal-anchor, and a small N-terminal ectodomain. While the membrane topology of BRV p15 remains undefined, this protein also lacks any evidence of a cleavable signal peptide, and contains a small, myristylated N-terminal domain and a basic region C-terminal to a predicted transmembrane anchor (Dawe and Duncan, 2002). However, p15 also contains a second potential membrane-spanning domain, leading to speculation that the protein may be a multi-spanning membrane protein (Dawe and Duncan, 2002). At present, no compelling evidence exists to rule out the possibility that p15, like the other reoviral FAST proteins, might also be a Type III ($N_{\text{exo}}/C_{\text{cyt}}$) membrane protein.

Co-translational translocation of the p14 myristylated ectodomain

Our discovery that the myristylated p14 N terminus is translocated across the membrane and resides outside the cell was surprising, but not without precedent. The Large Surface Antigen (LsAg) of both Hepatitis B virus and Duck Hepatitis B virus adopts two functional membrane topologies, of which one externalizes the myristylated N-terminal pre-S1 domain of the protein on the virion surface (Swameye and Schaller, 1997). When surface-exposed, the myristylated pre-S1 domain mediates effective entry of the virus into hepatocytes (Bruss *et al.*, 1996). Though LsAg externalizes its myristylated N terminus, this topology is achieved post-translationally (Swameye and Schaller, 1997).

When an interaction between the pre-S1 domain and the chaperone Hsc70 is prevented, the N-terminal domain is no longer retained in the cytoplasm and the myristylated domain co-translationally translocates into the ER lumen, as evidenced by N-glycosylation of asn4 (Gallina and Milanesi, 1993; Swameye and Schaller, 1997; Löffler-Mary *et al.*, 1997; Prange *et al.*, 1999). Co-translational translocation of a myristic acid occurs naturally with p14.

The RRV p14 protein is the first example of a Type III integral membrane protein that co-translationally translocates a myristylated N terminus, and the only example of a membrane fusion protein that requires a myristylated ectodomain. However, other examples may exist. The vaccinia virus L1R protein is an N-terminally myristylated polytopic protein located in the membrane of intracellular mature virions (Wolffe *et al.*, 1995). Information based on studies on disulfide bond formation in the cytoplasmic-facing central loop of L1R hint that the myristylated N terminus of L1R resides in the ER lumen (Senkevich *et al.*, 2000). More recent results confirm this supposition, as at least a proportion of L1R translocates its myristylated N terminus across the membrane (Dennis Hruby, personal communication). Similarly, CLN3 assumes $N_{\text{exo}}/C_{\text{cyt}}$ membrane topology and contains an N-terminal myristylation consensus sequence but the function of this motif has not been examined (Mao *et al.*, 2003). P14 is, therefore, the first example of a viral integral membrane protein that adopts a unique Type III ($N_{\text{exo}}/C_{\text{cyt}}$) membrane topology by co-translational translocation of its myristylated N terminus.

A myristylated ectodomain is essential for p14 fusion activity

Myristic acid is a 14-carbon fatty acid that, though interacting with lipid bilayers, is not sufficient on its own to mediate stable membrane association of an otherwise soluble protein, and requires a second signal (another lipid modification, electrostatic interaction) for stable binding (Peitzsch and McLaughlin, 1993). The unique ability of a myristylated cytosolic protein to associate on/off a membrane domain in response to the availability of a second signal is essential for a number of cellular signaling proteins (Randazzo *et al.*, 1995; Saouaf *et al.*, 1997; Resh, 1999). In addition, myristylation often contributes to the structural stability of the modified protein (Zheng *et al.*, 1993; Sowadski *et al.*, 1996) or viral capsid (Chow *et al.*, 1987). Though the addition of myristic acid to otherwise soluble proteins has been well characterized, the role of myristylation of integral membrane proteins remains controversial. Integral membrane proteins that are myristylated include the transferrin receptor (Nadler *et al.*, 1994), human CD36 cell adhesion receptor and new family member CLA-1 (Calvo and Vega, 1993), insulin receptor (Hedo *et al.*, 1987), tumor necrosis factor α preprotein (Stevenson *et al.*, 1992), interleukin 1 α preprotein (Stevenson *et al.*, 1993), and the cytochrome c oxidase subunit I of *Neurospora crassa* (Vassilev *et al.*, 1995). In the case of myristylated integral membrane proteins, stable membrane association derives from the transmembrane domain, and the myristic acid serves some undefined function other than protein anchoring in the membrane. The role of myristate in these integral membrane proteins is speculative, but is suggested to involve the regulation of enzymatic activity by modulating protein-protein or protein:lipid interactions, or by altering the ability of the protein to be modified.

In contrast, the essential myristic moiety present in p14 must exert its influence on p14-induced membrane fusion by interacting with the external leaflet of the membrane bilayer. Although the essential role of the p14 myristic acid is unclear, several possible roles can be envisioned. Acylation of both viral and cellular proteins can target these proteins to detergent-resistant membrane microdomains within the plasma membrane (Robbins *et al.*, 1995; Melkonian *et al.*, 1999). Although the myristylation-minus p14-G2A still trafficked to the cell surface (Fig 3.7.B), the loss of myristylation could influence p14 localization to membrane microdomains. A second possibility is based on the assumption that the myristate associates with the luminal leaflet of the ER membrane after translocation, in a manner analogous to the membrane association of signal peptides before their cleavage (Hegde and Lingappa, 1999; Heinrich *et al.*, 2000). Signal-peptide interactions with the luminal leaflet of the ER membrane can promote correct folding of the nascent protein (Wilson *et al.*, 1981); a similar situation could contribute to folding of the p14 ectodomain into a fusion-competent conformation. Addition of two HA-epitope tags into this domain abrogated p14-fusion (Fig 3.4.A), as did the site-specific alteration of valine 9 (V9T; Fig 3.9.A, panel a), highlighting the important nature of the hydrophobic patch motif in either the fusion mechanism itself, or in the promotion of a fusion-competent extracellular structure (discussed in Chapter 4). An intriguing third possibility reflects the unique ability of myristic acid to reversibly associate with a lipid bilayer (Resh, 1999). During the close apposition of membranes that must occur prior to fusion, the myristic acid may disassociate from the outer leaflet of the donor membrane and interact with the outer leaflet of the target membrane. Such interactions of myristic acid with the target and/or donor membranes could alter lipid packing of one or both

membranes during the fusion reaction. This hypothesis is supported by the greater membrane permeabilization exhibited by a myristylated hydrophobic peptide compared to its non-acylated partner (Joseph and Nagaraj, 1995). p14 may be the first example of a viral membrane fusion protein that commandeers the unique ability of myristate to reversibly associate with the exoplasmic leaflet of the membrane in an as-yet-undefined fusion mechanism.

Shared features of the FAST protein family

The detailed structural and topological analysis of p14 presented in my thesis expands our understanding about this group of unusual membrane fusion proteins. The reovirus FAST protein family has previously been defined by the following features: 1) nonstructural in nature; 2) integral membrane association; 3) the presence of a second region of hydrophobicity in addition to the transmembrane domain; 4) the presence of a membrane-proximal cluster of basic residues; 5) modification by myristate or palmitate; 6) the absence of key structural features found in enveloped-viral fusion proteins, including coiled-coil motifs or a typical fusion peptide; 7) small size; and 8) the only viral protein required to mediate membrane fusion (Dawe and Duncan, 2002). As a distinct new member of the reoviral fusion-protein family, p14 shares these features, and proves to be the second example of a Type III ($N_{\text{exo}}/C_{\text{cyt}}$) membrane fusion protein within this family. I propose that this topology is the ninth defining feature of the reoviral FAST protein family.

P14 is the first example of a membrane fusion protein that externalizes its myristylated N terminus by co-translational translocation across the ER membrane. The

discovery of this newest FAST protein with its unusual membrane topology further underscores the diversity of these Class III viral membrane fusion proteins. A collection of membrane-interaction motifs, including signal-anchors, hydrophobic patches, polybasic regions and, now, an externalized fatty acid, have been assembled into these rudimentary membrane fusion proteins. Though the mechanism of FAST-mediated membrane fusion remains undetermined, it is evident that these proteins do not have the size capability or structural features to promote membrane fusion using large energy-releasing conformational changes as described for the Class I and Class II fusion proteins (Skehel and Wiley, 1998; Heinz and Allison, 2001). The FAST proteins suggest a previously unrecognized diversity in membrane-fusion-protein structure. Continued structure-function analysis of the reovirus fusion proteins should provide additional insights into the minimal determinants of protein-mediated fusion of biological membranes.

3.5 Figures

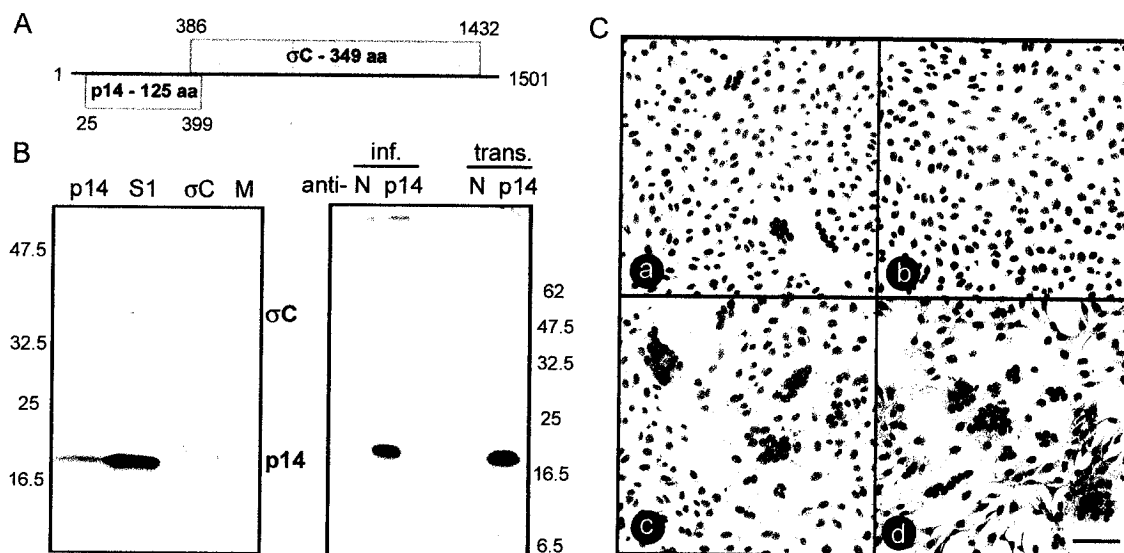


Fig 3.1 The first open reading frame on the RRV bicistronic S1 genome segment encodes a p14 fusion protein. **(A)** The name of the predicted gene product and the number of residues are shown within the shaded rectangles representing the orfs present in the RRV S1 genome segment. Numbers indicate the first and last nucleotides of the genome segment of each ORF (minus the termination codon). **(B)** Translation products generated by rabbit reticulocytes primed with *in vitro* transcribed mRNAs representing the S1 genome segment, the p14 ORF, the σ C ORF, or no exogenous mRNA (M) were detected by radiolabeling, SDS-PAGE and autoradiography (left panel). The locations of the p14 and σ C translation products are indicated, along with the relative migration of molecular-weight markers. Virus-infected (inf.) or p14-transfected (trans.) Vero cells were radiolabeled and immune precipitated with polyclonal anti-p14 serum (p14) or normal rabbit serum (N) (right panel). The relative migration of molecular-weight markers is indicated. **(C)** Cells were transfected with pcDNA3 expressing the bicistronic S1 genome segment (a), the σ C ORF (b), or the p14 ORF (c and d). Panels a-c are transfected Vero cells, Giemsa-stained at 18 hrs post-transfection. Panel d is transfected QM5 cells, Giemsa-stained at 8 hrs post-transfection. Syncytial foci are clearly visible in panels a, c, and d. Scale bar = 100 μ m.

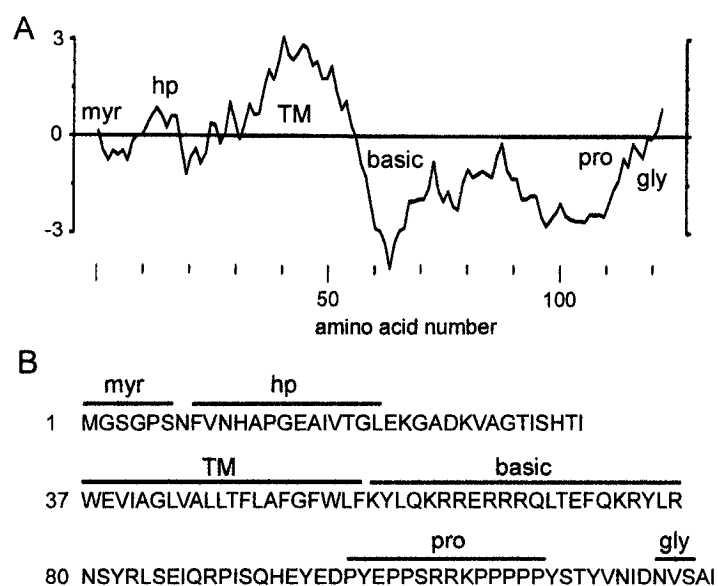


Fig 3.2 Sequence-predicted structural motifs in p14. **(A)** Hydropathy profile of the p14 protein averaged over a window of 11 residues. Hydrophobic residues are above the horizontal line. The locations of the myristylation consensus sequence (myr), hydrophobic patch (hp), transmembrane domain (TM), polybasic region (basic), polyproline region (pro), and N-linked-glycosylation consensus sequence (gly) are indicated. **(B)** Predicted amino acid sequence of p14. The locations of the structural motifs described in panel A are indicated above the sequence.

Fig 3.3 p14 is a surface-localized integral membrane protein. **(A)** The membrane pellet from radiolabeled, p14-transfected QM5 cells was isolated by centrifugation (left panel). Membrane pellets were treated with phosphate-buffered saline (PBS), or stripped with either high salt (salt) or high pH (pH) to remove peripheral proteins, and the integral membrane (M) and soluble (S) fractions were isolated by centrifugation. The presence of p14 in each fraction was detected by immunoprecipitation using anti-p14 polyclonal antisera. A similar analysis was performed on transfected cells expressing the soluble ARV σ C protein (right panel) as a control for the membrane isolation protocol. **(B)** p14-transfected QM5 cells were immunostained at 6 hrs post-transfection using an anti-p14 polyclonal antibody, and antibody distribution was detected by immunofluorescence microscopy using FITC-conjugated secondary antibody (panels a and c). Cells were permeabilized by methanol fixation prior to antibody staining to reveal intracellular p14 distribution (panels a and b), or stained live to reveal cell-surface expression of p14 (panels c and d). The corresponding DIC images overlaid with the fluorescent images are shown (panels b and d). Scale bar = 10 μ m. **(C)** Transfected Vero cells expressing p14 were treated with anti-p14 polyclonal antiserum (a) or normal rabbit serum (b). Cells were fixed with methanol at 14 hrs post-transfection and Giemsa stained to reveal the inhibition of syncytium formation by the anti-p14 antiserum. Scale bar = 100 μ m.

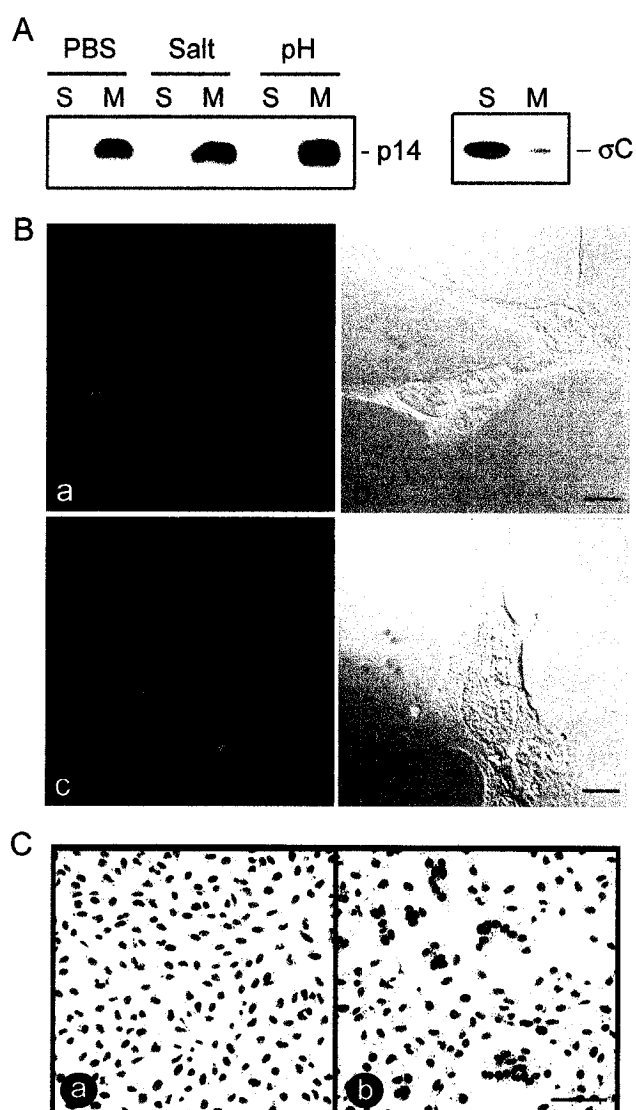


Fig 3.3 p14 is a surface-localized integral membrane protein.

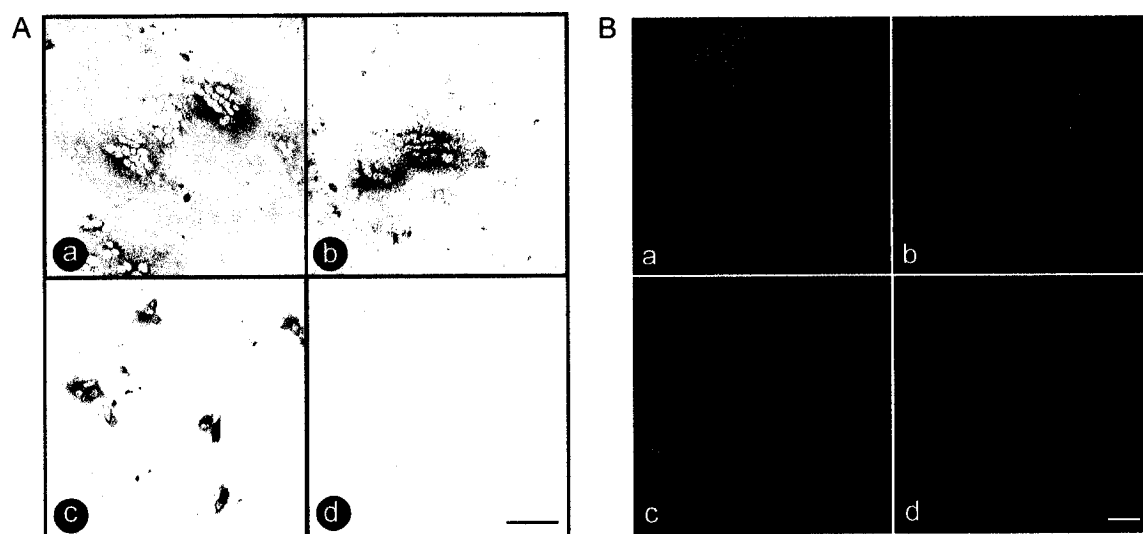


Fig 3.4 p14 assumes an N_{exo}/C_{cyt} surface membrane topology. (A) Vero cells were transfected with authentic p14 (a), p14-2HAC (b), p14-2HAN (c), or the pcDNA3 vector alone (d). Cells were immunostained at 18 hrs post-infection using anti-p14 antiserum and alkaline phosphatase-conjugated secondary antibody to reveal antigen-positive foci. p14-2HAC displayed reduced fusion kinetics while p14-2HAN was fusion-minus. Scale bar = 100 μ m. (B) Vero cells transfected with p14-2HAN (a, c) or p14-2HAC (b, d) were immunostained at 8 hours post-transfection using an anti-HA monoclonal antibody and FITC-conjugated secondary antibody. To detect intracellular p14, cells were fixed with methanol before staining (a, b); for surface-localized p14 (c, d), staining was performed on live cells. Scale bar = 10 μ m.

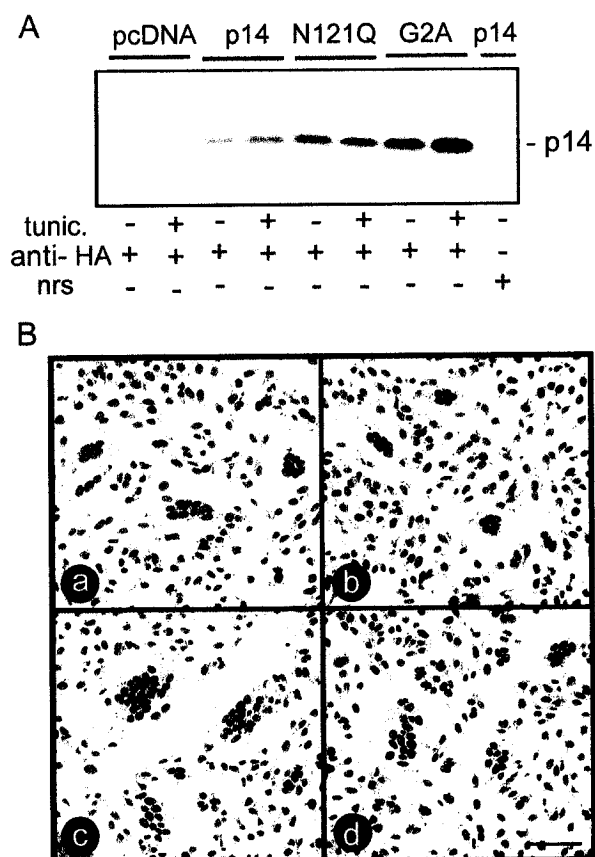


Fig 3.5 p14 is not N-glycosylated. (A) 2HAC-tagged p14-, p14-N121Q-, p14-G2A-, and pcDNA3-transfected Vero cells in the presence or absence of the N-linked glycosylation inhibitor tunicamycin (tunic.) were radiolabeled at 20 hrs post-transfection and immune precipitated using anti-HA monoclonal antibody (α HA) or normal rabbit serum (nrs). The relative gel mobilities of the precipitated p14 proteins were determined by SDS-PAGE and fluorography. (B) Vero cells transfected with either 2HAC-tagged p14 (a-b) or p14-N121Q (c-d) were incubated in the presence (b, d) or absence of tunicamycin. Giemsa staining at 18 hrs post-transfection revealed that neither the N121Q substitution nor treatment with the glycosylation inhibitor affected p14-induced cell fusion. Scale bar = 100 μ m.

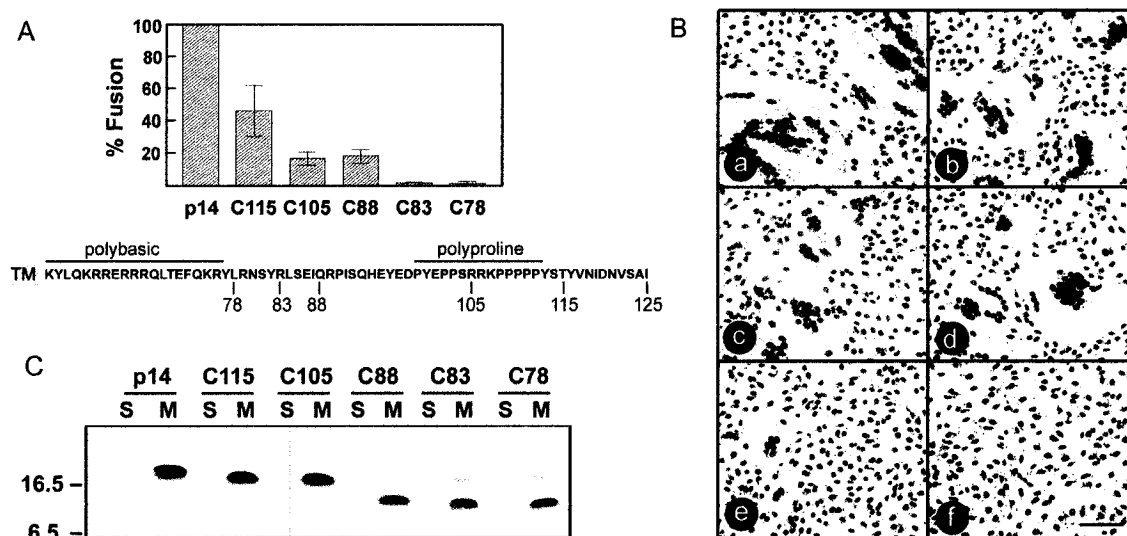


Fig 3.6 The C-terminal 37 amino acids of p14 are dispensable for fusion. **(A)** Vero cells transfected with authentic p14 or with various p14 C-terminal deletion constructs, named according to the number of the last C-terminal residue, were Giemsa-stained at 16 hrs post-transfection. The average number of nuclei present in syncytia was determined by microscopic examination of five random fields, and results are expressed as the percent of wild-type fusion \pm the standard error. The sequence of p14 from the transmembrane domain (TM) to the C terminus is shown, and the locations of the C-terminal truncations, the polybasic region, and the polyproline region are indicated. **(B)** Vero cells were transfected with p14 (a), C115 (b), C105 (c), C88 (d), C83 (e), or C78 (f) and Giemsa-stained at 24 hrs post-transfection. The C88-C115 truncations induced extensive syncytium formation in spite of the reduced speed of p14-mediated fusion indicated in A. The C83 truncation induced a limited number of small syncytia that failed to progress, while the C78 truncation was devoid of syncytium-inducing activity. **(C)** QM5 cells were transfected with p14 or the C-terminal deletion mutants (C115, C105, C88, C83, and C78), and the distribution of the p14 constructs in the soluble (S) and membrane (M) fractions was determined by radiolabelling and immunoprecipitation as described in Fig. 3A. The relative gel mobilities of molecular-weight standards are indicated on the left.

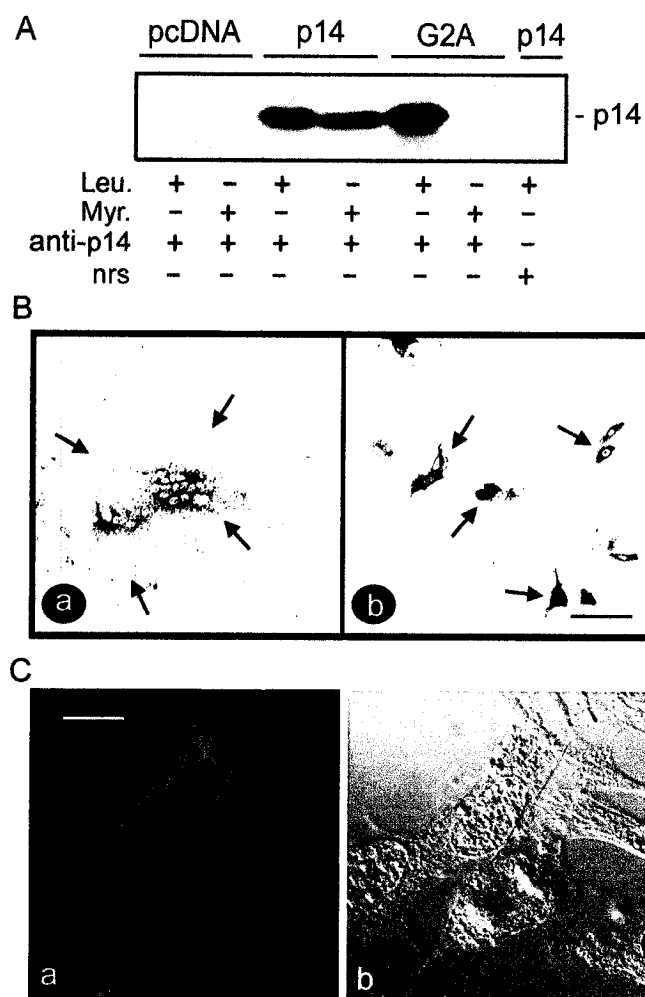


Fig 3.7 N-terminal myristylation of p14 is essential for cell fusion. (A) 2HAC-tagged p14-, p14-G2A-, and pcDNA3-transfected Vero cells were labeled with either [3 H]myristic acid (Myr.) or [3 H]leucine (Leu.), and immune precipitated using anti-p14 polyclonal antiserum (α p14) or normal rabbit serum (nrs). Precipitates were fractionated by SDS-PAGE and radiolabeled p14 detected by fluorography. (B) Vero cells transfected with either 2HAC-tagged p14 (a) or p14-G2A (b) were fixed with methanol at 18 hrs post transfection and immunostained using anti-p14 polyclonal antiserum and alkaline phosphatase-conjugated secondary antibody. Arrows indicate the limits of an antigen-positive syncytial cell (a) or individual antigen-positive cells expressing the fusion-minus p14-G2A construct (b). Scale bar = 100 μ m. (C) QM5 cells transfected with HAC-tagged p14-G2A were permeabilized with methanol and immunostained at 9 hrs post-transfection using anti-p14 polyclonal antiserum and FITC-conjugated secondary antibody. Fluorescence microscopy (a) revealed punctuate, perinuclear intracellular staining of p14-G2A and ring surface fluorescence characteristic of authentic p14. The corresponding DIC image overlaid with the fluorescent image is shown (b). Scale bar = 10 μ m.

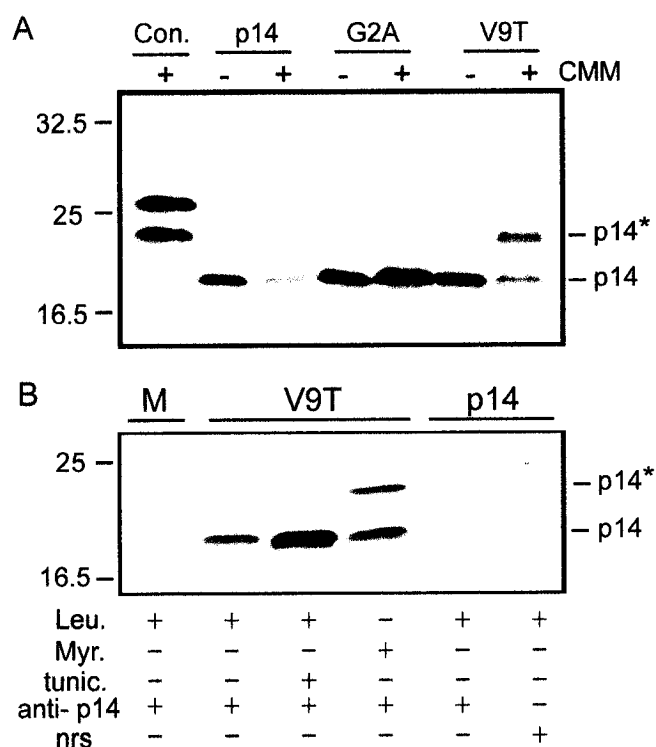


Fig 3.8 p14 translocates its myristylated N terminus across the membrane. **(A)** 2HAC-tagged p14, p14-G2A, or p14-V9T were *in vitro* transcribed and translated in the presence or absence of canine microsomal membranes (CMM). The relative gel mobilities of the radiolabelled authentic (p14) and glycosylated (p14*) species of p14 are indicated on the right, and molecular-weight markers on the left. The control lane (Con.) indicates the glycosylated and non-glycosylated species generated by translation of yeast α -factor mRNA. **(B)** Vero cells were transfected with 2HAC-tagged p14 or p14-V9T, or mock-transfected (M) with pcDNA3 vector. Transfected cells were labeled with [3 H]myristic acid (Myr.) or [3 H]leucine (Leu.) in the presence or absence of tunicamycin (tunic.), and immunoprecipitated using anti-p14 antiserum (α p14) or normal rabbit serum (nrs). The relative gel mobilities of the radiolabelled authentic (p14) and glycosylated (p14*) species of p14 are indicated on the right, and molecular-weight markers on the left.

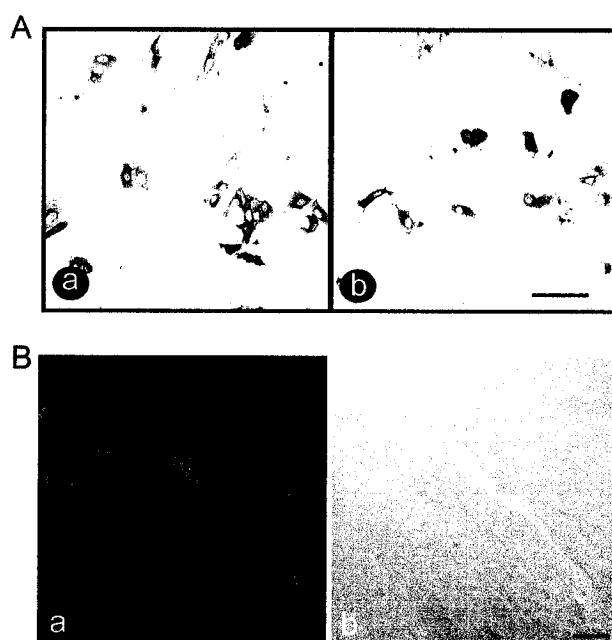


Fig 3.9 The V9T substitution eliminates p14-induced membrane fusion. (A) Vero cells were transfected with 2HAC-tagged p14-V9T in the absence (a) or presence (b) of tunicamycin. Cells were immunostained at 18 hrs post-transfection using anti-p14 antiserum and alkaline phosphatase-conjugated secondary antibody to reveal the single antigen-positive cells generated by the fusion-minus p14-V9T construct. Scale bar = 100 μ m. (B) Transfected QM5 cells were permeabilized with methanol and immunostained at 9 hrs post-transfection using anti-p14 antiserum and FITC-conjugated secondary antibody. Fluorescence microscopy revealed punctuate intracellular staining of p14-V9T and ring surface fluorescence characteristic of authentic p14. Scale bar = 10 μ m.

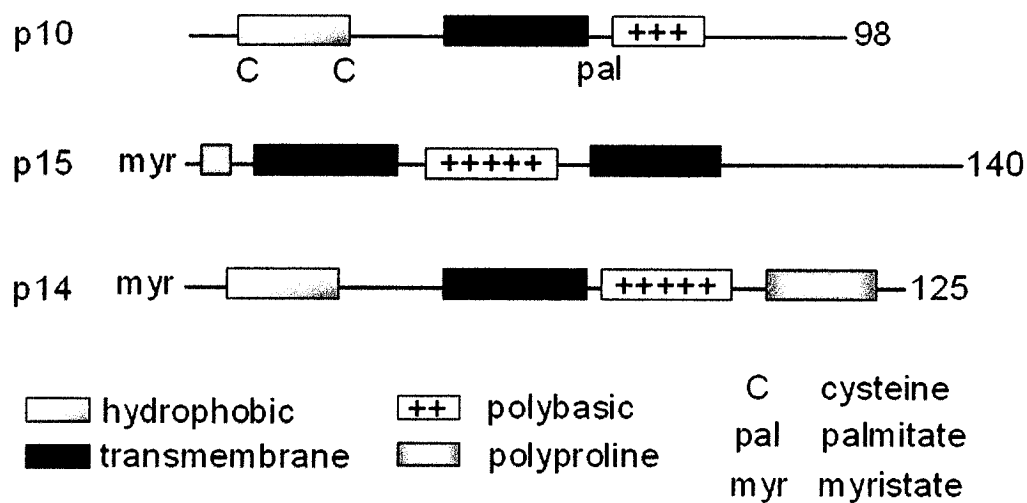


Fig 3.10 Structural motifs in the reovirus FAST proteins. The arrangement of structural motifs present in the RRV p14, ARV p10, and BRV p15 FAST proteins are depicted in a linear fashion, drawn to approximate scale. Numbers refer to amino acid residues.

Chapter 4

An atypical fusion protein from a nonenveloped virus contains a looped internal fusion peptide within its essential 40-residue N-terminal ectodomain.

4.1 Overview

Reptilian reovirus (RRV) is a non-enveloped virus that encodes a 14-kDa, 125-residue, Type III (N_{exo}/C_{cyt}) membrane fusion protein (p14). The approximately 40-amino-acid myristylated N-terminal ectodomain of p14 contains a potential internal fusion-peptide motif that I have termed the hydrophobic patch (HP). In an experiment performed by our collaborators, Drs. Epand and Epand, a synthetic HP peptide mediates lipid mixing in a liposome fusion assay, suggesting that the HP is a fusion-peptide motif. Drs. Epand and Epand also performed circular-dichroism spectroscopy, which suggested that the secondary structure of the p14 HP peptide lacked α -helical character and is likely comprised of a β -strand, turn, and random coil. When I reversed the position of two charged residues in the p14 HP, predicted to stabilize the structure, this result suggested that the HP may form a loop; however, when these same amino acids were replaced with alanine, but not with conservative residues, p14 retained fusion function. From structural calculations based on solution NMR spectroscopic data performed by our collaborators, Drs. Syvitski and Jakeman, the location of the β -structured loop was defined as proximal to the N terminus (residues 4/5-13/14), and the peptide was disordered in the C terminus. This is the first description of a detailed structure of an internal fusion-peptide motif from a reovirus FAST protein.

4.2 Introduction

Enveloped viruses encode and rely on a membrane fusion protein to mediate merger of their lipid envelope with the target cell membrane during virus entry (White, 1990). These fusion proteins are required to overcome the thermodynamic barrier that prevents fusion between opposing membranes (Zimmerberg *et al.*, 1993; Blumenthal *et al.*, 2003). Class I membrane fusion proteins, typified by influenza hemagglutinin (HA) protein and human immunodeficiency virus gp41, undergo triggered rearrangement of coiled coils that transition the fusion protein from a metastable to a low-energy form. This transition is believed to provide necessary energy to the system (Carr and Kim, 1993; Weissenhorn *et al.*, 1999). Though the direct target of this transduced energy is unknown (Bentz and Mittal, 2003), and the precise thermodynamic effects of structural remodeling in the fusion reaction are debatable (Epand and Epand, 2002, 2003; Remeta *et al.*, 2002), the triggered conformational change accomplishes a second essential role. Upon low-pH (the HA fusion trigger) exposure, the fusion peptide of HA moves approximately 100 Å relative to the rest of the molecule (Carr and Kim, 1993), mediating its membrane insertion and concomitant lipid-bilayer disruption. In this manner, the fusion peptide is thought to drive the initial interaction of the fusion-protein ectodomain with the target membrane (Nieva and Agirre, 2003). In combination with other membrane-interacting segments of the fusion protein (Peisajovich and Shai, 2003), the fusion peptide mediates sufficient membrane disruption for merger to result.

A second class of fusion proteins has been differentiated from Class I on the basis of structure. Class II fusion proteins are predominantly β -structured dimers that lie flat on

the viral membrane in an icosahedral scaffold (Rey *et al.*, 1995; Lescar *et al.*, 2001; Pletnev *et al.*, 2001; Kuhn *et al.*, 2002). For the Class II fusion proteins encoded by alpha- and flaviviruses, fusion-mediating structural rearrangements involve a redistribution from dimer to trimer of the proteins that comprise the icosahedral scaffold (Haag *et al.*, 2002). The multimer rearrangement is believed to impart energy to drive the membrane fusion reaction (Gibbons *et al.*, 2000; Heinz and Allison, 2001; Stiasny *et al.*, 2001; Haag *et al.*, 2002). Further, this structural rearrangement facilitates the subsequent interaction of the internal fusion peptide (located in a small loop at one end of each monomer, buried in the dimer and exposed upon trimerization) with the membrane (Heinz and Allison, 2001; Gibbons *et al.*, 2003).

Fusion peptides are typically highly conserved motifs within fusion proteins encoded by different virus strains, but display little sequence homology between virus families (Nieva and Agirre, 2003). These motifs are essential for fusion activity and sometimes even conservative single point mutations abolish function (Cross *et al.*, 2001; Epand *et al.*, 2001). Class I fusion proteins most often localize fusion peptide motifs at or near their N terminus, whereas fusion peptide motifs are embedded internally within the amino acid sequence of Class II proteins and the VSV G protein (Whitt *et al.*, 1990; Shome and Kielian, 2001; Skehel *et al.*, 2001). Most fusion peptide motifs are moderately hydrophobic and glycine/alanine-rich (Durell *et al.*, 1997). The latter residues impart conformational flexibility to the region, a feature believed important to the membrane-disruptive property of a fusion peptide (Davies *et al.*, 1998; P  cheur *et al.*, 2000; Wong, 2003). Internal fusion peptides often contain central proline residues, and are often less hydrophobic than their N-terminal counterparts; the fusion peptide of VSV

G protein is non-polar, and very proline-rich (Whitt *et al.*, 1990; Zhang and Ghosh, 1994). A number of internal fusion peptide motifs adopt looped structures, as evidenced by high-resolution structural analysis of the entire fusion protein (Rey *et al.*, 1995; Lescar *et al.*, 2001; Kuhn *et al.*, 2002) or mutagenesis of the region (Zhang and Ghosh, 1994; Frederickson and Whitt, 1995; Delos and White, 2000; Delos *et al.*, 2000; Allison *et al.*, 2001). Synthetic peptides that represent both N-terminal and internal fusion peptide motifs are used to mimic the structure and function of this region *in vitro*. To best understand how a fusion peptide motif functions to mediate hemifusion and/or membrane disruption requires the determination of the structural state of the fusion peptide during the membrane fusion process.

N-terminal fusion peptides are more hydrophobic than those found internally; this feature prevents the high aqueous solubility required for crystallographic and solution NMR techniques (Yang *et al.*, 2001). Spectroscopic techniques such as circular-dichroism or infrared spectroscopy have been used to assess overall secondary structure of many synthetic representations of fusion peptide motifs. Attenuated total reflection Fourier-transform infrared spectroscopy (ATR-FITR) is often used to determine orientation of these peptides in the plane of a lipid bilayer (Martin *et al.*, 2003), and may be used more in the future to detect alterations in fusion-peptide structure during the fusion process. Circular-dichroism spectroscopy on the HA fusion peptide indicated that it is predominantly α -helical when inserted into a membrane (Wharton *et al.*, 1988), while FITR suggests the fusion peptide inserts into the membrane at an oblique angle (Lüneberg *et al.*, 1995). The structure of the HIV fusion peptide has been more elusive, as experiments predict both α -helical and β -sheet secondary structure, or the conversion

of a β -sheet to an α -helix in the presence of a lipid membrane (Martin *et al.*, 1993; Martin *et al.*, 1996; Yang *et al.*, 2001). Different methods of preparation of an insoluble fusion peptide (i.e. solvents, detergents, lipids used, and relative concentration of peptide) can yield different results, as the conformation of a hydrophobic peptide in a lipid bilayer often depends on the solvent used in the reconstitution process (Han and Tamm, 2000b; Dennison *et al.*, 2002; Gordon *et al.*, 2002). Not all methods permit the formation of an equilibrium structure in membranes, as demonstrated for the hydrophobic peptide gramicidin A (Killian, 1992). To avoid this issue, Han *et al.* (2001) used a host-guest peptide design (Han and Tamm, 2000a) to render the HA fusion peptide water-soluble. They subsequently used NMR spectroscopy techniques to assess the role of pH on the structure of the HA fusion peptide in a lipid bilayer (Han *et al.*, 2001). Yang *et al.* (2001) used solid-state NMR while Gordon *et al.* (2002) utilized ^{13}C -enhanced FITR to determine the structure of the gp41 fusion peptide in a membrane environment.

The 125-amino-acid reptilian reovirus (RRV) p14 protein is a distinct member of the fusion-associated small transmembrane (FAST) proteins encoded by nonenveloped orthoreoviruses (Shmulevitz and Duncan, 2000; Dawe and Duncan, 2002; also see Chapter 3). The FAST proteins mediate cell-cell fusion and multinucleated syncytium formation in infected and transfected cells; moreover, they are non-structural and non-essential to virus entry (Duncan *et al.*, 1996; Shmulevitz and Duncan, 2000; Dawe and Duncan, 2002). The FAST proteins are unique fusion proteins, as they do not contain structural features typical of enveloped-virus fusion proteins, including large ectodomains or coiled coils. These proteins clearly do not have the size capability or structural features to undergo the fusion-mediating conformational rearrangement reported as

essential to membrane merger mediated by enveloped viruses. However, each member of the FAST protein family consists of its own signature arrangement of a subset of structural features that are common to all members of this unique class of fusion proteins. These common motifs include: Type III ($N_{\text{exo}}/C_{\text{cyt}}$) integral membrane association, a membrane-proximal cluster of basic residues, a C-terminal tail of 20-40 amino acids that is dispensable for fusion, modification by myristic or palmitic acid, and the presence of a second region of hydrophobicity (hydrophobic patch or HP) in addition to the transmembrane domain (Shmulevitz and Duncan, 2000; Dawe and Duncan, 2002; Chapter 3). The p10 protein of avian reovirus (ARV) utilizes this second region of hydrophobicity, located in the p10 ectodomain (p10HP), as an internal fusion peptide (Shmulevitz *et al.*, 2003a). RRV p14 also contains a region that is glycine/alanine-rich and moderately hydrophobic within its small N-terminal ectodomain. Previous studies have highlighted the importance of this region of p14 in the fusion mechanism. Insertion of two HA epitope tags, or the substitution of valine to threonine (V9T) to create an N-glycosylation motif in the ectodomain, eliminates fusion. Fusion was not restored upon treatment of p14-V9T-transfected cells with an inhibitor of glycosylation, tunicamycin (Fig 3.9.A; Chapter 3). To investigate whether this region is an internal fusion peptide motif important for the mechanism of p14-mediated fusion, I undertook biochemical and structural analyses of this motif. Certain experiments reported in this thesis chapter were performed by collaborators, as I did not possess the appropriate technical expertise.

From inter-proton distance information determined from solution NMR spectroscopic data, a three-dimensional structure of the p14 hydrophobic-patch motif was calculated by Drs. Syvitski and Jakeman. While reovirus fusion proteins

lack the size capability or structural features to promote membrane fusion using large energy-releasing triggered conformational changes (coiled-coil or multimer rearrangement), p14 and other FAST proteins may utilize a repertoire of membrane-interacting motifs similar to those found in the larger complex fusion proteins. This investigation of the structural nature of one such motif, the internal fusion peptide of p14, promises to contribute to an improved understanding of how p14, and the FAST proteins in general, facilitate membrane merger.

4.3 Results

The small 40-residue ectodomain of p14 contains a hydrophobic patch

A hydropathy plot indicates that there is a region of moderate hydrophobicity within the ectodomain of p14 that I termed the hydrophobic patch (HP) (Fig 4.1.A); both the 2HA-tag insertion and V9T substitution that eliminated fusion occur within this motif (Figs 3.4.A. and 3.9.A, Chapter 3). We examined this small region within the p14 ectodomain (Fig 4.1.B) to determine if p14 used its hydrophobic-patch motif as an internal fusion peptide.

The p14 hydrophobic patch is an internal fusion-peptide motif

We identified a core region of the hydrophobic patch (HP) that comprised amino acid residues 8-25 (Fig 4.1.A). This region contains a high percentage of glycine and alanine residues (6 of 18), and a moderate percentage of charged residues (4 of 18); these features are typical of amphipathic fusion peptides (White, 1992; Fig 4.1.A). The overall hydrophobicity of the core hydrophobic patch was calculated to be 0.45 using Eisenberg's normalized hydrophobicity scale (Eisenberg, 1984). This value is significantly greater than that of the internal fusion-peptide motif found within the ARV p10 membrane fusion protein (0.29; Shmulevitz *et al.*, 2003a); however, it is less hydrophobic than what is typically observed for fusion peptides of enveloped viruses (0.5-0.7; White, 1992). Thus, the hydrophobic patch of p14 is an atypical fusion-peptide motif.

I designed a synthetic peptide of the p14 HP to assess the ability of this region to mediate lipid mixing in an *in vitro* assay. The HP peptide (myr-30HP) is comprised of the first 30 amino acids of the p14 ectodomain, and thus spans the entire region of the core HP (Fig 4.1.A). Myr-30HP includes 6 residues N-terminal, and 6 residues C-terminal, to the core HP, and is myristylated at the N-terminal glycine residue. Modification with myristate is essential for fusion stimulated by the p14 protein (Fig 3.7.B, Chapter 3). Creation of an acylated peptide that is longer than the core region of interest should ensure that the core HP folds properly, and maximizes its membrane-penetration/lipid-mixing potential (Han and Tamm, 2000a). For example, inclusion of a polar region C-terminal to the actual hydrophobic fusion-peptide sequence of influenza HA and HIV gp41 markedly improved both penetration of the synthetic fusion peptide into the lipid bilayer, and lipid mixing (Peisajovich *et al.*, 2000a; Leikina *et al.*, 2001).

Our collaborators, Drs. R. F. Epand and R. M. Epand (McMaster University, Hamilton, ON), performed the lipid mixing studies reported in supplementary Fig 1.1, Appendix A. In this experiment, the myr-30HP peptide was added to large unilamellar vesicles (DOPC:DOPE:cholesterol ratio 1:1:1) and lipid mixing was quantified by a resonance energy transfer assay (Struck *et al.*, 1981). The myr-30HP peptide mediated efficient lipid mixing in a dose-dependent manner (Fig 1.1.A, Appendix A). Lipid mixing reached 50% at the highest concentration of peptide used (10 μ M). No lipid mixing occurred between vesicles in the absence of peptide (Fig 1.1.A, Appendix A). The lipid mixing mediated by 5 μ M p14 HP peptide plateaued at 25-30% (Fig 1.1.A, Appendix A), whereas 10 μ M of the ARV p10ehp peptide mediated only 10% lipid mixing, and 5 μ M of the simian immunodeficiency virus (SIV) gp32 fusion peptide, only 20% (Shmulevitz

et al., 2003a). Furthermore, lipid mixing with the myr-30HP peptide was very rapid, as evidenced by its rapid increase within the first few seconds to the maximum value (Fig 1.1.A, Appendix A). The ratio of lipid/peptide did not greatly affect the ability of the myr-30HP peptide to induce lipid mixing, as a given concentration of peptide yielded approximately the same percent of lipid mixing in 200 seconds with varying lipid concentrations (Fig 1.1.B, Appendix A).

Circular-dichroism spectroscopy predicts that the myr-30HP peptide lacks α -helical secondary structure

Circular-dichroism spectroscopy can identify overall secondary-structure character within a given fusion peptide, and how this secondary structure alters in the presence of solvent or lipid. Though useful, this technique has yielded conflicting results and drastically different secondary-structure determinations for the same fusion peptide depending on experimental conditions (Chang *et al.*, 1997; Yang *et al.*, 2001; Gordon *et al.*, 2002). Some investigators suggest that this variability results from inherent structural plasticity of the glycine/alanine-rich fusion peptides that is essential for their role as membrane-destabilizing modules (Davies *et al.*, 1998; Pécheur *et al.*, 2000; Wong, 2003). Despite much debate, the conclusion derived from many of these structural studies is that the fusion-competent conformation of an N-terminal fusion peptide is α -helical, while β -structures represent an inactive, aggregated form of a fusion peptide (Epand, 2003; Tamm, 2003). Conversely, internal fusion peptides do not form extensive secondary structures (Epand, 2003), and the majority of the structural information regarding these

regions has been obtained from the crystal structure of a fusion protein (Rey *et al.*, 1995; Lescar *et al.*, 2001; Kuhn *et al.*, 2002).

I modeled the p14 core HP motif as both an α -helix and a β -strand (Fig 4.2). When modeled as an α -helix a hydrophobic face results, but the modeled structure does not display clustering of bulky hydrophobic residues or a glycine/alanine ridge (Fig 4.2); both features have been reported as essential to the activity of the fusion peptides of HA and gp41 (Tamm, 2003; Wong, 2003). When modeled as a β -strand, one face is more glycine/alanine rich, whereas the other contains the majority of the bulky hydrophobic residues (Fig 4.2). Circular dichroism spectroscopy was performed on the myr-30HP peptide (in water at various concentrations) by our collaborators, Drs. R. F. Epand and R. M. Epand. CD spectra demonstrated a notable absence of minima at 208 and 222 nm, suggesting an almost complete lack of α -helical structure (Fig 1.2, Appendix A). A high percentage of β -structure, turn, and random coil was estimated to be present in the soluble myr-30HP peptide at the higher concentrations (Table 1.1, Appendix A, calculations performed by Drs. Epand and Epand); however, at peptide concentrations of 40 or 80 μ M, self-association and aggregation of the peptide is likely and aggregated peptide can artificially increase β -secondary structure (R. F. Epand and R. M. Epand, personal communication). In contrast, even at low concentration (10 μ M) in the presence of lipid vesicles (lipid:peptide ratio of 10:1; Fig 1.2.B, Appendix A) or in a helix-promoting solvent, trifluoroethane (TFE; Fig 1.2.C, Appendix A), the myr-30HP peptide demonstrated increased α -helical propensity (Table 1.1, Appendix A), suggesting that the p14 fusion peptide may adopt a more ordered secondary structure upon membrane interaction.

Fusion peptide motifs located internal to the amino acid sequence of a fusion protein often form looped structures (Rey *et al.*, 1995; Delos and White, 2000; Allison *et al.*, 2001; Lescar *et al.*, 2001; Kuhn *et al.*, 2002; Shmulevitz *et al.*, 2003a). A kinked, inverted-V structure is integral to the mechanism of membrane insertion utilized by the N-terminal fusion peptides of influenza HA and possibly HIV gp41 (Han *et al.*, 2001; Gordon *et al.*, 2002). When modeled as a β -turn- β strand structure, the p14 core HP is comprised of a central pro-gly pair (residues 13-14) predicted to promote the turn, while electrostatic interactions between the charged residues his11 and glu15 are predicted to stabilize the resulting loop (Fig 4.2). The proposed proline kink is on the opposite face of the β -strand as a glycine/alanine ridge, a feature which has been suggested to be an important component in the mechanism of action of the HA fusion peptide (Tamm, 2003).

P14 constructs with site-specific substitutions in the hydrophobic patch that alter the putative loop or its hydrophobic face, but not overall hydrophobicity, impair fusion

The p14 HP motif was altered in the context of the whole p14 protein to determine whether changing the residues predicted to form the loop, or the alanine/glycine hydrophobic face, would affect fusion. All p14 constructs were expressed in QM5 cells from the pcDNA3 mammalian expression vector, as assessed by radiolabeling and immunoprecipitation with polyclonal α -p14 (Fig 4.3.A). Immunofluorescence was used to qualitatively assess the surface localization of each mutant construct. As demonstrated for a subset of p14 constructs shown in Fig 4.3.C, all reached the cell surface, in

approximately equal amounts according to the staining pattern. As previously observed for authentic p14, only a subset of the total population of the protein localized to the cell periphery; the remainder was found in perinuclear and punctuate intracellular fluorescence (Fig 3.3.B, Chapter 3). When N-glycosylation mapping was used to determine the Type III ($N_{\text{exo}}/C_{\text{cyt}}$) membrane topology of p14 (Fig 3.8, Chapter 3), P14-V9T was N-glycosylated at the engineered site in the N-terminal ectodomain. This is confirmed here by the retarded gel mobility of the glycosylated proportion of p14-V9T in Fig 4.3.A. Authentic p14 lacks the N-terminal engineered site, but does contain a non-functional, non-essential native glycosylation site (asn121) within the C-terminal endodomain. This site is not modified by N-glycan addition in authentic p14 (Fig 3.8, Chapter 3), or in any of the p14 mutant constructs (Fig 4.3.A), as indicated by the lack of p14 with a retarded gel mobility. As the C-terminal glycosylation site is not modified in any of the p14 HP mutants, we infer that all have adopted the correct $N_{\text{exo}}/C_{\text{cyt}}$ membrane topology.

To assess the effect of each site-specific substitution on the ability of p14 to mediate fusion, we quantified the formation of multinucleated syncytia after each construct was transfected into Vero cells. The transfection efficiency of each construct was approximately equal as assessed by expression analysis (Fig 4.3.A). The ability of each to mediate fusion is expressed as a percent of authentic p14 fusion ability (Fig 4.3.B, left axis). The fusion ability of each mutant does not correlate with the overall hydrophobicity of the core hydrophobic patch, calculated using Eisenberg's normalized hydrophobicity scale (Eisenberg, 1984; Fig 4.3.B, right axis); fusion does not increase with a more hydrophobic fusion peptide motif and decrease with a more hydrophilic one

(Fig 4.3.B). This suggests that the lack of fusion observed for some of the p14 HP mutants is a result of the disruption of a residue-specific role(s) in promoting the formation of a fusion-competent structure, or in the interaction with the membrane itself.

Alanine was used to replace many of the residues within the core HP motif. Ala replacement of gly14 did not markedly alter p14 fusion (Fig 4.3.B). This substitution is tolerated among other fusion peptides, even in the N-terminal position of the HA fusion peptide (Qiao *et al.*, 1999; Epand *et al.*, 2001). Ala could replace pro13 (a residue that we predicted was essential to the formation of the loop) with only a moderate effect on fusion (Fig 4.3.B). In the ASLV env internal fusion peptide motif, proline can be replaced with alanine or glycine, but not with charged or bulky amino acids (Balliet *et al.*, 2000; Delos *et al.*, 2000). This suggests that the peptide turn can be mediated in absence of a proline residue, if the region still retains sufficient flexibility. Ala replacement of the two charged residues that I predicted to stabilize the loop, his11 and glu15, was surprisingly well-tolerated. Though speed with which p14 mutants H11A and E15A mediate fusion was decreased compared to authentic p14, their ability to mediate syncytium formation (Fig 4.3.B), and fuse the entire cell monolayer over time (data not shown), was unimpaired. This result contradicts my hypothesis that the putative loop is stabilized by electrostatic interactions between his11 and glu15, and argues that these charged residues are not essential for loop formation/stabilization. P14 constructs that contained conservative substitutions of these same residues (H11R, E15D) were expected to retain function (as was observed for I17V, and to a lesser extent for V9I; Fig 4.3.B); however, in both cases p14 fusion function was eliminated (Fig 4.3.B). Though H11R could be fusion-inactive as a result of the increased size and/or charge of the replacement arg, the

inability of asp to replace glu15 is unusual and suggests that these charged residues do not play the loop-stabilizing role I predicted.

Reversal of the position of charged residues within the p14 hydrophobic patch restores fusion

His11 was replaced with glu to test the effect of two negatively charged residues, and the resulting charge repulsion, on the ability of p14 to cause fusion. In accordance with my predicted model, H11E was unable to mediate membrane fusion (Fig 4.3.B, Fig 4.4). To test this model further, the position of each charged residue relative to the other was reversed (H11E/E15H). In Vero cells transfected with H11E/E15H, some fusion ability was restored to the previously non-fusogenic H11E construct (Fig 4.4). However, the fusion ability of H11E/E15E was much impaired relative to authentic p14 (Fig 4.3.B), and multinucleated syncytium formation did not progress beyond multinucleated cells with approximately 10 nuclei (Fig 4.4). The ability of H11E/E15H to restore partial fusion to H11E supported the hypothesized role of these charged residues as essential for loop stabilization, but suggests that they may also play other roles in the fusion mechanism.

Structural characterization of the acetyl-30HP peptide by solution NMR spectroscopy (details in Syvitski *et al.*, manuscript in preparation)

Mutational analysis of the HP motif within the p14 protein indicated that individual residues are important in the formation of a fusion-competent secondary or tertiary structure (Fig 4.3.B). Secondary-structure prediction for the myr-30HP peptide based on

CD spectroscopy (Fig 1.2.A-C, Appendix A) suggested that the HP structure is comprised of β -strand, random coil, and turns; however, this method does not provide information about the position of individual residues in a given structure. Our collaborators, Drs. R. Syvitski and D. Jakeman (Faculty of Pharmacy, Dalhousie University), used solution NMR spectroscopy to investigate the N-terminal water-soluble acetyl-30HP peptide. This peptide is identical to the myr-30HP with the exception that the N-terminal myristate has been replaced with an acetyl group. In solubility studies using the myr-30HP and acetyl-30HP peptides, I observed that the myr-30HP peptide behaved like a detergent in aqueous solution (data not shown). Thus, Drs. Syvitski and Jakeman could not perform the solution NMR analyses using the myr-30HP, as the myristic acid was believed to cause this peptide to form micelles in solution, preventing structural characterization.

Sequence-specific assignments were determined through routine NMR techniques performed by Drs. Syvitski and Jakeman (Roberts, 1993; Wuthrich, 1986) using two-dimensional ^1H TOCSY (Griesinger *et al.*, 1988) and NOESY (Jeener *et al.*, 1979) spectra. For three-dimensional protein-structure calculations, inter-proton distances were determined using ^1H NOESY NMR spectra and the $\text{NH-H}\alpha$ and $\text{H}\alpha\text{-H}\beta$ dihedral angles were determined using E-COSY (Syvitski *et al.*, manuscript in preparation) spectra. Structure calculations were based on previous procedures using the simulated-annealing molecular dynamics protocol in the X-PLOR software package (Brunger, 1992; Kuszewski *et al.*, 1992; Nilges *et al.*, 1988; Nilges *et al.*, 1991). Out of 100 simulations, a total of 14 calculated structures were retained. For these retained structures, the difference between the inputted inter-proton distance and that which was calculated was

$>0.4 \text{ \AA}$ and dihedral angle constraint violations $>25^\circ$. The overall quality of these refined structures was examined and with the exception of the random-coil section (gly14-thr31) all backbone dihedral angles reside in the well defined, acceptable regions of the Ramchandran plot. For the structured loop section (pro5 through pro13) the root mean-square deviation among the structures is $\sim 0.4 \text{ \AA}$.

The 14 retained structures of the p14 HP motif from solution NMR spectroscopy are shown in Figure 1.3, Appendix A. The N-terminal region of acetyl-30HP is much more ordered than the C terminus, and contains a looped region (Fig 1.3.B, Appendix A); however, the location of the loop is not as predicted by my model. From the calculated structure, a pro-gly pair (residues 4-5) facilitates the first turn (Fig 1.3.A, Appendix A) and a second pro-gly pair (residues 13-14, the region that was predicted to be a central turn in the looped HP) facilitates a second turn (Fig 1.3.A, Appendix A). This creates a looped structure at the N terminus of the p14 HP motif. Those residues located between the proline hinges form a β -sheet-like structure, whereas the residues after the second turn are disordered (Fig 1.3.B, Appendix A).

We have identified an internal fusion peptide motif in the p14 fusion protein of RRV. This is the first NMR solution structure solved for an internal fusion peptide and the first detailed structural information provided about the atypical FAST proteins encoded by non-enveloped orthoreoviruses.

4.4 Discussion

The p14 fusion protein of RRV contains a looped internal fusion-peptide motif

I have identified an internal fusion peptide motif, termed the hydrophobic patch (HP), within the N-terminal ectodomain of the RRV p14 membrane fusion protein. Like other internal fusion peptides, it forms a β -structured loop (Rey *et al.*, 1995; Lescar *et al.*, 2001; Kuhn *et al.*, 2002). Like N-terminal fusion peptides, the C-terminal region of the p14 HP motif is disordered (Han *et al.*, 2001). This is the first high-resolution structural information determined for a FAST protein, and the first attempt to use solution NMR spectroscopy to elucidate the structure of an internal fusion peptide.

The ARV p10 fusion protein also contains a hydrophobic-patch motif (p10HP) within its N-terminal ectodomain that functions as an internal fusion peptide (Shmulevitz *et al.*, 2003). That region is predicted by circular dichroism spectroscopy to form a β -structured loop and Shmulevitz *et al.* (2003a) suggest that two cysteine residues that flank the p10HP motif promote loop formation and stability through an intramolecular disulfide bond. Though the predicted structure of the p10 HP is similar to what I have predicted (Fig 4.2) and Drs. Epand, Epand, Syvitski and Jakeman have shown for p14 (Fig 1.2.A-C, 1.3, Table 1.1, Appendix A), p10 and p14 constructs with altered residues within the HP motif respond differently to mutation. An alteration in the overall hydrophobicity of the p14 HP did not correlate with either an increase or decrease in fusion ability of the modified protein (Fig 4.3.B), whereas decreased hydrophobicity of the p10HP decreased the fusogenicity and increased the half-life of the mutant protein(s)

(Shmulevitz *et al.*, 2003a). Those authors suggest that ARV p10 has evolved to contain a weak fusion peptide with low overall hydrophobicity (0.29 versus 0.45 for p14) that offers a means by which ARV slows, and thereby controls, the formation of multinucleated syncytia during the course of infection. No such regulation exists for p14. Instead, mutagenesis suggests residue-specific roles for many amino acids within the p14 HP motif, in the promotion of a fusion-competent secondary or tertiary structure or in membrane interactions predicted to occur during fusion itself. Unlike p14 and p10, the BRV p15 fusion protein does not contain a hydrophobic patch within its small ectodomain (Dawe and Duncan, 2002). However, it does contain a region that is similar in amino acid composition to the p14 HP within its endodomain. This internal HP motif is comprised of two pro-gly pairs separated by 9 amino acids, with similar positioning of asp, ala, his, and val residues (Fig 4.5). Whether this internal HP motif functions as a fusion peptide or plays an alternative role in the fusion mechanism of p15 remains to be determined.

P14 hydrophobic-patch structure

Synthetic peptide analogues to fusion peptide motifs make useful models for studying the membrane association of a fusion peptide, its perturbation functions, and structural conformation (Nieva and Agirre, 2003). In this regard, *in vitro* lipid mixing (Fig 1.1, Appendix A) and circular-dichroism spectroscopy (Fig 1.2, Appendix A) using the myr-30HP synthetic peptide indicated that the p14 hydrophobic-patch (HP) motif is a β -structured loop, typical for an internal fusion peptide. However, site-directed mutagenesis yielded some inexplicable results: though swapping the proposed loop stabilizing

residues his11 and glu15 restored fusion ability to p14 (Fig 4.4), many site-specific changes did not yield the expected effect (Fig 4.3.B), specifically, the ability of ala, but not arg or asp, to replace his11 and glu15, respectively, and yield a fusogenic protein. That conservative amino acids cannot replace these charged residues is unexpected, and suggests that his and glu do not play a loop-stabilizing role. The ability of ala to replace pro13 with little effect on fusion has also been observed for other proline-containing looped internal fusion peptides (Balliet *et al.*, 2000; Delos *et al.*, 2000). I wanted to verify the role of this pro residue, and others, in the formation of the putative HP loop.

Our collaborators, Drs. Syvitski and Jakeman (Faculty of Pharmacy, Dalhousie University) utilized solution NMR spectroscopy as a residue-specific technique to determine the structure of the acetyl-30HP peptide, and to investigate whether the core HP indeed forms a loop. The extended HP peptide was ideal for this technique; it is water-soluble, and contains flanking residues that may influence the folding/stability of the core HP. Using solution NMR spectroscopy, Drs. Syvitski and Jakeman elucidated that the p14 HP motif contains a looped region proximal to the N terminus (pro5-pro13; Fig 1.3.A, Appendix A) that is displaced from the location I had predicted from examining the amino acid sequence (phe8-gly20, with a central pro13-gly14 pair). The remainder of the myr-30HP peptide (glu15-thr31) is disordered and does not adopt a discrete secondary fold (Fig 1.3.B, Appendix A). This pattern is similar to the helix-hinge-helix structure that has recently been described for the N-terminal fusion peptides of influenza HA (derived from NMR spectroscopic analysis; Han *et al.*, 2001) and HIV gp41 (derived from FTR spectroscopy of ^{13}C -labeled fusion peptide; Gordon *et al.*, 2002). In the HA fusion peptide, the amino acids N-terminal to the hinge (gly13) form an

α -helix at both neutral and acidic pH; however, the region C-terminal to the hinge is disordered at neutral pH, whereas it adopts a 3_{10} -helix at a fusion-activating low pH (Han *et al.*, 2001). This inverted V-structure places the bulky hydrophobic residues into a pocket within the V, and places a ridge of glycine residues on the surface-exposed edge of the N-terminal α -helix (Tamm, 2003). It is possible that the internal fusion peptide motif of p14 is inherently disordered when inactive, and adopts secondary and/or tertiary structure when membrane-embedded. Preliminary evidence for this structural change is an increase in α -helical secondary structure (CD spectra) of myr-p14HP in the presence of lipid (Fig 1.2.B, Appendix A). NMR spectroscopic studies are currently underway to corroborate these CD observations. Alternatively, the lack of structure for the residues gly14 to thr31 in the acetyl-p14HP observed by NMR spectroscopy may result from the inherent plasticity of this internal fusion peptide, a hallmark feature of other fusion peptides (Davies *et al.*, 1998; Pécheur *et al.*, 2000; Wong 2003). This region may adopt a secondary or tertiary structure within the entire p14 protein (when the N-terminal myristic acid and transmembrane domain embed in the membrane) or within a membrane environment. Such a structural interconversion may be essential to the role of the p14 HP motif as an internal fusion peptide. Unfortunately, the myr-p14HP peptide appeared to form large micelles in solution, inhibiting a detailed NMR spectroscopic study on the role of the N-terminal myristate in the HP structure (R. Syvitski, personal communication).

What is the role of the fusion peptide motif in an enveloped-virus fusion protein

Fusion peptides have been predicted to play essential roles in the membrane-fusion ability of all enveloped-virus fusion proteins. These regions have been shown to interact

with and embed into membranes, mediate membrane destabilization, and promote lipid mixing using *in vitro* assays. Recent development of a host-guest system that renders the HA fusion peptide water-soluble (Han and Tamm, 2000) allowed an investigation of the thermodynamics of fusion-peptide insertion into a lipid bilayer. Li *et al.* (2003) have demonstrated that for the HA N-terminal fusion peptide, membrane insertion is a thermodynamically favorable event driven by enthalpy (Li *et al.*, 2003). These amphipathic peptides are also believed to mediate dehydration of the intercellular water layer (Han *et al.*, 1999), one of the predominant thermodynamic barriers that prevents biological membrane fusion (Zimmerberg *et al.*, 1993). Synthetic fusion peptides possess the ability to modulate membrane curvature, as evidenced by assays that measure their ability to induce non-bilayer lipid phases in pure bilayer systems (Epad and Epad, 2000; Siegel and Epad, 2000; Peisajovich *et al.*, 2000a). Fusion-protein multimerization may promote the self-association of fusion peptides in the biological setting to further promote their action. This has been mimicked *in vitro* using cross-linked synthetic fusion peptides, which display enhanced fusogenicity compared to the monomeric form (Yang *et al.*, 2003b). Many investigators believe that one of the reasons it has been so difficult to pinpoint the 'functional' structure of fusion peptide motifs within a membrane environment is due to the inherent structural plasticity of these peptides. Synthetic constructs of fusion peptides can readily interconvert between α -helical and β -structured conformations (Epad, 1998). It is possible that the conversion between the more compact α -helices and the extended β -conformations plays an important role in fusion function (Peisajovich *et al.*, 2000a), or that conversion of a disordered extended β -structure to a compact α -helix facilitates the membrane insertion/disruption necessary for

fusion (Tamm, 2003). In either case, secondary-structure interconversion is likely an important contributor to the ability of fusion peptides to mediate membrane disruption and lipid mixing (Davies *et al.*, 1998; P  cheur *et al.*, 2000; Wong 2003).

What is the role of the internal fusion peptide motif in p14-mediated fusion

I envision that the p14 HP motif plays a role in the membrane-fusion mechanism similar to that which has been ascribed to the fusion peptide motifs from enveloped-viral fusion proteins. That the p14 HP motif mediates membrane interaction and lipid mixing is clear (Fig 1.1, Appendix A); however, it is unknown whether this region facilitates membrane merger by an interaction with the donor or target membrane or both. I propose that the inherent structural plasticity of this region, as demonstrated by different secondary-structural propensity in water and lipid (Fig 1.2, Appendix A) and by the disorder of the C-terminal portion of the acetyl-30HP peptide (Fig 1.3, Appendix A), is important to the mechanism of p14-fusion. Perhaps in the context of the whole p14 protein, secondary or tertiary structure is imposed on the HP motif (a region that would otherwise remain largely disordered as in Fig 1.3.B, Appendix A) by the propensity of the transmembrane domain and/or N-terminal myristic acid to embed in the donor membrane. If so, the p14 ectodomain may contain potential energy that could be released upon the interaction of the HP motif and/or myristic acid with a target membrane, to drive the fusion reaction. As the insertion of the HA fusion peptide into a membrane is favored by enthalpy, this interaction may not be promoted solely by the hydrophobic effect (Li *et al.*, 2003). If for p14 the HP fusion-peptide membrane insertion is energetically favored, this event, in combination with the hypothetical release of potential energy from a constrained loop

within the ectodomain, and the subsequent refolding of the internal fusion peptide upon membrane interaction, may provide significant thermodynamic impetus for fusion.

Enveloped-viral fusion proteins rely on large conformational changes in protein structure or multimerization to provide energy to drive the membrane fusion reaction (Carr and Kim, 1993; Weissenhorn *et al.*, 1999; Gibbons *et al.*, 2000; Stiasny *et al.*, 2001). P14 and the other FAST proteins are much smaller membrane fusion proteins that are not part of the virus particle, do not play a role in mediating virus entry, and are not essential to the virus life cycle in cell culture. A small, unregulated fusion protein may utilize only small alterations in its ectodomain similar to those secondary-structure alterations already described to occur within fusion peptides encoded by enveloped viruses. That, in combination with the thermodynamically favorable membrane insertion of a fusion peptide and the ability of these motifs to dehydrate the intercellular space between adjacent cells and alter membrane curvature, may be sufficient for p14 to mediate membrane merger. That said, it is difficult to envision how the small approximately 40-amino-acid p14 ectodomain can span the distance between two opposing membranes. However, the first 127 amino acids of HA2 induced lipid mixing between cells that had been treated previously to establish cell-cell contacts (Leikina *et al.*, 2001). If close cell-cell contact is maintained by other means, perhaps p14 can use a simpler thermodynamic profile of discrete structural alterations, without a requirement for the extensive structural remodeling necessary for the membrane fusion activity of enveloped-virus fusion proteins. We propose that p14, and the other members of the FAST protein family, contain the minimal arrangement of protein motifs, including

membrane-interacting regions that are similar to those found in larger more complex fusion proteins, to mediate biological-membrane fusion.

4.5 Figures and Tables

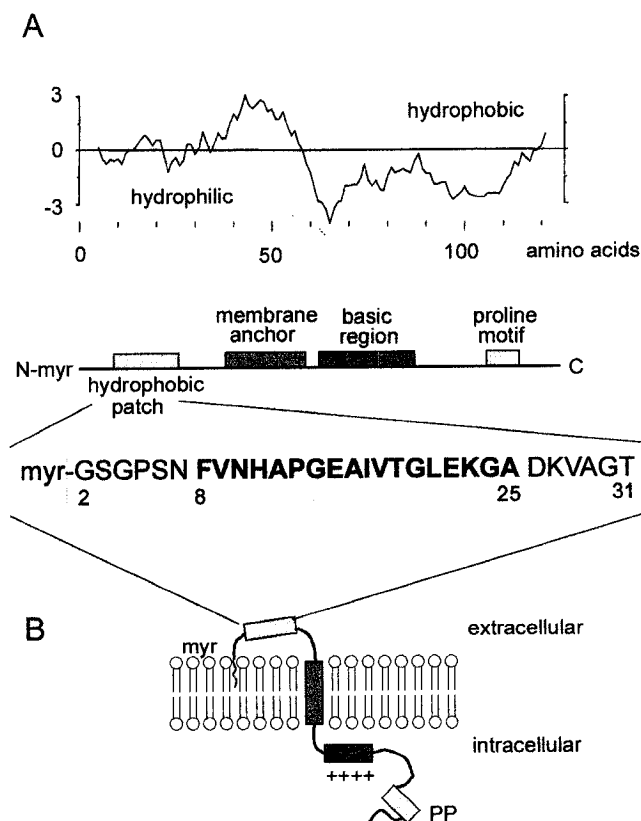


Fig 4.1 p14 contains a hydrophobic patch in its ectodomain. **(A)** A hydropathy profile of the p14 protein averaged over a window of 11 residues is shown. The locations of the myristate modification, hydrophobic patch, transmembrane anchor, polybasic region, and polyproline region are indicated in a linear **(A)** and structural model of p14 **(B)**. The p14 hydrophobic-patch motif is located within the small approximately 40-residue ectodomain of p14. The core region of the hydrophobic patch is comprised of residues 8-25 (bold); the p14 hydrophobic patch peptide (myr-30HP) spans residues 2-31 (shaded) and includes the N-terminal myristate modification.

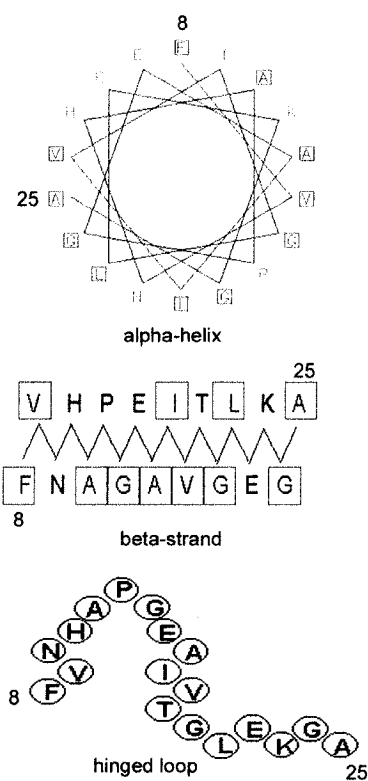


Fig 4.2 The p14 hydrophobic patch lacks α -helical character and may form a loop. The core region of the p14 hydrophobic patch (residues 8-25) modeled as a α -helix, β -strand, and β -structured loop. Amino acid numbers are indicated and squares surround hydrophobic residues.

Fig 4.3 Site-specific substitution of amino acids within the p14 hydrophobic patch motif that alter the predicted loop or its hydrophobic face, but not overall hydrophobicity, impair fusion. **(A)** p14 constructs that contained site-specific substitutions within the HP were transfected into QM5 cells. At 12 hours post-transfection, cells were radiolabeled with [3 H]-leucine and immune precipitated with polyclonal anti-p14. **(B)** The ability of these p14 constructs to mediate cell-cell fusion by transfected Vero cells was quantified by a syncytial indexing assay (bar graph, left axis). The average number of nuclei present in syncytia was determined by microscopic examination of five random fields, and results are expressed as the percent of authentic p14 fusion \pm the standard error. The relative hydrophobicity of the core HP (residues 8-25) of each p14 construct was calculated using Eisenberg's normalized hydrophobicity scale (line graph, right axis). H/E = H11E/E15H p14 construct. **(C)** QM5 cells transfected with p14 mutant constructs were assessed for cell-surface localization by immunofluorescence microscopy using polyclonal anti-p14 antibody and FITC-conjugated goat anti-rabbit secondary antibody. Scale bar = 10 μ m.

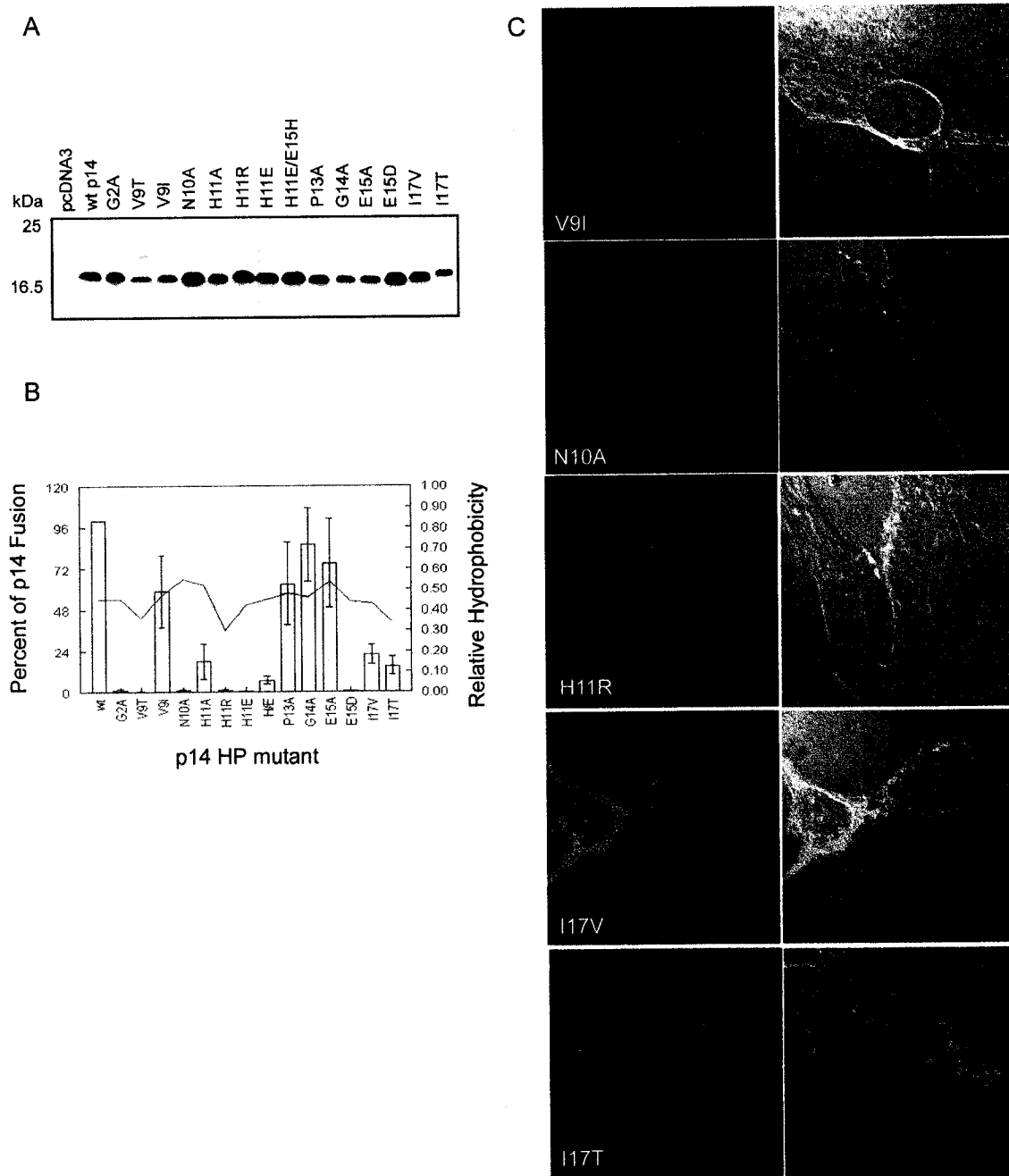


Fig 4.3 Site-specific substitution of amino acids within the p14 hydrophobic patch motif that alter the predicted loop or its hydrophobic face, but not overall hydrophobicity, impair fusion.

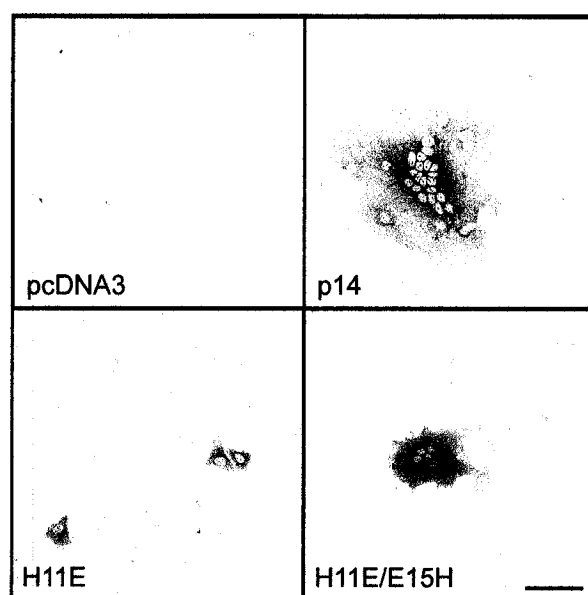


Fig 4.4 Reversal of the positions of the loop-stabilizing charged residues within the p14 hydrophobic-patch motif restores fusion. Vero cells were transfected with authentic p14, p14 constructs containing site-specific amino acid substitutions (H11E, H11E/E15H), or the pcDNA3 vector. At 20 hours post-transfection, cells were immunostained with polyclonal anti-p14 antibody and alkaline phosphatase-conjugated goat anti-rabbit secondary antibody to visualize p14-expressing cells. Scale bar = 100 μ m.

p14 HP 2-GSGPSNFVNHAPGEAIV-18
p15 HP 77-AHNPGSVISATPIYKGP-93

Fig 4.5 The amino acid sequence of the p14 hydrophobic patch is compared with a moderately hydrophobic stretch within the cytoplasmic domain of BRV p15 (S. Dawe, personal communication). The shaded region in p14 represents the N-terminal loop identified in Fig 3.6. It is compared to a similar motif in p15.

Chapter 5

The 14-kDa membrane fusion protein of reptilian reovirus is a homomultimer

5.1 Overview

Reptilian reovirus (RRV) is one of the few known examples of a non-enveloped virus capable of inducing cell fusion. RRV encodes an unusual 125-amino-acid, 14-kDa membrane fusion protein. Mutagenic analysis to identify essential p14 functional motifs revealed that certain substituted or tagged p14 constructs exerted a dominant-negative effect on syncytium formation when expressed with the authentic protein in co-transfected cells. The dominant-negative effect suggested that p14 is either a homomultimer or interacts with a limiting host factor to mediate cell fusion. To address this issue, I undertook several approaches to determine the multimeric status of p14. Following co-transfection of both authentic p14 and a C-terminally HA-tagged version of the protein, both forms of p14 were immune precipitated by an anti-HA monoclonal antibody. This co-immune precipitation occurred under different detergent conditions, which all solubilized the total cellular population of p14. *In vitro* chemical cross-linking confirmed the close association of p14 monomers, and suggested that p14 forms dimers. Fluorescence microscopy showed that p14 traffics through the ER-Golgi pathway to the cell surface. A preliminary assessment of the p14 assembly process, using pulse-chase analysis, suggested that p14 multimers form within the first 15 minutes after synthesis, and thus assembly likely occurs in the endoplasmic reticulum. This continued dissection of p14 multimerization, the regions of p14 that mediate these interactions, and the role of multimer formation in the fusion process will contribute to an understanding of how this unusual small fusion protein, encoded by a non-enveloped virus, has the ability to facilitate membrane merger.

5.2 Introduction

Enveloped viruses encode membrane fusion proteins that embed in the lipid envelope and mediate merger with the cell membrane to effect virus entry (White, 1990). Two classes of these viral membrane fusion proteins have been described, that differ markedly in structure. However, despite structural dissimilarity, each class facilitates fusion by utilizing triggered conformational changes of a multimeric fusion protein, which is believed to provide the energy to overcome the thermodynamic barrier that exists between opposing membranes (Carr and Kim, 1993; Zimmerberg *et al.*, 1993; Weissenhorn *et al.*, 1999; Blumenthal *et al.*, 2003). For the Class I membrane fusion proteins, typified by influenza hemagglutinin (HA) protein and human immunodeficiency virus (HIV) gp41, rearrangement involves coiled coils that both mediate trimerization and comprise the bulk of the ectodomain. For the Class II fusion proteins encoded by alpha- and flaviviruses, structural rearrangement redistributes the fusion protein, arranged in an icosahedral scaffold around the lipid envelope, from a metastable dimer to low-energy homotrimer (Rey *et al.*, 1995; Lescar *et al.*, 2001; Kielian, 2002; Kuhn *et al.*, 2002). Though structural remodeling plays a role in regulating the fusion activity of these proteins, it is possible that the energy produced by such rearrangements may not drive the fusion reaction (Epand and Epand, 2002, 2003; Remeta *et al.*, 2002). Instead, key elements that mediate membrane fusion are the membrane-interacting motifs found within these proteins. Fusion peptide motifs mediate lipid destabilization and mixing (Epand, 2003; Nieva and Agirre, 2003), and membrane-spanning domains assist in multimerization and donor-membrane destabilization, as well as stable anchoring in the viral envelope (Melikyan *et al.*, 1999; Tong and Compans, 2000; Patel *et al.*, 2001). In

combination with other membrane-interacting segments of the fusion protein (Peisajovich and Shai, 2003), these essential domains disrupt two opposing bilayers sufficiently to mediate membrane merger.

The role of multimer formation in enveloped-viral fusion proteins is not clear (Doms *et al.*, 1993). The formation of fusion-protein oligomers often occurs before the folding of individual monomers is complete; thus, oligomerization is an essential step in their folding pathway (Yewdell *et al.*, 1988; Tatu *et al.*, 1995; Mulvey and Brown, 1996). If these proteins fail to oligomerize they are often retained in the endoplasmic reticulum (ER) and subsequently degraded (Copeland *et al.*, 1988; Doms *et al.*, 1993; Oomens *et al.*, 1995). More recently it has been suggested that properly folded trimers are the necessary minimum functional unit of the fusion reaction (Markovic *et al.*, 1998), and that only properly assembled multimers can proceed to the formation of large fusion-protein aggregates deemed essential for the initiation of fusion (Danieli *et al.*, 1996; Markovic *et al.*, 1998; Bentz, 2000b; Markovic *et al.*, 2001; Roche and Gaudin, 2002).

The 125-amino-acid reptilian reovirus (RRV) p14 protein is a member of the fusion-associated small transmembrane (FAST) proteins encoded by certain non-enveloped orthoreoviruses (Shmulevitz and Duncan, 2000; Dawe and Duncan, 2002; Chapter 3). The FAST proteins mediate cell-cell fusion and multinucleated syncytium formation in infected and transfected cells and are the only viral proteins required for this process. Moreover, they are non-structural and non-essential to virus entry (Duncan *et al.*, 1996; Shmulevitz and Duncan, 2000; Dawe and Duncan, 2002). Significant comparative analysis of the structural features of three members of the FAST protein family (RRV p14, avian reovirus (ARV) p10, and baboon reovirus (BRV) p15) has identified a subset

of structural features common to this class of fusion proteins. These include Type III ($N_{\text{exo}}/C_{\text{cyt}}$) integral membrane association, a membrane-proximal cluster of basic residues, a C-terminal tail of 20-40 amino acids that is dispensible for fusion, modification by myristate or palmitate, and the presence of a second region of hydrophobicity (hydrophobic patch or HP) in addition to the transmembrane domain (Shmulevitz and Duncan, 2000; Dawe and Duncan, 2002; Chapter 3). The FAST proteins do not contain structural features typical of enveloped-virus fusion proteins, such as large ectodomains or coiled coils. These proteins clearly do not have the size or the structural features to undergo the fusion-mediating rearrangements reported as essential to membrane merger mediated by enveloped viruses (Weissenhorn *et al.*, 1999).

As a preliminary step towards an understanding of how p14 manages to overcome the thermodynamic barrier that prevents membrane merger, I investigated the oligomeric structure of p14. Using both a co-immune precipitation assay and chemical cross-linking I discovered that p14 is a homomultimer, and may exist as a dimer. This is the first report of a multimeric FAST protein, and this evidence is compared with previous findings that suggest that the ARV p10 protein is a monomer (Shmulevitz *et al.*, 2003b). These studies also confirmed that p14 traffics through the ER-Golgi to the cell surface, and preliminary results have suggested that multimer formation may occur in the endoplasmic reticulum shortly after protein synthesis. While the p14 multimer lacks the size or the structural features to promote membrane fusion using large energy-releasing triggered conformational changes, it may utilize a repertoire of membrane-interacting motifs, in co-operation with other p14 multimers, to drive the fusion reaction. Further studies on the p14 multimer, and the multimeric status of other members of the FAST protein family,

promise to complement our understanding of the co-operative nature of protein-mediated membrane fusion in all biological systems.

5.3 Results

Substituted/tagged p14 constructs act in a *trans*-dominant negative fashion to inhibit authentic p14-mediated fusion

The ectodomain of p14 is comprised of an essential myristate moiety on the N-terminal glycine residue (Fig 3.7, 3.8, Chapter 3), and a hydrophobic patch that may form a looped structure and acts like an internal fusion peptide to mediate lipid mixing *in vitro* (Figs 1.1, 1.2, 1.3, Appendix A; illustrated in Fig 5.1). Given the important role of this region in the mechanism of p14-mediated membrane fusion, mutations altering the hydrophobic patch often disrupt fusion (Fig 4.3, Chapter 4). I decided to investigate whether these p14 mutants had any effect on the ability of authentic p14 to cause cell-cell fusion. Mutated forms of other multimeric proteins can exert such a dominant negative effect (p53 tumor suppressor protein, Joers *et al.*, 1998; dynamin-1, Lee *et al.*, 1999; human T-cell leukemia virus type 1 env protein, Rosenberg *et al.*, 1999).

Vero cells were co-transfected with authentic p14 and p14 constructs that contain site-specific substitutions within the hydrophobic patch. These mutant proteins are expressed, adopt the correct topology, and localize to the cell surface (Fig 4.3, Chapter 4). Many of these mutant versions of p14 altered the rate of authentic p14-mediated fusion (Fig 5.2.B); a subset displayed a *trans*-dominant negative effect on the ability of authentic p14 to mediate fusion (Fig 5.2.A). A myristylation-minus construct (G2A), a hydrophobic-patch substituted construct (H11E), and a non-fusogenic construct with two HA epitopes inserted within the hydrophobic patch (2HAN) all displayed the dominant

negative phenotype and eliminated fusion. No negative effect was observed when p14 was co-transfected with the pcDNA3 vector (Fig 5.2.A). Other non-fusogenic p14 constructs did not completely inhibit the ability of authentic p14 to cause syncytium formation; however, many impaired the overall extent of authentic fusion when co-transfected into the same cell (Fig 5.2.B).

Non-fusogenic constructs of p14 possess the ability to interfere with the mechanism of authentic p14-mediated fusion when expressed in the same cell; this suggests that there may be a direct interaction between p14 monomers. If so, the mutant and authentic p14 interact and form a p14 multimer that is fusion-inactive/impaired possibly because p14 mutants may disrupt the folding of a fusion-competent structure, and its subsequent activity (Joers *et al.*, 1998; Lee *et al.*, 1999; Rosenberg *et al.*, 1999). It is also possible that the presence of mutant p14 and authentic p14 in the same cell results in competition for a cellular factor that is essential to the fusion mechanism. If such a cellular factor is limiting, the presence of an equal amount of mutant p14 could impair or inhibit fusion. This second possibility suggests that p14 could be a heteromultimer; however, immune precipitation with anti-p14 antibody does not co-precipitate any additional protein species (data not shown), and multimeric enveloped-virus fusion proteins do not require interaction(s) with a cellular partner to mediate membrane fusion (these proteins act in the absence of cellular proteins in liposome fusion assays; White *et al.*, 1982; Lapidot *et al.*, 1987). I believe that my observation that some p14 mutants completely eliminate fusion, while others decrease the speed of the fusion reaction, suggests a direct interaction between p14 monomers.

Co-immune precipitation indicates interactions between p14 monomers

I used co-immune precipitation as a direct approach to investigate p14 homomultimerization. These experiments utilized expression clones for authentic p14 and for a C-terminally HA-tagged construct of p14 (p14-2HAC) that retains the ability to mediate cell-cell fusion (Fig 3.4, Chapter 3). When co-transfected together, p14/p14-2HAC mediated multinucleated-syncytium formation at a speed that was slower than that of authentic p14 and faster than that of p14-2HAC (data not shown). I used immune precipitated co-transfected QM5 cell lysates to examine whether authentic p14 and p14-2HAC interact. To ensure the specificity of this procedure, control immune-precipitation experiments were performed (Fig 5.3.A). When cells were co-transfected with authentic p14 and the pcDNA3 vector, and immune precipitated with anti-p14, the authentic p14 protein was detected, whereas when the same cell lysate was treated with anti-HA, normal rabbit serum, or an isotype control, p14 was not precipitated (Fig 5.3.A). When cells were co-transfected with p14-2HAC and pcDNA3, both anti-p14 and anti-HA recognized the slow migrating p14-2HAC, while normal rabbit serum and an isotype control did not (Fig 5.3.A). Under these same conditions, cells were also co-transfected with p14 and p14-2HAC. Both forms of p14 were precipitated with anti-p14, indicating that authentic and HA-tagged p14 were expressed, and that the expression levels of the two proteins were approximately equal when co-transfections were performed using a 1:1 DNA ratio (Fig 5.3.A, B). Immune precipitation with anti-p14 also demonstrated that the two forms of p14 were easily distinguished by their different mobilities when subjected to gel electrophoresis (Fig 5.3.A). Immune precipitation with a mouse monoclonal anti-

HA (IgG2b) antibody recognized p14-2HAC and authentic p14, indicating that p14 and p14-2HAC interacted under the immune-precipitation conditions used (Fig 5.3.A, B).

Co-transfected cells were lysed using both mild (1% Triton X-100, 1% NP-40) and harsh (RIPA, high salt) conditions and immune precipitated. As previously observed, p14 and p14-2HAC were both precipitated by anti-HA as well as by anti-p14, but not by control antibodies (normal rabbit serum or mouse IgG2b; Fig 5.3.B). I performed p14/p14-2HAC co-transfection experiments with varying ratios of DNA in an attempt to increase the intensity of the authentic p14 band after anti-HA immune precipitation of the p14 multimer. By varying the amount of input DNA for each p14 construct, I also hoped to decipher the multimeric status of p14. When a 2:1 (Fig 5.3.A) or 3:1 (Fig 5.3.B) ratio of authentic p14:HA-tagged p14 were used in co-transfections, the expression levels of each protein were altered; this was reflected by the relative amounts of each protein after anti-p14 immune precipitation (Fig 5.3.A, B). Anti-HA did not precipitate an increased proportion of authentic p14, but rather a lower amount of authentic p14. By decreasing the population of p14 multimers that contained an HA-tagged version of p14, I decreased the proportion of authentic p14 immune precipitated by anti-HA (Fig 5.3.A, B). This effect is illustrated in Fig 5.3.C.

The co-immune precipitation technique used in my experiments required the presence of a detergent to solubilize p14. The use of Triton X-100 in these procedures can be cause for concern, as this detergent is frequently used to isolate membrane microdomains (Brown and Rose, 1992; Brown and London, 1998). If so, the positive co-immune precipitation results could be due to isolation of p14-containing detergent-resistant microdomains with the anti-HA antibody. To ensure that the interaction

observed between authentic p14 and p14-2HAC reflected true protein-protein interactions and not solely co-localization of the two proteins into the same detergent-resistant microdomain, or detergent micelle, I utilized a number of different immune-precipitation conditions (Fig 5.3.B), all of which do not preserve p14 microdomain localization (see Fig 6.2, Chapter 6). Further, each detergent was used at a concentration in excess of its critical micellar concentration (CMC), and the ratio of detergent to protein in the cell lysate was estimated to be well in excess of the 10:1 ratio required to effect proper membrane-lipid solubilization (Ostermeyer *et al.*, 1999). In addition, the relative amount of authentic and HA-tagged p14 protein that was precipitated by anti-HA did not reflect the input amount, and is different than the relative amount of protein precipitated by anti-p14 (Fig 5.3.A, B). If p14 and p14-2HAC were co-precipitated because the two proteins co-localize to the same detergent-resistant membrane microdomain or detergent micelle, the ratio of each protein to the other would be expected to reflect the ratio of input DNA, as is observed for anti-p14 precipitation. That this ratio differs with anti-HA, supports my assertion that p14 monomers directly interact. Despite this evidence, I attempted to confirm p14 multimerization using a second approach.

P14 monomers can be cross-linked *in vitro*

Homo- or heterotypic chemical cross-linking reagents often provide structural information about non-covalently interacting complexes in cells and *in vitro* (Bennett *et al.*, 2000). These chemicals interact with amino acid side chains to covalently link closely associated proteins together. P14 does not contain any cysteine residues; however, many compounds also react with primary amines, and p14 contains two lysine residues within

its ectodomain and four in the endodomain. I used three *N*-hydroxysuccinimide (NHS) esters, (1) dithiobis(sulfosuccinimidylpropionate) or DTSSP, (2) ethylene glycobis(succinimidylsuccinate) or EGS, and (3) disuccinimidyl tartrate or DST, to cross-link lysine residues and thereby demonstrate close association of p14 monomers. I also used a fourth compound, *p*-azidophenyl glyoxal monohydrate (APG), that specifically reacts with the side chain of arginine (p14 contains eleven arginines within the endodomain). APG cross-links an arginine-containing protein non-specifically to any neighbouring molecule(s) when photoactivated with UV light (Konishi and Fujioka, 1987). This group of reagents (summarized in Table 5.1) provides a range of span distance (the spacer arm, and thus the optimal cross-linking distance between proteins is different for each reagent) and solubility, as it has been previously shown that not all proteins within close proximity can be covalently linked together by the same cross-linker (Finel, 1987; Mulvey and Brown, 1996).

When p14-transfected cells were treated with the four chemical cross-linkers (in either DMSO, or buffer plus 1% NP-40 to allow water-soluble reagents to cross the cell membrane), no high-molecular-weight p14 multimers were observed. A representative experiment is shown in Fig 5.4.A. Even upon prolonged exposure (Fig 5.4.A, lanes 7-11, 14-15) the banding pattern of high-molecular-weight background was not as expected for multiples of 14 kDa, and did not differ from the pattern in the control lanes 2, 7, 12, and 14 (treated with DMSO alone or with a water-soluble cross-linker and no detergent). Though the monomeric form of p14 was no longer visible by SDS-PAGE after p14-transfected cells were treated with DTSSP, a high-molecular-weight form of p14 did not appear (Fig 5.4.A, lanes 5, 10). However, when DTSSP treatment and anti-p14 immune

precipitation was followed with β -mercaptoethanol to cleave the cross-linker, monomeric p14 re-appeared (Fig 5.4.A, lanes 6, 11). The absence of monomeric p14 after DTSSP treatment occurred in numerous experiments; however, in each I failed to detect a low-mobility cross-linked form of p14 (data not shown). The disappearance of monomeric protein upon DTSSP cross-linking, and its reappearance after cleavage of the cross-linker by β -mercaptoethanol (without any visible appearance of high-molecular-weight complexes in either case) has been observed by other investigators (see Fig 3A of Friedrichson and Kurzchalia, 1998).

I decided to use DTSSP for a more thorough investigation of p14 multimerization. As many cross-linking reagents function optimally at a precise ratio of reagent to protein of interest (Wiemken *et al.*, 1981; Mulvey and Brown, 1996; Gosselin *et al.*, 2001), I hypothesized that the actual amount of p14 protein present in the total cell extract from p14-transfected cells was too low and that the presence of such an excess of cellular protein would compete with p14 for DTSSP. As well, NHS esters are readily hydrolyzed, especially in alkaline or dilute protein solutions (Jung *et al.*, 1983). In an attempt to overcome these potential problems, I decided to add varying amounts of DTSSP directly to a concentrated solution of pure p14 protein, thereby minimizing hydrolysis of the reagent (Colacino *et al.*, 1997; Moore-Hoon and Turner, 2000). This second set of experiments was performed using a concentrated source of the p14 protein, expressed and purified from the baculovirus expression system. Octylglucoside (OG) micelles maintained p14 in solution; however, as a detergent micelle does not mimic the natural membrane environment, and may alter the multimeric status of p14, I also performed cross-linking experiments using purified p14 that had been embedded in liposomes.

When DTSSP powder was added directly to either preparation of concentrated p14 (in OG micelles or in liposomes), high-molecular-weight forms of p14 were detected by silver stained SDS-PAGE (Figs 5.4.B). These bands represent multimeric p14, as they were not present in preparations of p14 that were not treated with DTSSP. When the cross-linking reaction was performed using p14-OG micelles, the band pattern corresponded to 1X, 2X, 3X, and 4X the predicted molecular weight of baculovirus-expressed p14 (Fig 5.4.B, left panel), whereas, cross-linked p14-liposomes gave a two-band pattern of monomeric and dimeric p14 (Fig 5.4.B, right panel). The concentration of protein in p14 OG-micelles is approximately five times greater than that of the p14-liposomes and the environment of a detergent micelle is artificial. Thus, I hypothesize that the cross-linking results obtained using p14-liposomes reflect a more accurate representation of p14 in a cell membrane and may indicate that p14 is a homodimer. At the very least, however, these *in vitro* experiments have confirmed my co-immune precipitation results, as both approaches indicate that p14 is a homomultimer.

The assembly of p14 into homomultimers

P14 is an integral membrane protein that localizes exclusively to the membrane fraction after co-translational translocation across the endoplasmic reticulum (ER) membrane (Fig 3.3, Chapter 3). The perinuclear and punctate immunofluorescence staining pattern observed for p14-transfected cells (Fig 3.4, Chapter 3) suggested that p14 traffics to the cell surface using the ER-Golgi pathway. This was confirmed by co-fluorescence experiments using a p14 construct that was C-terminally tagged with green fluorescent protein (p14-GFP), and organelle-specific staining with Texas Red (Fig 5.5). P14-GFP

retained fusion function (Fig 5.5, panels d, j, m) and also adopted the perinuclear and punctate staining pattern previously observed for intracellular p14 (Fig 5.5, panels a, g, m). When p14-GFP-transfected cells were treated with Brefeldin A (BFA) to cause the redistribution of the Golgi membranes into the ER (Doms *et al.*, 1989), the reticular staining coalesced and became more perinuclear (Fig 5.5, panels d, j, p). Abnormally large membraneous structures often observed after BFA treatment (Pelham, 1991) were visible (Fig 5.5 panel p). P14-GFP transfected cells were co-stained using primary antisera against the organelle markers (Theiler and Compton, 2002) calnexin (ER) (Fig 5.5, panels b, e), β -COP (Golgi apparatus) (Fig 5.5, panels h, k), and TGN38 (*trans*-Golgi network) (Fig 5.5, panels n, q) and a Texas Red-conjugated secondary antibody. As observed in the case of p14-GFP, these organelle markers all adopted a more perinuclear, clumped staining pattern after BFA treatment (Fig 5.5, panels e, k, q). Co-fluorescence indicated that p14-GFP partially co-localized with all three organelle markers (Fig 5.5, panels c, i, o). Co-localization was increased significantly when both p14-GFP containing vesicles and the specific organelle in question were induced to collapse following BFA treatment (Fig 5.5, panels f, l, r).

These co-localization studies established that p14 utilizes the ER-Golgi pathway to traffic to cell surface. I attempted pulse-chase analysis to determine when p14 multimer formation occurs. Cells were co-transfected with authentic p14 and p14-2HAC, pulse-labeled for 15 minutes, and immune precipitated. Anti-p14 precipitated both forms of p14 by co-immune precipitation, whereas both normal rabbit serum and the isotype control recognized neither p14 nor p14-2HAC (Fig 5.6.A). However, immune precipitation with anti-HA precipitated only the HA-tagged version of p14 (Fig 5.6.A).

This suggested that p14 multimer formation does not occur within the first 15 minutes after protein synthesis. Pulse-labeled, co-transfected cells were chased for various lengths of time to determine when p14 and p14-2HAC interact. Despite numerous attempts, (a representative experiment is shown in Fig 5.6.A) Anti-HA did not precipitate authentic p14 after any of the chase times (0, 15, 30, 45, 60 minutes) analyzed.

I hypothesized that the inability of anti-HA to detect both forms of p14 in our pulse-chase experiments may have resulted from the weak intensity of the signal following the 15-minute pulse-labeling period. A short half-life could make this approach fruitless. It has previously been demonstrated (Shmulevitz *et al.*, manuscript in preparation), and confirmed in this study (Fig 5.7), that the ARV p10 fusion protein has an extremely short half-life when expressed in transfected cells. Shmulevitz *et al.* (manuscript in preparation) speculated that the rapid degradation of p10 occurs in the ER, and that any p10 that escapes the ER to successfully reach the cell surface remains stable. Therefore, I analyzed the stability of p14. Authentic p14 demonstrated a rapid degradation profile (Fig 5.6.B). The half-life of p14-2HAC was not assessed; however, the half-life of C-terminally HA-tagged p10 and authentic p10 are indistinguishable (J. Salsman, M. Shmulevitz, and R. Duncan, unpublished data) suggesting that this is also the case for p14 and p14-2HAC. When the degradation profile of p14 was compared to that of p10 (Fig 5.7), it appeared that a greater proportion of p14 escaped the degradation machinery. This correlates with the ability of p14 to mediate fusion in transfected cells much more rapidly than ARV p10. At the time of pulse-labeling in Fig 4.7, syncytia were only approximately 5 nuclei/cell, whereas p14 had fused the entire monolayer of QM5 cells by 16 hours post-transfection (Fig 3.1, Chapter 3; Fig 5.6.B).

I attempted to co-immune precipitate p14/p14-2HAC using co-transfected cells that had been pulse-labeled and chased at a time point when the cell monolayer was completely fused. Anti-HA did not appear to precipitate authentic p14 unless I used a long labeling period (1 hour) and no chase (data not shown). However, after prolonged exposure, HA-tagged and authentic forms of the p14 protein were detected in both anti-p14 and anti-HA immune precipitates in both the 1-hour and 15-minute pulse-labeled lanes (Fig 5.6.C). The ability of anti-HA to precipitate both forms of p14 was inversely proportional to the length of the chase period until a time when authentic p14 was no longer detectable in the complex (after 30-minute chase, Fig 5.6.C). This observation is likely due to the short half-life of p14, and not dissociation of the p14 multimer. These studies suggest, but do not prove, that p14 and p14-2HAC interact within the first 15 minutes of their synthesis. As the trafficking of membrane proteins from the ER to the Golgi complex usually is the rate-limiting step in their transport (Copeland *et al.*, 1988), this assembly process likely occurs in the ER. As well, these experiments may suggest that multimerization of p14 is an inefficient process, as the p14 multimer is difficult to detect.

5.4 Discussion

P14 is a homomultimer

Using co-immune precipitation and chemical cross-linking, I provide evidence that the RRV p14 fusion protein is a homomultimer (Figs 5.3, 5.4). The co-immune precipitation assay indicated that authentic p14 and HA-tagged p14 interact under a number of different detergent and salt conditions (Fig 5.3.B), and taken together these assays provide evidence to suggest p14 homomultimerization. Immune precipitation using anti-p14 also fails to precipitate specific cellular proteins (data not shown), suggesting that p14 is unlikely to exist in a heteromultimeric complex with a cellular co-factor(s). Immune precipitation was also used to investigate the multimeric status of the avian reovirus (ARV) p10 fusion protein, with the opposite result (Shmulevitz *et al.*, 2003b) supporting the specificity of this assay.

In vitro cross-linking of liposome-embedded p14 protein suggested that p14 may be a dimer (Fig 5.4.B, right panel), whereas cross-linking of p14 in OG micelles resulted in high-molecular-weight species that corresponded to dimeric, trimeric, and tetrameric p14 (Fig 5.4.B, left panel). The membrane environment of p14, when liposome-embedded, more closely resembles a cellular membrane than p14 solubilized by a detergent micelle. I estimate that p14 comprises less than 10 % of the total liposome surface area (D. Top, personal communication), suggesting that the cross-linking result is not due to artificial crowding of p14 in the liposomal membrane. All membrane fusion proteins encoded by enveloped viruses are either homo- or heteromultimers (Doms *et al.*,

1993). Indeed, the statistical probability of protein-protein interactions within a membrane environment (based on the estimated concentration of integral membrane proteins in a cell membrane) suggests that membrane proteins are one million-fold more likely to form oligomers than to exist in a monomeric state (Grasberger *et al.*, 1986). Thus, that p14 is a homomultimer, and likely a dimer, is not in itself surprising, except for the evidence that another member of the FAST protein family, ARV p10, is believed to be a monomer (Shmulevitz *et al.*, 2003b).

In this study, I attempted pulse-chase analysis to understand the assembly process for p14. Pulse-chase analysis has been a useful assay to assess the assembly of other viral fusion proteins, and has illustrated that the half-life of the multimerization process differs greatly for different proteins. Assembly can occur very rapidly: 6-8 minutes for VSV G protein (Doms *et al.*, 1987) and 5-10 minutes for influenza HA (Copeland *et al.*, 1988; Yewdell *et al.*, 1988); or very slowly: 30 min for HIV-1 gp160 (Otteken *et al.*, 1996) and 80 minutes for Rous sarcoma virus env (Einfeld and Hunter, 1988). Similarly, for other small membrane proteins the folding and oligomerization time varies: e.g., for Simian virus 5 HN, the half-life of oligomerization is 25 –30 minutes (Ng *et al.*, 1989). Because p14 does not contain any methionine residues after N-terminal modification with myristate, I used [³H]-leucine for pulse-labeling experiments. The 15-minute pulse, coupled with the short half-life of p14, did not generate a strong pulse-labeling signal (Figs 5.6.A, B). I did not want to alter the authentic protein, and were hesitant to increase the pulse-labeling time, as many proteins are synthesized and assembled within a 15-minute time frame (Doms *et al.*, 1987; Copeland *et al.*, 1988; Yewdell *et al.*, 1988). In addition, an attempt to C-terminally methionine-tag authentic p14 resulted in a p14

construct that was only weakly fusogenic (J. Salsman, personal communication). These assays were not very successful; however, the prolonged exposure of one autoradiogram of an co-immune precipitation experiment after pulse-chase suggested that p14 multimers assemble within the first 15 minutes of p14 synthesis (during the 15 minute pulse; Fig 5.6.C). Though these data await confirmation, current evidence indicates that p14 multimers may assemble in the endoplasmic reticulum (ER). Folding and oligomerization of many membrane proteins, including the influenza HA trimer and the Sindbis virus trimer of E1:E2 heterodimers, occurs in the endoplasmic reticulum shortly after synthesis (Tatu *et al.*, 1995; Mulvey and Brown, 1996). Brefeldin A (BFA)-treated co-transfected cells and my co-immune precipitation assay will be used to discover if p14 multimers assemble when they are retained in the ER by this inhibitor (Otteken *et al.*, 1996). A p14 mutant with an N-glycosylation site engineered into the ectodomain (p14-V9T) can be used to study the sensitivity of p14 multimers to various compartment-specific endoglycosidases (Parks and Pohlmann, 1995). This experiment will allow me to distinguish the subcellular compartment in which p14 multimerizes.

The difficulty I encountered with the pulse-chase co-immune precipitation assay may suggest that p14 multimerization is an inefficient process. If p14 assembly is inefficient and a large quantity of monomeric p14 is retained in the ER, this could explain the rapid-degradation profile observed for p14 (Fig 5.6.A, B). If oligomeric proteins do not fold or assemble correctly, quality-control mechanisms retain the misfolded protein in the ER and can target the protein for ER-associated degradation (Nehls *et al.*, 2000; Ellgaard and Helenius, 2003). In the case of Simian virus 5 HN protein, ER retention correlates with a defect in folding and oligomerization (Ng *et al.*, 1990), and monomeric

forms of the baculovirus gp64 trimer are not transported to the cell surface, but are retained in the ER and degraded (Oomens *et al.*, 1995). The ARV p10 fusion protein has a more extreme degradation profile than that of p14, as a smaller proportion of p10 appears to escape rapid destruction (compare Fig 5.6.B and Fig 5.7; Shmulevitz *et al.*, manuscript in preparation). P10 is believed to function as a monomeric fusion protein (Shmulevitz *et al.*, 2003b). Perhaps the inability of Shmulevitz *et al.* (2003b) to detect multimeric p10 (using co-immune precipitation and cross-linking assays) resulted from an extremely inefficient p10 assembly process, such that a large proportion of p10 was retained in the ER and degraded (Shmulevitz *et al.*, manuscript in preparation). If a more sensitive assay can be developed as a tool to study the assembly process of the p14 multimer, perhaps such an assay will elucidate whether p10 may also assemble, albeit inefficiently, into multimers. Interestingly, the fusion proteins of vesicular stomatitis virus and Simian immunodeficiency virus 1 exist in equilibrium between monomeric and trimeric forms (Zagouras and Rose, 1993; Caffrey *et al.*, 1999); perhaps this situation may also apply to the FAST proteins. The multimeric status of the BRV p15 fusion protein is unknown; however, a number of non-fusogenic p15 mutants exert a *trans*-dominant negative effect on the ability of authentic p15 to mediate syncytium formation (S. Dawe, personal communication). The multimeric status of the three FAST proteins must be examined further. It would be unusual for this family of proteins to assemble into such disparate fusion-competent structures, one monomeric and the other multimeric, especially when their overall membrane topologies and subsets of structural features appear to be otherwise similar (Shmulevitz and Duncan, 2000; Dawe and Duncan, 2002; Chapter 3).

Regions involved in p14 multimerization

Oligomeric membrane proteins can interact through three possible regions: the extracellular/luminal, membrane-spanning, and/or cytoplasmic domain(s) (Bormann and Engelman, 1992). Influenza virus HA, parainfluenza virus type-2 F, and human immunodeficiency virus-1 gp160 that lack a membrane-spanning domain (MSD) and cytoplasmic domain can trimerize (Doms and Helenius, 1986; Tong and Compans, 2000; Zhang *et al.*, 2001). The oligomerization domain of baculovirus gp64 is comprised of an amphipathic α -helix within its ectodomain (Monsma and Blissard, 1995). Many small membrane proteins, including the prototypical example of the sialoglycoprotein of erythrocyte membranes, glycophorin A (Lemmon *et al.*, 1992), the erythropoietin receptor (EpoR; Constantinescu *et al.*, 2001), and the Simian virus 5 HN protein (Parks and Pohlmann, 1995), use the MSD to mediate protein-protein interactions. MSDs of enveloped-virus fusion proteins also contribute to multimerization. Sequences within the MSD are required for the formation of native E1:E2 heterodimers in hepatitis C virus (Patel *et al.*, 2001).

At 125 amino acids, p14 is small and thus is comprised of only few regions available for interaction between p14 monomers. We have previously demonstrated that the C-terminal 37 amino acids of p14 are not essential to the fusion mechanism of the protein (Fig 3.6, Chapter 3). This non-essential region encompasses a proline-rich domain and includes a predicted proline helix, a motif often involved in protein-protein interactions (Kay *et al.*, 2000; Blott *et al.*, 2001). The proline-rich region of p14 would be

an ideal candidate multimerization domain, if indeed the region were required for p14-fusion. The essential basic membrane-proximal region contains eleven positively charged residues, a property that makes this region unlikely to be responsible for the association between p14 monomers. The ectodomain of p14 is approximately 38 amino acids in size, and consists of an N-terminal myristate (Fig 3.7, 3.8, Chapter 3) and a looped hydrophobic patch (Fig 4.3, Chapter 4; Figs 1.1, 1.2, 1.3, Appendix A), both essential to the mechanism of p14-mediated fusion. The p14 mutants that exert a *trans*-dominant negative effect on the ability of authentic p14 to mediate fusion are those that disrupt either myristylation (G2A) or the proposed folding of the hydrophobic patch (2HAN, H11E) (Fig 5.2.A). This suggests that they interact with authentic p14 in a manner that disrupts proper multimer formation, making it unlikely that this region is the sole multimerization domain. For example, if a dominant negative p14 construct such as p14-2HAN was not interacting with authentic p14 due to the 2HAN insertion into the region of multimerization, then it is not likely to be a *trans* dominant negative. I propose that the MSD of p14, either alone or in combination with residues in the ectodomain, is responsible for the association between p14 monomers (Fig 5.8).

Membrane-spanning domains are no longer assumed to play the single role of hydrophobic membrane anchor. Enveloped-virus fusion proteins can use the MSD as a multimerization domain, and as a region of the protein that contributes to the fusion mechanism (Melikyan *et al.*, 1999; Tong and Compans, 2000; Patel *et al.*, 2001). The influenza HA MSD is not essential for trimer formation at neutral pH, but the HA trimer dissociates more readily upon low pH exposure when the MSD is removed, implicating this region in promoting trimer stability after low-pH conformational changes (Doms and

Helenius, 1986). However, the prototypical model of a small membrane protein that oligomerizes using its MSD is the SDS-resistant dimer glycoporphin A (Lemmon *et al.*, 1992). The residues important for dimerization include small hydrophobic amino acids within the motif GVXXGV. The NMR structure of glycoporphin A confirmed biochemical studies that indicated that the interaction is mediated by this region (MacKenzi *et al.*, 1997). This structural study demonstrated a close association of the two transmembrane α -helices at the N terminus (where two alpha carbon atoms are only 6.2 Å apart), but widening of the dimer interface within C terminus of the MSD (MacKenzi *et al.*, 1997). The MSD of p14 has an amino acid character similar to that of glycoporphin A (Fig 5.1): the MSD consists of many small hydrophobic residues in its N-terminus, while its C-terminal region is bulky, with five of the last nine residues either phe or trp. It is possible that the p14 MSD mediates monomer:monomer interaction using the valine- and glycine-rich narrow end of the transmembrane α -helix. This feature of the p14 MSD, a narrow N-terminal region and a wide base comprised of bulky hydrophobic residues, is also found in the other FAST proteins (ARV p10 and BRV p15). Future studies may demonstrate the importance of this unique MSD character in the multimerization or fusion activities of both or all members of the FAST protein family.

Role of p14 multimerization in fusion

The multimerization of enveloped-virus fusion proteins is essential for the proper folding, processing, and trafficking of these proteins. It is also a means of regulating fusion activity, as the oligomers are inactive metastable structures, and are believed to use conformational rearrangement to provide the energy required to drive fusion when

exposed to the appropriate trigger (Carr and Kim, 1993; Weissenhorn *et al.*, 1999). That said, the G protein encoded by rabies virus exists in a reversible equilibrium between native, active, and inactive forms (Roche and Gaudin, 2002); thus, the energy produced upon each conformational alteration must be small to allow for such reversibility. As well, recent thermodynamic analysis of HA suggests that this fusion protein may not exist in a metastable state (Epand and Epand, 2002, 2003). For p14 and the other members of the FAST protein family, their small size and non-essential nature negates the important role of energy-producing structural remodeling in the mechanism of fusion.

If the assembly of a p14 multimer is not important for creating a metastable structure, what role, if any, does the p14 multimer have? As discussed above, and similar to enveloped-virus fusion proteins, multimerization of p14 is believed to assist monomeric p14 in proper folding and trafficking to the cell surface (Figs 5.5 and 5.6). However, I believe that the p14 multimer may also possess functional significance more directly related to the fusion process. Many fusion proteins are predicted to use a co-operative mechanism to mediate fusion. Such models suggest that a minimum of three (Danieli *et al.*, 1996), six (Blumenthal *et al.*, 1996) or eight (Bentz, 2000b) HA trimers, 13-19 rabies virus G protein trimers (Roche and Gaudin, 2002), ten baculovirus gp64 trimers (Markovic *et al.*, 1998), and 5-6 Semliki Forest virus E1 homotrimers (Gibbons *et al.*, 2003) must aggregate at the site of fusion initiation. These studies also suggest that the trimeric form of these fusion proteins is the minimum functional unit for fusion. The energy that is predicted to result from the conformational change of one HA trimer (calculated to be approximately 40 kcal/mol in artificial lipid bilayers) is insufficient to overcome the thermodynamic barrier that prevents spontaneous fusion (Lee and Lentz,

1998); thus, if this energy release does drive the fusion reaction, then the co-ordinated conformational alteration of multiple trimers is necessary. However, the precise step(s) that require co-operation between fusion multimers is unknown. It has been suggested that co-operativity may facilitate the interactions of the fusion peptide with the membrane (Daneli *et al.*, 1996), the synchronized release of energy from triggered conformational changes (Markovic *et al.*, 2001), or a late-stage fusion step after the conformational change has occurred (Markovic *et al.*, 1998). As I hypothesize that p14 does not use energy-producing conformational changes to drive the fusion reaction, I speculate that its membrane-interacting domains, comprised of an internal fusion peptide (Chapter 4) and transmembrane anchor, disrupt both donor and target membranes to mediate membrane merger. A p14 multimer contains greater potential for bilayer disruption than a monomer, as fusion-protein multimerization may promote the self-association of fusion peptides in the biological setting to further promote their action (Han and Tamm, 2000b). This has been mimicked *in vitro* using cross-linked synthetic fusion peptides, which display enhanced fusogenicity (Yang *et al.*, 2003b). I propose that a significant number of p14 multimers co-operate, their membrane-interacting segments disturb the donor and target membranes, lower the energy barrier that prevents membrane merger, and drive the fusion reaction.

I have shown that RRV p14 forms a homomultimer. I propose that p14-multimer formation is not only integral to the correct folding and trafficking of p14 to the cell surface, but may play a more direct role in the mechanism of this fusion protein. P14-multimer formation is the first step in a co-operative process that results in membrane disruption significant enough to facilitate membrane merger. Future studies in our lab

will investigate the role of p14 microdomain localization as the second step in a process that requires the convergence of a critical number of p14 multimers to the fusion initiation site.

5.5 Figures and Tables

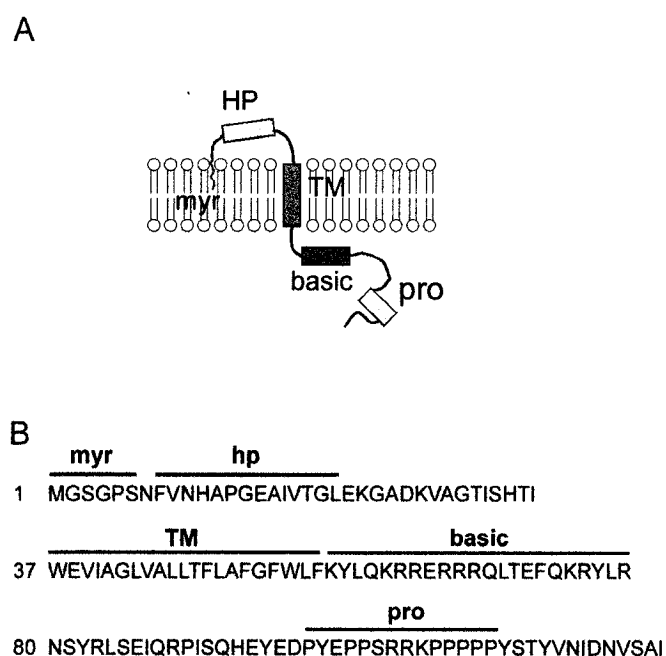
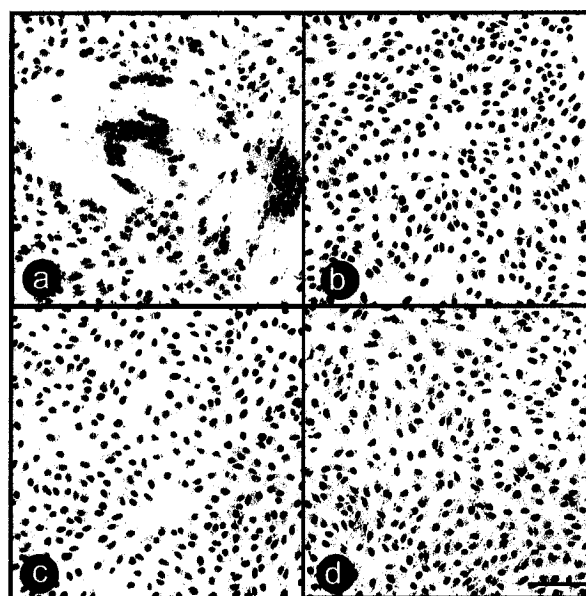


Fig 5.1 Structural motifs in p14. **(A)** The locations of the myristylation site (myr), hydrophobic patch (HP), transmembrane domain (TM), polybasic region (basic), and polyproline region (pro) are indicated on the topological model of p14. **(B)** Predicted amino acid sequence of p14. The locations of the structural motifs described in panel A are indicated above the sequence.

A



B

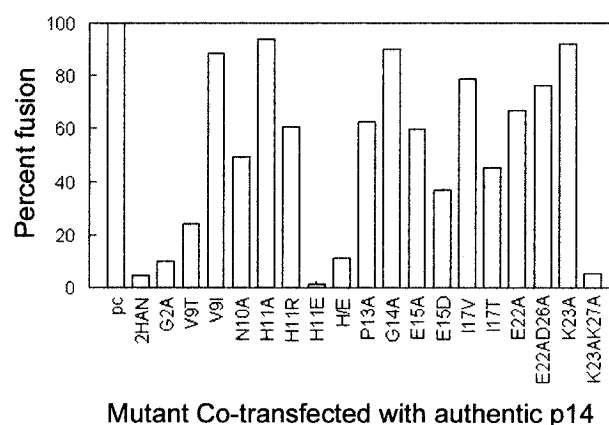


Fig 5.2 Substituted or tagged p14 constructs exert a *trans*-dominant negative effect on the ability of authentic p14 to mediate fusion. **(A)** Cells were co-transfected with authentic p14 and pcDNA3 vector (a), p14-2HAN (b), p14-G2A (c), or p14-H11E (d) in a 1:1 DNA ratio, and the ability of authentic p14 to mediate fusion was visualized by Giemsa-staining of cell monolayers. Scale bar = 100 μ m. **(B)** The *trans*-dominant negative effect was quantified by a syncytial index assay. The average number of nuclei present in syncytia was determined by microscopic examination of five random fields, and results are expressed as the percent of fusion observed when authentic p14 was co-transfected with the pcDNA3 vector. All co-transfections were performed using a 1:1 DNA ratio. pc = pcDNA3 vector, H/E = H11E/E15H p14 construct.

Fig 5.3 Co-immune precipitation indicates that p14 interacts as a homomultimer. **(A)** Authentic p14 and p14-2HAC (1:1 or 2:1 DNA ratio) were co-transfected into QM5 cells, radiolabeled at 14 hours post-transfection, and immune precipitated with polyclonal anti-p14 antibody (14), monoclonal anti-HA antibody (HA) normal rabbit serum (N) or an IgG2b isotype control (I) monoclonal antibody. Co-immune precipitation reactions were performed in RIPA buffer. **(B)** Authentic p14 and p14-2HAC (1:1 or 3:1 [indicated by *] DNA ratio) were co-transfected into QM5 cells, and co-immune precipitation reactions were performed as in (A) under various detergent conditions (RIPA, TxTNE, NpTNE, and TxTNE with 1 M NaCl). **(C)** Expected band intensities for co-immune precipitation with anti-p14 and anti-HA if p14 is a homodimer.

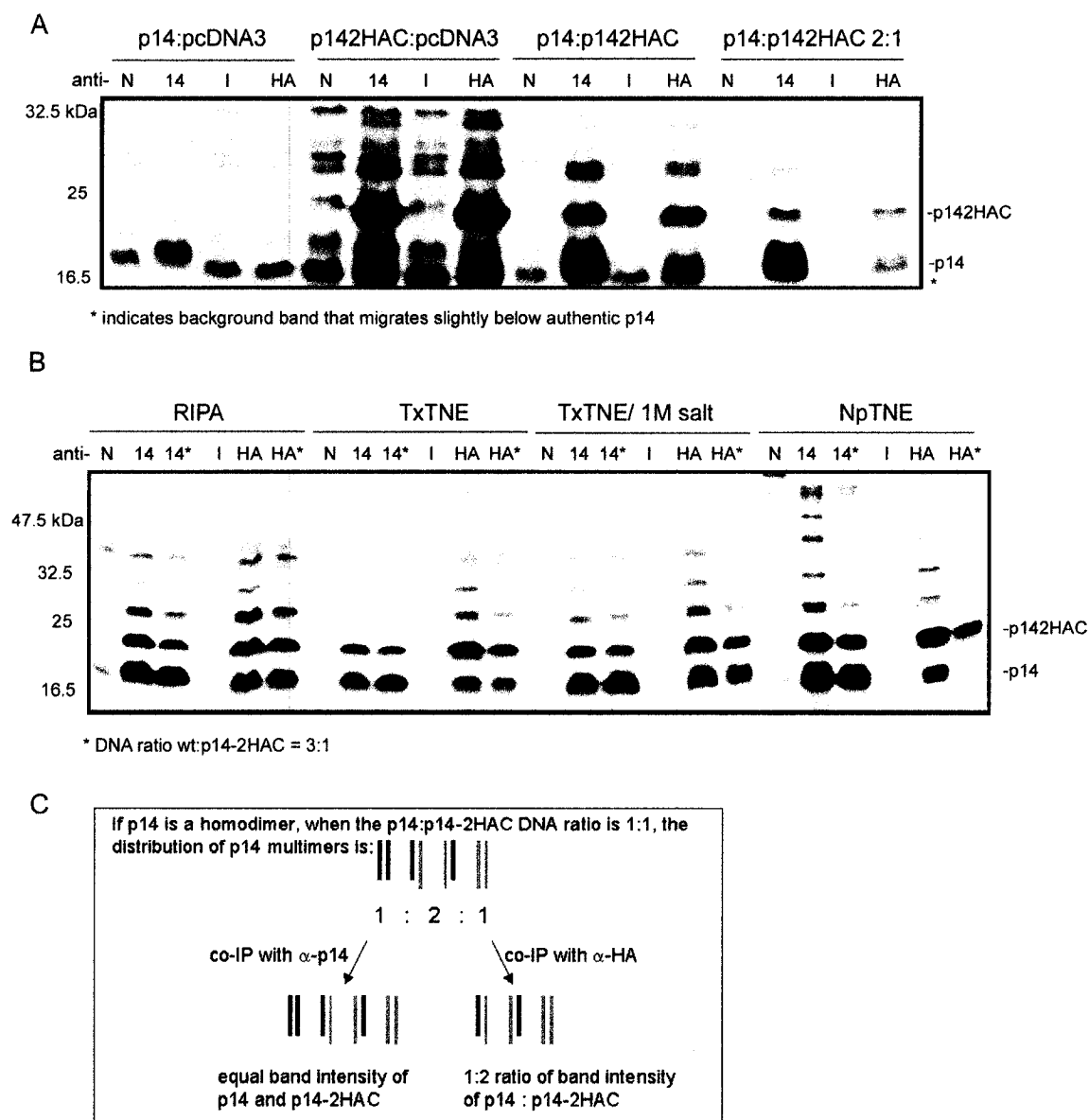


Fig 5.3 Co-immune precipitation indicates that p14 interacts as a homomultimer.

Table 5.1 Cross-linking reagents

Cross-linking Reagent	Abbrev	Solubility	Final Conc. (mM)	Spacer Arm (Å)	Cleavable
Dithiobis(sulfosuccinimidylpropionate)	DTSSP	Na citrate	5	12	reduction
Ethylene glycobis(succinimidylsuccinate)	EGS	DMSO	2.5	16.1	hydroxylamine
Disuccinimidyl tartrate	DST	DMSO	2.5	6.4	oxidation
p-Azidophenyl glyoxal monohydrate	APG	PBS	2.5	9.3	no
Dimethyl sulfoxide control	DMSO	-	-	-	-

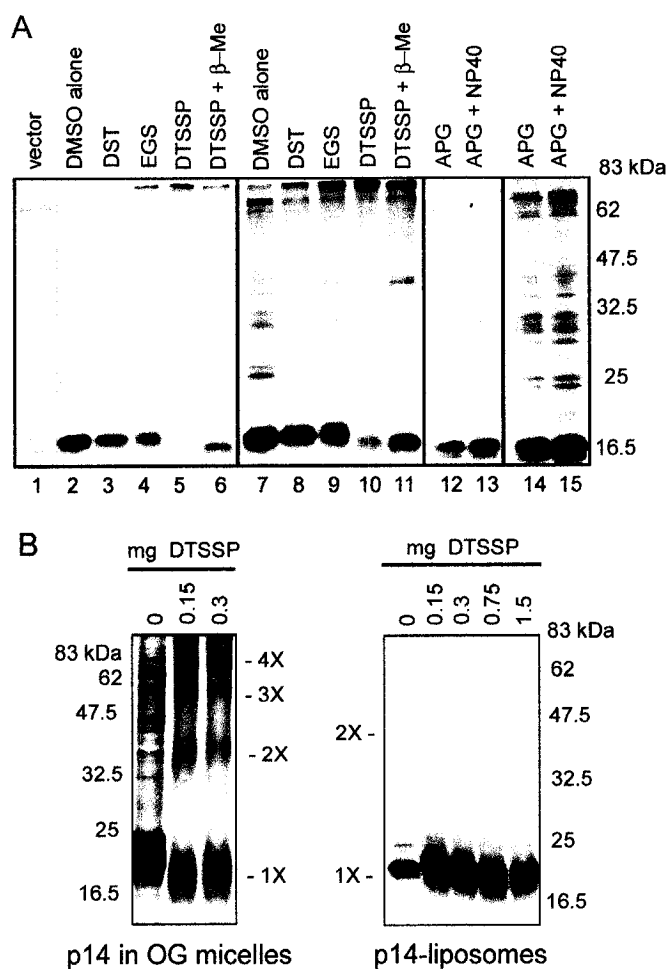


Fig 5.4 *In vitro* chemical cross-linking of p14 in liposomes supports that p14 is a homomultimer. **(A)** pcDNA3 vector- or p14-transfected cells were radiolabeled at 14 hours post-transfection, and cell suspensions were treated with the indicated chemical cross-linker (reaction conditions outlined in Table 3.I), or DMSO alone, and immune precipitated with anti-p14 antibody. **(B)** *In vitro* chemical cross-linking, with the indicated amount of DTSSP, of p14 in octylglucoside micelles (left panel) and p14 embedded in liposomes (right panel).

Fig 5.5 p14 traffics through the ER-Golgi pathway to the cell surface. P14-GFP-transfected QM5 cells were co-stained with antisera for organelle markers: ER (calnexin, panels a-f), Golgi apparatus (β -COP, panels g-l), and trans-Golgi network (TGN38, panels m-r) and examined for co-localization (yellow) of p14 (green) with each organelle marker (red). Where indicated, p14-GFP-transfected cells were treated with the vesicular-transport inhibitor brefeldin A (BFA), which results in a redistribution of the Golgi into the ER.

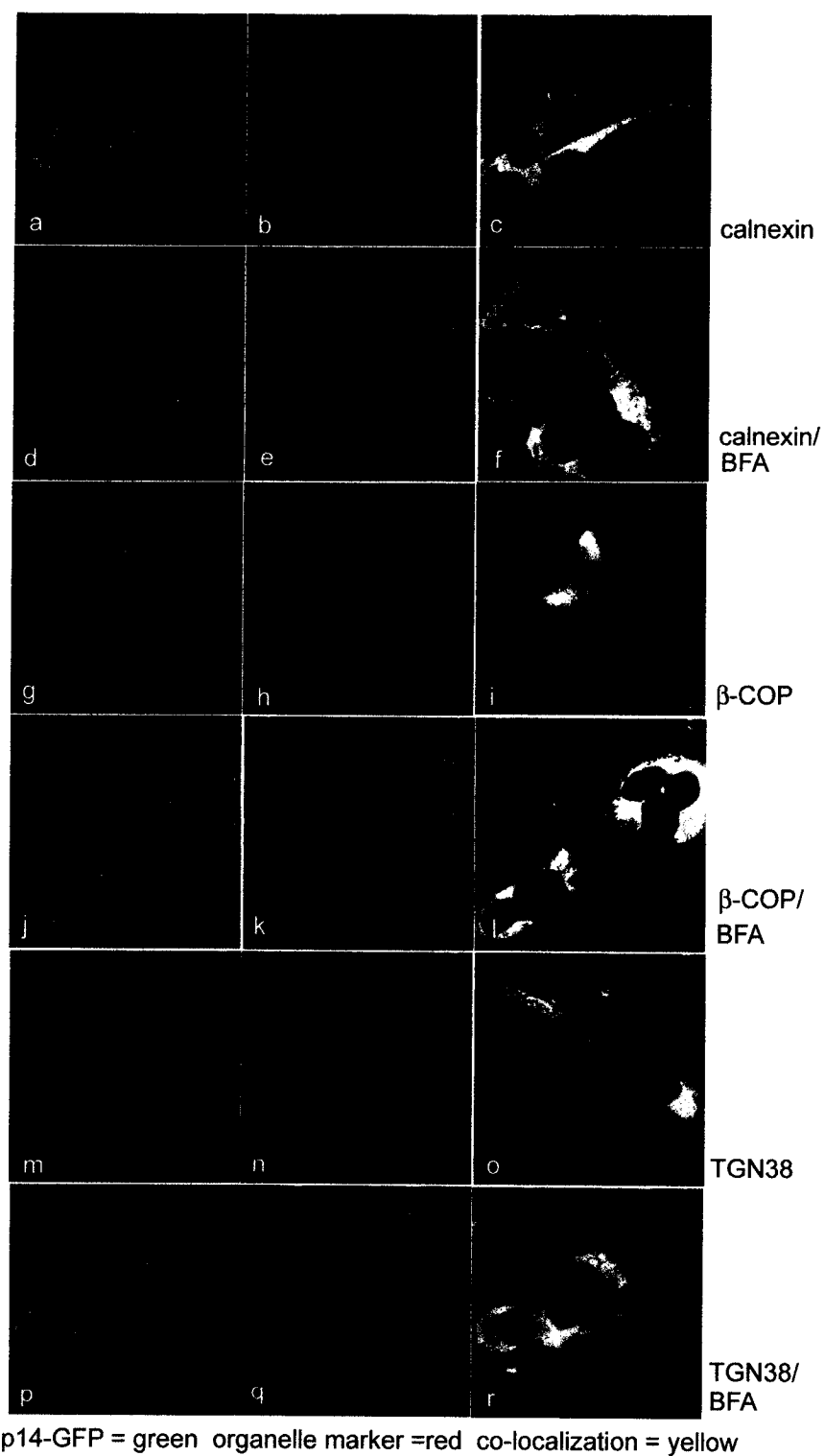


Fig 5.5 p14 traffics through the ER-Golgi pathway to the cell surface.

Fig 5.6 p14 multimerization may occur within the first 15 minutes of protein synthesis. **(A)** p14/p14-2HAC co-transfected QM5 cells were pulse-labeled for 15 minutes at 12 hours post-transfection and chased with a 3000-fold excess of unlabelled leucine for the times indicated. Cell lysates were immune precipitated with anti-p14 antibody (14), anti-HA antibody (HA), normal rabbit serum (N) or an IgG2b isotype control monoclonal antibody (I). As an additional control, co-transfected cells were pulse-labeled in chase medium (C) before immune precipitation. **(B)** To determine the half-life of p14 and assess the optimal time post-transfection for co-immune precipitation, p14- or pcDNA3 vector (v)-transfected cells were pulse-labeled as in (A), chased for the times indicated, and immune precipitated with anti-p14 antibody. Transfected cell lysates labeled in chase medium (C) were used as a control. **(C)** When syncytia were extensive (approximately 15 hours post-transfection), co-transfected QM5 cells were either labeled for 1 hour (no chase) or pulse-chased as in (A), solubilized and then immune precipitated in either RIPA (top panel) or TxTNE buffer (bottom panel) to determine the timing of p14 multimerization.

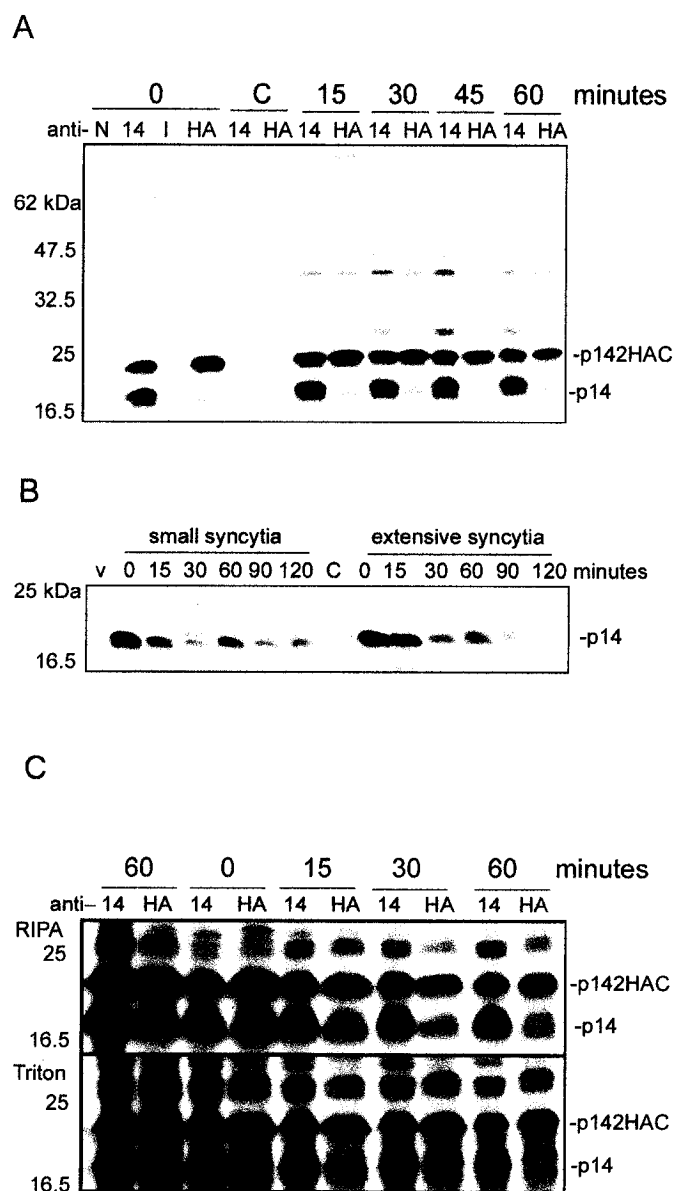


Fig 5.6 p14 multimerization may occur within the first 15 minutes of protein synthesis.

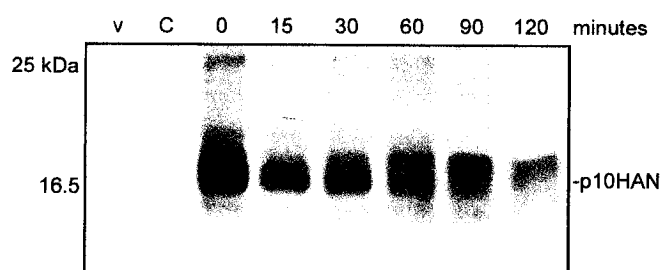


Fig 5.7 The degradation profile of the ARV p10 protein. p10-2HAN- or pcDNA3 vector (v)-transfected QM5 cells were pulse-labeled for 15 minutes at 24 hours post-transfection and chased with a 3000-fold excess of unlabelled leucine for the times indicated. Cell lysates were immune precipitated with anti-HA antibody (HA). P10-2HAN-transfected cell lysates labeled in chase medium (C) were used as a control. P10-induced syncytia formation was minimal at the time of pulse-labeling.

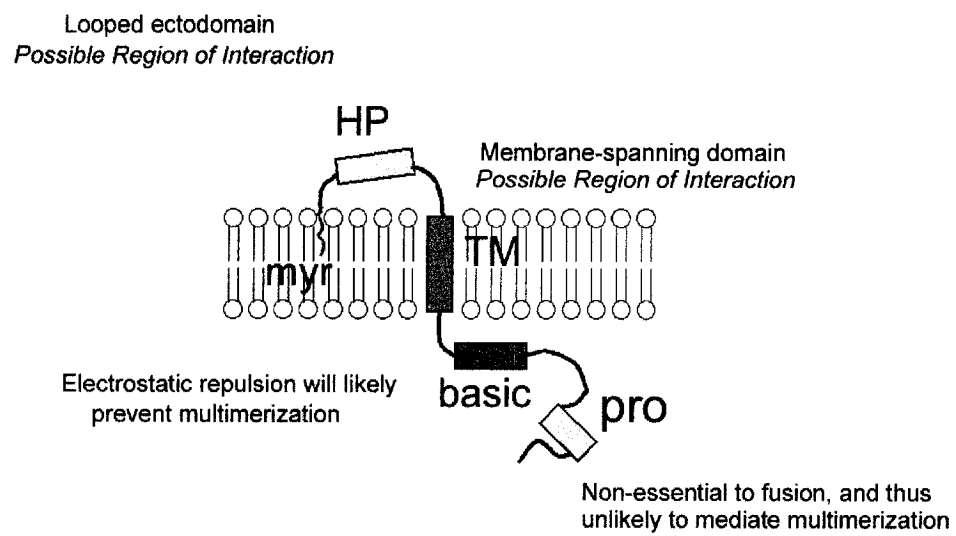


Fig 5.8 A structural model of p14 indicates possible regions of interaction between p14 monomers.

Chapter 6

A nonenveloped-virus membrane fusion protein localizes to lubrol-resistant membrane microdomains: possible role of cell protrusions in the mechanism of p14-mediated cell-cell fusion.

6.1 Overview

Reptilian reovirus is a member of a small group of nonenveloped orthoreoviruses that cause cell-cell fusion and multinucleated syncytium formation in cell culture. Its 125-amino-acid fusion protein, p14, lacks the typical large ectodomain found in fusion proteins from enveloped viruses. P14 and the other reovirus-encoded fusion-associated small transmembrane (FAST) proteins lack the size to extend the distance between two opposing membranes, and are unlikely to mediate fusion using energy-producing structural remodeling. I now show that, like some enveloped-virus fusion proteins, the mechanism used by p14 to mediate membrane merger is dependent on the presence of cholesterol in the plasma membrane. Reducing membrane cholesterol content with methyl- β -cyclodextrin (M β CD), Lovastatin or U-18666A inhibited p14-mediated fusion activity. After extraction of p14-transfected cells with Lubrol WX, Brij 56, and Brij 58, p14 was detected in the detergent-insoluble pellet after ultracentrifugation, whereas lysis with RIPA, Triton X-100, or octylglucoside rendered p14 soluble. High-salt treatment did not affect Lubrol insolubility, while cholesterol depletion reduced the amount of p14 that remained insoluble in Lubrol (Lubrol-resistant p14). Upon sucrose density gradient analysis, p14 was present in both Lubrol- and Triton X-100-resistant membrane complexes in the low-density sucrose fractions. While the population of p14 in Lubrol-resistant membranes was sensitive to cholesterol depletion with M β CD, Triton X-100-resistant p14 was not. Fluorescence microscopy of p14-GFP-transfected cells

demonstrated that a greater population of the protein resided in cholesterol-dependent Lubrol-resistant membrane microdomains than in those membranes isolated by extraction with Triton X-100. p14 appeared to localize preferentially to regions of Lubrol-resistant membrane, which displayed the same sensitivity to cholesterol depletion as did the fusion mechanism itself. Based on these results, I propose that p14 utilizes Lubrol-resistant membrane microdomains to target cell-membrane protrusions as its preferred site of fusion initiation.

6.2 Introduction

The plasma membrane, once thought to exist as a fluid mosaic of lipid and protein, is now believed to exhibit lateral organization between lipids (Brown and Rose, 1992; Simons and Ikonen, 1997; Brown and London, 2000). A liquid-ordered membrane phase is proposed to form as a result of interactions between the long saturated acyl chains of sphingolipids (SGL); cholesterol molecules then preferentially incorporate into the spaces between the acyl chains (Rietveld and Simons, 1998). Certain proteins associate with these liquid-ordered microdomains, including many that are acylated and GPI-anchored (Schroeder *et al.*, 1998; Melkonian *et al.*, 1999). Upon cell lysis with Triton X-100 at 4°C, sphingolipid- and cholesterol-rich regions of the cell membrane remain insoluble. These detergent-resistant membranes (DRMs) can be separated from soluble membrane components either by ultracentrifugation (to pellet DRMs) or by sucrose-density centrifugation and are often termed lipid rafts (Brown and Rose, 1992; Scheiffele *et al.*, 1997). The addition of antibodies before cell fixation results in coalescence of known lipid raft antigens into larger patches that are visible by fluorescence optical microscopy (Harder *et al.*, 1998; Kozak *et al.*, 2002; Lu *et al.*, 2002; Holm *et al.*, 2003). This technique is often used to visualize membrane raft domains, or to identify new raft proteins. Extraction of membrane cholesterol both disrupts the formation of DRMs and antigen patching (Brown and Rose, 1992; Simons and Ikonen, 1997; Harder *et al.*, 1998; Brown and London, 2000). Despite the technical manipulations required to analyze membrane rafts, evidence for clustered membrane microdomains in living cells (Friedrichson and Kurzchalia, 1998; Varma and Mayor, 1998) and the formation of

detergent-resistant membranes at physiological temperatures (Drevot *et al.*, 2002) supports their existence. Whether the proteins and lipids that are isolated in a given DRM preparation actually associate with each other *in vivo* is still a matter of debate (Mayor and Maxfield, 1995; Schuck *et al.*, 2003).

Contrary to initial theory, the majority of the plasma-membrane lipid content exists in a liquid-ordered state, cholesterol-rich and resistant to extraction with cold Triton X-100 (Mayor and Maxfield, 1995; Hao *et al.*, 2001). This suggests that the plasma membrane may resemble a dense assembly of discrete microdomains that differ in the degree of lipid order, detergent solubility, protein content, and size (Madore *et al.*, 1999). This contrasts with the relatively small proportion of plasma-membrane proteins that are found to be resistant to cold Triton X-100 extraction (Hao *et al.*, 2001; Schuck *et al.*, 2003). It is also becoming clear that different classes of lipid rafts exist in mammalian cells (Galbiati *et al.*, 2001). Distinct membrane microdomains can be isolated from the same cells based on susceptibility to different nonionic detergents (Madore *et al.*, 1999; Röper *et al.*, 2000; Holm *et al.*, 2003; Schuck *et al.*, 2003), from morphologically different regions of the cell membrane (Röper *et al.*, 2000; Gomez-Mouton *et al.*, 2001), based on buoyant density in sucrose (Oliferenko *et al.*, 1999; Lindwasser and Resh, 2001), by association with different protein scaffolds (Bickel *et al.*, 1997; Lang *et al.*, 1998; Okamoto *et al.*, 1998; Lindwasser and Resh, 2001; Salzer and Prohaska 2001), by variable susceptibility to cholesterol depletion (Röper *et al.*, 2000), or any combination of these techniques.

Membrane microdomains serve as platforms for the transport of selected components or as organizational centers for intracellular signaling molecules (Brown and

London, 1998; Simons and Ikonen, 1997; Brown and London, 2000). Many viruses use membrane microdomains as organizational domains during the assembly process (Scheiffele *et al.*, 1997; Nguyen and Hildreth, 2000; Ali *et al.*, 2000; Manie *et al.*, 2000; Sapin *et al.*, 2002; Cuadras and Greenberg, 2003; Halwani *et al.*, 2003). Viral glycoproteins, including fusion proteins, are found selectively in raft microdomains (Scheiffele *et al.*, 1997; Mañes *et al.*, 2000). Those fusion proteins that target raft domains do not always require the character of this membrane region for the fusion process. The receptor and co-receptors for HIV-1, CD4 and CXCR4/CCR5, respectively, localize to cholesterol- and sphingolipid-rich domains; thus, the HIV-1 virus requires the effective formation of these regions in the target cell membrane for entry (Mañes *et al.*, 2000). Raft lipids are also believed to play a more direct role in modulating the fusion ability of HIV-1 (Guyader *et al.*, 2002). Cholesterol and/or cholesterol-rich domains are essential for the entry of mouse hepatitis virus and murine leukemia virus (Daya *et al.*, 1988; Lu *et al.*, 2002); however, the detailed step of the entry process that requires cholesterol is undefined. Alphaviruses require the presence of cholesterol and sphingolipid in the target membrane (Vashishtha *et al.*, 1998; Smit *et al.*, 1999; Kielian *et al.*, 2000; Waarts *et al.*, 2000; Ahn *et al.*, 2002; Chatterjee *et al.*, 2002). The lipid dependency of alphaviruses is not due to clustering of the virus receptor in a raft domain, and does not require raft formation at all, but rather the presence of both molecules (clustered or unclustered) in the target membrane (Ahn *et al.*, 2002; Waarts *et al.*, 2002).

The fusion-associated small transmembrane protein (FAST) family is comprised of a group of small (95-140 amino acid), non-essential, non-structural fusion proteins

encoded by members of the reovirus family (Duncan *et al.*, 1996; Shmulevitz and Duncan, 2000; Dawe and Duncan, 2002; Chapter 3). These proteins lack the structural features typical of large fusion proteins encoded by enveloped viruses (Weissenhorn *et al.*, 1999; Heinz and Allison, 2001) and thus the mechanism by which they mediate cell-cell fusion promises to be novel. I was interested in discerning whether lipid composition and/or cholesterol- and sphingolipid-rich raft membranes play a role in the unusual fusion mechanism of the FAST proteins. These studies were initiated using the FAST protein p14 encoded by a reptilian reovirus (Duncan *et al.*, 2003). P14 is a myristylated Type III (N_{exo}/C_{cyt}) cell-surface protein. The N-terminal myristate modification is essential for fusion (Fig 3.7, Chapter 3). Live p14-transfected cells demonstrated patchy cell-surface staining using indirect immunofluorescence (Fig 3.3.B, Chapter 3) suggesting that p14 may cluster in lipid rafts or other plasma membrane microdomains. Here I report that p14 localizes preferentially to Lubrol-resistant DRMs and that this localization, and the mechanism of p14-mediated fusion, is highly sensitive to depletion of membrane cholesterol. These results suggest that p14 may localize to a membrane microdomain characterized by resistance to the nonionic detergent Lubrol WX and residence at plasma membrane protrusions (Röper *et al.*, 2000). I propose that p14 localization to cell membrane protrusions is an important step in the fusion mechanism of this FAST protein.

6.3 Results

P14-mediated fusion requires plasma membrane cholesterol

I treated p14-transfected Vero cells with methyl- β -cyclodextrin (M β CD) prior to the initiation of fusion. M β CD is a cholesterol-solubilizing agent, which stimulates cholesterol efflux from cells when added exogenously to the cell culture media (Klein *et al.*, 1995). The addition of M β CD to p14-transfected cells inhibited fusion (Fig 6.1, panel b) when compared to untreated p14-transfected cells (Fig 6.1, panel a). To ensure that the inhibition of fusion resulted from a decrease in the cholesterol content of the cell membrane, the ability of different concentrations of M β CD to remove [3 H]-cholesterol from the membrane was assessed by J. Salsman (collaborator, Dalhousie University). Mr. Salsman both performed the experiment and generated the figure shown in 1.4.A, Appendix A. Under all serum conditions, 20 mM M β CD removed greater than 90% of the cholesterol, while 2mM M β CD (the concentration used to generate the data shown in Fig 6.1) removed greater than 60% of the [3 H]-cholesterol (Fig 1.4.A, Appendix A). When M β CD was removed from cells, p14-mediated fusion activity was restored (data not shown), suggesting that the inhibition of fusion was due to the effect of M β CD on cellular cholesterol. If M β CD was preventing p14-mediated fusion as a result of other toxic effects, replenishing cell membrane cholesterol would not restore fusion ability (Viard *et al.*, 2002).

The effect of cholesterol-depleting agents on the mechanism of p14-mediated fusion was examined and quantified by J. Salsman (collaborator, Dalhousie University),

who both performed and generated the figure shown in 1.4.B, Appendix A. As observed for Vero cells (Fig 6.1), 2 mM M β CD inhibited p14-mediated fusion by more than 80% for QM5 cells (Fig 1.4.B, Appendix A). Lovastatin, which prevents *de novo* cholesterol synthesis (Rodal *et al.*, 1999), also inhibited greater than 80% of p14-mediated fusion (Fig 1.4.B, Appendix A). U18666A, which prevents the normal recycling of cholesterol from the endosome to the plasma membrane and induces a Niemann-Pick C phenotype (cholesterol accumulates in the lysosomal/endosomal system; Higgins *et al.*, 1999), inhibited p14-mediated fusion by greater than 90% (Fig 1.4.B, Appendix A). N-BP-2 cells are CHO cells with a defect in the chromosomal site-2 protease needed to activate the SREBP-responsive genes, but are stably transfected with an inducible version of the gene (Pai *et al.*, 1998). Without induction, N-BP-2 cells require exogenous cholesterol. When exogenous cholesterol is withdrawn, these cells are cholesterol-deficient and under these conditions, p14-mediated fusion was inhibited by more than 50% compared to what was seen for N-BP-2 cells that were grown in the presence of cholesterol (Fig 1.4.B, Appendix A).

P14 membrane domains are Lubrol-resistant and Triton X-100-sensitive

The mechanism of p14-mediated fusion is cholesterol-dependent. The fusion process of alphaviruses also requires cholesterol, but is not dependent on the association of its fusion protein, E1, in membrane microdomains (Kielian *et al.*, 2000; Ahn *et al.*, 2002; Chatterjee *et al.*, 2002). I wanted to determine whether p14 cholesterol-dependence resulted from association with cholesterol-rich membrane microdomains, or reflected a requirement for cholesterol itself.

I investigated the ability of p14 to associate with cholesterol/sphingolipid rafts. These rafts can be isolated as detergent-resistant membranes upon cold solubilization of cells with nonionic detergent (Scheiffele *et al.*, 1997). After lysis of p14-transfected cells on ice and fractionation by ultracentrifugation, I assessed the presence of p14 in the supernatant (S100) and pellet (P100) fractions by immune precipitation and SDS-PAGE (15%). When no detergent was used, p14 resided exclusively in the P100 membrane fraction of p14-transfected cells (Fig 6.2.A; Fig 3.3, Chapter 3). When p14-transfected cells were treated with RIPA buffer (which contains two ionic detergents, sodium dodecyl sulphate and sodium deoxycholate), p14 was completely solubilized (Fig 6.2.A). Triton X-100, used to isolate classical cholesterol- and sphingolipid-rich membrane rafts (Brown and Rose, 1992), solubilized the entire population of p14 (Figs 6.2.A-B); however, a small proportion of p14 remained Triton X-100-resistant (Fig 6.2.C). Taken together, this data suggest that only a small proportion of p14 resides in Triton X-100 DRMs. Other nonionic detergents, such as Lubrol (Röper *et al.*, 2000) and members of the Brij series (Röper *et al.*, 2000; Drevot *et al.*, 2002; Holm *et al.*, 2003), have also been used to isolate detergent-resistant membranes (DRMs). When p14-transfected cells were treated with Lubrol WX, Brij 56, and Brij 58, approximately 50% of the total population of p14 remained detergent-insoluble (Fig 6.2.A, 6.2.B, and 6.2.C). Lubrol WX, Brij 56, and Brij 58 each possess a greater hydrophilic-lipophilic balance than does Triton X-100, and Lubrol in particular was used to isolate a subset of plasma membrane microdomains different from classical rafts (Röper *et al.*, 2000). My results suggest that p14 may reside in these non-classical rafts.

I determined whether the Lubrol-resistant property of p14 resulted from its localization to a detergent-resistant membrane microdomain distinct from the classical Triton raft. One such distinct population of membrane microdomains are those containing the marker protein prominin, that can be isolated by extraction with Lubrol and centrifugation of Lubrol-DRMs at low speeds (17,000 x g) (Röper *et al.*, 2000). I determined if the detergent-resistant membrane fraction of p14 could be isolated by lower speed centrifugation (17,000 x g). p14 remained in the soluble fraction after Triton X-100 and Lubrol WX lysates were subjected to centrifugation for 30 minutes at 17,000 x g (Fig 6.2.C). The inability of p14 to sediment under these conditions is a feature that is observed for proteins that localize to classical lipid rafts assessed by Triton X-100 lysis (e.g. placental alkaline phosphatase [PLAP]; Brown and Rose, 1992), and not typical of Lubrol-resistant prominin rafts (see discussion).

To ensure that p14 insolubility in Lubrol WX did not result from its anchoring to cytoskeleton elements that would also be present in the P100 membrane fraction, I lysed p14-transfected cells in octylglucoside (OG). OG is believed to preserve the cytoskeleton and associated proteins (Kunimoto *et al.*, 1989); under these conditions p14 was located in the S100 fraction (Fig 6.2.A), consistent with the ability of OG to solubilize classical rafts (Melkonian *et al.*, 1999). I also included a high salt concentration (1 M NaCl) in the Lubrol WX lysis buffer to weaken any potential p14-cytoskeleton interactions. The high-salt treatment did not disrupt the Lubrol-resistance property of p14, and the protein still localized to the P100 fraction (Fig 6.2.C). As p14 localization to the P100 fraction appeared to result from the resistance of p14-containing membranes to Lubrol, and not from an interaction with components of the cytoskeleton, I tested if these DRMs are

sensitive to cholesterol extraction. P14-transfected cells were pretreated with M β CD before Lubrol lysis and ultracentrifugation. The amount of p14 in the membrane fraction decreased by approximately 50% compared to an untreated control (Fig 6.2.B), suggesting that p14 localized to cholesterol-rich Lubrol-resistant membranes.

P14 is present in both Lubrol- and Triton X-100-resistant membrane microdomains identified by sucrose density gradient analysis

If Lubrol-resistant p14 is associated with a Lubrol-resistant membrane microdomain, this population (approximately 50% in Fig 6.2) of p14 should float to the low-density fractions in a sucrose density gradient (Brown and Rose, 1992). P14-transfected cells were treated with both Lubrol WX and Triton X-100, to isolate Lubrol- and classical Triton X-100-insoluble membranes, respectively. P14 floated to the low-density fractions (approximately 10-15% sucrose) after transfected cells were lysed with either detergent (Fig 6.3, panels A and B; herein referred to as Lubrol- and Triton X-100-rafts). A GPI-linked Triton X-100 raft-resident protein, placental alkaline phosphatase (PLAP), demonstrated exclusive localization to the low-density sucrose fractions when PLAP-transfected cells were analyzed in the same manner (Fig 6.4.B). For p14, some of the protein remained soluble in Triton X-100 (in the high-density fractions), whereas the p14-containing DRMs floated to low-density (10-15 %) sucrose fractions (Fig 6.3, panel A). However, the distribution of p14 in the sucrose density gradient following Lubrol extraction differed. Though both the low-density (10-15 %) and high-density sucrose fractions were enriched in p14, the protein was also present throughout the fractions of intermediate sucrose density (Fig 6.3, panel B). The distribution of a Lubrol-resistant

protein throughout a sucrose gradient has been observed for another Lubrol-raft protein, prominin (Röper *et al.*, 2000). P14 was also present in low-density sucrose fractions when 0.1% Lubrol was included in each fraction of the gradient (Fig 6.3, panel H). In all, a lesser proportion of p14 is observed in the low-density fractions of sucrose than was observed for the PLAP control (Fig 6.4.B). Nonetheless, these results indicate that a portion of p14 localized to both Lubrol- and Triton X100-DRMs or rafts.

P14 does not require N-terminal myristylation for DRM localization

The addition of a fatty acid moiety to an otherwise soluble protein has been suggested as a means not only to target the protein to a cell membrane, but also to target it to detergent-resistant membrane microdomains. However, many of the proteins that target classical rafts are dually acylated, or use their acyl chains in combination with another raft targeting signal (Melkonian *et al.*, 1999; Zacharias *et al.*, 2002). Not all dually acylated proteins are targeted to classical rafts, underscoring the current view of microdomain heterogeneity (McCabe and Berthiaume, 2001; Pierini and Maxfield, 2001). The role of acyl groups in targeting integral membrane proteins to rafts is less well understood. Integral membrane proteins often use other features, such as a membrane-spanning domain, to target cholesterol/sphingolipid raft domains (Scheiffele *et al.*, 1997). Myristylation of p14 is essential for its fusion mechanism (Fig 3.7, Chapter 3), and this may be a result of the ability of myristate to target p14 to membrane rafts. I investigated whether N-terminal modification of p14 with myristate is a necessary signal for Triton X-100-raft localization. Preliminary analysis of the detergent resistance of a myristylation-minus construct of p14 (G2A) in Triton X-100 was performed. P14-G2A was present in

the low-density fractions of a sucrose gradient (Fig 6.3, panel G), suggesting that the myristate moiety may not be essential for p14 microdomain localization. Future analysis of the detergent resistance of p14-G2A in Lubrol will confirm whether p14 utilizes its myristate moiety to target detergent-resistant membrane microdomains.

P14-containing Lubrol-rafts are sensitive to cholesterol depletion

The mechanism of p14-mediated fusion requires the presence of membrane cholesterol (Fig 6.1 and Fig 1.4, Appendix A). Cholesterol is necessary to maintain the integrity of DRMs (Brown and Rose, 1992; Scheiffele *et al.*, 1997). To demonstrate a correlation between p14 raft localization and its ability to cause fusion, I pretreated p14-transfected cells with 20 mM M β CD at 37 °C (depleted > 90% of the cholesterol in Fig 1.4.A, Appendix A) before lysis with either Lubrol or Triton X-100. M β CD treatment decreased the proportion of low-density p14 in the Lubrol sucrose gradient (Fig 6.3, panel D), but did not have an appreciable effect on the presence of p14 at the top of the Triton X-100 gradient (Fig 6.3, panel C). This is unusual, as most raft proteins, including the classical raft marker protein used in these studies (PLAP), are sensitive to M β CD treatment (Fig 6.4.B). 10 mM M β CD has been shown to eliminate the association of both influenza hemagglutinin and PLAP with DRM pellet (Scheiffele *et al.*, 1997). When cholesterol-depleted p14-transfected cells were supplied with M β CD-cholesterol complexes before detergent lysis and sucrose density gradient analysis, p14 returned to the low-density sucrose fractions in the Lubrol gradient (Fig 6.3, panel F), indicating that the ability of p14 to localize to Lubrol-resistant microdomains requires the presence of cell membrane cholesterol, as does the ability of p14 to cause cell-cell fusion (Fig 6.1). Again, the

pattern of p14 in the Triton X-100 gradient was not noticeably different after cholesterol repletion (Fig 6.3, compare panels A, C, E).

The different sensitivities to cholesterol depletion exhibited by p14-containing Lubrol-DRMs versus Triton-DRMs suggests that p14 may reside in two different membrane microdomains. Indeed, different microdomains show different sensitivities to extraction with different detergents (Schuck *et al.*, 2003) and different responses to cholesterol depletion (Röper *et al.*, 2000); in addition, Lubrol-rafts have previously been demonstrated to contain a subset of cellular proteins that differs from those isolated in Triton X-100 rafts (Röper *et al.*, 2000). This suggests that the insolubility of p14 in Lubrol is not due to a lower efficiency of this detergent in solubilizing bulk membrane, but rather to microdomain localization to cholesterol-sensitive regions of the cell membrane. Furthermore, the behavior of p14 Lubrol rafts in response to M β CD-mediated cholesterol depletion and repletion correlates with the ability of membrane-cholesterol content to modulate p14-mediated fusion activity (Fig 6.1). I propose that the localization of p14 to Lubrol-rafts, and not Triton X-100-rafts, may be more relevant to the fusion process of p14.

Fluorescence microscopy indicates that p14 localizes preferentially to Lubrol-resistant rafts

Isolation of DRMs by ultracentrifugation suggested that p14 localized preferentially to Lubrol- rather than Triton-rafts (Fig 6.2); however, sucrose density gradient analysis did not clearly distinguish which type of membrane microdomain p14 resides in (Fig 6.3). However, the p14-containing Lubrol-resistant membrane fraction displayed cholesterol

sensitivity similar to that observed for the fusion process itself (Fig 6.1 and 6.3). Despite this correlation, some questions remain. Does p14 localize to Lubrol-rafts, to Triton X-100-rafts, or to both? Are both these DRM domains biologically relevant to the p14 fusion mechanism?

I used a p14-GFP construct that retains the ability to cause cell-cell fusion (Fig 5.5, Chapter 5) to discern whether p14 preferentially localizes to Lubrol DRMs. P14-GFP-transfected cells were grown on coverslips, pretreated with either 0 or 20 mM M β CD, and briefly immersed in either buffer, or Lubrol WX, or Triton X-100. Confocal fluorescence microscopy was used to visualize the population of detergent-resistant p14-GFP. When no detergent was used, p14-GFP-transfected cells displayed saturating levels of intracellular perinuclear fluorescence, making it difficult to distinguish the surface-localized population of p14 (Fig 6.5, panel a); pre-treatment with M β CD did not alter this pattern (Fig 6.5, panel b). When p14-GFP transfected cells were treated with Triton X-100 and photographed using the same capture parameters as for panels a and b, only speckled background fluorescence that likely represents p14-containing membrane debris was observed (Fig 6.5, panel d). After Lubrol treatment, the saturating intracellular fluorescence signal (Fig 6.5, panel a) was no longer visible, while an outline of the cell periphery remained visible (Fig 6.5, panel c). These detergent treatments suggest that a greater portion of the cell membrane p14 is Lubrol-resistant than Triton X-100 resistant. When p14-GFP cells were pretreated with M β CD before detergent extraction, both Lubrol and Triton X-100 treatments extracted p14-GFP and only background fluorescence remained (Fig 6.5, panels e and f). These findings suggested that p14 localizes predominantly to Lubrol rafts, and that the formation of these rafts requires

cholesterol (Fig 6.5, panels d and f). The results of my sucrose density gradient centrifugation analyses suggested that both Lubrol- and Triton-rafts contain a significant proportion of p14 (Fig 6.3), while detergent extraction followed by either ultracentrifugation (Fig 6.2) or fluorescence microscopy (Fig 6.5) suggested that a greater proportion of p14 is present in Lubrol-rafts. The preferential localization of p14 in Lubrol DRMs, and the cholesterol requirement exhibited by these domains, suggests that these membrane microdomains are more biologically relevant for the fusion mechanism of p14.

P14 may localize to plasma membrane extensions

Lubrol-rafts have been previously described as unique membrane microdomains that preferentially localize to microvilli in epithelial cells, and to protrusions and filopodia on non-epithelial cells (Weigmann *et al.*, 1997; Röper *et al.*, 2000; Corbeil *et al.*, 2001). Immunofluorescence microscopy of p14-GFP transfected cells (green) that were co-stained for cellular organelle markers (red) indicated that p14 is found in membrane extensions of the QM5 fibroblast cells used for transfection (Fig 6.6, panels a-d). I speculate that p14 preferentially targets Lubrol-rafts as a means to localize to cell extensions or protrusions, and that the localization of p14 to such regions of the cell surface may play an important role in the fusion mechanism of p14.

6.4 Discussion

P14 localization to Lubrol-insoluble membrane domains is cholesterol-dependent

I demonstrated that the p14 fusion protein of reptilian reovirus requires the presence of plasma-membrane cholesterol for fusion (Fig 6.1 and Fig 1.4, Appendix A) and localizes to DRMs isolated by the detergents Lubrol WX and Triton X-100 (Fig 6.3). Membrane-fractionation experiments and fluorescence microscopy indicated that p14 preferentially resides in those membrane microdomains that are isolated by Lubrol extraction (Figs 6.2, 6.5, 6.6). As the p14-containing Lubrol-rafts are sensitive to cholesterol depletion using M β CD, while the p14 Triton X-100 rafts are not, I propose that p14 resident in Lubrol-rafts may be the fusion-active population (Fig 6.1, Fig 6.3). These results suggest that p14 requires cholesterol because it localizes to membrane raft domains, and thus the cholesterol dependence of p14 differs from that of the alphavirus family (Kielian *et al.*, 2000; Waarts *et al.*, 2000; Ahn *et al.*, 2002; Chatterjee *et al.*, 2002).

The localization of a classical Triton X-100 raft marker protein, placental alkaline phosphatase (PLAP), to Triton X-100 rafts was also sensitive to cholesterol depletion using M β CD. However, the distribution of PLAP in the sucrose density gradient differed from that of p14 (both in Lubrol and Triton X-100 gradients). As distinct membrane microdomains can be differentiated on the basis of numerous techniques including susceptibility to nonionic detergents, sensitivity to cholesterol extraction, and buoyant density in sucrose (Madore *et al.*, 1999; Oliferenko *et al.*, 1999; Röper *et al.*, 2000; Lindwasser and Resh, 2001; Holm *et al.*, 2003; Schuck *et al.*, 2003), I believe that PLAP

and p14 are not likely to exist in the same microdomain. Röper *et al.* (2000) observed that the microvillar protein prominin localizes to Lubrol-rafts that were extremely sensitive to cholesterol depletion, while PLAP insolubility in Triton X-100 was resistant to M β CD treatment. Röper *et al.* (2000) used a gentle cholesterol-extraction protocol (50 mM M β CD for 30 minutes at 4 °C), whereas our M β CD treatment was similar to that which has been previously used to demonstrate the cholesterol dependence of PLAP DRMs (Scheiffele *et al.*, 1997). The character of the Lubrol rafts we have isolated does agree with the observations of Röper *et al.*, (2000), as both p14 and prominin insolubility in Lubrol is sensitive to treatment with M β CD (Fig 6.3, panels B and D; Röper *et al.*, 2000). However, Lubrol-insoluble complexes containing prominin can be pelleted at a moderate centrifugal force (17,000 x g; Röper *et al.*, 2000), whereas p14-containing Lubrol complexes remain in the soluble fraction after this procedure (Fig 6.2.B). Röper *et al.* (2000) suggest that prominin resides in Lubrol rafts of two sizes, with the newly formed small domains becoming larger by coalescence at the apical surface. The sizes of 'rafts' have been estimated using a wide array of approaches, and the results range from 10 to 300 nm in diameter (summarized in Anderson and Jacobson, 2002; Drevot *et al.*, 2002; Varma and Mayor, 1998). However, lipid rafts are generally believed to be small dynamic microdomains that can be recruited into larger assemblies (sometimes visualized by optical microscopy) in response to signals (Pierini and Maxfield, 2001). That p14 DRMs require greater centrifugal force suggests that these domains remain small. Unfortunately, I was unable to obtain a mammalian expression clone of prominin to be used as a Lubrol-raft marker in a direct comparison with p14-containing Lubrol-resistant membranes.

Analysis of DRMs prepared by different detergents suggests that some detergents, such as Lubrol WX, are less selective, disrupt fewer protein-lipid interactions, and thus allow the DRM association of a larger number of proteins, while others effect greater solubilization of membrane lipids and dissolution of protein-lipid interactions (Schuck *et al.*, 2003). However, experimental evidence of individual protein insolubility in Lubrol and solubility in Triton X-100 (a more stringent nonionic detergent according to Schuck *et al.*, 2003) indicates otherwise. The macrophage protein CD11b remains Triton X-100-insoluble but Lubrol-soluble even though in general Triton X-100 extracts a greater proportion of membrane lipids (Drobnik *et al.*, 2002). The protein profile of polarized MDCK cells extracted with Lubrol differs from that of the Triton X-100 extract (Röper *et al.*, 2000). In addition, it has been suggested that the majority of the plasma-membrane lipid remains insoluble after extraction with cold Triton X-100, even though the majority of the proteins are soluble (Mayor and Maxfield, 1995; Hao *et al.*, 2001). If all nonionic detergents, even those typically considered as more stringent (Schuck *et al.*, 2003), actually preserve the bulk of the plasma membrane, does this make the different protein solubility profiles in these different detergents more relevant? If each nonionic detergent disrupts a particular subset of protein-lipid interactions, perhaps it possible to use the differential protein solubility profiles these detergents generate to define their membrane environment.

If p14 localization to Lubrol-rafts is biologically relevant to the fusion mechanism, why is a portion of p14 also found in Triton-X-100-insoluble membrane complexes? Both Triton X-100 microdomains and Lubrol membrane microdomains are believed to form in the *trans*-Golgi network, as the cholesterol/sphingolipid concentration

and membrane bilayer thickness increases (Simons and Ikonen, 1997; van Meer, 1998; Röper *et al.*, 2000; Gkantiragas *et al.*, 2001). That p14 is found in both types of membrane microdomains may suggest that the p14 protein cannot distinguish between these two rafts, and even though the population in Lubrol-insoluble membranes may be the functional one for fusion, a portion of the p14 population resides in other cholesterol- and sphingolipid-rich microdomains. Alternatively, Triton X-100 DRMs and Lubrol DRMs may be formed together in the *trans*-Golgi, travel in the same vesicle to the apical plasma membrane, and physically segregate into planar and non-planar regions (e.g. membrane protrusions or microvilli) of the membrane only when they reach the cell surface (Röper *et al.*, 2000). If this model of Lubrol-raft formation is correct, it is easy to envision why a small proportion of p14 would associate with Triton X-100 DRMs during the trafficking process, while the bulk of the protein localizes to Lubrol-rafts. My results support the latter theory, as p14 is insoluble in both detergents, but ultracentrifugation and fluorescence microscopy suggest that a greater proportion of p14 resides in Lubrol-rafts (Figs 6.2 and 6.5).

P14 localization to DRMs is myristylation-independent

Cellular signaling proteins and viral proteins involved in assembly have been shown to target DRMs by virtue of their acyl (myristate and palmitate) groups (Resh, 1999; Rodgers, 2002; Ding *et al.*, 2003). However, recent evidence has suggested that not all acylated proteins target rafts, and that those that do are dually acylated or require a second signal for raft localization (Melkonian *et al.*, 1999; McCabe and Berthiaume, 2001; Zacharias *et al.*, 2002). The role of acylation in targeting integral membrane

proteins to membrane microdomains is unclear. Palmitoylation of HIV-1 gp160 governs raft association and is critical for infectivity of the virus (Rousso *et al.*, 2000). However, interaction of influenza hemagglutinin (HA) with sphingolipid- and cholesterol-rich microdomains requires residues in its transmembrane domain (Scheiffele *et al.*, 1997), and palmitoylation of the protein is not required for efficient trafficking to the cell surface, virus assembly or entry (Naim *et al.*, 1992). My preliminary data suggest that p14 targets DRMs in a myristylation-independent manner (Fig 6.3, panel G). However, the region of p14 that is required to mediate raft localization is unknown at this time.

Other members of the FAST protein family are also modified by acylation. The p10 protein from avian reovirus (ARV) is di-palmitoylated at two internal cysteine residues (Shmulevitz *et al.*, 2003b), while baboon reovirus (BRV) p15 is N-terminally myristylated. Both proteins localize to the cell surface independently of acylation; however, these modifications are required for fusion activity (Shmulevitz *et al.*, 2003b; Dawe *et al.*, manuscript in preparation). Interestingly, the fusion mechanisms of both p10 and p15 have recently been shown to be sensitive to cholesterol depletion by M β CD (J. Salsman and R. Duncan, unpublished data), suggesting that other members of the FAST protein family may also target cholesterol- and sphingolipid-rich membrane microdomains.

Possible role of microvilli/plasma-membrane protrusions in the fusion mechanism of p14

Prominin has been described as a marker protein for both microvilli and plasma-membrane protrusions, and Lubrol WX-insoluble membranes (Weigmann *et al.*, 1997;

Röper *et al.*, 2000; Corbeil *et al.*, 2001). I show that the small membrane fusion protein p14 may also localize preferentially to Lubrol-DRMs (Figs 6.2, 6.3, 6.5). The preferential localization to these microdomains has been previously described only for prominin; thus it is unknown if other proteins behave in the same manner. For example, are all microvilli-localized proteins, by definition Lubrol-insoluble? Are all Lubrol-insoluble proteins found in microvilli/membrane protrusions? These questions remain unanswered. For p14, Lubrol-raft localization does correlate with the localization of a proportion of p14 to plasma-membrane protrusions on the fibroblast cells used in my studies (Fig 6.6).

Microvilli and/or other plasma-membrane protrusions (filopodia, ruffles) may play important roles in cell-cell fusion. The character of non-planar regions of the cell membrane differs from that of planar membrane, as extremely cholesterol-rich. Immunoelectron microscopy using a modified and biotinylated derivative of the cholesterol-binding toxin perfringolysin O showed a high concentration of plasma-membrane cholesterol in highly curved structures such as filopodia (2.9 times more cholesterol than in flat plasma membrane; Möbius *et al.*, 2002). Microvilli contain an abundance of sphingolipids, mostly sphingomyelin (Milhiet *et al.*, 2001), giving renal brush-border membranes a lipid content similar to that proposed for raft membranes (Brown and Rose, 1992), and suggesting that non-planar regions of the plasma membrane are likely to be detergent-resistant domains. Cholesterol depletion of brush-border membranes has been shown not to disrupt microdomain localization of the marker protein galectin-4 (Hansen *et al.*, 2001), causing the cholesterol-dependent nature of non-planar microdomains to be questioned. However, galectin-4 is an extracellular lectin that may act as a stabilizing factor for cholesterol-depleted DRMs, enhancing their detergent-

resistance in the absence of cholesterol (Braccia *et al.*, 2003). Conversely, Lubrol-rafts containing the microvillar marker protein prominin are sensitive to M β CD extraction of membrane cholesterol (Röper *et al.*, 2000). Non-planar regions of membrane also possess a high degree of membrane curvature, making these membranes unstable and thus more susceptible to fusion-initiating events (Zimmerberg *et al.*, 1993; Epand, 1997; Lee and Lentz, 1998; Hague *et al.*, 2001).

There are a number of biological systems that suggest that non-planar regions of a membrane are sites of fusion initiation (summarized in Wilson and Snell, 1998). HIV-1 has been shown to selectively enter and fuse with microvillar membrane. This is likely the result of homogenous clustering of the two HIV-1 receptors, CD4 and CXCR4, less than one virus diameter apart on tips of microvilli (Singer *et al.*, 2001). Sites of HIV-1 entry correlate with receptor clustering; these clusters co-localize with actin and are cholesterol-dependent (Viard *et al.*, 2002). HIV-1-infected cells adhere to neighbouring cells prior to cell-cell fusion using microspikes (Dimitrov and Blumenthal, 1994). During fertilization, sperm selectively bind to the microvillus-rich portion of the egg plasma membrane (Wilson and Snell, 1998, and references therein). Fertilization in the alga *Chlamydomonas* requires the formation of a microvillus-like fertilization tubule (approximately 50 nm in diameter); binding between gametes is initiated at the tip of the fertilization tubule (Wilson *et al.*, 1997). Ultrastructure studies show that microvilli are the sites of cell-cell fusion (Knutton and Pasternek, 1979).

I propose that p14 may use a preferential association with Lubrol-insoluble membrane complexes to localize to plasma-membrane extensions or protrusions. I plan to confirm this theory using immunoelectron microscopy to directly visualize p14

localization in these cell surface structures. If the localization of p14 to such structures is confirmed, this may provide the missing clue to explain how a small membrane fusion protein (approximately 40-amino-acid ectodomain) can extend the distance between two opposing membranes and mediate the thermodynamically unfavorable membrane fusion process. I propose that plasma-membrane protusions may play the following role in this fusion mechanism. (1) P14 localizes to plasma-membrane extensions in cholesterol-dependent membrane rafts (Lubrol insoluble) such that p14 clusters in high density on these structures. Other fusion proteins are predicted to use a co-operative mechanism to mediate fusion. A minimum of three (Danieli *et al.*, 1996), six (Blumenthal *et al.*, 1996) or eight (Bentz, 2000) HA trimers, 13-19 rabies virus G protein trimers (Roche and Gaudin, 2002), and ten baculovirus gp64 trimers (Markovic *et al.*, 1998) aggregate at the site of fusion initiation. The mechanism of p14-mediated fusion is also likely to require the convergence of a critical number of p14 multimers to the fusion initiation site (see Chapter 5). (2) Microvilli/membrane protrusions are often rich in cell-cell adhesion molecules (Springer, 1990; Chaitin *et al.*, 1994; Von Andrian *et al.*, 1995). As p14 is a non-structural fusion protein that plays no role in virus entry, it is not believed to contain a receptor-binding domain, and thus likely requires prior cellular adhesion before it can initiate membrane merger. The first 127 amino acids of HA2 (lacking the membrane anchor and receptor-binding domain) can induce lipid mixing between cells that are treated previously to establish cell-cell contacts (Leikina *et al.*, 2001). P14 clustering within membrane protrusions would also place p14 at regions of close cell-cell contact. (3) P14 is a small fusion protein that is not likely to undergo energy-producing structural rearrangements like those described for the fusion mechanism of many enveloped-viral

fusion proteins (Weissenhorn *et al.*, 1999). Non-planar membrane structures are highly curved areas of cell membrane (even non-epithelial and non-adherent cells such as B cells possess plasma-membrane protrusions approximately 200 nm in diameter; Möbius *et al.*, 2002) that are unstable in comparison to planar regions of the membrane. The activation energy barrier that prevents merger of two opposing bilayers is reduced in such highly curved membrane structures (Zimmerberg *et al.*, 1993; Epand, 1997; Lee and Lentz, 1998; Hague *et al.*, 2001), which could facilitate the process of p14-induced membrane fusion.

P14 and the other FAST proteins may use membrane protrusions as a means to establish close apposition of cell bilayers, and cluster at these membrane sites that are less stable and susceptible to the lipid rearrangements that precede membrane merger. If close cell-cell contact is maintained, perhaps p14 can use a simpler thermodynamic profile of discrete structural alterations, without the requirement for the extensive structural remodeling necessary for the membrane fusion activity of enveloped-virus fusion proteins.

6.5 Figures

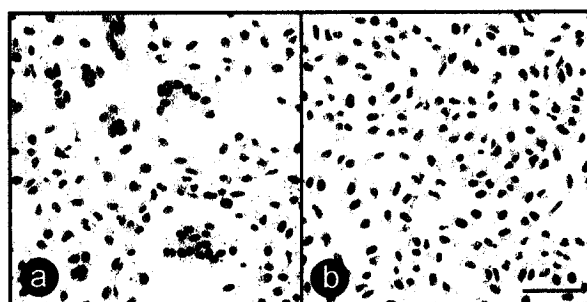


Fig 6.1 p14-mediated fusion requires plasma-membrane cholesterol. p14-transfected Vero cells were treated with 2mM M β CD before fusion initiation (approximately 12 hours post transfection). Scale bar = 100 μ m.

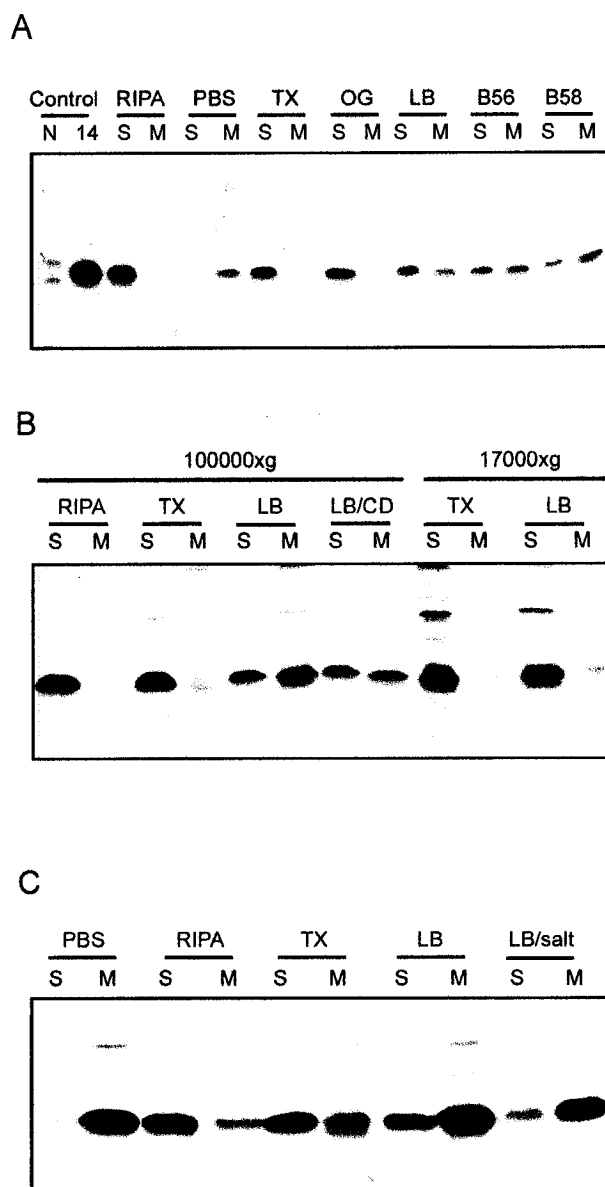


Fig 6.2 p14 localizes to the Lubrol-resistant membrane fraction by ultracentrifugation. **(A)** P14-transfected QM5 cells were treated/lysed with PBS, RIPA, Triton X-100 (TX), Lubrol WX (LB), octylglucoside (OG), Brij 56 (B56), or Brij 58 (B58) on ice for 45 minutes, and the detergent-resistant membrane fraction (M) isolated from the detergent-soluble fraction (S) by ultracentrifugation at 100000 x g. The membrane and soluble fractions were immune precipitated with polyclonal anti-p14 antibody (14). Control immune precipitation using anti-p14 antibody (14) and normal rabbit serum (N) were performed on RIPA whole-cell lysates. **(B)** p14-transfected QM5 cells were pretreated with 50 mM M β CD on ice for 30 minutes before lysis with Lubrol (LB/CD) and isolated by ultracentrifugation at 100000 x g. Lubrol- and Triton X-100-resistant membrane fractions were isolated at 17000 x g and compared with those isolated at 100000xg. **(C)** P14-transfected QM5 cells were treated with Lubrol in a high-salt buffer (1 M NaCl; LB/salt) before isolation of the Lubrol-resistant membrane fraction as above.

Fig 6.3 p14 localizes to Lubrol- and Triton X-100-resistant membrane microdomains as indicated by sucrose density gradient analysis. P14-transfected QM5 cells were treated with 20 mM M β CD at 37°C for 40 minutes (C, D), or treated with M β CD at 37 °C for 40 minutes followed immediately by cholesterol repletion using cholesterol-M β CD complexes (cholesterol at 6 mg/ml complexed with 20 mM M β CD) (E, F). These cells, and untreated p14-transfected cells (A, B, H), were lysed with Triton X-100 (A, C, E) or Lubrol (B, D, F, H). After sucrose density gradient ultracentrifugation for 16-18 hours at 332000 x g, 0.5-ml fractions of each gradient were analyzed for the presence of p14 by immune precipitation with polyclonal anti-p14 antibody. P14-transfected cells lysed in Lubrol were analyzed by sucrose gradient analysis with 0.1% (w/v) Lubrol in each step of the sucrose gradient (H). For all panels except G (p14-G2A), the percent of sucrose in each fraction of the gradient was 31, 29, 27, 25, 23.5, 19, 13, 7.5, 5 % for lanes 1-9, respectively. A preliminary analysis of p14-G2A-transfected QM5 cells lysed in Triton X-100 and analyzed by sucrose density gradient ultracentrifugation is shown in panel G. The sucrose gradients used to analyze the p14-G2A mutant has a different composition; thus, panel G cannot be directly compared to panels A, C, and E.

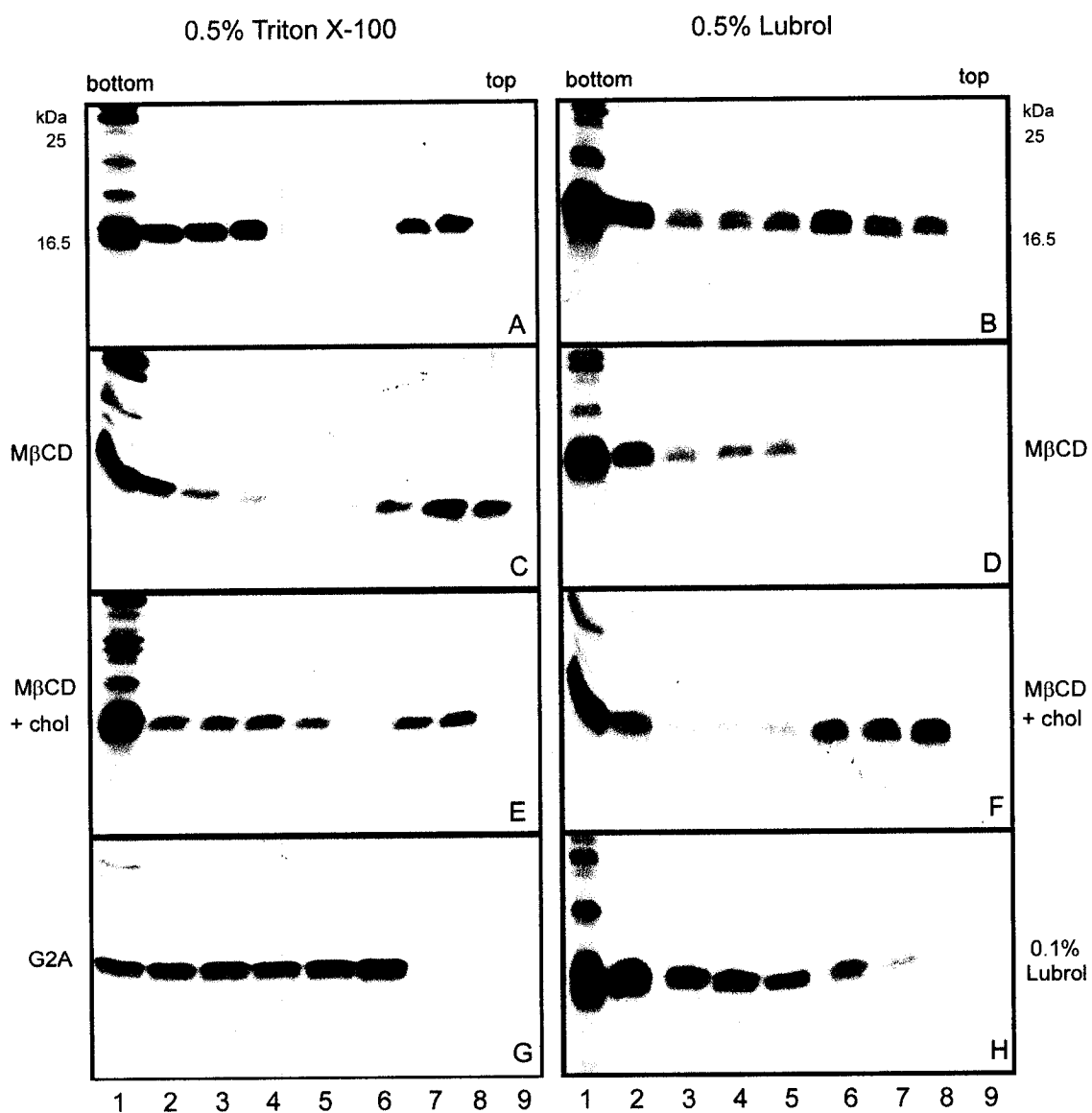


Fig 6.3 p14 localizes to Lubrol- and Triton X-100-resistant membrane microdomains as indicated by sucrose density gradient analysis.

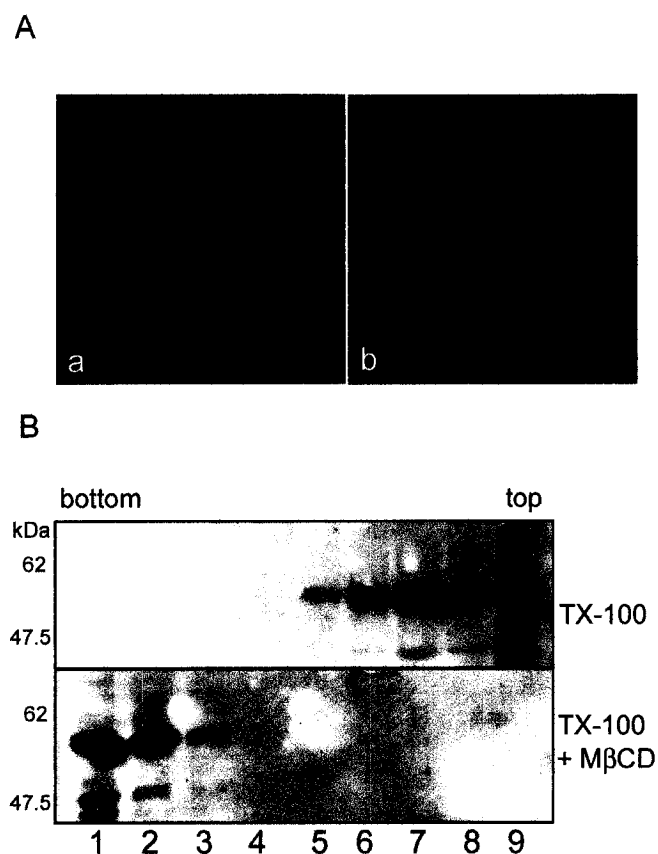


Fig 6.4 Placental alkaline phosphatase (PLAP) localizes to Triton X-100-resistant membrane microdomains. **(A)** PLAP-transfected QM5 cells (a) were assessed for expression by immunofluorescence staining with a mouse monoclonal anti-PLAP antibody and a secondary antibody conjugated to FITC. pcDNA3 vector-transfected QM5 cells (b) were subjected to the same staining procedure as a control. Scale bar = 10 μ m. **(B)** PLAP-transfected QM5 cells were lysed in Triton X-100, with or without previous treatment with 20 mM M β CD at 37 $^{\circ}$ C for 50 minutes, and subjected to sucrose density gradient ultracentrifugation at 332000 \times g for 16-18 hours. Each 0.5-ml fraction was analyzed for the presence of PLAP by 10%-SDS-PAGE and immunoblotting with monoclonal anti-PLAP antibody. The percent of sucrose in each fraction of the gradient was 32, 29, 27, 26, 22.5, 16.5, 9, and 6% for lanes 1-9, respectively.

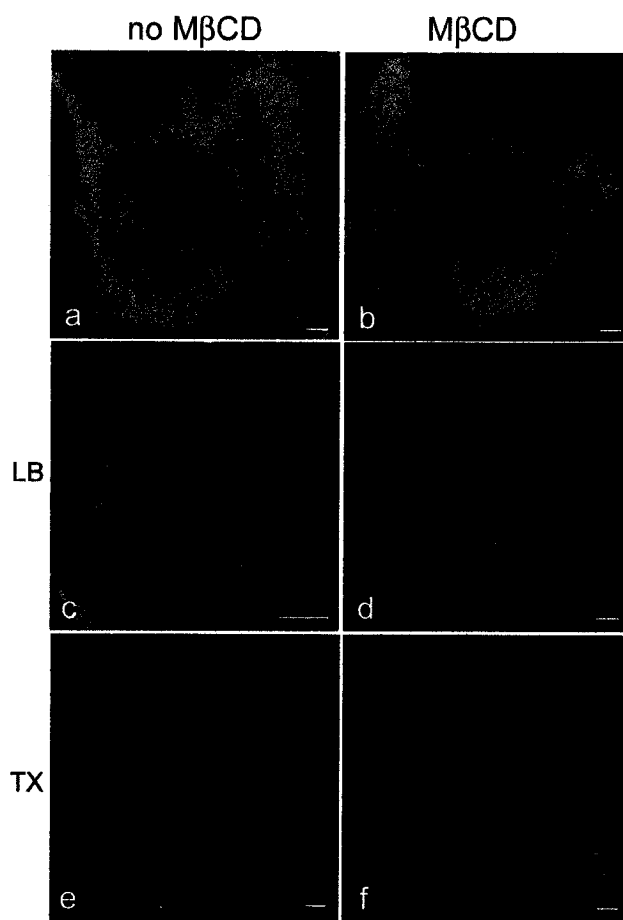


Fig 6.5 p14 localizes preferentially to Lubrol-rafts. P14-GFP-transfected QM5 cells grown on coverslips were either not treated (a, c, e), or treated with 20 mM M β CD in serum-free medium at 37 °C for 20 minutes (b, d, f). Cells on coverslips were then dipped in Hanks buffered saline solution (HBSS) alone (a, b), or HBSS containing Lubrol (c, d) or Triton X-100 (e, f), and examined for residual fluorescence by confocal microscopy. All images were captured using the same parameters on the confocal microscope. Scale bar = 10 μ m.

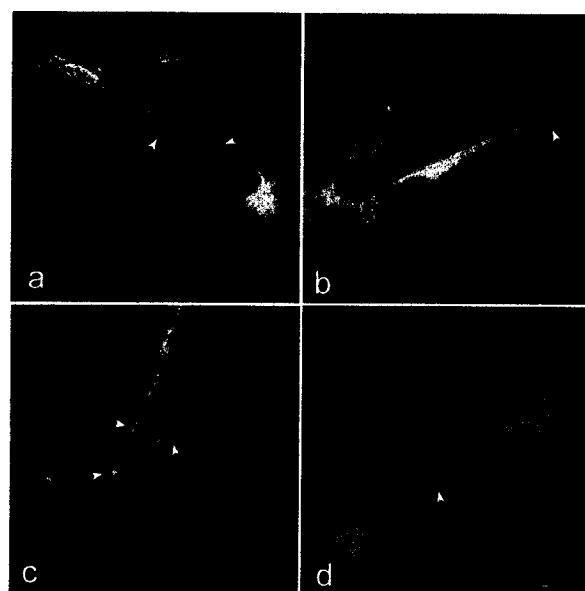


Fig 6.6 p14 is found in extensions of the cell membrane in QM5 cells. p14-GFP-transfected QM5 cells were co-stained with Texas Red using antisera to the organelle markers calnexin (ER; b) or TGN38 (*trans*-Golgi network; a and c). Arrows indicate p14-GFP in plasma membrane extensions. Scale bar = 10 μ m.

Chapter 7

Conclusions

7.1 Summary

The fusion-associated small transmembrane (FAST) proteins encoded by certain members of the nonenveloped virus family *Reoviridae* are non-essential and non-structural proteins (Duncan *et al.*, 1996; Shmulevitz and Duncan, 2000; Dawe and Duncan, 2002). FAST proteins do not play an essential role in the entry or exit mechanism of the virus that encodes them (Duncan *et al.*, 1996). Instead, the reovirus fusion proteins are believed to promote more rapid egress and cell-cell spread of fusogenic orthoreoviruses during the course of an infection (Duncan *et al.*, 1996; Duncan and Sullivan, 1998). As these proteins have no other role in the virus life cycle aside from the induction of multinucleated syncytia, their activity does not need to be regulated in time and space like that of membrane fusion proteins encoded by enveloped viruses or cells (Blumenthal *et al.*, 2003; Jahn *et al.*, 2003). FAST proteins do not act in response to a defined trigger and lack a regulatory domain(s). The FAST proteins are also unique in that they do not contain structural features typical of enveloped-virus fusion proteins, including large ectodomains or coiled coils (Skehel and Wiley, 1998; Heinz and Allison, 2001). These proteins clearly do not have the size capability or structural features to undergo the fusion-mediating conformational rearrangement reported as essential to membrane merger mediated by enveloped viruses (Weissenhorn *et al.*, 1999). Free from the constraints placed on most membrane fusion proteins, the FAST proteins may have evolved to contain only the minimal structural features necessary to mediate membrane merger.

This study identified and characterized a novel member of the reovirus FAST protein family, p14. Each member of the FAST protein family consists of its own signature arrangement of a subset of structural features that are common to all members of this class of fusion proteins. These common motifs include Type III ($N_{\text{exo}}/C_{\text{cyt}}$) integral membrane association, a membrane-proximal cluster of basic residues, a C-terminal tail of 20-40 amino acids that is dispensable for fusion, modification by myristic or palmitic acid, and the presence of a second region of hydrophobicity (hydrophobic patch or HP) in addition to the transmembrane domain (Shmulevitz and Duncan, 2000; Dawe and Duncan, 2002).

This study identified p14 as a surface-localized Type III ($N_{\text{exo}}/C_{\text{cyt}}$) integral membrane protein. Topological analysis revealed that p14 co-translationally translocates a myristylated N-terminal domain of approximately 40 amino acids into the ER; after trafficking, this domain resides outside the cell. N-terminal myristylation is essential for the fusion activity of the protein. Deletion mutagenesis determined that the C-terminal 38 amino acids of the protein (including a proline-rich region) are dispensable for p14-mediated syncytium formation. Smaller p14 constructs were still translocated and membrane-embedded, suggesting that an 88-amino-acid minimum size may be a requirement of the fusion process. Insertional and site-directed mutagenesis also identified a hydrophobic patch in the N-terminal ectodomain that functions like an internal fusion peptide in an *in vitro* fusion assay. Structural analysis using solution NMR spectroscopy (performed by our collaborators, Drs. Syvitski and Jakeman, Dalhousie University) showed that the N terminus of the HP motif forms a β -structured loop (gly2-pro13), while the C-terminal region remains unstructured. Co-immune precipitation and

cross-linking studies revealed that p14 is a homomultimer. Future studies will use site-directed mutagenesis to assess the role of the transmembrane domain and membrane-proximal basic motif in the fusion mechanism.

7.2 Model of p14-mediated membrane fusion

The small size, non-essential nature, and lack of a regulatory feature(s) common to most membrane fusion proteins force a reevaluation of current models of protein-mediated fusion when considering p14. I considered the steps defined by Lentz and Lee (1999) for the membrane fusion of two opposing pure lipid bilayers. These steps are aggregation, membrane destabilization, and fusion. Closely apposed pure lipid bilayers do not fuse unless the lipid packing in the outer leaflets is disrupted in some way, often by altered membrane curvature or increased membrane tension. These factors are believed to either destabilize the pre-fusion lipid bilayer state relative to the presumed high-energy intermediate state and/or promote the lipid rearrangement required to form the high-energy non-bilayer intermediate. In both cases, the activation energy barrier that prevents membrane fusion is reduced (Fig 7.1). How does p14 orchestrate these three fusion steps to overcome the thermodynamic barrier that prevents membrane fusion? My model combines the results obtained from this study with other results from the lab, and suggests a mechanism of p14-mediated membrane fusion. Although some elements of this proposed mechanism have not been confirmed experimentally, this model will serve as a working hypothesis for future studies in the laboratory.

Step 1 – aggregation

The small size of p14 makes it difficult to envision how p14 can bridge the distance between two opposing membranes. I do not believe that p14 or the other FAST proteins are cell-attachment proteins based on the limited sizes of their ectodomains and the ability of these proteins to fuse many different cell types (J. Salsman, M. Shmulevitz, and R. Duncan, unpublished results). However, a 127-amino-acid construct of influenza HA (lacking the cytoplasmic tail, the transmembrane anchor and the C-terminal half of the ectodomain) was able to mediate lipid mixing of two opposing cells when the cells were treated to establish cell-cell contacts (Leikina *et al.*, 2001). This suggests that a minimal fusion-protein construct can still interact with opposing bilayers if they are in close apposition. I believe that p14 may use its ability to associate with cholesterol-rich membrane microdomains to target regions in the plasma membrane involved in cell-cell contact. Further, p14 appeared to localize preferentially to membrane microdomains resistant to the nonionic detergent Lubrol; these membrane microdomains have been shown to be associated with microvilli and plasma-membrane protrusions of both epithelial and non-epithelial cells (Röper *et al.*, 2000). Preliminary fluorescence microscopy suggests that p14 may also associate extended regions of the cell membrane; the lab is currently pursuing this hypothesis using immunoelectron microscopy. Thus, the first assumption made by this model is that the fusion-active population of p14 localizes to non-planar regions of the plasma membrane that facilitate close bilayer apposition between two cells (Fig 7.2 illustrates cell protrusions; Fig 7.3 visualizes p14-fusion initiation at extended regions of the cell membrane).

The close aggregation of bilayers that must precede membrane fusion requires dehydration of the intercellular space. Hydrophobic fusion-peptide exposure is believed to locally dehydrate the cell surface (Han *et al.*, 1999). In an analogous manner, the p14 hydrophobic patch may mediate intercellular dehydration; furthermore, the presumed reversible association of the N-terminal myristate with the outer leaflet of the plasma membrane may aid in this regard.

Step 2 – membrane destabilization

For fusion to progress from an aggregated state, the activation energy barrier that prevents membrane merger must be overcome (Fig 7.1). For enveloped viruses, a large conformational rearrangement in structure from a metastable to a low-energy form is believed to provide energy that can then be captured to overcome this barrier and drive the membrane fusion reaction (Carr and Kim, 1993; Weissenhorn *et al.*, 1999). An alternative theory suggests that the activation energy barrier does not need to be overcome, but can be reduced by raising the energy state of the pre-fusion state or lowering the energy cost of the formation of the lipid intermediate(s) that precede fusion (Fig 7.1; Epand, 2003). Thus, if a fusion protein can favor the formation of non-bilayer structures, the thermodynamic barrier is lowered. Membrane-interacting regions of different fusion proteins have been implicated in playing such a role. Fusion peptides have been shown to alter the spontaneous curvature of a lipid bilayer to favor the non-lamellar Hexagonal II phase (Epand and Epand, 2000; Peisajovich *et al.*, 2000a). Fusion peptides have also been shown to cause perturbation of lipid bilayers and mixing of outer leaflets (Epand, 2003; Neiva and Agirre, 2003).

A synthetic peptide of the p14 hydrophobic patch mediated lipid mixing *in vitro*. The interaction of HP motif with either the donor or target membrane during the fusion process may perturb pre-fusion bilayers and/or stabilize highly curved lipid intermediates, thereby promoting stalk formation. P14 is also believed to localize preferentially to regions of the cell membrane that are highly curved. The putative presence of p14 in plasma-membrane protrusions is also likely to promote the fusion reaction. Indeed, cell-cell fusion events are often initiated at protrusion sites (Wilson and Snell, 1998).

It is possible that, despite the concerted action of the membrane-disrupting regions of p14, the activation energy barrier is lowered but not removed by these effects (for example, EA3 is reduced to EA1 or EA2 in the hypothetical free energy diagram, Fig 7.1). In such a scenario, an input of free energy is required to drive the fusion reaction forward. As p14 is unlikely to undergo large structural remodeling in a manner like that of enveloped-virus fusion proteins, where could this energy come from? Membrane insertion of the HA fusion peptide is a thermodynamically favorable event (Li *et al.*, 2003). Upon low-pH exposure, membrane insertion deepens and a portion of the V-shaped fusion peptide re-folds to a 3_{10} helix (Han *et al.*, 2001). Solution NMR spectroscopy indicated that the p14 hydrophobic patch is a β -structured loop in the N-proximal region, and random coil at its C terminus. Perhaps upon membrane interaction the C-terminal region adopts a distinct secondary fold. Circular-dichroism spectroscopy showed an increase in the helical propensity of the p14 HP peptide in the presence of membrane lipids. Such a discrete structural alteration is possible, even for a small fusion protein such as p14, and this in combination with thermodynamically favorable

membrane insertion may provide sufficient impetus for membrane fusion, especially if p14 has already modulated the activation energy barrier to a minimum.

One of the most interesting structural features of p14 is the externalized N-terminal myristate. Myristic acid can associate reversibly with a membrane (Resh, 1999). P14 may be the first membrane fusion protein to commandeer the reversible association of a fatty acid as critical feature of the fusion mechanism. Buried in a membrane, myristate has the potential to perturb that bilayer (Joseph and Nagaraj, 1995). If transiently located in the interbilayer space, this hydrophobic moiety will likely dehydrate membrane surfaces. Future studies plan to assess these putative roles *in vitro* by comparing the ability of myristylated and non-myristylated peptide analogues of the p14-ectodomain to modulate membrane stability and lipid mixing of liposomes.

This model assumes that the convergence of a critical number of p14 multimers to the site of fusion initiation is required. Each p14 multimer possesses greater potential to interact with the donor and/or target membrane than does one monomer alone. The membrane-destabilizing potential of an aggregate of p14 multimers is greater still. The localization of p14 to cholesterol-rich detergent-resistant membrane microdomains may be a means for p14 to travel to distinct regions of the plasma membrane and promote clustering at these sites. The lab is currently examining the possibility of p14 clustering at non-planar regions of the plasma membrane.

Structural remodeling of enveloped-virus fusion proteins is required to extrude the previously buried fusion peptide, which is then believed to interact with the target membrane (Carr and Kim, 1993). However, I do not assume that p14 HP motif must interact with the target membrane during the fusion process. Kozlov and Chernomordik

(1998) suggest an alternative model for HA-mediated fusion that suggests the fusion peptide of HA must interact with the HA-containing (donor) membrane. This results in the formation of a highly curved and stressed membrane dimple that reaches towards the target membrane and facilitates lipid intermixing and merger. The small size of the p14 ectodomain relative to that of other membrane fusion proteins suggests that the p14 HP may be used to destabilize the p14-containing membrane. Is it possible to consider the other, more classical scenario of target-membrane insertion? Given the relatively unstructured nature of the p14 ectodomain in solution, this region may be capable of bridging the distance between two closely apposed membranes. Assuming an axial length of 3.4 Å per amino acid (Zimmerberg *et al.*, 1993), and discounting the residues known to form the N-proximal β -structured loop, the p14 ectodomain can extend a maximum of 86 Å (25 amino acids x 3.4 Å/residue). Electron microscopy of the QM5 fibroblast cells that are used in my lab (that was performed and donated by J. Salsman) indicates that cells in culture possess many sites of close cell-cell contact (Fig 7.2 and Fig 7.3). These sites are especially prevalent between regions of cell protrusions, where two opposing membranes are only 2-3 nm apart (Fig 7.2). It is possible that reversible disassociation of myristic acid leads to the extension of both the N-proximal loop of the HP motif and the fatty acid toward the target membrane, where they embed.

Step 3- fusion

I have not discussed the transmembrane domain and membrane-proximal basic motif of p14. These domains are likely to play an important role(s) in destabilizing the donor membrane during fusion. The transmembrane domains of enveloped-virus fusion proteins

have been implicated in playing an essential role in fusion-pore formation; replacement of these domains with a lipid anchor results in hemifusion (Salzwedel *et al.*, 1993; Kemble *et al.*, 1994). The boomerang model of HA-mediated fusion suggests that the fusion peptide and transmembrane domain must interact for complete fusion-pore formation (Tamm, 2003). The p14 transmembrane anchor may play a similar role in p14-fusion-pore formation; current studies undertaken in the laboratory include swapping this domain between different members of the FAST protein family, and between the FAST proteins and unrelated integral membrane polypeptides. Mutagenesis of the membrane-proximal positively charged residues or of transmembrane-domain glycine residues in ARV p10 abolished fusion (Shmulevitz and Duncan, 2000), suggesting the essential nature of both motifs in p14.

This study is a preliminary characterization of the p14 membrane fusion protein of a reptilian reovirus. An understanding of how p14 works to modulate membrane structure and elicit the lipid rearrangements necessary for membrane merger is in its infancy, especially in comparison to the years of study on enveloped-virus fusion proteins such as influenza HA, HIV-1 gp41, paramyxovirus F, and rhabdovirus G protein. Nonetheless, based on the first structural characterization of p14 I propose a working hypothesis for p14-mediated membrane fusion (Fig 7.2); studies are underway in the laboratory to confirm or refute these ideas.

It is assured that p14, as a small, unregulated fusion protein, does not possess the size capability or structural features to promote membrane fusion using large energy-releasing triggered conformational changes. However, p14 and other FAST proteins may

utilize a repertoire of membrane-interacting motifs (fusion peptide, transmembrane domain), similar to those found in larger, more complex fusion proteins, to disrupt two opposing bilayers. After membrane disruption, p14 may require only small alterations in its ectodomain similar to those secondary-structure alterations already described to occur within fusion peptides encoded by enveloped viruses. That, in combination with the thermodynamically favorable membrane insertion of the hydrophobic patch and/or myristic acid, dehydration of the intercellular layer, and alteration of membrane curvature, may be sufficient impetus for membrane merger. I propose that p14 utilizes a simpler thermodynamic profile of discrete structural alterations, without the requirement for extensive structural remodeling. This study has characterized a distinct new member of the reovirus FAST protein family, p14, and supports the assertion that the FAST proteins represent a new class of fusion proteins that contain the minimal arrangement of protein motifs essential for biological-membrane fusion.

7.3 Figures

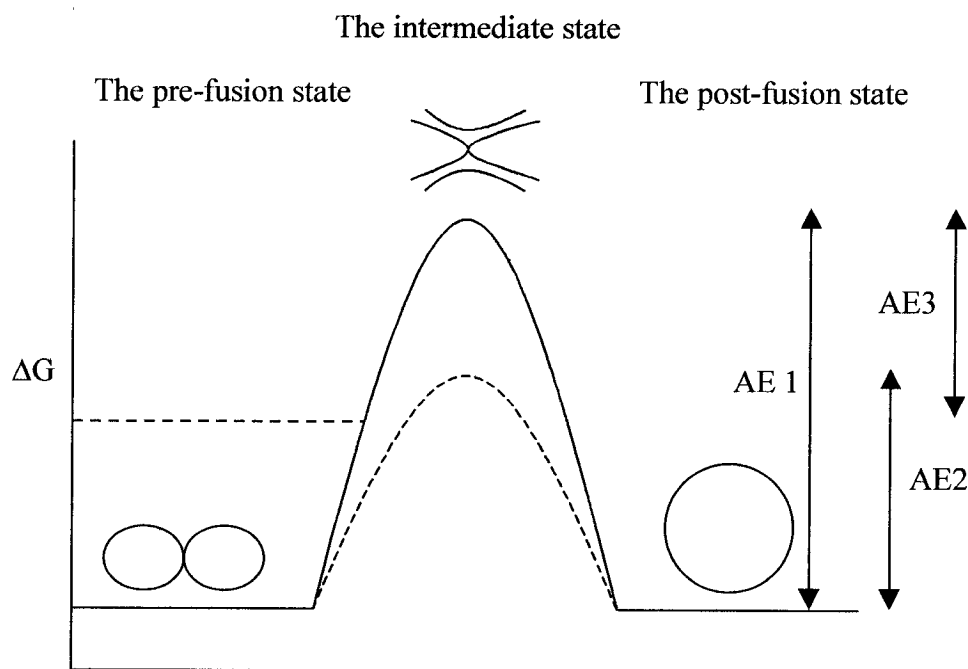


Fig 7.1 A hypothetical free-energy diagram of the membrane fusion reaction. The Gibbs free energy (ΔG) of pre- and post-fusion bilayer states is depicted as equal, as the free energy of the starting structures and the products of the fusion process are believed to be similar (Epan, 2003). The reaction is represented as having one high-energy intermediate state; however, it is likely that more than one lipidic intermediate exists (Lentz and Lee, 1999). If the free energy of the pre-fusion bilayers remains low, and the free energy of the intermediate state remains high (solid lines) the activation energy barrier that prevents membrane fusion is large (AE1). If the free energy of the pre-fusion bilayer is raised or the free energy of the intermediate state is lowered (dashed lines), then the activation energy barrier is decreased substantially (AE2 or AE3).

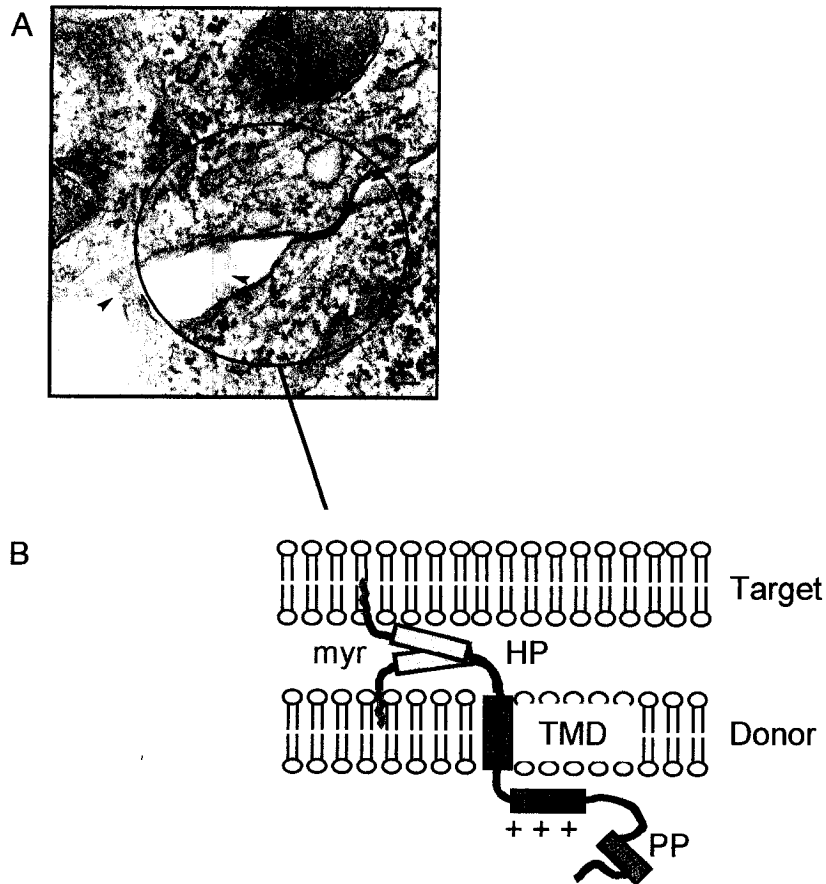


Fig 7.2 A model of p14-mediated membrane fusion. **(A)** Sites of cell-cell contact in QM5 fibroblast cells. Two adjacent QM5 cells demonstrate multiple sites of close cell-cell contact at plasma-membrane protrusions (black arrows) and a gap-junction-like structure (white arrow). The intercellular space is 2-3 nm. Scale bar = 100 nm. This figure was contributed by J. Salsman. **(B)** At sites of close cell apposition (approximately 2-3 nm), p14 may use its membrane-interacting domains (externalized myristate [red line], hydrophobic patch [orange], transmembrane domain [red], and basic motif [blue]) to mediate the intercellular dehydration and perturbation of the donor and/or target lipid bilayer(s) required to elicit membrane merger.

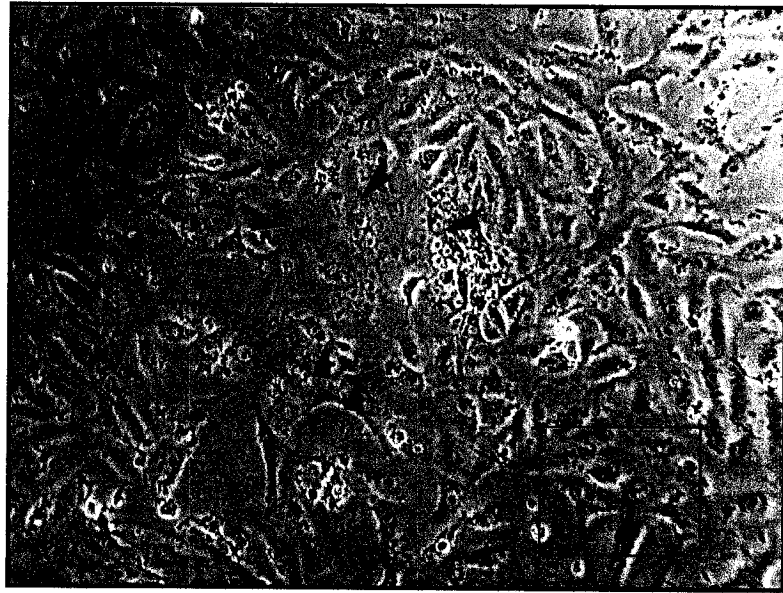


Fig 7.3 The p14 fusion protein in action, as illustrated by a short video. P14-transfected Vero cells (16 hours post transfection) were photographed every 5 minutes for 4 hours. The individual frames were then compiled into a movie using Image Pro Plus software. During the video, note the large multinucleated syncytium as indicated by the black arrows and the two cells within the boxed area (the intercellular junction is indicated by an arrow). The movie demonstrates that fusion of two individual cells is initiated by plasma-membrane protrusions.

References

- Abell, B., S. High, and M. M. Moloney. 2002. Membrane protein topology of Oleosin is constrained by its long hydrophobic domain. *J. Biol. Chem.* **277** 8602-8610.
- Adler, R. R., A. K. Ng, and N. S. Rote. 1995. Monoclonal antiphosphatidylserine antibody inhibits intercellular fusion of the choriocarcinoma line, JAR. *Biol. Reprod.* **53** 905-910.
- Ahn, A., D. L. Gibbons, and M. Kielian. 2002. The fusion peptide of Semliki forest virus associates with sterol-rich membrane domains. *J. Virol.* **76** 3267-3275.
- Ahne, W., I. Thomsen, and J. Winton. 1987. Isolation of a reovirus from the snake, *Python regius*. *Arch. Virol.* **94** 135-139.
- Ali, A., R. T. Avalos, E. Ponimaskin, and D. P. Nayak. 2000. Influenza virus assembly: effect of influenza virus glycoproteins on the membrane association of M1 protein. *J. Virol.* **74** 8709-8719.
- Allison, S. L., J. Schlich, K. K. Stiasny, C. W. Mandl, and F. X. Heinz. 2001. Mutational evidence for an internal fusion peptide in flavivirus envelope protein E. *J. Virol.* **75** 4268-4275.
- Almers, W. 2001. Fusion needs more than SNAREs. *Nature* **409** 567-568.
- Ames, B. N. 1966. *Methods Enzymol.* **8** 115-118.
- Anderson, R. G. W. and K. Jacobson. 2002. A role for lipid shells in targeting proteins to caveolae, rafts, and other lipid domains. *Science* **296** 1821-1825.
- Antin, P. B. and C. P. Ordahl. 1991. Isolation and characterization of an avian myogenic cell line. *Dev. Biol.* **143** 111-121.
- Armstrong, R. T., A. S. Kushnir, and J. M. White. 2000. The transmembrane domain of influenza hemagglutinin exhibits a stringent length requirement to support the hemifusion to fusion transition. *J. Cell Biol.* **151** 425-437.
- Arnold, K., L. Pratsch, and K. Gawrisch. 1983. Effect of poly(ethylene glycol) on phospholipid hydration and polarity of the external phase. *Biochim. Biophys. Acta* **728** 121-128.
- Attoui, H., P. Biagini, J. Stirling, P. P. Mertens, J. F. Cantaloube, A. Meyer, P. de Micco, and X. de Lamballerie. 2001. Sequence characterization of Ndelle virus genome

segments 1, 5, 7, 8, and 10: evidence for reassignment to the genus Orthoreovirus, family Reoviridae. *Biochem. Biophys. Res. Commun.* **287** 583-588.

Attoui, H., Q. Fang, F. M. Jaafar, J.-F. Cantaloube, P. Biagini, P. de Micco, and X. de Lamballerie. 2002. Common evolutionary origin of aquareoviruses and orthoreoviruses revealed by genome characterization of Golden shiner reovirus, Grass carp reovirus, Striped bass reovirus and golden ide reovirus (genus *Aquareovirus*, family Reoviridae). *J. Gen. Virol.* **83** 1941-1951.

Avitable, E., G. Lombardi, and G. Campadelli-Fiume. 2003. Herpes simplex virus glycoprotein K, but not its syncytial allele, inhibits cell-cell fusion mediated by the four fusogenic glycoproteins, gD, gB, gH, and gL. *J. Virol.* **77** 6836-6844.

Baker, K. A., R. E. Dutch, R. A. Lamb, T. S. Jardetzky. 1999. Structural basis for paramyxovirus-mediated membrane fusion. *Mol. Cell* **3** 309-319.

Balliet, J. W., K. Gendron, and P. Bates. 2000. Mutational analysis of the subgroup A avian sarcoma leukosis virus putative fusion peptide domain. *J. Virol.* **74** 3731-3739.

Bax, A. and D. G. Davis. 1985. MLEV-17-based two-dimensional homonuclear magnetization transfer spectroscopy. *J. Magn. Reson.* **65** 355-360.

Bennett, K. L., M. Kussmann, P. Bjork, M. Godzwon, M. Mikkelsen, P. Sorensen, and P. Roepstorff. 2000. Chemical cross-linking with thiol-cleavable reagents combined with differential mass spectrometric peptide mapping – a novel approach to assess intramolecular protein contacts. *Prot. Sci.* **9** 1503-1518.

Bentz, J. 2000a. Membrane fusion mediated by coiled coils: a hypothesis. *Biophys. J.* **78** 886-900.

Bentz, J. 2000b. Minimal aggregate size and minimal fusion unit for the first fusion pore of influenza hemagglutinin-mediated membrane fusion. *Biophys. J.* **78** 227-245.

Bentz, J. and A. Mittal. 2003. Architecture of the influenza hemagglutinin membrane fusion site. *Biochem. Biophys. Acta* **1614** 24-35.

Berger, J., A. D. Howard, L. Gerber, B. R. Cullen, and S. Udenfriend. 1987. Expression of active, membrane-bound human placental alkaline phosphatase by transfected simian cells. *Proc. Natl. Acad. Sci. USA* **84** 4885-4889.

Bickel, P. E., P. E. Scherer, J. E. Schnitzer, P. Oh, M. P. Lisanti, and H. F. Lodish. 1997. Flotillin and epidermal surface antigen define a new family of caveolae-associated integral membrane proteins. *J. Biol. Chem.* **272** 13793-13802.

Bigler, D., M. Chen, S. Waters, and J. M. White. 1997. A model for sperm-egg binding and fusion based on ADAMs and integrins. *Trends Cell Biol.* **7** 65-72.

- Blahak, S., I. Ott, and E. Vieler. 1995. Comparison of six different reoviruses of various reptiles. *Vet. Res.* **26** 470-476.
- Blobel, C. P., T. G. Wolfsberg, C. W. Turck, D. G. Myles, P. Primakoff and J. M. White. 1992. A potential fusion peptide and integrin ligand domain in sperm-egg membrane fusion. *Nature* **356** 248-252.
- Blott, E. J., G. Bossi, R. Clark, M. Zvelebil, and G. M. Griffiths. 2001. Fas ligand is targeted to secretory lysosomes via a proline-rich domain in its cytoplasmic tail. *J. Cell Sci.* **114** 2405-2416.
- Blum, H., H. Beier, and H. J. Gross. 1987. Improved silver staining of plant proteins, RNA, and DNA in polyacrylamide gels. *Electrophoresis* **8** 93-99.
- Blumenthal, R., D. P. Sarkar, S. Durrell, D. E. Howard, and S. L. Morris. 1996. Dilation of the influenza hemagglutinin fusion pore revealed by the kinetics of individual cell-cell fusion events. *J. Cell Biol.* **135** 63-71.
- Blumenthal, R. M. J. Clague, S. R. Durell, and R. M. Epand. 2003. Membrane fusion. *Chem. Rev.* **103** 53-69.
- Bock, J. B., H. T. Matern, A. A. Peden, and R. H. Scheller. 2001. A genomic perspective on membrane compartment organization. *Nature* **409** 839-841.
- Bonafous, P. and T. Stegmann. 2000. Membrane perturbation and fusion pore formation in influenza hemagglutinin-mediated membrane fusion. *J. Biol. Chem.* **275** 6160-6166.
- Bonner, W. M. 1984. Fluorography for detection of radioactivity in gels. *Methods Enzymol.* **104** 460-465.
- Bormann, B. J. and D. M. Engelman. 1992. Intramembrane helix-helix association in oligomerization and transmembrane signaling. *Annu. Rev. Biophys. Biomol. Struct.* **21** 223-242.
- Bosch, B. J., R. van der Zee, C. A. M. de Haan, and P. J. M. Rottier. 2003. The coronavirus spike protein is a Class I virus fusion protein: structural and functional characterization of the fusion core complex. *J. Virol.* **77** 8801-8811.
- Braccia, A., M. Villani, L. Immerdel, L.-L. Niels-Christiansen, B. T. Nyström, G. H. Hansen, and E. M. Danielsen. 2003. Microvillar membrane microdomains exist at physiological temperature. *J. Biol. Chem.* **278** 15679-15684.
- Brown, D. A. and J. K. Rose. 1992. Sorting of GPI-anchored proteins to glycolipid-enriched membrane subdomains during transport to the apical cell surface. *Cell* **68** 533-544.

Brown, D. A. and E. London. 1998. Functions of lipid rafts in biological membranes. *Annu. Rev. Cell Dev. Biol.* **14** 111-136.

Brown, D. A. and E. London. 2000. Structure and function of sphingolipid- and cholesterol-rich membrane rafts. *J. Biol. Chem.* **275** 17221-17224.

Brun, G., X. Bao, and L. Prevec. 1995. The relationship of Piry virus to other vesiculoviruses: a re-evaluation based on the glycoprotein gene sequence. *Intervirology* **38** 274-282.

Brunger, A. T. XPLOR. [3.1]. 1992. Yale University, 260 Whitney Avenue, P.O. Box 6666, New Haven, CT 06511, The Howard Hughes Medical Institute and Department of Molecular Biophysics and Biochemistry. 1992. Ref Type: Computer Program.

Brunger, A. T. 2001. Structural insights into the molecular mechanism of calcium-dependent vesicle-membrane fusion. *Curr. Opin. Struct. Biol.* **11** 163-73.

Bruss, V., J. Jagelstein, E. Gerhardt, and P. R. Galle. 1996. Myristylation of the large surface protein is required for hepatitis B virus *in vitro* infectivity. *Virology* **218** 396-399.

Buckland, R., C. Gerald, R. Barker, and T. F. Wild. 1987. Fusion glycoprotein of measles virus: nucleotide sequence of the gene and comparison with other paramyxoviruses. *J. Gen. Virol.* **68** 1695-1703.

Bullough, P. A., F. M. Hughson, J. J. Skehel, and D. C. Wiley. 1994. Structure of influenza haemagglutinin at the pH of membrane fusion. *Nature* **371** 37-43.

Caffrey, M., M. Cai, J. Kaufman, S. J. Stahl, P. T. Wingfield, D. G. Covell, A. M. Gronenborn, and G. M. Clore. 1998. Three-dimensional solution structure of the 44 kDa ectodomain of SIV gp41. *EMBO J.* **17** 4572-4584.

Caffrey, M., J. Kaufman, S. Stahl, P. Wingfield, A. M. Gronenborn, and G. M. Clore. 1999. Monomer-trimer equilibrium of the ectodomain of SIV gp41: insight into the mechanism of peptide inhibition of HIV infection. *Protein Sci.* **8** 1904-1907.

Calvo, D. and M. A. Vega. 1993. Identification, primary structure, and distribution of CLA-1, a novel member of the CD36/LIMPII gene family. *J. Biol. Chem.* **268** 18929-18935.

Carneiro, F. A., A. S. Ferradosa, and A. T. Da Poian. 2001. Low pH-induced conformational changes in vesicular stomatitis virus glycoprotein involve dramatic structure reorganization. *J. Biol. Chem.* **276** 62-67.

Carr, C. M., and P. S. Kim. 1993. A spring-loaded mechanism for the conformational change of influenza hemagglutinin. *Cell* **73** 823-832.

Carr, C. M., C. Chaudhry, and P. S. Kim. 1997. Influenza hemagglutinin is spring-loaded by a metastable native conformation. *Proc. Natl. Acad. Sci. USA* **94** 14306-14313.

Chaitin, M. H., H. S. Wortham, and A. M. Brun-Zinkernagel. 1994. Immunocytochemical localization of CD44 in the mouse retina. *Exp. Eye Res.* **58** 359-365.

Chambers, P., N. S. Millar, and P. T. Emmerson. 1986. Nucleotide sequence of the gene encoding the fusion glycoprotein of Newcastle disease virus. *J. Gen. Virol.* **67** 2685-2694.

Chan, D. C., D. Fass, J. M. Berger, and P. S. Kim. 1997. Core structure of gp41 from the HIV envelope glycoprotein. *Cell* **89** 263-273.

Chang, D., S. Cheng, and W. Chien. 1997. The amino-terminal fusion domain peptide of human immunodeficiency virus type I gp41 inserts into the sodium dodecyl sulfate micelle primarily as a helix with a conserved glycine at the micelle-water interface. *J. Virol.* **71** 6593-6602.

Chanturiya, A., L. V. Chernomordik, and J. Zimmerberg. 1997. Flickering fusion pores comparable with initial exocytotic pores occur in protein-free phospholipid bilayers. *Proc. Natl. Acad. Sci. USA* **94** 14423-14428.

Chanturiya, A., P. Scaria, M. C. Woodle. 2000. The role of membrane lateral tension in calcium-induced membrane fusion. *J. Membr. Biol.* **176** 67-75.

Chatterjee, P. K., C. H. Eng, and M. Kielian. 2002. Novel mutations that control the sphingolipid and cholesterol dependence of the Semliki virus fusion protein. *J. Virol.* **76** 12712-12722.

Chen, J., J. J. Skehel, and D. C. Wiley. 1999. N- and C-terminal residues combine in the fusion-pH influenza hemagglutinin HA(2) subunit to form an N cap that terminates the triple-stranded coiled coil. *Proc. Natl. Acad. Sci. USA* **96** 8967-8972.

Chen, L., J. J. Gorman, J. McKimm-Breschkin, L. J. Lawrence, P. A. Tulloch, B. J. Smith, P. M. Colman, and M. C. Lawrence. 2001. The structure of the fusion glycoprotein of Newcastle disease virus suggests a novel paradigm for the molecular mechanism of membrane fusion. *Structure* **9** 255-266.

Chernomordik, L., A. Chanturiya, J. Green, and J. Zimmerberg. 1995a. The hemifusion intermediate and its conversion to complete fusion: regulation by membrane composition. *Biophys. J.* **69** 922-929.

Chernomordik, L., M. M. Kozlov, and J. Zimmerberg. 1995b. Lipids in biological membrane fusion. *J. Membr. Biol.* **146** 1-14.

Chernomordik, L. V., V. A. Frolov, E. Leikina, P. Bronk, and J. Zimmerberg. 1998. The pathway of membrane fusion catalyzed by influenza hemagglutinin: restriction of lipids, hemifusion, and lipidic pore formation. *J. Cell Biol.* **140** 1369-1382.

Chernomordik, L. K., E. Leikina, M. M. Kozlov, V. A. Frolov, and J. Zimmerberg. 1999. Structural intermediates in influenza haemagglutinin-mediated fusion. *Mol. Membr. Biol.* **16** 33-42.

Cho, C., H. Ge, D. Branciforte, P. Primakoff, and D. G. Myles. 2000. Analysis of mouse fertilin in wild-type and fertilin beta(-/-) sperm: evidence for C-terminal modification, α/β dimerization, and lack of essential role of fertilin α in sperm-egg fusion. *Dev. Biol.* **222** 289-295.

Chow, M., J. F. Newman, D. Filman, J. M. Hogle, D. J. Rowlands, F. Brown. 1987. Myristylation of picornavirus capsid protein VP4 and its structural significance. *Nature* **327** 482-486.

Cladera, J., I. Martin, J.-M. Ruyschaert, and P. O'Shea. 1999. Characterization of the sequence of interactions of the fusion domain of simian immunodeficiency virus with membranes. *J. Biol. Chem.* **274** 29951-29959.

Clague, M. J., C. Schoch, L. Zech, and R. Blumenthal. 1990. Gating kinetics of pH-activated membrane fusion of vesicular stomatitis virus with cells: stopped-flow measurements by dequenching of octadecylrhodamine fluorescence. *Biochemistry* **29** 1303-1308.

Cleverley, D. Z. and J. Lenard. 1998. The transmembrane domain in viral fusion: essential role for a conserved glycine residue in vesicular stomatitis virus G protein. *Biochemistry* **95** 3425-3430.

Colacino, J. M., N. Y. Chirgadze, E. Garman, G. Murti, R. J. Loncharich, A. J. Baxter, K. A. Staschke, and W. G. Laver. 1997. A single sequence change destabilizes the influenza virus neuraminidase tetramer. *Virology* **236** 66-75.

Constantinescu, S. N., T. Keren, M. Socolovsky, H.-S. Nam, Y. I. Henis, and H. F. Lodish. 2001. Ligand-independent oligomerization of cell-surface erythropoietin receptor is mediated by the transmembrane domain. *Proc. Natl. Acad. Sci. USA* **98** 4379-4384.

- Coonrod, S. A., S. Naaby-Hansen, J. Shetty, H. Shibahara, M. Chen, J. M. White, and J. C. Herr. 1999. Treatment of mouse oocytes with PI-PLC releases 70-kDa (pI 5) and 35- to 45-kDa (pI 5.5) protein clusters from the egg surface and inhibits sperm-oolemma binding and fusion. *Dev. Biol.* **207** 334-349.
- Cooper, A., N. Paran, and Y. Shaul. 2003. The earliest steps in hepatitis B virus infection. *Biochim. Biophys. Acta* **1614** 89-96.
- Copeland, C. S., K. P. Zimmer, K. R. Wagner, G. A. Healey, I. Mellman, and A. Helenius. 1988. Folding, trimerization, and transport are sequential events in the biogenesis of influenza virus hemagglutinin. *Cell* **53** 197-209.
- Corbeil, D., K. Röper, C. A. Fargeas, A. Joester, and W. B. Huttner. 2001. Prominin: a story of cholesterol, plasma membrane protrusions and human pathology. *Traffic* **2** 82-91.
- Crimmins, D., W. Mehard, and S. Schlesinger. 1983. Physical properties of a soluble form of the glycoprotein of vesicular stomatitis virus at neutral and acidic pH. *Biochemistry* **22** 5790-5796.
- Cross, K. J., S. A. Wharton, J. J. Skehel, D. C. Wiley, and D. A. Steinhauer. 2001. Studies on influenza haemagglutinin fusion peptide mutants generated by reverse genetics. *EMBO J.* **20** 4432-4442.
- Crystal, A. S., V. A. Morais, T. C. Pierson, D. S. Pijak, D. Carlin, V. M.-Y. Lee, and R. M. Doms. 2003. Membrane topology of γ -secretase component PEN-2. *J. Biol. Chem.* **278** 20117-20123.
- Cuadras, M. A. and H. B. Greenberg. 2003. Rotavirus infectious particles use lipid rafts during replication for transport to the cell surface *in vitro* and *in vivo*. *Virology* **313** 308-321.
- Cullis, P. R., M. J. Hope, and C. P. Tilcock. 1986. Lipid polymorphism and the roles of lipids in membranes. *Chem. Phys. Lipids* **40** 127-144.
- Dalgarno, L., C. M. Rice, and J. H. Strauss. 1983. Ross River virus 26 S RNA: complete nucleotide sequence and deduced sequence of the encoded structural proteins. *Virology* **129** 170-187.
- Danieli, T., S. L. Pelletier, Y. I. Henis, and J. M. White. 1996. Membrane fusion mediated by the influenza virus hemagglutinin requires the concerted action of at least three hemagglutinin trimers. *J. Cell Biol.* **133** 559-569.
- Daniels, R., B. Kurowski, A. E. Johnson and D. N. Hebert. 2003. N-linked glycans direct the cotranslational folding pathway of *Influenza* hemagglutinin. *Mol. Cell* **11** 79-90.

- Davies, S. M. A., S. M. Kelly, N. C. Price, and J. P. Bradshaw. 1998. Structural plasticity of the feline leukaemia virus fusion peptide: a circular dichroism study. *FEBS Lett.* **425** 415-418.
- Dawe, S. and R. Duncan. 2002. The S4 genome segment of baboon reovirus is bicistronic and encodes a novel fusion-associated small transmembrane protein. *J. Virol.* **76** 2131-2140.
- Dawe, S. J., J. A. Corcoran, and R. Duncan. Determination of the membrane orientation of the baboon reovirus fusion-inducing protein reveals the absence of an externalized hydrophobic peptide. *Manuscript in preparation*.
- Daya, M., M. Cervin, and R. Anderson. 1988. Cholesterol enhances mouse hepatitis virus-mediated cell fusion. *Virology* **163** 276-283.
- Delos, S. E. and J. M. White. 2000. Critical role for the cysteines flanking the internal fusion peptide of avian sarcoma/leukosis virus envelope glycoprotein. *J. Virol.* **74** 9738-9741.
- Delos, S. E., J. M. Gilbert, and J. M. White. 2000. The central proline of an internal viral fusion peptide serves two important roles. *J. Virol.* **74** 1686-1693.
- Dennison, S. M., N. Greenfield, J. Lenard, and B. R. Lentz. 2002. VSV transmembrane domain (TMD) peptide promotes PEG-mediated fusion of liposomes in a conformationally sensitive fashion. *Biochemistry* **41** 14925-14934.
- Denzer, A. J., C. E. Nabholz, and M. Spiess. 1995. Transmembrane orientation of signal-anchor proteins is affected by the folding state but not the size of the N-terminal domain. *EMBO J.* **14** 6311-6317.
- Deubel, V., R. M. Kinney, and D. W. Trent. 1986. Nucleotide sequence and deduced amino acid sequence of the structural proteins of dengue type 2 virus, Jamaica genotype. *Virology* **155** 365-377.
- Dimitrov, D. S. and R. Blumenthal. 1994. Photoactivation and kinetics of membrane fusion mediated by human immunodeficiency type 1 enveloped glycoprotein. *J. Virol.* **68** 1956-1961.
- Ding, L., A. Derdowski, J.-J. Wang, and P. Spearman. 2003. Independent segregation of human immunodeficiency virus type 1 gag protein complexes and lipid rafts. *J. Virol.* **77** 1916-1926.
- Doms, R. W. and A. Helenius. 1986. Quaternary structure of influenza virus hemagglutinin after acid treatment. *J. Virol.* **60** 833-839.

- Doms R. W., A. Helenius, and J. M. White. 1985. Membrane fusion activity of the influenza virus hemagglutinin. The low pH-induced conformational change. *J. Biol. Chem.* **260** 2973-2981.
- Doms, R. W., D. S. Keller, A. Helenius, and W. E. Batch. 1987. Role of adenosine triphosphate in regulating the assembly and transport of vesicular stomatitis virus G protein trimers. *J. Cell Biol.* **105** 1957-1969.
- Doms, R. W., G. Russ, and J. W. Yewdell. 1989. Brefeldin A redistributes resident and itinerant Golgi proteins to the endoplasmic reticulum. *J. Cell Biol.* **109** 61-72.
- Doms, R. W., R. A. Lamb, J. K. Rose, and A. Helenius. 1993. Folding and assembly of viral membrane proteins. *Virology* **193** 545-562.
- Drevot, P., C. Langlet, X.-J. Guo, A.-M. Bernard, O. Colard, J.-P. Chauvin, R. Lasserre, H.-T. He. 2002. TCR signal initiation machinery is pre-assembled and activated in a subset of membrane rafts. *EMBO J.* **21** 1899-1908.
- Drobnik, W., H. Borsukova, A. Bottcher, A. Pfeiffer, G. Liebisch, G. J. Schutz, H. Schindler, and G. Schmitz. 2002. Apo AI/ABCA1-dependent and HDL3-mediated lipid efflux from compositionally distinct cholesterol-based microdomains. *Traffic* **3** 268-278.
- Duncan, R. 1999. Extensive sequence divergence and phylogenetic relationships between the fusogenic and nonfusogenic orthoreoviruses: a species proposal. *Virology* **260** 316-328.
- Duncan, R. and K. Sullivan. 1998. Characterization of two avian reoviruses that exhibit strain-specific quantitative differences in their syncytium-inducing and pathogenic capabilities. *Virology* **250** 263-272.
- Duncan, R., F. A. Murphy, and R. R. Mirkovic. 1995. Characterization of a novel syncytium-inducing baboon reovirus. *Virology* **212** 752-756.
- Duncan, R., Z. Chen, S. Walsh, and S. Wu. 1996. Avian reovirus-induced syncytium formation is independent of infectious progeny virus production and enhances the rate, but is not essential, for virus-induced cytopathology and virus egress. *Virology* **224** 453-464.
- Duncan R., J. A. Corcoran, D. Stoltz, J. Shou. 2003. Reptilian reovirus represents a new species in the fusogenic subgroup of Orthoreoviruses. *Virology*. In press.
- Durell, S. R., I. Martin, J.-M. Ruyschaert Y. Shai, R. Blumenthal. 1997. What studies of fusion peptides tell us about viral envelope glycoprotein-mediated membrane fusion. *Mol. Membr. Biol.* **14** 97-112.

Dutch, R. E., G. P. Leser, and R. A. Lamb. 1999. Paramyxovirus fusion protein: characterization of the core trimer, a rod-shaped complex with helices in anti-parallel orientation. *Virology* **254** 147-159.

Eckert, D. M. and P. S. Kim. 2001. Mechanisms of viral membrane fusion and its inhibition. *Annu. Rev. Biochem.* **70** 777-810.

van den Eijnde, S. M., M. J. B. van den Hoff, C. P. M. Reutelingsperger, W. L. van Heerde, M. E. R. Henfling, C. Varmeij-Keers, B. Schutte, M. Borgers, and F. C. S. Ramaekers. 2001. Transient expression of phosphatidylserine at cell-cell contact areas is required for myotube formation. *J. Cell Sci.* **114** 3631-3642.

Einfeld, D. and E. Hunter. 1988. Oligomeric structure of a prototype retrovirus glycoprotein. *Proc. Natl. Acad. Sci. USA* **85** 8688-8692.

Eisenberg, D. 1984. Three dimensional structure of membrane and surface proteins. *Annu. Rev. Biochem.* **53** 595-623.

Ellens, H., J. Bentz and F.C. Szoka. 1985. H^+ and Ca^{2+} -induced fusion and destabilization of liposomes. *Biochemistry* **24** 3099-3106.

Ellgaard, L. and A. Helenius. 2003. Quality control in the endoplasmic reticulum. *Nat. Rev. Mol. Cell Biol.* **4** 181-191.

Engelsberg, A., R. Hermosilla, U. Karsten, R. Schüle, B. Dörken, and A. Rehn. 2003. The Golgi protein RCAS1 controls cell surface expression of tumor-associated O-linked glycan antigens. *J. Biol. Chem.* **278** 22998-23007.

Epand, R. F. and R. M. Epand. 2003. Irreversible unfolding of the neutral pH form of influenza hemagglutinin demonstrates that it is not in a metastable state. *Biochemistry* **42** 5052-5057.

Epand, R. F., J. C. Macosko, C. J. Russell, Y.-K. Shin and R. M. Epand. 1999. The ectodomain of HA2 of influenza virus promotes rapid pH dependent membrane fusion. *J. Mol. Biol.* **286** 489-503.

Epand, R. M. 1997. Studies of membrane physical properties and their role in biological fusion. *Biochem. Soc. Trans.* **25** 1073-1078.

Epand, R. M. 1998. Lipid polymorphism and protein-lipid interactions. *Biochim. Biophys. Acta* **1376** 353-368.

Epand, R. M. 2003. Fusion peptides and the mechanism of viral fusion. *Biochim. Biophys. Acta* **1614** 116-121.

- Epand, R. M. and R. F. Epand. 1994. Relationship between the infectivity of influenza virus and the ability of its fusion peptide to perturb bilayers. *Biochem. Res. Comm.* **202** 1420-1425.
- Epand, R. M. and R. F. Epand. 2000. Modulation of membrane curvature by peptides. *Biopolymers* **55** 358-363.
- Epand, R. M. and R. F. Epand. 2001. Factors contributing to the fusogenic potency of foamy virus. *Biochem. Biophys. Res. Comm.* **284** 870-874.
- Epand, R. M. and R. F. Epand. 2002. Thermal denaturation of influenza virus and its relationship to membrane fusion. *Biochem. J.* **365** 841-848.
- Epand, R. M., R. F. Epand, I. Martin, and J. Ruyschaert. 2001. Membrane interactions of mutated forms of the influenza fusion peptide. *Biochemistry* **40** 8800-8807.
- Fass, D., S. C. Harrison, and P. S. Kim. 1996. Retrovirus envelope domain at 1.7 angstrom resolution. *Nat. Struct. Biol.* **3** 465-469.
- Finel, M. 1987. Studies on the oligomeric state of isolated cytochrome oxidase using cross-linking reagents. *Biochem. Biophys. Acta* **894** 174-179.
- Fredericksen, B. L. and M. A. Whitt. 1995. Vesicular stomatitis virus glycoprotein mutations that affect membrane fusion activity and abolish virus infectivity. *J. Virol.* **69** 1435-1443.
- Friedrichson, T. and T. V. Kurzchalia. 1998. Microdomains of GPI-anchored proteins in living cells revealed by cross-linking. *Nature* **394** 802-805.
- Frolov, V. A., M. S. Cho, P. Bronk, T. S. Reese, and J. Zimmerberg. 2000. Multiple local contact sites are induced by GPI-linked influenza hemagglutinin during hemifusion and flickering pore formation. *Traffic* **1** 622-630.
- Fujiki, Y., A. L. Hubbard, S. Fowler, and P. B. Lazarow. 1982. Isolation of intracellular membranes by means of sodium carbonate treatment: application to endoplasmic reticulum. *J. Cell Biol.* **93** 97-108.
- Galbiati, F. B. Razani, and M. P. Lisanti. 2001. Emerging themes in lipid rafts and caveolae. *Cell* **106** 403-411.
- Gallina, A. and G. Milanesi. 1993. Trans-membrane translocation of a myristylated protein amino terminus. *Biochem. Biophys. Res. Comm.* **195** 637-642.
- Gard, G. and R. W. Compans. 1970. Structure and cytopathic effects of Nelson Bay virus. *J. Virol.* **6** 100-106.

Garoff, H., A. M. Frischau, K. Simons, H. Lehrach, and H. Delius. 1980. Nucleotide sequence of cDNA coding for Semliki Forest virus membrane glycoproteins. *Nature* **288** 2362-2341.

Garry, R. F. and S. Dash. 2003. Proteomics computational analyses suggest that hepatitis C virus E1 and pestivirus E2 envelope glycoproteins are truncated class II fusion proteins. *Virology* **307** 255-265.

Gaudin, Y. 2000. Reversibility in fusion protein conformational changes: the intriguing case of rhabdovirus-induced membrane fusion. *Subcell. Biochem.* **34** 379-408.

Gaudin, Y., C. Tuffèreau, D. Segretain, M. Knossow, and A. Flamand. 1991. Reversible conformational changes and fusion activity of rabies virus glycoprotein. *J. Virol.* **65** 4853-4859.

Gaudin, Y., R. W. H. Ruigrok, and J. Brunner. 1995. Low-pH induced conformational changes in viral fusion proteins: implications for the fusion mechanism. *J. Gen. Virol.* **76** 1541-1556.

Gelberg, H. B., W. F. Hall, G. N. Woode, E. J. Basgall, and G. Scherba. 1990. Multinucleate enterocytes associated with experimental group A porcine rotavirus infection. *Vet. Pathol.* **27** 453-454.

Gerst, J. E. 2003. SNARE regulators: matchmakers and matchbreakers. *Biochim. Biophys. Acta* **1641** 99-110.

Ghosh, J. K. and Y. Shai. 1999. Direct evidence that the N-terminal heptad repeat of Sendai virus fusion protein participates in membrane fusion. *J. Mol. Biol.* **292** 531-546.

Ghosh, J. K., S. G. Peisajovich, and Y. Shai. 2000. Sendai virus internal fusion peptide: structural and functional characterization and a plausible mode of viral entry inhibition. *Biochemistry* **39** 11581-11592.

Gibbons, D. L., A. Ahn, P. K. Chatterjee, and M. Kielian. 2000. Formation and characterization of the trimeric form of the fusion protein of Semliki forest virus. *J. Virol.* **74** 7772-7780.

Gibbons, D. L., I. Erk, B. Reilly, J. Navaza, M. Kielian, F. A. Rey, and J. Lepault. 2003. Visualization of the target-membrane-inserted fusion protein of Semliki Forest Virus by combines electron microscopy and crystallography. *Cell* **114** 573-583.

Gilpin, B. J., F. Loechel, M. G. Mattei, E. Engvall, R. Albrechtsen, and U. M. Wewer. 1998. A novel, secreted form of human ADAM 12 (meltrin alpha) provokes myogenesis *in vivo*. *J. Biol. Chem.* **273** 157-166.

Gkantiragas, I., B. Brügger, E. Stüven, D. Kaloyanova, X.-Y. Li, K. Löhr, F. Lottspeich, F. T. Wieland, and J. B. Helms. 2001. Sphingomyelin-enriched microdomains at the Golgi complex. *Mol. Biol. Cell* **12** 1819-1833.

Goder, V. and M. Spiess. 2001. Topogenesis of membrane proteins: determinants and dynamics. *FEBS Lett.* **504** 87-93.

Gómez-Moutón, C., J. L. Abad, E. Mira, R. A. Lacalle, E. Gallardo, S. Jimenez-Baranda, I. Illa, A. Bernad, S. Manes, and C. Martínez-A. 2001. *Proc. Natl. Acad. Sci. USA* **98** 9642-9647.

Gong, S., C. Lai, and M. Esteban. 1990. Vaccinia virus induces cell fusion at acid pH and this activity is mediated by the N-terminus of the 14-kDa virus envelope protein. *Virology* **178** 81-91.

Gordon, L. M., P. W. Mobley, R. Pilpa, M. A. Sherman, and A. J. Waring. 2002. Conformational mapping of the N-terminal peptide of HIV-1 gp41 in membrane environments using ¹³C-enhanced Fourier transform infrared spectroscopy. *Biochim. Biophys. Acta* **1559** 96-120.

Gosselin, M. A., W. Guo, and R. J. Lee. 2001. Efficient gene transfer using reversibly cross-linked low molecular weight polyethylenimine. *Bioconjugate Chem.* **12** 989-994.

Gottlieb, H. E., V. Kotlyar, and A. Nudelman. 1997. NMR chemical shifts of common laboratory solvents as trace impurities. *J. Organic Chem.* **62** 7512-7515.

Grasberger, B., A. P. Minton, C. DeLisi, and H. Metzger. 1986. Interactions between proteins localized in membranes. *Proc. Natl. Acad. Sci. USA* **83** 6258-6262.

Grgacic, E. V., C. Kuhn, and H. Schaller. 2000. Hepadnavirus envelope topology: insertion of a loop region in the membrane and role of S in L protein translocation. *J. Virol.* **74** 2455-2458.

Griesinger, C., G. Otting, K. Wuthrich, and R. R. Ernst. 1988. Clean TOCSY for proton spin system identification in macromolecules. *J. Am. Chem. Soc.* **110** 7870-7872.

Gruenke, J. A., R. T. Armstrong, W. W. Newcomb, J. C. Brown, and J. M. White. 2002. New insights into the spring-loaded conformational change of influenza virus hemagglutinin. *J. Virol.* **76** 4456-4466.

Guyader, M. E. Kiyokawa, L. Abrami, P. Turelli, and D. Trono. 2002. Role for human immunodeficiency virus Type 1 membrane cholesterol in viral internalization. *J. Virol.* **76** 10356-10364.

Haag, L., H. Garoff, L. Xing, L. Hammar, S.-T. Kan, and R. H. Cheng. 2002. Acid-induced movements in the glycoprotein shell of an alphavirus turn the spikes into membrane fusion mode. *EMBO J.* **21** 4402-4410.

Hague, M. E., T. J. McIntosh, and B. R. Lentz. 2001. Influence of lipid composition on physical properties and PEG-mediated fusion of curved and uncurved model membrane vesicles: "nature's own" fusogenic lipid bilayer. *Biochemistry* **40** 4340-4348.

Hallenberger, S., V. Bosch, H. Angliker, E. Shaw, H. D. Klenk, and W. Garten. 1992. Inhibition of furin-mediated cleavage activation of HIV-1 glycoprotein gp160. *Nature* **360** 358-361.

Halwani, R., A. Khorchid, S. Cen, and L. Kleinman. 2003. Rapid localization of Gag/GagPol complexes to detergent-resistant membrane during the assembly of human immunodeficiency virus Type 1. *J. Virol.* **77** 3973-3984.

Han, X. and L. K. Tamm. 2000a. A host-guest system to study structure-function relationships of membrane fusion peptides. *Proc. Natl. Acad. Sci. USA* **97** 13097-13102.

Han, X. and L. K. Tamm. 2000b. pH-dependent self-association of influenza hemagglutinin fusion peptides in lipid bilayers. *J. Mol. Biol.* **304** 953-965.

Han, X., D. A., Steinhauer, S. A. Wharton, and L. K. Tamm. 1999. Interaction of mutant influenza virus hemagglutinin fusion peptides with lipid bilayers: probing the role of hydrophobic residue size in the central region of the fusion peptide. *Biochemistry* **38** 15052-15059.

Han, X., J. H. Bushweller, D. S. Cafiso, and L. K. Tamm. 2001. Membrane structure and fusion-triggering conformational change of the fusion domain from influenza hemagglutinin. *Nat. Struct. Biol.* **8** 715-720.

Hansen, G. H., L. Immerdal, E. Thorsen, L.-L. Niels-Christiansen, B. T. Nystrom, E. J. F. Demant, and E. M. Danielsen. 2001. Lipid rafts exist as stable cholesterol-independent microdomains in the brush border membrane of enterocytes. *J. Biol. Chem.* **276** 32338-32344.

Hao, M., S. Mukherjee, and F. R. Maxfield. 2001. Cholesterol depletion induces large scale domain segregation in living cell membranes. *Proc. Natl. Acad. Sci.* **98** 13072-13077.

Haque, M. E., T. J. McIntosh, and B. R. Lentz. 2001. Influence of lipid composition on physical properties and PEG-mediated fusion of curved and uncurved model membrane vesicles: nature's own fusogenic lipid bilayer. *Biochemistry* **40** 4340-4348.

Harder, T., P., Scheiffele, P. Verkade, and K. Simons. 1998. Lipid domain structure of the plasma membrane revealed by patching of membrane components. *J. Cell Biol.* **141** 929-942.

- Harlow, E., and D. Lane. 1988. Antibodies: a laboratory manual. Cold Spring Harbor Laboratory Press, Cold Spring Harbor, New York.
- Harman, A., H. Browne, and T. Minson. 2002. The transmembrane domain and cytoplasmic tail of herpes simplex virus type 1 glycoprotein H play a role in membrane fusion. *J. Virol.* **76** 10708-10716.
- Hedo, J. A., E. Collier, and A. Watkinson. 1987. Myristyl and palmityl acylation of the insulin receptor. *J. Biol. Chem.* **262** 954-957.
- Hegde, R. S. and V. R. Lingappa. 1999. Regulation of protein biogenesis at the endoplasmic reticulum membrane. *Trends Cell Biol.* **9** 132-137.
- von Heijne, G. and Y. Gavel. 1988. Topogenic signals in integral membrane proteins. *Eur. J. Biochem.* **174** 671-678.
- Heiman, M. G. and P. Walter. 2000. Prmlp, a pheromone-regulated multispinning membrane protein, facilitates plasma membrane fusion during yeast mating. *J. Cell Biol.* **151** 719-730.
- Heinrich, S. U., W. Mothes, J. Brunner and T. A. Rapoport. 2000. The Sec61p complex mediates the integration of a membrane protein by allowing lipid partitioning of the transmembrane domain. *Cell* **102** 233-244.
- Heinz, F. A. and S. L. Allison. 2001. The machinery for flavivirus fusion with host cell membranes. *Curr. Opin. Microbiol.* **4** 450-455.
- Helm, C. A., J. N. Israelachvili, and P. M. McGuiggan. 1989. Molecular mechanisms and forces involved in the adhesion and fusion of amphiphilic bilayers. *Science* **246** 919-922.
- Higgins, M. E., J. P. Davies, F. W. Chen, Y. A. Ioannou. 1999. Niemann-Pick C1 is a late endosome-resident protein that transiently associates with lysosomes and the trans-Golgi network. *Mol. Genet. Metab.* **68** 1-13.
- High, S. and V. Laird. 1997. Membrane protein biosynthesis – all sewn up? *Trends Cell Biol.* **7**, 206-210.
- Hirayama, E., M. Nakanishi, N. Honda, and J. Kim. 1999. Mouse C2 myoblast cells resist HVJ (Sendai virus)-mediated cell fusion in the proliferating stage but become capable of fusion after differentiation. *Differentiation* **64** 213-223.
- Hockstra, D., T. de Boer, K. Klappe, and J. Wilschut. 1984. Fluorescence method for measuring the kinetics of fusion between biological membranes. *Biochemistry* **23** 5675-5681.

- Holm, K., K. Weclawicz, R. Hewson, and M. Suomalainen. 2003. Human immunodeficiency virus Type 1 assembly and lipid rafts: Pr55^{gag} associates with membrane domains that are largely resistant to Brij 98 but sensitive to Triton X-100. *J. Virol.* **77** 4805-4817.
- Hu, C., M. Ahmed, T. J. Melia, T. H. Söllner, T. Mayer, and J. E. Rothman. 2003. Fusion of cells by flipped SNAREs. *Science* **300** 1745-1749.
- Huovila, A.-P. J., E. A. C. Almeida, and J. M. White. 1996. ADAMs and cell fusion. *Curr. Opin. Cell Biol.* **8** 692-699.
- Huppertz, B., H. G. Frank, F. Reister, J. Kingdom, H. Korr, and P. Kaufmann. 1999. Apoptosis cascade progresses during turnover of human trophoblast: analysis of villous cytotrophoblast and syncytial fragments *in vitro*. *Lab Invest.* **79** 1687-1702.
- Jahn, R. T. and T. C. Südhof. 1994. Synaptic vesicles and exocytosis. *Annu. Rev. Neurosci.* **17** 219-246.
- Jahn, R., T. Lang, and T. C. Südhof. 2003 Membrane fusion. *Cell* **112** 519-533.
- Jeener, J., B. H. Meier, P. Bachmann, and R. R. Ernst. 1979. Investigation of exchange processes by two-dimensional NMR spectroscopy. *J. Chem. Phys.* **71** 4546-4553.
- Jeetendra, E., C. S. Robinson, L. M. Albritton, and M. A. Whitt. 2002. The membrane-proximal domain of vesicular stomatitis virus G protein functions as a membrane fusion potentiator and can induce hemifusion. *J. Virol.* **76** 12300-12311.
- Joers, A., A. Kristjuhan, L. Kadaja, and T. Maimets. 1998. Tumour associated mutants of p53 can inhibit transcriptional activity of p53 without heterooligomerization. *Oncogene* **17** 2351-2358.
- Joseph, M. and R. Nagaraj. 1995. Interaction of peptide corresponding to fatty acylation sites in proteins with model membranes. *J. Biol. Chem.* **270** 16749-16755.
- Joshi, S. B., R. E. Dutch, and R. A. Lamb. 1998. A core trimer of the paramyxovirus fusion protein: parallels to influenza virus hemagglutinin and HIV gp41. *Virology* **246** 20-34.
- Jung, S. M., and M. Moroi. 1983. Cross-linking of platelet glycoprotein 1b by N-succinimidyl(4-azidophenylthio)propionate and 3,3'-dithiobis(sulfo-succinimidyl propionate). *Biochem. Biophys. Acta* **761** 152-162.
- Kaji, K., S. Oda, T. Shikano, T. Ohnuki, Y. Uematsu, J. Sakagami, N. Tada, S. Miyazaki, and A. Kudo. 2000. The gamete fusion process is defective in eggs of CD9-deficient mice. *Nat. Genet.* **24** 279-282.

- Kawamura, H., F. Shimizu, M. Maeda, and H. Tsubahara. 1965. Avian reovirus: its properties and serological classification. *Nat. Inst. Anim. Health Quart.* **5** 115-124.
- Kay, B. K., M. P. Williamson, and M. Sudol. 2000. The importance of being proline: the interaction of proline-rich motifs in signaling proteins with their cognate domains. *FASEB J.* **14**, 231-241.
- Kemble, G. W., T. Danieli, and J. M. White. 1994. Lipid-anchored influenza hemagglutinin promotes hemifusion, not complete fusion. *Cell* **76** 383-391.
- Kida, Y., M. Sakaguchi, M. Fukuda, K. Mikoshiba, and K. Mihara. 2000. Membrane topogenesis of a Type I signal-anchor protein, mouse synaptotagmin II, on the endoplasmic reticulum. *J. Cell Biol.* **150** 719-729.
- Kielian, M. 2002. Structural surprises from the flaviviruses and alphaviruses. *Mol. Cell* **9** 454-456.
- Kielian, M., P. K. Chatterjee, D. L. Gibbons, and Y. E. Lu. 2000. Specific roles for lipids in virus fusion and exit: examples from the alphaviruses. *Subcell. Biochem.* **34** 409-455.
- Killian, J. A. 1992. Gramicidin and gramicidin-lipid interactions. *Biochim. Biophys. Acta* **1113** 391-425.
- Klein, U., G. Gimpl, and F. Fahrenholz. 1995. Alteration of plasma membrane cholesterol content with beta cyclodextrin modulates the binding affinity of the oxytocin receptor. *Biochemistry* **34** 13784-13793.
- Kliger, Y., S. G. Peisajovich, R. Blumenthal, and Y. Shai. 2000. Membrane-induced conformational change during the activation of HIV-1 gp41. *J. Mol. Biol.* **301** 905-914.
- Knutton, S. and C. A. Pasternak. 1979. The mechanism of cell-cell fusion. *Trends Biochem. Sci.* **4** 220-223.
- Kobe, B., R. J. Center, B. E. Kemp and P. Pountourios. 1999. Crystal structure of human T cell leukemia virus type 1 gp21 ectodomain crystallized as a maltose-binding protein chimera reveals structural evolution of retroviral transmembrane proteins. *Proc. Natl. Acad. Sci. USA* **96** 4319-4324.
- Konishi, K. and M. Fujioka. 1987. Chemical modification of a functional arginine residue of rat liver glycine methyltransferase. *Biochemistry* **26** 8496-8502.
- Kozak, S. L., J. M. Heard, and D. Kabat. 2002. Segregation of CD4 and CXCR4 into distinct lipid microdomains in T lymphocytes suggests a mechanism for membrane destabilization by human immunodeficiency virus. *J. Virol.* **76** 1802-1815.

Kozlov, M. M. and V. S. Markin. 1983 Possible mechanism of membrane fusion. *Biofizika* **28** 242-247.

Kozlov, M. M. and L. V. Chernomordik. 1998. A mechanism of protein-mediated fusion: coupling between refolding of influenza hemagglutinin and lipid rearrangements. *Biophys. J.* **75** 1384-1396.

Kozlov, M. M., S. L. Leikin, L. V. Chernomordik, V. S. Markin, and Y. A. Chizmadzhev. 1989. Stalk mechanism of vesicle fusion. Intermixing of aqueous contents. *Eur. Biophys. J.* **17** 121-129.

Kozlovsky, Y. and M. M. Kozlov. 2002. Stalk model of membrane fusion: solution of energy crisis. *Biophys. J.* **82** 882-895.

Kuhn, R. J., W. Zhang, M. G. Rossmann, S. V. Pletnev, J. Corver, E. Lenches, C. T. Jones, S. Mukhopadhyay, P. R. Chipman, E. G. Strauss, T. S. Baker, and J. H. Strauss. 2002. Structure of Dengue virus: implications for flavivirus organization, maturation, and fusion. *Cell* **108** 717-725.

Kunimoto, M., K. Shibata, and T. Miura. 1989. Comparison of the cytoskeleton fractions of rat red blood cells prepared with nonionic detergents. *J. Biochem.* **105** 190-195.

Kuntz-Simon, G., G. Le Gall-Reculé, C. de Boissésou, and V. Jestin. 2002. Muscovy duck reovirus σ C protein is atypically encoded by the smallest genome segment. *J. Gen. Virol.* **83** 1189-1200.

Kuszewski, J., M. Nilges, and A. T. Brunger. 1992. Sampling and Efficiency of Metric Matrix Distance Geometry - A Novel Partial Metrization Algorithm. *J. Biomol. NMR* **2** 33-56.

Lamb, R. A., S. L. Zebedee, C. D. Richardson. 1985. Influenza virus M2 protein is an integral membrane protein expressed on the infected-cell surface. *Cell* **40** 627-733.

Lamirande, E. W., D. K. Nichols, J. W. Owens, J. M. Gaskin, and E. R. Jacobson. 1999. Isolation and experimental transmission of a reovirus pathogenic in ratsnakes (*Elaphe* species). *Virus Res.* **63** 135-141.

Lang, D. M., S. Lommel, M. Jung, R. Ankerhold, B. Petrusch, U. Laessing, M. F. Wiechers, H. Plattner, and C. A. Stuermer. 1998. Identification of reggie-1 and reggie-2 as plasmamembrane-associated proteins which co-cluster with activated GPI-anchored cell adhesion molecules in non-caveolar micropatches in neurons. *J. Neurobiol.* **37** 502-523.

Lapidot, M., O. Nussbaum, and A. Loyter. 1987. Fusion of membrane vesicles bearing only the influenza hemagglutinin with erythrocytes, living cultured cells, and liposomes. *J. Biol. Chem.* **262** 13736-13741.

- Lee, A., D. W. Frank, M. S. Marks, and M. A. Lemmon. 1999. Dominant-negative inhibition of receptor-mediated endocytosis by a dynamin-1 mutant with a defective pleckstrin homology domain. *Curr. Biol.* **9** 261-264.
- Lee, J.-K. and B. R. Lentz. 1997a. Evolution of lipidic structures during model membrane fusion and the relation of this process to cell membrane fusion. *Biochemistry* **36** 6251-6259.
- Lee, J.-K. and B. R. Lentz. 1997b. Outer leaflet-packing defects promote poly(ethylene glycol)-mediated fusion of large unilamellar vesicles. *Biochemistry* **36** 421-431.
- Lee, J.-K. and B. R. Lentz. 1998. Secretory and viral fusion may share mechanistic events with fusion between curved lipid bilayers. *Proc. Natl. Acad. Sci. USA* **95** 9274-9279.
- Leikina, E. and L. V. Chernomordik. 2000. Reversible merger of membranes at the early stage of influenza hemagglutinin-mediated fusion. *Mol. Biol. Cell* **11** 2359-2371.
- Leikina, E., D. L. LeDuc, J. C. Macosko, R. Epand, Y. K. Shin, and L. V. Chernomordik. 2001. The 1-127 HA2 construct of influenza virus hemagglutinin induces cell-cell hemifusion. *Biochemistry* **40** 8378-8386.
- Lemmon, M. A., J. M. Flanagan, J. F. Hunt, B. D. Adair, B.-J. Bormann, C. E. Dempsey, and D. M. Engelman. 1992. Glycophorin A dimerization is driven by specific interactions between transmembrane α -helices. *J. Biol. Chem.* **267** 7683-7689.
- Lentz, B. R. and J.-K. Lee. 1999. Poly(ethylene glycol) (PEG)-mediated fusion between pure lipid bilayers: a mechanism in common with viral fusion and secretory vesicle release? *Mol. Membr. Biol.* **16** 279-296.
- Lentz, B. R., G. F. McIntyre, D. J. Parks, J. C. Yates, and D. Massenburg. 1992. Bilayer curvature and certain amphipaths promote poly(ethylene glycol)-induced fusion of dipalmitoylphosphatidylcholine unilamellar vesicles. *Biochemistry* **31** 2643-2653.
- Lescar, J., A. Roussel, M. W. Wien, J. Navaza, S. D. Fuller, G. Wengler, G. Wengler, and F. A. Rey. 2001. The fusion glycoprotein shell of Semliki Forest virus: an icosahedral assembly primed for fusogenic activation at endosomal pH. *Cell* **105** 137-148.
- Li, Y., X. Han, and L. K. Tamm. 2003. Thermodynamics of fusion peptide-membrane interactions. *Biochemistry* **42** 7245-7251.
- Lindwasser, O. W. and M. D. Resh. 2001. Multimerization of human immunodeficiency virus Type 1 Gag promotes its localization to barges, raft-like membrane microdomains. *J. Virol.* **75** 7913-7924.

- Löffler-Mary, H., M. Werr, and R. Prange. 1997. Sequence-specific repression of cotranslational translocation of the hepatitis B virus envelope proteins coincides with the binding of heat shock protein Hsc70. *Virology* **18** 144-152.
- Lorenz, I. C., S. L. Allison, F. X. Heinz, and A. Helenius. 2002. Folding and dimerization of Tick-borne encephalitis virus envelope proteins prM and E in the endoplasmic reticulum. *J. Virol.* **76** 5480-5491.
- Lu, X., Y. Xiong, and J. Silver. 2002. Asymmetric requirement for cholesterol in receptor-bearing but not envelope-bearing membranes for fusion mediated by ecotropic murine leukemia virus. *J. Virol.* **76** 6701-6907.
- Lüneberg, J., I. Martin, F. Nussler, J. M. Ruysschaert, and A. Herrmann. 1995. Structure and topology of the influenza virus fusion peptide in lipid bilayers. *J. Biol. Chem.* **270** 27606-27614.
- Lyden, T. W., A. K. Ng, and N. S. Rote. 1993. Modulation of phosphatidylserine epitope expression by BeWo cells during forskolin treatment. *Placenta* **14** 177-186.
- MacKenzi, K. R., J. H. Prestegard, and D. M. Engelman. 1997. A transmembrane helix dimer: structure and implication. *Science* **276** 131-133.
- Madore, N., K. L. Smith, C. H. Graham, A. Jen, K. Brady, S. Hall, and R. Morris. 1999. Functionally different GPI proteins are organized into different microdomains on the neuronal surface. *EMBO J.* **18** 6917-6926.
- Malashkevich, V. N., D. C. Chan, C. T. Chutkowski, and P. S. Kim. 1998. Crystal structure of the simian immunodeficiency virus (SIV) gp41 core: conserved helical interactions underlie the broad inhibitory activity of gp41 peptides. *Proc. Natl. Acad. Sci. USA* **95** 9134-9139.
- Malashkevich, V. N., B. J. Schneider, M. L. McNally, M. A. Milhollen, J. X. Pang, and P. S. Kim. 1999. Core structure of the envelope glycoprotein GP2 from Ebola virus at 1.9-Å resolution. *Proc. Natl. Acad. Sci. USA* **96** 2662-2667.
- Malashkevich, V. N., M. Singh, and P. S. Kim. 2001. The trimer-of-hairpins motif in membrane fusion: Visna virus. *Proc. Natl. Acad. Sci. USA* **98** 8502-8506.
- Mañes, S., G. del Real, R. A. Lacalle, P. Lucas, C. Gómez-Moutón, S. Sánchez-Palomino, R. Delgado, J. Alcamí, E. Mira, and C. Martínez-A. 2000. Membrane raft microdomain assemblies required for HIV-1 infection. *EMBO Rep.* **1** 190-196.
- Manie, S. N., S. Debreyne, S. Vincent, and D. Gerlier. 2000. Measles virus structural components are enriched into lipid raft microdomains: a potential cellular location for virus assembly. *J. Virol.* **74** 305-311.

- Mao, Q., B. J. Foster, H. Xia, B. L. Davidson. 2003. Membrane topology of CLN3, the protein underlying Batten disease. *FEBS Lett.* **541** 40-46.
- Markovic, I., H. Pulyaeva, A. Sokoloff, and L. V. Chernomordik. 1998. Membrane fusion mediated by baculovirus gp64 involves assembly of stable gp64 trimers into multiprotein aggregates. *J. Cell Biol.* **143** 1155-1166.
- Markovic, I., E. Leikina, M. Zhukovsky, J. Zimmerberg, and L. V. Chernomordik. 2001. Synchronized activation and refolding of influenza hemagglutinin in multimeric fusion machines. *J. Cell Biol.* **155** 833-843.
- Martin, I., F. Defrise-Quertain, E. Decroly, M. Vandenbranden, R. Brasseur, and J.-M. Ruyschaert. 1993. Orientation and structure of the NH2-terminal HIV-1 gp41 peptide in fused and aggregated liposomes. *Biochim. Biophys. Acta* **1145** 124-133.
- Martin, I., H. Schaal, A. Scheid, and J.-M. Ruyschaert. 1996. Lipid membrane fusion induced by the human immunodeficiency virus type 1 gp41 N-terminal extremity is determined by its orientation in the lipid bilayer. *J. Virol.* **70** 298-304.
- Martin, I., E. Goormaghtigh, and J.-M. Ruyschaert. 2003. Attenuated total reflection IR spectroscopy as a tool to investigate the orientation and tertiary structure changes in fusion proteins. *Biochem. Biophys. Acta* **1614** 97-103.
- Massenburg, D. and B. R. Lentz. 1993. Poly(ethylene glycol)-induced fusion and rupture of dipalmitoylphosphatidylcholine large, unilamellar extruded vesicles. *Biochemistry* **32** 9172-9180.
- Mathews, C. K. and K. E. van Holde, Eds. 1996. Chapter 10: Lipids, membranes, and cellular transport. In *Biochemistry*, 2nd ed. The Benjamin/Cummings Publishing Company. Menlo Park, California, USA.
- Mayer, A. 1999. Intracellular membrane fusion: SNAREs only? *Curr. Opin. Cell Biol.* **11** 447-452.
- Mayor, S. and F. R. Maxfield. 1995. Insolubility and redistribution of GPI-anchored proteins at the cell surface after detergent treatment. *Mol. Biol. Cell* **6** 929-944.
- McCabe, J. B. and L. G. Berthiaume. 2001. N-terminal protein acylation confers localization to cholesterol, sphingolipid-enriched membranes but not to lipid rafts/caveolae. *Mol. Biol. Cell* **12** 3601-3617.
- McGinnes, L. W. and T. G. Morrison. 1986. Nucleotide sequence of the gene encoding the Newcastle disease virus fusion protein and comparisons of paramyxovirus fusion protein sequences. *Virus Res.* **5** 343-356.

- McIntosh, J. R. 2001. Electron microscopy of cells: a new beginning for a new century. *J. Cell Biol.* **153** F25-F32.
- McNew, J. A., T. Weber, F. Parlati, R. J. Johnston, T. J. Melia, T. H. Söllner, and J. E. Rothman. 2000. Close is not enough: SNARE-dependent membrane fusion requires an active mechanism that transduces force to membrane anchors. *J. Cell Biol.* **150** 105-117.
- van Meer, G. 1998. Lipids of the Golgi membrane. *Trends Cell Biol.* **8** 29-33.
- Melikyan, G. B., S. Lin, M. G. Roth, and F. S. Cohen. 1999. Amino acid sequence requirements of the transmembrane and cytoplasmic domains of influenza virus hemagglutinin for viable membrane fusion. *Mol. Biol. Cell* **10** 1821-1836.
- Melikyan, G. B., R. M. Markosyan, H. Hemmati, M. K. Delmedico, D. M. Lambert, and F. S. Cohen. 2000. Evidence that the transition of HIV-1 gp41 into a six-helix bundle, not the bundle configuration, induces membrane fusion. *J. Cell Biol.* **151** 413-423.
- Melkonian, K. A., A. G. Ostermeyer, J. Z. Chen, M. G. Roth, and D. A. Brown. 1999. Role of lipid modifications in targeting proteins to detergent-resistant membrane rafts. *J. Biol. Chem.* **274** 3910-3917.
- Mi, S., X. Lee, X. Li, G. M. Veldman, H. Finnerty, L. Racie, E. LaVallie, X.-Y. Tang, P. Edouard, S. Howes, J. C. Keith Jr., and J. M. McCoy. 2000. Syncytin is a captive retroviral envelope protein involved in human placental morphogenesis. *Nature* **403** 785-789.
- Milhiet, P. E., C. Domec, M.-C. Giocondi, N. V. Mau, F. Heitz, and C. Le Grimellec. 2001. Domain formation in models of the renal brush border membrane outer leaflet. *Biophys. J.* **81** 547-555.
- Miyado, K., G. Yamada, S. Yamada, H. Hasuwa, Y. Nakamura, F. Ryu, K. Suzuki, K. Kosai, K. Inoue, A. Ogura, M. Okabe, and E. Mekada. 2000. Requirement of CD9 on the egg plasma membrane for fertilization. *Science* **287** 321-324.
- Möbius, W., Y. Ohno-Iwashita, E. G. van Donselaar, V. M. J. Oorschot, Y. Shimada, T. Fujimoto, H. F. G. Heijnen, H. J. Geuze, and J. W. Slot. 2002. Immunoelectron microscopic localization of cholesterol using biotinylated and non-cytolytic perfringolysin O. *J. Histochem. Cytochem.* **50** 43-55.
- Mohler, W. A., J. S. Simske, E. M. Williams-Masson, J. D. Hardin, and J. G. White. 1998. Dynamics and ultrastructure of developmental cell fusions in the *Caenorhabditis elegans* hypodermis. *Curr. Biol.* **8** 1087-1090.

- Mohler, W. A., G. Shemer, J. del Campo, C. Valansi, E. Opoku-Serebuoh, V. Scranton, N. Assaf, J. G. White, and B. Podbilewicz. 2002. The type 1 membrane protein EFF-1 is essential for developmental cell fusion. *Dev. Cell* **2** 355-362.
- Monsma, S. A. and G. W. Blissard. 1995. Identification of a membrane fusion domain and an oligomerization domain in the baculovirus gp64 envelope fusion protein. *J. Virol.* **69** 2583-2595.
- Moore-Hoon, M. L. and R. J. Turner. 2000. The structural unit of the secretory Na⁺-K⁺-2Cl⁻ Cotransporter (NKCC1) is a homodimer. *Biochemistry* **39** 3718-3724.
- Muggeridge, M. I. 2000. Characterization of cell-cell fusion mediated by herpes simplex virus 2 glycoproteins gB, gD, gH, and gL in transfected cells. *J. Gen. Virol.* **81** 2017-2027.
- Mulvey, M. and D. T. Brown. 1996. Assembly of the Sinbis virus spike protein complex. *Virology* **219** 125-132.
- Munoz-Barroso, I., K. Salzwedel, E. Hunter, and R. Blumenthal. 1999. Role of membrane-proximal domain in the initial stages of human immunodeficiency virus Type 1 envelope glycoprotein-mediated membrane fusion. *J. Virol.* **73** 6089-6092.
- Nadler, M. J., X. E. Hu, J. M. Cassady, R. L. Geahlen. 1994. Posttranslational acylation of the transferrin receptor in LSTRA cells with myristate, palmitate and stearate: evidence for distinct acyltransferases. *Biochim. Biophys. Acta* **1213** 100-106.
- Naim, H. Y., B. Amarneh, N. T. Ktistakis, and M. G. Roth. 1992. Effects of altering palmitoylation sites on biosynthesis and function of the influenza virus hemagglutinin. *J. Virol.* **66** 585-588.
- Nehls, S., E. L. Snapp, N. B. Cole, K. J. M. Zaal, A. K. Kenworthy, T. H. Roberts, J. Ellenberg, J. F. Presley, E. Siggia, and J. Lippincott-Schwartz. 2000. Dynamics and retention of misfolded proteins in native ER membranes. *Nat. Cell Biol.* **2** 288-295.
- Neumann G., H. Feldmann, S. Watanabe, I. Lukashevich, and Y. Kawaoka. 2002. Reverse genetics demonstrates that proteolytic processing of the Ebola virus glycoprotein is not essential for replication in cell culture. *J. Virol.* **76** 406-410.
- Ng, D. T. W., R. E. Randall, and R. A. Lamb. 1989. Intracellular maturation and transport of the simian virus 5 type II glycoprotein hemagglutinin-neuraminidase: specific and transient association with GRP-78-BiP in the endoplasmic reticulum and extensive internalization from the cell surface. *J. Cell Biol.* **109** 3273-3289.
- Ng, D. T. W., S. W. Hiebert, and R. A. Lamb. 1990. Different roles of individual N-linked oligosaccharide chains in folding, assembly, and transport of simian virus 5 hemagglutinin-neuraminidase. *Mol. Cell. Biol.* **10** 1989-2001.

- Nguyen, D. H. and J. E. K. Hildreth. 2000. Evidence for budding of human immunodeficiency virus Type 1 selectively from glycolipid-enriched membrane lipid rafts. *J. Virol.* **74** 3264-3272.
- Nibert, M. L. and L. Schiff. 2001. Reoviruses and their replication. *In* Fundamental Virology. (D. M. Knipe and P. M. Howley, Eds.) 4th ed. Lippincott Williams and Wilkins, Philadelphia, Pennsylvania, USA.
- Nieva, J. L. and A. Agirre. 2003. Are fusion peptides a good model to study viral cell fusion? *Biochim. Biophys. Acta* **1614** 104-115.
- Nieva, J. L. and T. Suarez. 2000. Hydrophobic-at-interface regions in viral fusion protein ectodomains. *Biosci. Rep.* **20** 519-533.
- Nilges, M., G. M. Clore, and A. M. Gronenborn. 1988. Determination of three-dimensional structures of proteins from interproton distance data by hybrid distance geometry-dynamical simulated annealing calculations. *FEBS Lett.* **229** 317-324.
- Nilges, M., J. Kuszewski and A. T. Brunger. 1991. *Computational Aspects of the Study of Biological Macromolecules by NMR*. Plenum Press, New York.
- Oberhauser, A. F., J. R. Monck, and J. M. Fernandez. 1992. Events leading to the opening and closing of the exocytotic fusion pore have markedly different temperature dependencies. Kinetic analysis of single fusion events in patch-clamped mouse mast cells. *Biophys. J.* **61** 800-809.
- Odell, D., E. Wanas, J. Yan, and H. P. Ghosh. 1997. Influence of membrane anchoring and cytoplasmic domains on the fusogenic activity of vesicular stomatitis virus glycoprotein G. *J. Virol.* **71** 7996-8000.
- Ohki, S. 1982. A mechanism of divalent ion-induced phosphatidylserine membrane fusion. *Biochem. Biophys. Acta* **689** 1-11.
- Okamoto, T., A. Schlegel, P. E. Scherer, and M. P. Lisanti. 1998. Caveolins, a family of scaffolding proteins for organizing 'preassembled signaling complexes' at the plasma membrane. *J. Biol. Chem.* **273** 5419-5422.
- Oliferenko, S., K. Paihi, T. Harder, T. Gerke, C. Schwarzler, H. Schwarz, H. Beug, U. Gunthert, and L. A. Huber. 1999. Analysis of CD44-containing lipid rafts: Recruitment of annexin II and stabilization by the actin cytoskeleton. *J. Cell Biol.* **146** 843-854.
- Oomens, A. G., S. A. Monsma, and G. W. Blissard. 1995. The baculovirus gp64 envelope fusion protein: synthesis, oligomerization, and processing. *Virology* **209** 592-603.

Ostermeyer, A. G., B. T. Beckrich, K. A. Ivarson, K. E. Grove, and D. A. Brown. 1999. Glycosphingolipids are not essential for formation of detergent-resistant membrane rafts in melanoma cells. methyl-beta-cyclodextrin does not affect cell surface transport of a GPI-anchored protein. *J. Biol. Chem.* **274** 34459-34466.

Otteken, A., P. L. Earl., and B. Moss. 1996. Folding, assembly, and intracellular trafficking of the human immunodeficiency virus type 1 envelope glycoprotein analyzed with monoclonal antibodies recognizing maturational intermediates. *J. Virol.* **70** 3407-3415.

Pai, J. T., O. Guryev, M. S. Brown, and J. L. Goldstein. 1998. Differential stimulation of cholesterol and unsaturated fatty acid biosynthesis in cells expressing individual nuclear sterol regulatory element-binding proteins. *J. Biol. Chem.* **273** 26138-26148.

Parks, G. D. and S. Pohlmann. 1995. Structural requirements in the membrane-spanning domain of the paramyxovirus HN protein for the formation of a stable tetramer. *Virology* **213** 263-270.

Patel, J., A. H. Patel, and J. McLauchlan. 2001. The transmembrane domain of the Hepatitis C virus E2 glycoprotein is required for correct folding of the E1 glycoprotein and native complex formation. *Virology* **279** 58-68.

Pécheur, E.-I., I. Martin, A. Bienvenüe, J.-M. Ruyschaert, and D. Hoekstra. 2000. Protein-induced fusion can be modulated by target membrane lipids through a structural switch at the level of the fusion peptide. *J. Biol. Chem.* **275** 3936-3942.

Peisajovich, S. G., R. F. Epand, M. Pritsker, Y. Shai, R. M. Epand. 2000a. The polar region consecutive to the HIV fusion peptide participates in membrane fusion. *Biochemistry* **39** 1826-1833.

Peisajovich, S. G., O. Samuel, and Y. Shai. 2000b. Paramyxovirus F1 protein has two fusion peptides: implications for the mechanism of membrane fusion. *J. Mol. Biol.* **296** 1353-1365.

Peisajovich, S. G. and Y. Shai. 2003. Viral fusion proteins: multiple regions contribute to membrane fusion. *Biochim. Biophys. Acta* **1614** 122-129.

Peitzsch, R. M. and S. McLaughlin. 1993. Binding of acylated peptides and fatty acids to phospholipid vesicles: pertinence to myristoylated proteins. *Biochemistry* **32** 10436-10443.

Pelham, H. R. B. 1991. Multiple targets for Brefeldin A. *Cell* **67** 449-451.

Pertel, P. E., A. Fridberg, M. L. Parish, and P. G. Spear. 2001. Cell fusion induced by herpes simplex virus glycoproteins gB, gD, and gH-gL requires a gD receptor but not necessarily heparan sulfate. *Virology* **279** 313-324.

- Peters, C., M. J. Bayer, S. Bühler, J. S. Andersen, M. Mann, and A. Mayer. 2001. *Trans*-complex formation by proteolipid channels in the terminal phase of membrane fusion. *Nature* **409** 581-588.
- Pierini, L. M. and F. R. Maxfield. 2001. Flotillas of lipid rafts fore and aft. *Proc. Natl. Acad. Sci. USA* **98** 9471-9473.
- Piotto, M., V. Saudek, and V. Sklenar. 1992. Gradient-Tailored Excitation for Single-Quantum Nmr-Spectroscopy of Aqueous-Solutions. *J. Biomol. NMR* **2** 661-665.
- Pique, C., C. Lagaudrière-Gesbert, L. Delamarre, A. R. Rosenberg, H. Conjeaud and M.-C. Dokhélart. 2000. Interaction of CD82 tetraspanin proteins with HTLV-1 envelope glycoproteins inhibits cell-to-cell fusion and virus transmission. *Virology* **276** 455-465.
- Pletnev, S. V., W. Zhang, S. Mukhopadhyay, B. R. Fisher, R. Hernandez, D. T. Brown, T. S. Baker, M. G. Rossmann, and R. J. Kuhn. 2001. Locations of carbohydrate sites on alphavirus glycoproteins show that E1 forms an icosahedral scaffold. *Cell* **105** 127-136.
- Poggioli, G. J., T. S. Dermody, and K. L. Tyler. 2001. Reovirus-induced signals-dependent G(2)/M phase cell cycle arrest is associated with inhibition of p34(cdc2). *J. Virol.* **75** 7429-7434.
- Pötgens, A. J. G., U. Schmitz, P. Bose, A. Versmold, P. Kaufmann, and H.-G. Frank. 2003. Mechanisms of syncytial fusion: a review. *Placenta* **23A** S107-S113.
- Prange, R., M. Werr, and H. Löffler-Mary. 1999. Chaperones involved in hepatitis B virus morphogenesis. *Biol. Chem.* **380** 305-314.
- Puri, A., F. P. Booy, R. W. Doms, J. M. White, and R. Blumenthal. 1990. Conformational changes and fusion activity of influenza virus hemagglutinin of the H2 and H3 subtypes: effects of acid pretreatment. *J. Virol.* **64** 3824-3832.
- Qiao, H., R. T. Armstrong, G. B. Melikyan, F. S. Cohen, and J. M. White. 1999. A specific point mutant at position 1 of the influenza hemagglutinin fusion peptide displays a hemifusion phenotype. *Mol. Biol. Cell* **10** 2759-2769.
- Ragheb, J. A. and W. F. Anderson. 1994. Uncoupled expression of Moloney murine leukemia virus envelope polypeptides SU and TM: a functional analysis of the role of TM domains in viral entry. *J. Virol.* **68** 3207-3219.
- Rand, R. P. 1981. Interacting phospholipid bilayers: measured forces and induced structural changes. *Annu. Rev. Biophys. Bioeng.* **10** 277-314.

- Rand, R. P. and V. A. Parsegian. 1984. Physical force considerations in model and biological membranes. *Can. J. Biochem. Cell Biol.* **62** 752-759.
- Randazzo, P. A., T. Terui, S. Sturch, H. M. Fales, A. G. Ferrige, and R. A. Kahn. 1995. The myristoylated amino terminus of ADP-ribosylation factor is a phospholipid- and GTP-sensitive switch. *J. Biol. Chem.* **270** 14809-14815.
- Reiersen, H. and A. R. Rees. 2001. The hunchback and its neighbors: proline as an environmental modulator. *Trends Biochem. Sci.* **26** 679-684.
- Remeta, D. P., M. Krumbiegel, C. A. S. A. Minetti, A. Puri, A. Ginsburg, and R. Blumenthal. 2002. Acid-induced changes in thermal stability and fusion activity of influenza hemagglutinin. *Biochemistry* **41** 2044-2054.
- Resh, M. D. 1999. Fatty acid acylation: new insights into membrane targeting of myristoylated and palmitoylated proteins. *Biochim. Biophys. Acta* **1451** 1-16.
- Rey, F. A., F. X. Heinz, C. Mandl, C. Kunz, and S. C. Harrison. 1995. The enveloped glycoprotein from tick-borne encephalitis virus at 2 Å resolution. *Nature* **375** 291-298.
- Rietveld, A. and K. Simons. 1998. Differential miscibility of lipids as the basis for the formation of functional membrane rafts. *Biochim. Biophys. Acta* **1376** 467-479.
- Rigaud, J. L., B. Pitard, and D. Levy. 1995. Reconstitution of membrane proteins into liposomes: application to energy-transducing membrane proteins. *Biochim. Biophys. Acta* **1231** 223-246.
- Rigaud, J. L., M. T. Paternostre, and A. Bluzat. 1988. Mechanisms of membrane protein insertion into liposomes during reconstitution procedures involving the use of detergents. 2. Incorporation of the light-driven proton pump bacteriorhodopsin. *Biochemistry* **27** 2677-2688.
- Robbins, S. M., N. A. Quintrell, and J. M. Bishop. 1995. Myristoylation and differential palmitoylation of *HCK* protein-tyrosine kinases govern their attachment to membranes and association with caveolae. *Mol. Cell. Biol.* **15** 3507-3515.
- Roberts, G. C. K., Ed. 1993. *NMR of Macromolecules: A Practical Approach* Oxford University Press, Oxford.
- Roche, S. and Y. Gaudin. 2002. Characterization of the equilibrium between the native and fusion-inactive conformation of rabies virus glycoprotein indicates that the fusion complex is made of several trimers. *Virology* **297** 128-135.
- Rodal, S. K., G. Skretting, O. Garred, F. Vilhardt, B. van Deurs, and K. Sandvig. 1999. Extraction of cholesterol with methyl-beta-cyclodextrin perturbs formation of clathrin-coated endocytic vesicles. *Mol. Biol. Cell* **10** 961-974.

Rodgers, W. 2002. Making membranes green: construction and characterization of GFP-fusion proteins targeted to discrete plasma membrane domains. *Biotechniques* **32** 1044-1051.

Rodriguez, D., J. R. Rodriguez, and M. Esteban. 1993. The vaccinia virus 14-kilodalton fusion protein forms a stable complex with the processed protein encoded by the vaccinia virus A17L gene. *J. Virol.* **67** 3435-3440.

Rodriguez-Crespo, I., J. Gomez-Gutierrez, J. A. Encinar, J. M. Gonzalez-Rose, J. P. Albar, D. L. Peterson, and F. Gavilanes. 1996. Structural properties of the putative fusion peptide of hepatitis B virus upon interaction with phospholipids. *Eur. J. Biochem.* **242** 243-248.

Roos, D. S. and P. W. Choppin. 1985. Biochemical studies on cell fusion. II. Control of fusion response by lipid alteration. *J. Cell Biol.* **101** 1591-1598.

Röper, K., D. Corbeil, and W. B. Huttner. 2000. Retention of prominin in microvilli reveals distinct cholesterol-based lipid microdomains in the apical plasma membrane. *Nat. Cell Biol.* **2** 582-592.

Rösch, K., D. Naeher, V. Liard, V. Goder, and M. Spiess. 2000. The topogenic contribution of uncharged amino acids on signal sequence orientation in the endoplasmic reticulum. *J. Biol. Chem.* **275** 14916-14922.

Rosenberg, A. R., L. Delamarre, C. Pique, I. LeBlanc, G. Griffith, and M.-C. Dokh  lar. 1999. Early assembly step of a retroviral envelope glycoprotein: analysis using a dominant negative assay. *J. Cell Biol.* **145** 57-68.

Rousso, I., M. B. Mixon, B. K. Chen, and P. S. Kim. 2000. Palmitoylation of the HIV-1 enveloped glycoprotein is critical for viral infectivity. *Proc. Natl. Acad. Sci. USA* **97** 13523-13525.

Ruigrok, R. W., S. R. Martin, S. A. Wharton, J. J. Skehel, P. M. Bayley, and D. C. Wiley. 1986. Conformational changes in the hemagglutinin of influenza virus which accompany heat-induced fusion of virus with liposomes. *Virology* **155** 484-497.

Russell, C. J., T. S. Jardetzky, and R. A. Lamb. 2001. Membrane fusion machines of paramyxoviruses: capture of intermediates of fusion. *EMBO J.* **20** 4024-4040.

Salzwedel, K., P. B. Johnston, S. J. Roberts, J. W. Dubay, and E. Hunter. 1993. Expression and characterization of glycopospholipid-anchored human immunodeficiency virus type 1 envelope glycoproteins. *J. Virol.* **67** 5279-5288.

Salzwedel, K., West JT, Hunter E. 1999. A conserved tryptophan-rich motif in the membrane-proximal region of the human immunodeficiency virus type 1 gp41

ectodomain is important for Env-mediated fusion and virus infectivity. *J. Virol.* **73** 2469-2480.

Samuel, O. and Y. Shai. 2001. Participation of two fusion peptides in measles virus-induced membrane fusion: emerging similarity with other paramyxoviruses. *Biochemistry* **40** 1340-1349.

Saouaf, S. J., A. Wolven, M. D. Resh, and J. B. Bolen. 1997. Palmitoylation of Src family tyrosine kinases regulates functional interaction with a B-cell substrate. *Biochem. Biophys. Res. Comm.* **234** 325-329.

Sapin, C., O. Colard, O. Delmas, C. Tessier, M. Breton, V. Enouf, S. Chwetzoff, J. Ouanich, J. Cohen, C. Wolf, and G. Trugnan. 2002. Rafts promote assembly and atypical targeting of a nonenveloped virus, rotavirus, in Caco-2 cells. *J. Virol.* **76** 4591-4602.

Sato, T., M. Sakaguchi, K. Mihara, and T. Omura. 1990. The amino-terminal structures that determine topological orientation of cytochrome P-450 in microsomal membrane. *EMBO J.* **9** 2391-2397.

Scheiffele, P., M. G. Roth, and K. Simons. 1997. Interaction of influenza virus haemagglutinin with sphingolipid-cholesterol membrane domains via its transmembrane domain. *EMBO J.* **16** 5501-5508.

Schlöndorff, J. and C. P. Blobel. 1999. Metalloprotease-disintegrins: modular proteins capable of promoting cell-cell interactions and triggering signals by protein-ectodomain shedding. *J. Cell Sci.* **112** 3603-3617.

Schmid, E., A. Zurbriggen, U. Gassen, B. Rima, V. ter Meulen, and J. Schneider-Schaulies. 2000. Antibodies to CD9, a tetraspan transmembrane protein, inhibit canine distemper virus-induced cell-cell fusion but not virus-cell fusion. *J. Virol.* **74** 7554-7561.

Schroeder, R. J., S. N. Ahmed, Y. Zhu, E. London, and D. A. Brown. 1998. Cholesterol and sphingolipid enhance the Triton X-100 insolubility of glycosylphosphatidylinositol-anchored proteins by promoting the formation of detergent-insoluble ordered membrane domains. *J. Biol. Chem.* **273** 1150-1157.

Schroth-Diez, B., K. Ludwig, B. Baljinnyam, C. Kozerski, Q. Huang, and A. Herrmann. 2000. The role of the transmembrane domain and of the intraviral domain of glycoproteins in membrane fusion of enveloped viruses. *Biosci. Rep.* **20** 571-595.

Schuck, S., M. Honsho, K. Ekroos, A. Shevchenko, and K. Simons. 2003. Resistance of cell membranes to different detergents. *Proc. Natl. Acad. Sci. USA* **100** 5795-5800.

Seif, I., P. Coulon, P. E. Rollin, and A. Flamand. 1985. Rabies virulence: effect on pathogenicity and sequence characterization of rabies virus mutations affecting antigenic site III of the glycoprotein. *J. Virol.* **53** 926-934.

Senkevich, T. G., C. L. White, E. V. Koonin, and B. Moss. 2000. A viral member of the ERV1/ALR protein family participates in a cytoplasmic pathway of disulfide bond formation. *Proc. Natl. Acad. Sci. USA* **97** 12068-12073.

Shemer, G. and B. Podbilewicz. 2003. The story of cell fusion: big lessons from little worms. *BioEssays* **25** 672-682.

Shmulevitz, M. and R. Duncan. 2000. A new class of fusion-associated small transmembrane (FAST) proteins encoded by the non-enveloped fusogenic reoviruses. *EMBO J.* **19** 902-912.

Shmulevitz, M., R. F. Epand, R. M. Epand, and R. Duncan. 2003a. Structural and functional properties of an unusual internal fusion peptide in a nonenveloped virus membrane fusion protein. *Submitted*.

Shmulevitz, M. J. Salsman, and R. Duncan. 2003b. Palmitoylation, membrane-proximal basic residues, and transmembrane glycine residues in the reovirus p10 protein are essential for syncytium formation. *J. Virol.* **77** 9769-9779.

Shmulevitz, M., J. A. Corcoran, J. Salsman, and R. Duncan. The ER-associated degradation pathway restricts the kinetics of cell-cell fusion induced by a nonenveloped virus membrane fusion protein. *Manuscript in preparation*.

Shome, S. G., and M. Kielian. 2001. Differential roles of two conserved glycine residues in the fusion peptide of Semliki forest virus. *Virology* **279** 146-160.

Siegel, D. P. 1993. Energetics of intermediates in membrane fusion: comparison of stalk and inverted micellar intermediate mechanisms. *Biophys. J.* **65** 2124-40.

Siegel, D. P. 1999. The modified stalk mechanism of lamellar/inverted phase transitions and its implications for membrane fusion. *Biophys. J.* **76** 291-313.

Siegel, D. P. and R. M. Epand. 1997. The mechanism of lamellar-to-inverted hexagonal phase transitions in phosphatidylethanolamine: implications for membrane fusion mechanisms. *Biophys. J.* **73** 3089-3111.

Siegel, D. P. and R. M. Epand. 2000. Effect of influenza hemagglutinin fusion peptide on lamellar/inverted phase transitions in dipalmitoleoylphosphatidylethanolamine: implications for membrane fusion mechanisms. *Biochim. Biophys. Acta* **1468** 87-98.

Simons, K. and E. Ikonen. 1997. Functional rafts in cell membranes. *Nature* **387** 569-572.

Singer, I. I., S. Scott, D. W. Kawka, J. Chin, B. L. Daugherty, J. A. DeMartino, J. DiSalvo, S. L. Gould, J. E. Lineberger, L. Malkowitz, M. D. Miller, L. Mitnaul, S. J.

- Siciliano, M. J. Staruch, H. R. Williams, H. J. Zweerink, and M. S. Springer. 2001. CCR5, CXCR4, and CD4 are clustered and closely apposed on microvilli of human macrophages and T cells. *J. Virol.* **75** 3779-3790.
- Skehel, J. J. and D. C. Wiley. 1998. Coiled coils in both intracellular vesicle and viral membrane fusion. *Cell* **95** 871-874.
- Skehel, J. J., P. M. Bayley, E. B. Brown, S. R. Martin, M. D. Waterfield, J. M. White, I. A. Wilson, and D. C. Wiley. 1982. Changes in the conformation of influenza virus hemagglutinin at the pH optimum of virus-mediated membrane fusion. *Proc. Natl. Acad. Sci. USA* **79** 968-792.
- Skehel, J. J., K. Cross, D. Steinhauer, and D. C. Wiley. 2001. Influenza fusion peptides. *Biochem. Soc. Trans.* **29** 623-626.
- Smit, J. M., R. Bittman, and J. Wilschut. 1999. Low-pH-dependent fusion of Sinbis virus with receptor-free cholesterol-and sphingolipid-containing liposomes. *J. Virol.* **73** 8476-8484.
- Smit, J. M., W. B. Klimstra, K. D. Ryman, R. Bittman, R. E. Johnston, and J. Wilschut. 2001. PE2 cleavage mutants of Sinbis virus: correlation between viral infectivity and pH-dependent membrane fusion activation of the spike heterodimer. *J. Virol.* **75** 11196-11204.
- Smith, D. E. and D. J. Haymet. 1993. Free energy, entropy, and internal energy of hydrophobic interactions: computer simulations. *J. Chem. Phys.* **98** 6445-6454.
- Söllner, T., M. K. Bennett, S. W. Whiteheart, R. H. Scheller, and J. E. Rothman. 1993. A protein assembly-disassembly pathway in vitro that may correspond to sequential steps of synaptic vesicle docking, activation, and fusion. *Cell* **75** 409-18.
- Sowadski, J. M., C. A. Ellis, and Madhusudan. 1996. Detergent binding to unmyristylated protein kinase A – structural implications for the role of myristate. *J. Bioenerg. Biomembr.* **28** 7-12.
- Spiess, M. 1995. Heads or tails – what determines the orientation of proteins in the membrane. *FEBS Lett.* **369** 76-79.
- Springer, T. A. 1990. Adhesion receptors of the immune system. *Nature* **346** 425-434.
- Sreerama, N., S. Y. Venyaminov, and R. W. Woody. 1999. Estimation of the number of alpha-helical and beta-strand segments in proteins using circular dichroism spectroscopy. *Protein Sci.* **8** 370-380.
- Stadler, K., Allison SL, Schlich J, Heinz FX. 1997. Proteolytic activation of tick-borne encephalitis virus by furin. *J. Virol.* **71** 8475-8481.

- Stiasny, K., S. L. Allison, C. W. Mandl, and F. X. Heinz. 2001. Role of metastability and acidic pH in membrane fusion by tick-borne encephalitis virus. *J. Virol.* **75** 7392-7398.
- Stegmann, T. 2000. Membrane fusion mechanisms: the influenza hemagglutinin paradigm and its implications for intracellular fusion. *Traffic* **1** 598-604.
- Stegmann, T., R. W. Doms, and A. Helenius. 1989. Protein-mediated membrane fusion. *Annu. Rev. Biophys. Chem.* **18** 187-211.
- Stevenson, F. T., S. L. Bursten, R. M. Locksley and D. H. Lovett. 1992. Myristyl acylation of the tumor necrosis factor alpha precursor on specific lysine residues. *J. Exp. Med.* **176** 1053-1062.
- Stevenson, F. T., S. L. Bursten, C. Fanton, R. M. Locksley and D. H. Lovett. 1993. The 31-kDa precursor of interleukin 1 α is myristoylated on specific lysines within the 16 kDa N-terminal propiece. *Proc. Natl. Acad. Sci. USA* **90** 7245-7249.
- Stoye, J. P. and J. M. Coffin. 2000. A provirus put to work. *Nature* **403** 715-716.
- Struck, D. K., D. Hoekstra, and R. E. Pagano. 1981. Use of resonance energy transfer to monitor membrane fusion. *Biochemistry* **20** 4093-4099.
- Stutzin, A. 1986. A fluorescence assay for monitoring and analyzing fusion of biological membrane vesicles *in vitro*. *FEBS Lett.* **197** 274-280.
- Suárez, T., W. R. Gallaher, A. Agirre, F. M. Goñi, and J. L. Nieva. 2000. Membrane interface-interacting sequence within the ectodomain of the human immunodeficiency virus type 1 envelope glycoprotein: putative role during viral fusion. *J. Virol.* **74** 8038-8047.
- Suárez, T., M. J. Gómara, F. M. Goñi, I. Mingarro, A. Muga, E. Pérez-Payá, and J. L. Nieva. 2003. Calcium-dependent conformational changes of membrane-bound Ebola fusion peptide drive vesicle fusion. *FEBS Lett.* **535** 23-28.
- Sutton, R. B., D. Fasshauer, R. Jahn, and A. T. Brunger. 1998. Crystal structure of a SNARE complex involved in synaptic exocytosis at 2.4 Å resolution. *Nature* **395** 347-353.
- Swameye, I. and H. Schaller. 1997. Dual topology of the large envelope protein of duck hepatitis B virus: determinants preventing pre-S translocation and glycosylation. *J. Virol.* **71** 9434-9441.
- Syvitski, R. T, I. Burton, R. Duncan, and D. L. Jakeman. Calculation of all E-COSY type spectra from s Single 3D NMR Experiment: Applications for Protein Structure Determination *Manuscript in preparation*.

- Tachibana, I. and M. E. Hemler. 1999. Role of transmembrane 4 superfamily (TM4SF) proteins CD9 and CD81 in muscle cell fusion and myotube maintenance. *J. Cell Biol.* **146** 893-904.
- Taguchi, F. 1993. Fusion formation by the uncleaved spike protein of murine coronavirus JHMV variant cl-2. *J. Virol.* **67** 1195-1202.
- Talbot, P., B. D. Shur and D. G. Myles. 2003. Cell adhesion and fertilization: steps in oocyte transport, sperm-zona pellucida interactions, and sperm-egg fusion. *Biol. Reprod.* **68** 1-9.
- Talbot, W. A., L. X. Zheng, and B. R. Lentz. 1997. Acyl chain unsaturation and vesicle curvature alter outer leaflet packing and promote poly(ethylene glycol)-mediated membrane fusion. *Biochemistry* **36** 5827-5836.
- Tamm, L. K. 2003. Hypothesis: spring-loaded boomerang mechanism of influenza hemagglutinin-mediated membrane fusion. *Biochim. Biophys. Acta* **1614** 14-23.
- Tan, K., J. Liu, J. Wang, S. Shen, and M. Lu. 1997. Atomic structure of a thermostable subdomain of HIV-1 gp41. *Proc. Natl. Acad. Sci. USA* **94** 12303-12308.
- Tatu, U., C. Hammond, and A. Helenius. 1995. Folding and oligomerization of influenza virus hemagglutinin in the ER and the intermediate compartment. *EMBO J.* **14** 1340-1348.
- Taylor, G. M. and D. A. Sanders. 1999. The role of the membrane-spanning domain sequence in glycoprotein-mediated membrane fusion. *Mol. Biol. Cell* **10** 2803-2815.
- Taylor, M. V. 2000. Muscle development: molecules of myoblast fusion. *Curr. Biol.* **10** 646-648.
- Theil, K. W. and C. McCloskey. 1991. Rabbit syncytium virus is a Kemerovo serogroup orbivirus. *J. Clin. Microbiol.* **29** 2059-2062.
- Theil, K. W. and L. J. Saif. 1985. *In vitro* detection of porcine rotavirus-like virus (group B rotavirus) and its antibody. *J. Clin. Microbiol.* **1** 844-846.
- Theiler R. N. and T. Compton. 2002. Distinct glycoprotein O complexes arise in a post-Golgi compartment of cytomegalovirus-infected cells. *J. Virol.* **76** 2890-2898.
- Tong, S. and R. W. Compans. 2000. Oligomerization, secretion, and biological function of an anchor-free parainfluenza virus Type 2 (PI2) fusion protein. *Virology* **270** 368-376.

- Tong, S., P. Yi, A. Martin, Q. Yao, M. Li, and R. W. Compans. 2001. Three membrane-proximal amino acids in the human parainfluenza type 2 (HPIV 2) F protein are critical for fusogenic activity. *Virology* **280** 52-61.
- Towler, D. A., S. P. Adams, S. R. Eubanks, D. S. Towery, E. Jackson-Machelski, L. Glaser, and J. I. Gordon. 1988. Myristoyl CoA:protein N-myristoyltransferase activities from rat liver and yeast possess overlapping yet distinct peptide substrate specificities. *J. Biol. Chem.* **263** 1784-1790.
- Ungermann, C., K. Sato, and W. Wickner. 1998. Defining the functions of trans-SNARE pairs. *Nature* **396** 543-548.
- Vahishtha, M., T. Phalen, M. T. Marquardt, J. S. Ryu, A. C. Ng, and M. Kielian. 1998. A single point mutation controls the cholesterol dependence of Semliki forest virus entry and exit. *J. Cell Biol.* **140** 91-99.
- Varma, R. and S. Mayor. 1998. GPI-anchored proteins are organized in submicron domains at the cell surface. *Nature* **394** 798-801.
- Vassilev, A. O., N. Plesofsky-Vig, and R. Brambl. 1995. Cytochrome c oxidase in *Neurospora crassa* contains myristic acid covalently linked to subunit 1. *Proc. Natl. Acad. Sci. USA* **92** 8680-8684.
- Vázquez, M.-I. and M. Esteban. 1999. Identification of functional domains in the 14-kilodalton envelope protein (A27L) of Vaccinia virus. *J. Virol.* **73** 9098-9109.
- Vázquez, M.-I. G. Rivas, D. Cregut, L. Serrano, and M. Esteban. 1998. The vaccinia virus 14-kilodalton (A27L) fusion protein forms a triple coiled-coil structure and interacts with the 21-kilodalton (A17L) virus membrane protein through a C-terminal alpha-helix. *J. Virol.* **72** 10126-10137.
- Veit, M., E. Kretzschmar, K. Kuroda, W. Garten, M. F. Schmidt, H. D. Klenk, and R. Rott. 1991. Site-specific mutagenesis identifies three cysteine residues in the cytoplasmic tail as acylation sites of influenza virus hemagglutinin. *J. Virol.* **65** 2491-2500.
- Viard, M., I. Parolini, M. Sargiacomo, K. Fecchi, C. Ramoni, S. Ablan, F. W. Ruscetti, J. M. Wang, and R. Blumenthal. 2002. Role of cholesterol in Human Immunodeficiency virus Type 1 envelope protein-mediated fusion with host cells. *J. Virol.* **76** 11584-11595.
- Vieler, E., W. Baumgärtner, W. Herbst, and G. Köhler. 1994. Characterization of a reovirus isolate from a rattle snake, *Crotalus viridis*, with neurological dysfunction. *Arch. Virol.* **138** 341-344.
- Volchkov, V. E., H. Feldmann, V. A. Volchkova, H. D. Klenk. 1998. Processing of the Ebola virus glycoprotein by the proprotein convertase furin. *Proc. Natl. Acad. Sci. USA* **95** 5762-5767.

- Von Andrian, U. H., S. R. Hasslen, R. D. Nelson, S. L. Erlandsen, and E. C. Butcher. 1995. A central role for microvillous receptor presentation in leukocyte adhesion under flow. *Cell* **82** 989-999.
- Vonderfecht, S. L., A. C. Huber, J. Eiden, L. C. Mader, and R. H. Yolken. 1984. Infectious diarrhea of infant rats produced by a rotavirus-like agent. *J. Virol.* **52** 94-98.
- Waarts, B.-L., R. Bittman, and J. Wilschut. 2002. Sphingolipid- and cholesterol-dependence of alphavirus membrane fusion. *J. Biol. Chem.* **277** 38141-38147.
- Wahlberg, J. M. and M. Spiess. 1997. Multiple determinants direct the orientation of signal-anchor proteins: the topogenic role of the hydrophobic signal domain. *J. Cell Biol.* **137** 555-562.
- Waters, S. I. and J. M. White. 1997. Biochemical and molecular characterization of bovine fertilin α and β (ADAM 1 and ADAM 2): a candidate sperm-egg binding/fusion complex. *Biol. Reprod.* **56** 1245-1254.
- Weber, T., B. V. Zemelman, J. A. McNew, B. Westermann, M. Gmachl, F. Parlati, T. H. Söllner, and J. E. Rothman. 1998. SNAREpins: minimal machinery for membrane fusion. *Cell* **92** 759-772.
- Weigmann, A., D. Corbeil, A. Hellwig, and W. B. Huttner. 1997. Prominin, a novel microvilli-specific polytopic membrane protein of the apical surface of epithelial cells, is targeted to plasmalemmal protrusions of non-epithelial cells. *Proc. Natl. Acad. Sci. USA* **94** 12425-12430.
- Weissenhorn, W. A. Dessen, S. C. Harrison, J. J. Skehel, and D. C. Wiley. 1997. Atomic structure of the ectodomain from HIV-1 gp41. *Nature* **387** 426-430.
- Weissenhorn W., A. Carfi, K. H. Lee, J. J. Skehel, and D. C. Wiley. 1998a. Crystal structure of the Ebola virus membrane fusion subunit, GP2, from the envelope glycoprotein ectodomain. *Mol. Cell* **2** 605-616.
- Weissenhorn W., L. J. Calder, S. A. Wharton, J. J. Skehel, D. C. Wiley. 1998b. The central structural feature of the membrane fusion protein subunit from the Ebola virus glycoprotein is a long triple-stranded coiled coil. *Proc. Natl. Acad. Sci. USA* **95** 6032-6036.
- Weissenhorn, W., A. Dessen, L. J. Calder, S. C. Harrison, J. J. Skehel, and D. C. Wiley. 1999. Structural basis for membrane fusion by enveloped viruses. *Mol. Membr. Biol.* **16** 3-9.
- Weng, Y. and C. D. Weiss. 1998. Mutational analysis of residues in the coiled-coil domain of human immunodeficiency virus type 1 transmembrane protein gp41. *J. Virol.* **72** 9676-9682.

- Wharton, S. A., J. J. Skehel, and D. C. Wiley. 2000. Temperature dependence of fusion by sendai virus. *Virology* **271** 71-78.
- Wharton, S. A., S. R. Martin, R. W. Ruigrok, J. J. Skehel, and D. C. Wiley. 1988. Membrane fusion by peptide analogues of influenza virus haemagglutinin. *J. Gen. Virol.* **69** 1847-57.
- White, J. M. 1990. Viral and cellular membrane fusion proteins. *Annu. Rev. Physiol.* **52** 675-697.
- White, J. M. 1992. Membrane fusion. *Science* **258** 917-924.
- White, J. M. and I. A. Wilson. 1987. Anti-peptide antibodies detect steps in a protein conformational change: low-pH activation of the influenza virus hemagglutinin. *J. Cell Biol.* **105** 2887-2896.
- White, J. M., J. Kartenbeck, and A. Helenius. 1982. Membrane fusion activity of influenza virus. *EMBO J.* **1** 217-222.
- Whitt, M. A., P. Zagouras, B. Crise, and J. K. Rose. 1990. A fusion-defective mutant of vesicular stomatitis virus glycoprotein. *J. Virol.* **64** 4907-4913.
- Wiemken, V., R. Theiler, and R. Bachofen. 1981. Lateral organization of proteins in the chromatophore membrane of *Rhodospirillum rubrum* studied by chemical cross-linking. *J. Bioenerg. Biomembr.* **13** 181-194.
- Wild, C. T., D. C. Shugars, T. K. Greenwell, C. B. McDanal, and T. J. Matthews. 1994. Peptides corresponding to a predictive α -helical domain of human immunodeficiency virus type 1 gp41 are potent inhibitors of virus infection. *Proc. Natl. Acad. Sci. USA* **91** 9770-9774.
- Wilk, T., T. Pfeiffer, A. Bukovsky, G. Moldenhausser, and V. Bosch. 1996. Glycoprotein incorporation and HIV-1 infectivity despite exchange of the gp160 membrane spanning domain. *Virology* **218** 269-274.
- Willett, B. J., M. J. Hosie, A. Shaw, and J. C. Neil. 1997. Inhibition of feline immunodeficiency virus infection by CD9 antibody operates after virus entry and is independent of virus tropism. *J. Gen. Virol.* **78** 611-618.
- Wiley, R. L., R. A. Rutledge, S. Dias, T. Folks, T. Theodore, C. E. Buckler, and M. A. Martin. 1986. Identification of conserved and divergent domains within the envelope gene of the acquired immunodeficiency syndrome retrovirus. *Proc. Natl. Acad. Sci. USA* **83** 5038-5042.

Williams, M. A., and R. A. Lamb. 1986. Determination of the orientation of an integral membrane protein and sites of glycosylation by oligonucleotide-directed mutagenesis: influenza B virus NB glycoprotein lacks a cleavable signal sequence and has an extracellular NH₂-terminal region. *Mol. Cell. Biol.* **6** 4317-28.

Wilson, I. A., J. J. Skehel, and D. C. Wiley. 1981. Structure of the haemagglutinin membrane glycoprotein of influenza virus at 3 Å resolution. *Nature* **289** 366-373.

Wilson, N. F. and W. J. Snell. 1998. Microvilli and cell-cell fusion during fertilization. *Trends Cell Biol.* **8** 93-96.

Wilson, N. F., M. J. Foglesong, and W. J. Snell. 1997. The *Chlamydomonas* mating type plus fertilization tubule, a prototypic cell fusion organelle: isolation, characterization, and in vitro adhesion to mating type minus gametes. *J. Cell Biol.* **137** 1537-1553.

Winton, J. R., C. N. Lannan, J. L. Fryer, R. P. Hedrick, T. R. Meyers, J. A. Plumb, and T. Yamamoto. 1987. Morphological and biochemical properties of four members of a novel group of reoviruses isolated from aquatic animals. *J. Gen. Virol.* **68** 353-364.

Wolffe, E. J., S. Vijaya, and B. Moss. 1995. A myristylated membrane protein encoded by the vaccinia virus L1R open reading frame is the target of potent neutralizing monoclonal antibodies. *Virology* **211**, 53-63.

Wong, T. C. 2003 Membrane structure of the human immunodeficiency virus gp41 fusion peptide by molecular dynamics simulation II. The glycine mutants *Biochim. Biophys. Acta* **1609** 45-54.

Wuthrich, K. 1986. *NMR of Proteins and Nucleic Acids* John Wiley and Sons, New York.

Yagami-Hiromasa, T., T. Sato, T. Kurisaki, K. Kamijo, Y. Nabeshima, and A. Fujisawa-Sehara. 1995. A metalloprotease-disintegrin participating in myoblast fusion *Nature* **377** 652-656.

Yang, J., C. M. Gabrys, and D. P. Weliky. 2001. Solid-state nuclear magnetic resonance evidence for an extended β strand conformation of the membrane-bound HIV-1 fusion peptide. *Biochemistry* **40** 8126-8137.

Yang, L. and H. W. Huang. 2002. Observation of a membrane fusion intermediate structure. *Science* **297** 1877-1879.

Yang, L. and H. W. Huang. 2003. A rhombohedral phase of lipid containing a membrane fusion intermediate structure. *Biophys. J.* **84** 1808-1817.

Yang, L., L. Ding, and H. W. Huang. 2003a. New phases of phospholipids and implications of the membrane fusion problem. *Biochemistry* **42** 6631-6635.

- Yang, R., J. Yang, and D. P. Weliky. 2003b. Synthesis, enhanced fusogenicity, and solid state NMR measurements of cross-linked HIV-1 fusion peptides. *Biochemistry* **42** 3527-3535.
- Yang, Z. N., T. C. Mueser, J. Kaufman, S. J. Stahl, P. T. Wingfield, and C. C. Hyde. 1999. The crystal structure of the SIV gp41 ectodomain at 1.47 Å resolution. *J. Struct. Biol.* **126** 131-144.
- Yao, Y., K. Ghosh, R. F. Epand, R. M. Epand, and H. P. Ghosh. 2003. Membrane fusion activity of vesicular stomatitis virus glycoprotein G is induced by low pH but not by heat or denaturant. *Virology* **310** 319-332.
- Yewdell, J. W., A. Yellin, and T. Bächli. 1988. Monoclonal antibodies localize events in folding, assembly, and intracellular transport of the influenza virus hemagglutinin glycoprotein. *Cell* **52** 843-852.
- Zacharias, D. A., J. D. Violin, A. C. Newton, and R. Y. Tsien. 2002. Partitioning of lipid-modified monomeric GFPs into membrane microdomains of live cells. *Science* **296** 913-916.
- Zagouras, P. and J. K. Rose. 1993. Dynamic equilibrium between vesicular stomatitis virus glycoprotein monomers and trimers in the Golgi and at the cell surface. *J. Virol.* **67** 7533-7538.
- Zhang, C.W., Y. Chishti, R. E. Hussey, and E. L. Reinherz. 2001. Expression, purification, and characterization of recombinant HIV gp140. The gp41 ectodomain of HIV or simian immunodeficiency virus is sufficient to maintain the retroviral envelope glycoprotein as a trimer. *J. Biol. Chem.* **276** 39577-39585.
- Zhang, L., and H. P. Ghosh. 1994. Characterization of the putative fusogenic domain in vesicular stomatitis virus glycoprotein G. *J. Virol.* **68** 2186-2193.
- Zhang, X., M. Fugère, R. Day, and M. Kielian. 2003. Furin processing and proteolytic activation of Semliki forest virus. *J. Virol.* **77** 2981-2989.
- Zhao, X., M. Singh, V. N. Malashkevich, and P. S. Kim. 2000. Structural characterization of the human respiratory syncytial virus fusion protein core. *Proc. Natl. Acad. Sci. USA* **97** 14172-14177.
- Zheng, J. D. R. Knighton, N. H. Xuong, S. S. Taylor, J. M. Sowadski, L. F. Ten Eyck. 1993. Crystal structures of the myristylated catalytic subunit of cAMP-dependent protein kinase reveal open and closed conformations. *Protein Sci.* **2** 1559-1573.

Zimmerberg, J. 2001. How can proteolipids be central players in membrane fusion. *Trends Cell Biol.* **11** 233-235.

Zimmerberg, J., S. S. Vogel, L. V Chernomordik. 1993. Mechanisms of membrane fusion. *Annu. Rev. Biophys. Biomol. Struct.* **22** 433-466.

Zimmerberg, J., R. Blumenthal, D. P. Sarkar, M. Curran, and S. J. Morris. 1994. Restricted movement of lipid and aqueous dyes through pores formed by influenza hemagglutinin during cell fusion. *J. Cell Biol.* **127** 1885-189.

Appendix A

Supplementary material for experiments performed by collaborators

Supplementary Materials and Methods

1.1 Circular Dichroism (CD)

The CD spectra were recorded using an AVIV Model 215 Circular Dichroism Spectrometer (Proterion Corp). The sample was contained in a 1-mm pathlength quartz cell that was maintained at 25°C in a thermostated cell holder. The CD data are expressed as the mean residue ellipticity. All CD runs were made with peptide dissolved in water. For samples containing lipid, the lipid was first made into a dry film from a solution of chloroform/methanol. The film was hydrated by vortexing and freeze-thawing and the lipid suspension then sonicated to clarity to make small unilamellar vesicles (SUVs). Data were analyzed with the Self Consistent Method for CD Analysis, ver. 3 (Selcon 3) (Sreerama *et al.*, 1999).

1.2 Preparation of large unilamellar vesicles (LUVs)

Lipid films were made by dissolving appropriate amounts of lipid in a mixture of chloroform:methanol (2:1 v/v), followed by solvent evaporation under nitrogen to deposit the lipid as a film on the wall of a test tube. Final traces of solvent were removed in a vacuum chamber attached to a liquid nitrogen trap, for 2-3 hours. Dried films were kept under argon gas at -30°C if not used immediately. Films were hydrated with buffer, vortexed extensively at room temperature and then subjected to five cycles of freezing and thawing. The homogeneous lipid suspensions were then further processed by 10 passes through two stacked 0.1-μm polycarbonate filters (Nucleopore Filtration Products)

in a high-pressure barrel extruder (Lipex Biomembranes), at room temperature. LUVs were kept on ice and used within a few hours of preparation. Lipid phosphorous was determined by the method of Ames *et al.* (1966).

1.3 Lipid Mixing Assay

The resonance-energy transfer assay of Struck *et al.* (1981) was used to monitor lipid mixing. For each system, two populations of LUVs were prepared, one unlabeled and one labeled with 2 mol % each of N-Rh-PE (N-[lissamine Rhodamine B sulfonyl] phosphatidylethanolamine) and N-NBD-PE (N-[7-nitro-2,1,3-benzoxadiazol-4-yl] phosphatidylethanolamine).

A 9:1 molar ratio of unlabeled to labeled liposomes was used in the assay. Fluorescence was recorded in an SLM Aminco Bowman Series II spectrofluorimeter. The excitation and emission wavelengths were set at 465 nm and 530 nm, respectively, using a 490-nm cut-off filter between the cuvette and the emission monochromator, with slits set for 8-nm bandwidths. Siliconized glass cuvettes (1-cm pathlength) were used with continuous stirring in a thermostated cuvette holder. A freshly prepared solution of the peptide in water (p14 was found to precipitate in the presence of salt) was added to 2 ml water in the cuvette containing 25, 50 or 100 μ M LUVs of DOPC:DOPE:cholesterol (1:1:1). Fluorescence was recorded for several minutes and then 20 μ l of 10% Triton X-100 was added (final concentration 0.1%) to obtain the maximum fluorescence intensity value, F_{\max} . The initial fluorescence intensity prior to addition of peptide, F_0 , was taken as zero. Percent lipid mixing at time t is given by $[(F_t - F_0)/(F_{\max} - F_0)]100$, where F_t is defined as fluorescence at time t .

1.4 Solution NMR Spectroscopy

For NMR experiments two samples were prepared, both containing 5 mg of the lyophilized acetyl-p14 peptide. One sample was dissolved in a 500 μ L solution of 90% H_2O and 10% $^2\text{H}_2\text{O}$ buffered at pH 7.2 with a 50 mM potassium phosphate solution, and the other in a 500 μ L solution of >99% $^2\text{H}_2\text{O}$ buffered at pH 7.2 with a 20 mM potassium phosphate solution.

^1H NMR data were collected on a Bruker AVANCE 500 spectrometer operating at 500 MHz. 1D reference spectra for the P14 peptide were collected in both $^1\text{H}_2\text{O}$ and $^2\text{H}_2\text{O}$ at 5°C with a recycle time of 2 seconds using a standard one-pulse sequence with saturation of the water solvent signal, or *via* a "soft 3:9:19" pulse (Piotto *et al.*, 1992) to suppress the water signal. Chemical shifts are referenced to 2,2-dimethyl-2-silapentane-5-sulfonate (DSS) through the calibrated water resonance (Gottlieb *et al.*, 1997). 500 MHz phase sensitive NOESY (Jeener *et al.*, 1979) (mixing time of 250 ms), Clean-TOCSY (Griesinger *et al.*, 1988) (spin lock of 80 ms using MLEV-17 [Bax and Davis, 1985]) and COSY (Syvitski *et al.*, manuscript in preparation) data sets were recorded over a bandwidth of 6 KHz with a recycle time of 2s, using 512 t_1 blocks of 48, 48, and effectively 64 scans, respectively. 2048 complex points were collected in t_2 . Data sets were processed using Bruker XWIN software on a Silicon Graphics workstation.

1.5 Quantification of Cholesterol Effects of Fusion

To assess the ability of M β CD (2 mM or 20 mM) to deplete membrane cholesterol using serum-free 10 % FBS or 5% complete lipoprotein-deficient (cLPDS) media, QM5 cells were loaded with [3 H]-cholesterol (5 μ Ci/ml; ICN) for 4 hours, washed 4 times with HBSS, and treated with either 0, 2 mM or 20 mM M β CD for 1 hour at 37°C. After M β CD treatment, the cell supernatant (0.5 ml) was removed, the cell monolayer was washed with PBS (0.5 ml) and the supernatant and PBS samples were pooled. The cell monolayer was then lysed in 200 μ l RIPA buffer, the volume increased to 1 ml with PBS, and both the cell lysate and the cell supernatant were counted on a Wallace Liquid Scintillation Counter (Beckman). The results were expressed as the percent of total [3 H]-cholesterol that was extracellular (cpm supernatant/[cpm supernatant + cpm cell lysate] x 100) and are the average of three independent experiments +/- the SE.

Various cholesterol-depleting agents were compared. QM5 cells were treated to deplete plasma-membrane cholesterol after p14 transfection using 2 mM M β CD in 5% cLPDS or, 24 hours prior to and throughout p14-transfection, using either Lovastatin (25 μ M; blocks *de novo* cholesterol synthesis) or U18666A (2 μ g/ml; prevents cholesterol recycling from the endosome to the plasma membrane), both in 10% FBS medium. Cells were fixed at 6-8 hours post transfection, stained with Wright-Giemsa, and assessed for fusion ability as described above. Results are the average of three experiments +/- the SE. N-BP-2 cells (CHO cells deficient in the ability to synthesize cholesterol *de novo*) were starved of exogenous cholesterol in DMEM 5% cLPDS for 48 hours prior to and throughout p14 transfection, fixed at 8-12 hours post transfection, Giemsa-stained and assessed for fusion ability. P14-mediated fusion by cholesterol-deficient cells was

compared to that observed in N-BP-2 cells that were provided with cholesterol (5% FBS).

Results are the average of three experiments \pm the SE.

1.6 Supplementary Figures and Tables

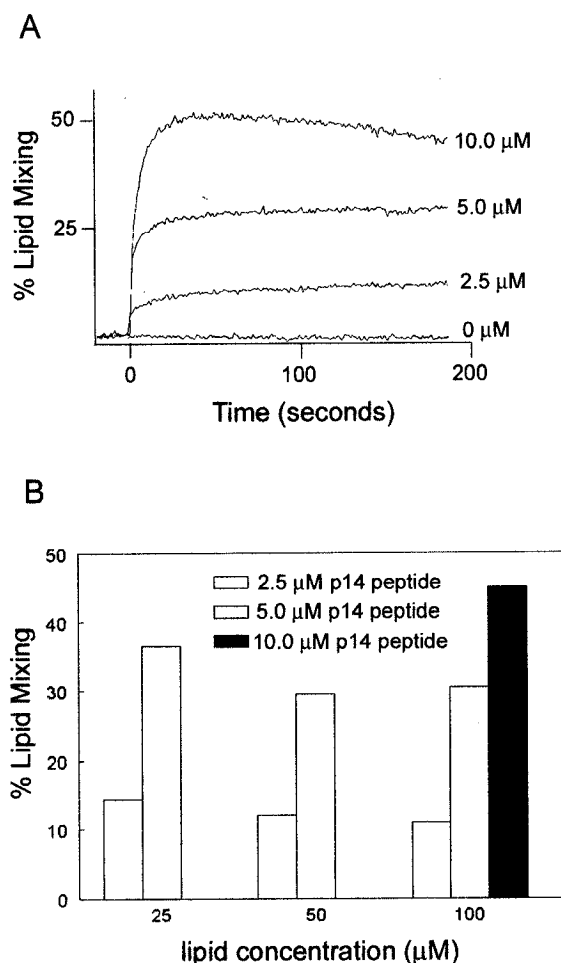


Fig 1.1 The p14 hydrophobic-patch peptide (myr-30HP) induces lipid mixing. **(A)** Various amounts of the myr-30HP peptide were added to LUVs, and lipid mixing was assayed by resonance energy transfer. Results are expressed as a percent of total lipid mixing that occurred when Triton X-100 was added to the LUVs. **(B)** The ratio of lipid:peptide was altered and the ability of the p14 peptide to induce lipid mixing was assayed. Results are expressed as a percent of total lipid mixing at 200 seconds. These experiments were performed and the figures generated by our collaborators, Drs. R. F. Epand and R. M. Epand (McMaster University).

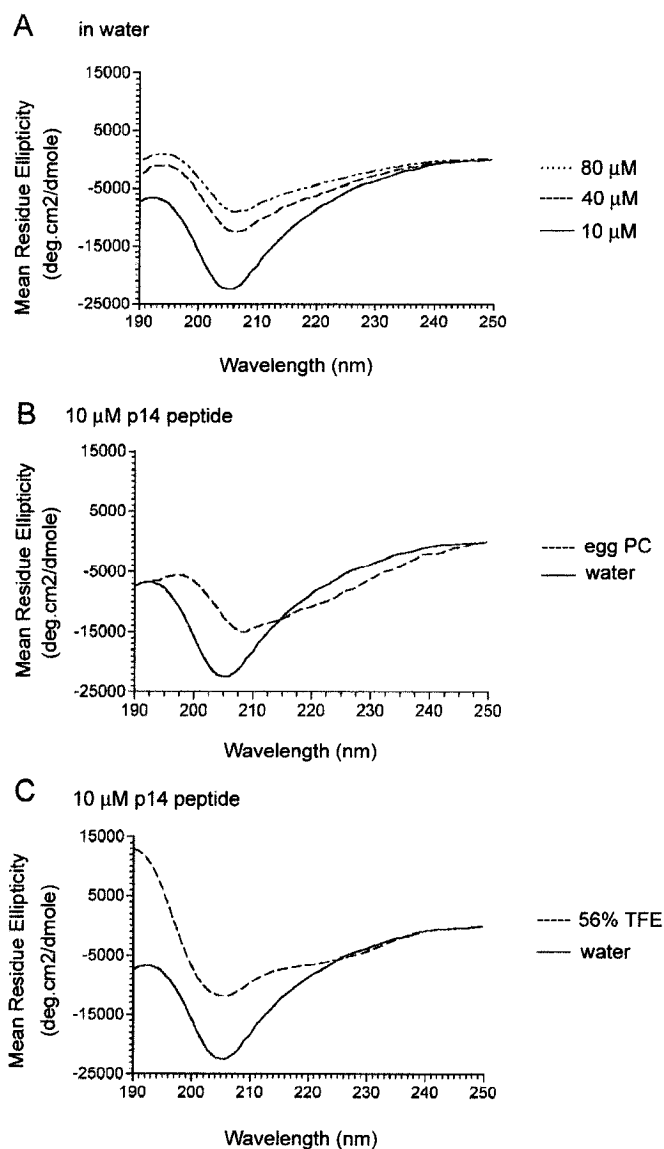


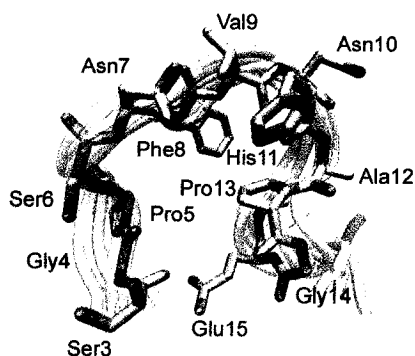
Fig 1.2 Circular dichroism of the p14 hydrophobic patch peptide. **(A)** Circular dichroism (CD) spectra of the myr-30HP peptide at varying concentrations in water. **(B)** CD spectra of the myr-30HP peptide (10 μ M) in water and in 100 μ M egg phosphatidylcholine (PC) liposomes (L/P = 10). **(C)** CD spectra of the myr-30HP peptide (10 μ M) in water and in 56 % trifluorethane (TFE). These experiments and figures were contributed by Drs. R. F. Epand and R. M. Epand (McMaster University).

Table 1.1 Summary of circular dichroism spectroscopy observations

Assay Condition	% alpha helix	% beta sheet	% turn	% random
10 μ M in water	3	5	8	84
40 μ M in water	7	40	24	29
80 μ M in water	7	37	23	33
10 μ M in egg PC	24	23	23	30
80 μ M in egg PC	22	30	24	24
10 μ M in 56% TFE	33	22	15	30

Secondary structure was estimated with the program Selcon3 by Drs. R. F. Epand and R. M. Epand (McMaster University) using data shown in Fig 1.2, Appendix A.

A Ser3- Glu15



B Gly2 - Thr31



Fig 1.3 The N-terminal portion of the p14 hydrophobic patch forms a looped structure. Solution NMR spectroscopy was performed using the acetyl-30HP peptide. The 14 retained structures are shown: **(A)** residues ser3-glu15 and **(B)** the entire acetyl-30HP peptide (residues gly2-thr31). Red = acidic, blue = basic functional groups. The solution NMR spectra was performed and this figure was generated by our collaborators, Drs. R. Syvitski and D. Jakeman (Dalhousie University).

Fig 1.4 p14-mediated fusion requires plasma-membrane cholesterol. **(A)** p14-transfected QM5 cells were pre-labeled with [^3H]-cholesterol for 4 hours and then treated with 0, 2, or 20 mM M β CD using a variety of serum conditions (serum-free, 5% complete lipoprotein deficient [cLPDS], or 10% fetal calf serum [FCS]). The proportion of [^3H]-cholesterol extracted from the cells by M β CD was quantified by scintillation counting of the cell supernatant and the cell-associated radiolabel. Results are the average of three experiments \pm the standard error. **(B)** QM5 cells were treated with 2mM methyl- β -cyclodextrin (CD) after p14 transfection and approximately 1 hour before fusion initiation. Lovastatin (25 μM) or U18666A (2 $\mu\text{g/ml}$) were added to cells 24 hours before transfection and remained throughout the experiment. Cells were fixed 6-8 hours post-transfection, Giemsa-stained, and the fusion ability of p14 was quantified by a syncytial indexing assay. The average number of nuclei present in syncytia was determined by microscopic examination of five random fields, and results are expressed as the percent of inhibition (\pm the standard error) when compared with authentic p14 fusion. Data are an average of three experiments. N-BP-2 cells (CHO cells unable to synthesize *de novo* cholesterol) were grown for 48 hours in the presence or absence of exogenous cholesterol, transfected with p14, and assessed for fusion 8-12 hours post-transfection by Giemsa-staining and a syncytial indexing assay as above. (These experiments and figures were performed and generated by J. Salsman.

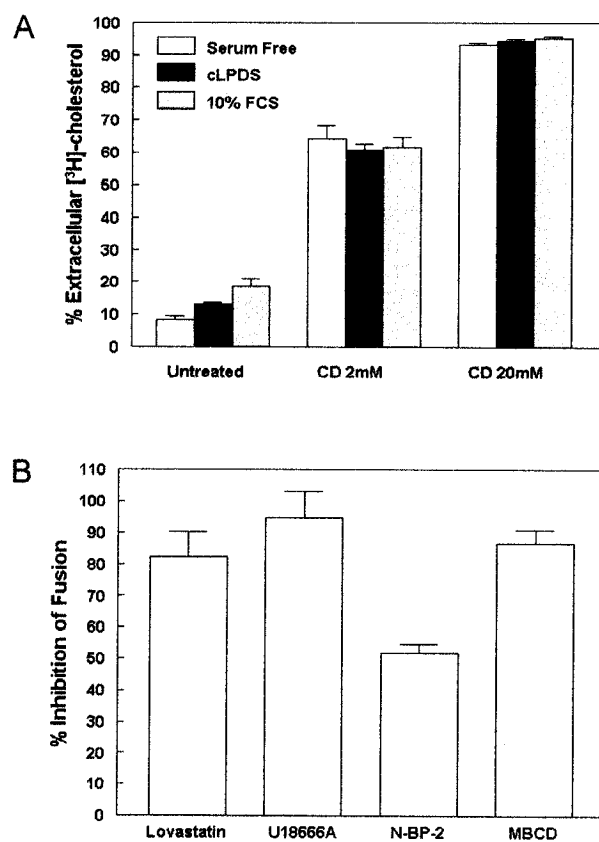


Fig 1.4 p14-mediated fusion requires plasma-membrane cholesterol.

Appendix B

Primers

Table 2.1 Primers used for Subcloning (underlined sequence binds template)

Primer	Sequence
S1FLF	5' -CCCAAGCTTACCATGGGGAGTGGACCCCTC
S1FLR	5' -AAGAATTCTCACGTCATCTGCCTAGCCCTC
p14HindIIIF	5' -CTAGATAAGCTTCCATGGGGAGTGGACCCCT
p14EcoR1R	5' -AATGAATTCTTAAATGGCTGAGACATTATCGATGTTG
σ CF	5' -CTAGATAAGCTTCCACCATGGCTCAGCCATTTAGTGATGAGC
σ CR	5' -AATGAATTCTCACGTCATCTGCCTAGCCCTC
p14SalIF	5' -CTAGATGTCGACCCACCATGGGGAGTGG ACCCTCTAATTTTCGTC
p146HisNotIR5'	TGAAGAAGCGGCCGCGTTAGTGATGGTGGTGATGGTGCTTGTCGTCGTCACAATGGCT GAGACATTATCGATGTTGACGTATGT
p14gfpHindIIIF	5' -ATGCATAAGCTTTTTTCCACCATGGGGAGTGGAC
p14gfpBamH1R	5' -ATGCATGGATCCTTAATGGCTGAGACATTATCG

Table 2.2 Primers used for Insertion and Deletion Mutagenesis (underlined sequence binds template, and the sequence of the HA epitope(s) is shown in bold)

Primer	Sequence
p14HANF	5' - CCCAAGCTTACCATGGGGAGTGGACCCCTCTAATT TACCCATACGATGTTCTGACTATGC GTTCGTCAATCACGCACCTGG
p142HANF	5' P- TATCCCTATGACGTCCCGGATTACGCAGGC TACCCATACGATGTTCTGACTATGCG
p142HANR	5' P-ATTAGAGGGTCCACTCCCCATGG
p14HACR	5' - AATGAATTCTTAC CGCATAGTCAGGAACATCGTATGGGTAAATGGCTGAGACATTATCGA TGTTG
p142HACR	5' - GCTACTGAATTCTCAT TGCGTAATCCGGGACGTCATAGGGATAGCCCGCATAGTCAGGAA CATCGTATGGGTA
p14C115R	5' -AATGAATTCTCATGTGCTATAAGGAGGAGGGGG
p14C105R	5' -AATGAATTCTCAACGACTTGGTGGCTCGTATGG
p14C88	5' -CTGGATCTCACTCAACCTGTAGC
p14C83	5' -AATGAATTCTCACCTGTAGCTATTCCGTAGATACC
p14C78	5' -TAGATACCGTTTTTGGAACTCAGTGAG
p14PFUdelf	5' -TAAGAATTCTGCAGATATCCATCACAC (for C88 and C78 only)

Table 2.3 Primers used for Site-directed Mutagenesis with altered nucleotide(s) in bold

Primer	Sequence	Template
p14G2AF	5' -CTTCCACCATGG C GAGTGGACCTC	p14 and p142HAC
p14G2AR	5' -GAGGGTCCACTC G CCATGGTGGAAG	p14 and p142HAC
p14V9TF	5' -CCCTCTAATTT C ACCAATCACGCACC	p14 and p142HAC
p14V9TR	5' -GGTGCGTGATTG G TGAAATTAGAGGG	p14 and p142HAC
p14V9IF	5' -CCCTCTAATTT C ATTAATCACGCACC	p14
p14V9IR	5' -GGTGCGTGATT A ATGAAATTAGAGGG	p14
p14N10AF	5' -CTCTAATTTTCGTC G CTCACGCACCTG	p14
p14N10AR	5' -CAGGTGCGTGAG C GACGAAATTAGAG	p14
p14H11AF	5' -CTAATTTTCGTC A TGCCGCACCTGGAG	p14
p14H11AR	5' -CTCCAGGTGCG G CATTGACGAAATTAG	p14
p14H11RF	5' -CTAATTTTCGTC A TGCCGCACCTGGAG	p14
p14H11RR	5' -CTCCAGGTGCG G CATTGACGAAATTAG	p14
p14H11EF	5'-CTAATTTTCGTC A TGAGGCACCTGGAG-3'	p14
p14H11ER	5' -CACCAGGTGC C TCATTGACGAAATTAG	p14
p14P13AF	5' -CGTCAATCACGC A GCTGGAGAAGCAATTG	p14
p14P13AR	5' -CAATTGCTTCTCCAG C TGCGTGATTGACG	p14
p14G14AF	5' -CACGCACCTG C AGAAGCAATTGTAAC	p14
p14G14AR	5'-GTTACAATTGCTTCT G CAGGTGCGTG-3'	p14
p14E15AF	5' -CACGCACCTGGAG C AGCAATTGTAACC	p14
p14E15AR	5' -GGTTACAATTGCT G CTCCAGGTGCGTG	p14
p14E15DF	5' -CACGCACCTGGAG A TGCAATTGTAACC	p14
p14E15DR	5' -GGTTACAATTG C ATCTCCAGGTGCGTG	p14
p14I17VF	5' -CCTGGAGAAGC A GTTGTAACCGGTTTGG	p14
p14I17VR	5' -CCAAACCGGTTACA A CTGCTTCTCCAGG	p14
p14I17TF	5' -CCTGGAGAAGC A CTGTAACCGGTTTGG	p14
p14I17TR	5' -CCAAACCGGTTACAGTTGCTTCTCCAGG	p14
p14H11E/E15HF	5' -GGCACCTGG A CACGCAATTGTAACC	p14-H11E
p14H11E/E15HR	5' -GGTTACAATTG C GTGTCCAGGTGCC	p14-H11E
p14E22AF	5' -GTAACCGGTTTGG C GAAAGGGGCAG	p14
p14E22AR	5' -CAGCCCCTTT C GCCAAACCGGTTAC	p14
p14E22A/D26AR	5' -GCGAAAGGGGC A GCTAAAGTAGCTGGAAC	p14-E22A
p14E22A/D26AR	5' -GTTCCAGCTACTTT A GCTGCCCCCTTTCGC	p14-E22A
p14K23AF	5' -GTAACCGGTTTGGAG G CAGGGGCAGATAAAGTAG	p14

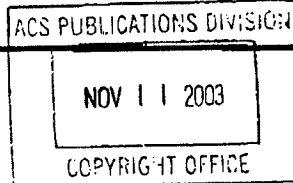
p14K23AR	5'-CTACTTTATCTGCCCCCTGCCTCCAAACCGGTTAC-3'	p14
p14K23A/K27AF	5'-GGCAGGGGCAGATGCAGTAGCTGGAACG-3'	p14-K23A
p14K23A/K27AR	5'-CGTTCCAGCTACTGCATCTGCCCCCTGCC-3'	p14K23A
p14N121QF	5'-GTCAACATCGATCAGGTCTCAGCCAT-3'	p14 and p142HAC
p14N121QR	5'-ATGGCTGAGACCTGATCGATGTTGAC-3'	p14 and p142HAC

Appendix C
Letters of copyright permission

Figures 1.2 and 1.3

Eric Slater

From:
Sent:
To:



Dear Sir or Madam,

I am writing to request permission from your journal to reproduce the following figures in my Ph.D. thesis.

Blumenthal et al., 2003. Membrane fusion. Chem. Rev. 103, 53-69
Figure 2, p. 58
Figure 3, p. 60

The figure will be used in the literature review, solely to illustrate the current research of the field. They will be used in the thesis only and are not going to be published in a scientific journal. If you require more information please do not hesitate to contact myself or my graduate supervisor (Dr. Roy Duncan: roy.duncan@dal.ca) further. I look forward to hearing from you.

Thanks

Jennifer

Jennifer Corcoran
Graduate Student
Department of Microbiology and Immunology


 PUBLICATIONS Division ACS 1155 - 16th St. NW Washington, DC 20036	PERMISSION TO REPRINT IS GRANTED BY THE AMERICAN CHEMICAL SOCIETY
	ACS COPYRIGHT CREDIT LINE REQUIRED. Please follow this sample: Reprinted with permission from (reference citation). Copyright (year) American Chemical Society.
VI-11-03	APPROVED BY ACS Copyright Office
<input type="checkbox"/> If this box is checked, author permission is also required. See original article for address.	

Figure 1.4.A

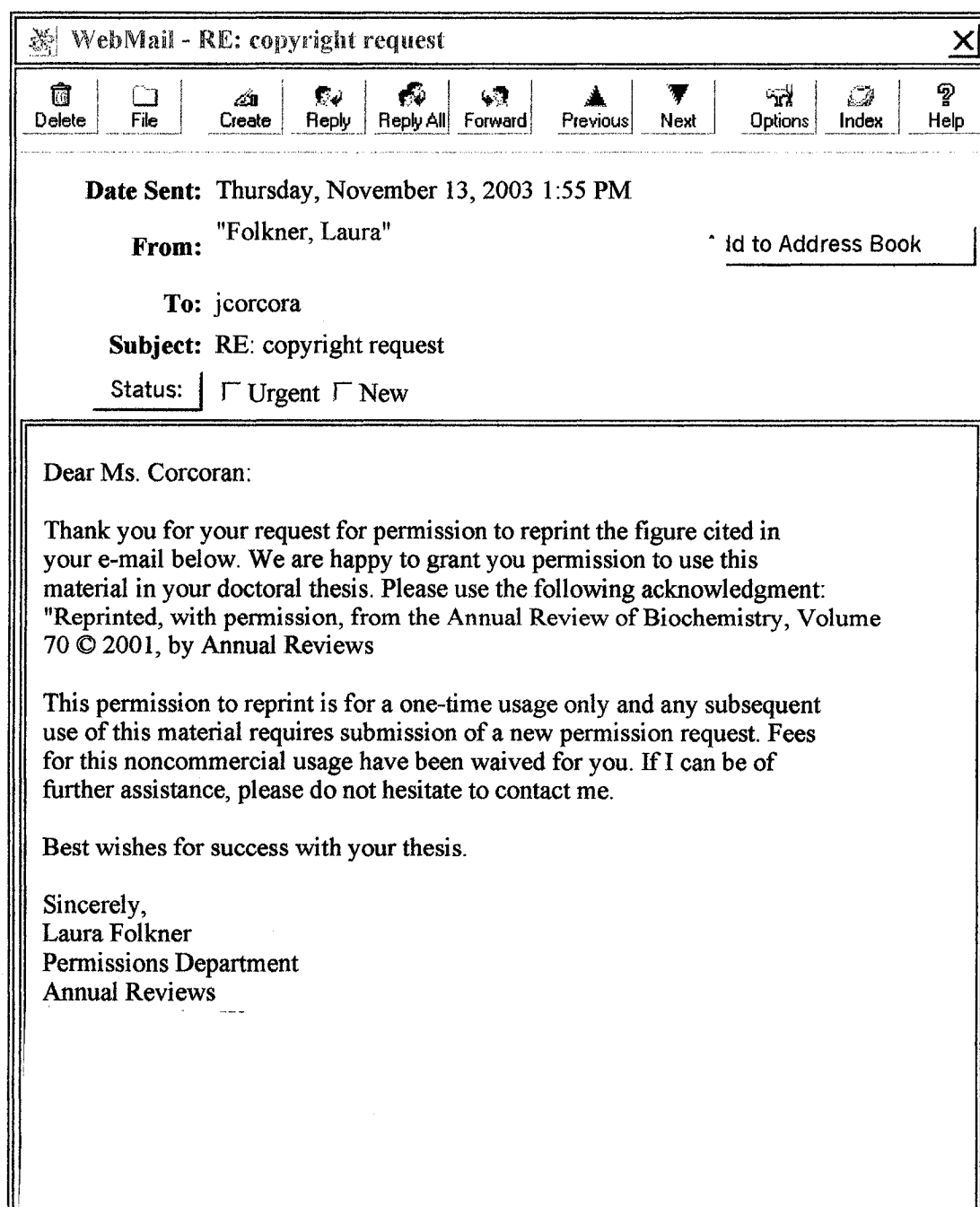


Figure 1.4.B



25 November 2003

Our ref: HW/ze.nov03.J077

Jennifer Corcoran
Dept of Microbiology and Immunology

Dear Ms Corcoran

CURRENT OPINION IN MICROBIOLOGY, Vol 4, 2001, pp450-455, Heinz et al, "The Machinery for..." 1 figure only.

As per your letter dated 10th November 2003, we hereby grant you permission to reprint the aforementioned material at no charge **in your thesis** subject to the following conditions:

1. If any part of the material to be used (for example, figures) has appeared in our publication with credit or acknowledgement to another source, permission must also be sought from that source. If such permission is not obtained then that material may not be included in your publication/copies.
2. Suitable acknowledgment to the source must be made, either as a footnote or in a reference list at the end of your publication, as follows:

"Reprinted from Publication title, Vol number, Author(s), Title of article, Pages No., Copyright (Year), with permission from Elsevier".
3. Reproduction of this material is confined to the purpose for which permission is hereby given.
4. This permission is granted for non-exclusive world **English** rights only. For other languages please reapply separately for each one required. Permission excludes use in an electronic form. Should you have a specific electronic project in mind please reapply for permission.
5. This includes permission for the National Library of Canada to supply single copies, on demand, of the complete thesis. Should your thesis be published commercially, please reapply for permission.

Yours sincerely

Helen Wilson
Rights Manager

Your future requests will be handled more quickly if you complete the online form at
www.elsevier.com/locate/permissions

Figure 1.5



26 November 2003

Our ref: HW/ND/Nov03/j102

Jennifer Corcoran
Department of Microbiology and Immunology
Dalhousie University

Dear Ms Corcoran

BIOCHIMICA ET BIOCHIMICA ACTA (BBA) - Biomembranes, Vol 1614, Issue 1, 2003, pp14-23, Tamm, "Hypothesis: spring-loaded boomerang mechanism...", 1 figure only

As per your letter dated 11 November 2003, we hereby grant you permission to reprint the aforementioned material at no charge in your thesis subject to the following conditions:

1. If any part of the material to be used (for example, figures) has appeared in our publication with credit or acknowledgement to another source, permission must also be sought from that source. If such permission is not obtained then that material may not be included in your publication/copies.
2. Suitable acknowledgment to the source must be made, either as a footnote or in a reference list at the end of your publication, as follows:

"Reprinted from Publication title, Vol number, Author(s), Title of article, Pages No., Copyright (Year), with permission from Elsevier".
3. Reproduction of this material is confined to the purpose for which permission is hereby given.
4. This permission is granted for non-exclusive world English rights only. For other languages please reapply separately for each one required. Permission excludes use in an electronic form. Should you have a specific electronic project in mind please reapply for permission.
5. This includes permission for the National Library of Canada to supply single copies, on demand, of the complete thesis. Should your thesis be published commercially, please reapply for permission.

Yours sincerely

Helen Wilson
Rights Manager

Your future requests will be handled more quickly if you complete the online form at
www.elsevier.com/locate/permissions

Figure 1.6



26 November 2003

Our ref: HW/ND/Nov03/j103

Jennifer Corcoran
Department of Microbiology and Immunology

Dear Ms Corcoran

VIROLOGY, Vol 260, 1999, pp316-328, Duncan, "Extensive sequence divergence and phylogenetic relationships between the fusogenic and nonfusogenic...", 1 figure only

As per your letter dated 11 November 2003, we hereby grant you permission to reprint the aforementioned material at no charge **in your thesis** subject to the following conditions:

1. If any part of the material to be used (for example, figures) has appeared in our publication with credit or acknowledgement to another source, permission must also be sought from that source. If such permission is not obtained then that material may not be included in your publication/copies.
2. Suitable acknowledgment to the source must be made, either as a footnote or in a reference list at the end of your publication, as follows:
"Reprinted from Publication title, Vol number, Author(s), Title of article, Pages No., Copyright (Year), with permission from Elsevier".
3. Reproduction of this material is confined to the purpose for which permission is hereby given.
4. This permission is granted for non-exclusive world English rights only. For other languages please reapply separately for each one required. Permission excludes use in an electronic form. Should you have a specific electronic project in mind please reapply for permission.
5. This includes permission for the National Library of Canada to supply single copies, on demand, of the complete thesis. Should your thesis be published commercially, please reapply for permission.

Yours sincerely

Helen Wilson
Rights Manager

Your future requests will be handled more quickly if you complete the online form at
www.elsevier.com/locate/permissions